

Hourly, In-Situ Quantitation of Organic Aerosol Marker Compounds

Final Report

ARB Award No. 03-324

STATE OF CALIFORNIA AIR RESOURCES BOARD

Principal Investigator

Dr. Allen H. Goldstein

Department of Environmental Science, Policy, and Management
Ecosystem Sciences Division
151 Hilgard Hall
University of California
Berkeley, CA 94720-3110
(510)643-2451
ahg@nature.berkeley.edu

Subcontract Co-Investigator

Dr. Susanne V. Hering

Aerosol Dynamics Inc.
Berkeley, CA

Contributing Researchers

Dr. Nathan M. Kreisberg
Brent J. Williams
Angela Miller

Contact for Contractual Matters:

David Garcia
Acting Assistant Director
Sponsored Project Office
University of California
336 Sproul Hall
Berkeley, CA 94720-5940
(510) 510-642-8114
(510) 642-8236 fax
email: dgarcia@uclink.berkeley.edu

April 25, 2008

ACKNOWLEDGEMENTS

Several individuals from the California Air Resources Board contributed to this project. We particularly want to thank Nehzat Motallebi for her steadfast encouragement and useful input throughout the contract period, along with William Vance and Chris Jakober for providing useful comments on the draft version of this report. The success of this study depended on the efforts of many individuals at UC Berkeley. In particular, Megan McKay from the Goldstein research group worked tirelessly to prepare for and then return from deployment to the research site and UC Riverside, and she was responsible for measurements of ozone, carbon monoxide, and meteorological variables, as well as purchasing, lab management, and many other details for the Goldstein Group. We thank Dave Rambeau for helping prepare our mobile laboratory and delivering it to and from the research site.

The measurements reported here were carried out during 2005 on the campus of the University of California at Riverside as part of the Study of Organic Aerosols at Riverside (SOAR). The overall research program was funded mainly EPA and CARB to investigate organic aerosol composition and sources. We are grateful to Paul Ziemann and his group at UC Riverside for hosting the SOAR campaign and allowing us to participate. We sincerely thank Jose Jimenez and Ken Docherty from the University of Colorado at Boulder for taking the lead in organizing the science team and planning the SOAR campaign. We thank Kim Prather and her group at UC San Diego, and Jamie Schauer and his group at University of Wisconsin, for important scientific collaborations associated with our measurements.

We gratefully acknowledge support for this research from the California Air Resources Board (award 03-324). Brent Williams acknowledges funding for a Graduate Student Fellowship from the Department of Energy Global Change Education Program.

TABLE OF CONTENTS

	<u>Page</u>
Acknowledgements.....	i
Table of Contents.....	ii
List of Acronyms.....	iv
List of Tables.....	v
List of Figures.....	vi
Abstract.....	ix
Executive Summary.....	x
Disclaimer.....	1
1. Introduction	2
1.1 Objectives	2
1.2 Background.....	2
1.3 Our Measurement Approach: Thermal desorption Aerosol GC (TAG).....	3
2. Field Measurement Site in Riverside California.....	4
3. Experimental Methods.....	5
3.1 Speciated organics in aerosols measured by TAG.....	5
3.1.1 Inlet Precut and Humidity Conditioning.....	5
3.1.2 Sampling Modes: Ambient / Filtered Ambient Blank / Zero Air Blanks.....	6
3.1.3 Collection-Thermal Desorption (CTD) Cell.....	6
3.1.4 Gas Chromatographic Separation.....	7
3.1.5 Mass Selective Detection (MSD) and Flame Ionization Detection (FID).....	8
3.1.6 Instrument Automation and Data Acquisition.....	8
3.1.7 Data Reduction and Analysis.....	8
3.1.8 Instrument Evaluation: Methods.....	9
3.1.8.1 Particle Collection Efficiency.....	9
3.1.8.2 Reproducibility for Ambient Sampling.....	9
3.1.9 Instrument Evaluation: Results.....	9
3.1.9.1 Particle Collection Efficiency.....	9
3.1.9.2 Reproducibility for Ambient Sampling.....	10
3.1.10 Instrument Summary.....	10
3.2 TAG Calibration and Quantification.....	11
3.2.1 Experimental Methods.....	11
3.2.1.1 Authentic standards.....	11
3.2.1.2 Assessment of precision and limits of quantitation.....	12
3.2.2 Calibration Methodology.....	12
3.2.3 Calibration and Quantification Results.....	13
3.2.3.1 Precision and LOQ.....	13
3.2.3.2 System stability and drift corrections.....	14
3.2.3.3 Time-independent, multi-point calibrations.....	15
3.2.3.4 Relative response factors for n-alkanes and PAHs.....	16

3.2.3.5 Alkane response factors.....	16
3.2.3.6 PAH response factors.....	17
3.2.3.7 Application of TAG calibration.....	17
3.2.3.8 Application to Riverside ambient measurements.....	18
3.2.4 Calibration and Quantification Summary.....	20
3.3 Gas Phase VOC measurements	20
3.4 Additional Measurements	22
4. Results and Discussion (SOAR Results).....	22
4.1 SOAR Speciated Organic Aerosol Measurements.....	22
4.2 Positive Matrix Factorization.....	23
4.3 Results.....	24
4.3.1 Drift Correction.....	24
4.3.2 Compound Identification.....	24
4.4 Source Apportionment.....	26
4.4.1 Summer PMF Results.....	27
4.4.1.1 Factors 1, 2, 3: SOA1, SOA2, and SOA3.....	27
4.4.1.2 Factors 4, 5: RegionalPrimaryAnthro and LocalVehicle.....	28
4.4.1.3 Factor 6: FoodCooking.....	30
4.4.1.4 BioParticle+Mixed.....	30
4.4.1.5 Factor 8: BioSemivolatile.....	31
4.4.1.6 Factor 9: BiomassBurning.....	31
4.4.2 Fall PMF Results.....	31
4.4.2.1 Factors 1, 2: SOA+FoodCooking1 and SOA+FoodCooking2.....	32
4.4.2.2 Factor 3: RegionalPrimaryAnthro.....	32
4.4.2.3 Factor 4: LocalVehicle.....	33
4.4.2.4 Factor 5: BioSemivolatile.....	33
4.4.2.5 Factor 6: BiomassBurning.....	33
4.4.3 PMF Residuals.....	33
4.5 Source Contributions to Organic Aerosol Mass.....	35
4.6 Average Diurnal Variations in Organic Aerosol Composition.....	36
5. Implications and Conclusions.....	37
6. References.....	38
7. Appendix A: Phase I Report.....	86

LIST OF ACRONYMS

AMS – Aerosol Mass Spectrometer
ATOFMS – Aerosol Time-Of-Flight Mass Spectrometer
BAM – Beta Attenuation Monitor
CPC – Condensation Particle Counter
CTD – Collection Thermal Desorption
DOY – Day Of Year
EC – Elemental Carbon
EI – Electron Impact
FID – Flame Ionization Detector
GC – Gas Chromatograph
HP – Hewlett-Packard
ICARTT – International Consortium for Atmospheric Research on Transport and Transformation
LOQ – Limit of Quantitation
LOWESS – Locally-Weighted Least-Squares Smoothed
MACR – Methacrolein
MDL – Method Detection Limit
MEK – Methyl Ethyl Ketone
MS – Mass Spectrometer
MSD – Mass Selective Detector
MVK – Methyl Vinyl Ketone
m/z – mass to charge ratio
OC – Organic Carbon
OM – Organic Matter
OVOC – Oxygenated Volatile Organic Aerosol
PAH – Polycyclic Aromatic Hydrocarbons
PAR – Photosynthetic Active Radiation
PM – Particulate Matter
PMF – Positive Matrix Factorization
RH – Relative Humidity
RSD – Relative Standard Deviation
SIM – Single Ion Mode
SOA – Secondary Organic Aerosol
SOAR – Study of Organic Aerosol at Riverside
TAG – Thermal desorption Aerosol Gas chromatograph
TS – Tracking Standard
UHP – Ultra High Purity
VOC – Volatile Organic Compound
VUV – Vacuum Ultraviolet Ionization

LIST OF TABLES

<u>Table No.</u>	<u>Page</u>
1. Subset of authentic standards used for TAG calibration during summer and fall Riverside field studies. The tracking standard was injected regularly throughout both study periods while the auxiliary standards were infrequently injected and primarily serve to confirm MS compound identification through retention times.	47
2. Compounds contained in the Tracking standard.	48
3. Relative response factors for PAHs in the EPA auxiliary standard relative to the tracking standard compound chrysene, as defined by equation (4). $R_{i,chy}$ is the response at the 1 ng injection level, and $\bar{R}_{i,chy}$ is the average response over a range of injection levels.	49
4. Summary statistics for aerosol concentrations and gas fractions for calibrated compounds during summer and fall intensive study periods.	50
5. MSD drift over seasonal focus periods July 29 - August 8 (summer) and November 4 - 14 (fall) as measured by daily-run tracking standard.	51
6. Compounds observed by TAG during SOAR campaigns.	52
7. Summer Positive Matrix Factorization profiles.	56
8. Fall Positive Matrix Factorization profiles.	58
9. Correlations ($-0.3 > r > 0.3$) between TAG-Defined Summer Factors and Other Relevant Parameters.	60
10. Correlations ($-0.3 > r > 0.3$) between TAG-Defined Fall Factors and Other Relevant Parameters.	61
11. Average Source Concentrations and Contributions to Total OA during SOAR 2005.	62

LIST OF FIGURES

<u>Figure No.</u>	<u>Page</u>
1. View of the ground-based field site at Riverside, CA (33°58'18''N, 117°19'17''W). Shown are anthropogenic PM _{2.5} -PRI emissions in short tons/ozone season day/grid cell, plotted on a 4-km Lambert-Conformal grid. This emission map was created using the NOAA-NESDIS/OAR Emission Inventory Mapviewer found at: (http://map.ngdc.noaa.gov/website/al/emissions/viewer.htm), maintained by Gregory Frost, NOAA.	63
2. Average daytime and nighttime winds for SOAR focus periods, separated by summer (July 29 – August 8) and fall (November 4 – 14) 2005. Concentric rings represent frequency of observations.	64
3. Schematic of the TAG system, showing flow configuration for two modes of operation: (a) concurrent sampling and analysis, and (b) thermal desorption. The thermal desorption mode is used for transfer of collected sample onto the chromatography column.	65
4. Current design of the collection and thermal desorption (CTD) cell provides in-situ calibrations of TAG via an integrated injection port. Fixed-volume injections of varying concentrations of authentic standards in solution are deposited near the impaction region of the collection cell on the same passivated surface as used for aerosol collection.	66
5. Collection efficiency curves for 9 and 12-jet impactors. The oleic aerosol is a nonhygroscopic oil, while potassium chloride aerosol is a solid particle (84% deliquescence), which was introduced to the cell at 60-70% RH. Data were obtained using the CPC counting method (see text).	67
6. Comparison of peak areas for independent, collocated samples of ambient air in Berkeley California. Line shows 1:1 correspondence.	67
7. Relationship of injection repeatability (RSD) versus the ratio of LOQ to the individual compound injection mass level M. Compounds that elute before hexadecane were excluded. For these less-volatile species, the baseline precision for calibration standards can be taken as the limit of LOQ/M~0, which is the intercept of the regression line=1.3% RSD.	68
8. Fall instrument response trends are shown for four selected tracking standard compounds used in this analysis. Plotted is the detector peak area divided by each compound's average response versus hour of study. Mean single ion areas are 6.7x10 ⁵ (cholestane), 4.0x10 ⁶ (chrysene), 2.2x10 ⁶ (eicosane) and 4.2x10 ⁶ (octacosane). These compounds demonstrate a consistent, downward trend in MSD response as a function of time. For a uniformly distributed subset of the tracking standard data, the cholestane FID data show no significant trend. Different filled symbols indicate distinct standard solutions. Drift regressions shown exclude the first set of standard solutions (triangles) due to uncertainty in that standard's concentrations.	69

<u>Figure No. (cont.)</u>	<u>Page</u>
9. Summer instrument response trends are shown for four selected tracking standard compounds used in this analysis. Plotted is the detector peak area divided by each compound's average response versus hour of study. Mean single ion areas are 8.4×10^5 (cholestane), 6.3×10^6 (chrysene), 2.6×10^6 (eicosane) and 5.6×10^6 (octacosane). These compounds demonstrate a consistent, downward trend in MSD response as a function of time. For a uniformly distributed subset of the tracking standard data, the cholestane FID data shows no significant trend. Different filled symbols are for two standard concentration levels with the indicated stock dilution ratio. The more dilute response data was scaled up to the more concentrated level by application of a preliminary calibration using the more concentrated subset of data.	70
10. Time-independent calibration of TAG for four of the tracking standard compounds for the Summer SOAR study. Non-linear fits (solid lines) are shown to be superior to linear fits (broken lines) for all four compounds, especially near the limits of detection of the instrument (insets). Vertical spread in calibration points indicates residual variation of data after de-trending.	71
11. Relative response factors for n-alkanes defined as the ratio of the single ion peak areas (57 m/z) for compound C_n to the reference compound eicosane (C_{20}) for summer and fall periods. Sensitivity to mass level is indicated at both the low and high volatility ends of the carbon number spectrum. Response factors from the alkane auxiliary standard (triangles, squares) provide the complete range of response for TAG and are in general agreement with similar ratios obtained from the multipoint calibration data using C_{16} , C_{20} and C_{28} in the tracking standard (circles), shown with $1-\sigma$ error bars, over the indicated mass injection levels.	72
12. Calibrated TAG response for octacosane, chrysene and the sum of two hopanes, during the fall study. The calibration for the tracking standard cholestane was applied to each of the hopane responses with a relative response factor prior to summing. Gaps greater than 2 hours are shown with line breaks indicating when calibrations or other interruptions of normal operation occurred.	73
13. AMS total organics, carbon monoxide (CO), and ozone (O_3) concentrations during SOAR 2005. a) The summer period (July 29 – August 8) displays regular diurnal patterns, with very high O_3 concentrations every afternoon. The summer focus period (outlined in grey) is consistent with the general trend of the entire summer study. b) The fall period (November 4 - 14) is dominated by meteorological “events”, with lower O_3 concentrations than observed in summer. The fall focus period (outlined in grey) is representative of a period high in particulate concentrations and CO concentrations.	74
14. Summer PMF profiles. Only compounds with loadings of at least 30% into a single source are displayed (at least 25% for RegionalPrimaryAnthro).	75
15. Fall PMF profiles. Only compounds with loadings of at least 50% into a single source are displayed (at least 33% for SOA+FoodCooking1).	76

<u>Figure No. (cont.)</u>	<u>Page</u>
16. Rose plots of the 9 summer aerosol sources (plus the Residual factor) using only concentrations > 1 standard deviation to emphasize dominant source directions. Frequency of observations are represented by the length of each wedge, and labeled by concentric rings. The shade of each wedge represents source concentrations in quartiles (dark = higher concentrations).	77
17. Rose plots of the 6 fall aerosol sources (plus the Residual factor) using only concentrations > 1 standard deviation to emphasize dominant source directions. Frequency of observations are represented by the length of each wedge, and labeled by concentric rings. The shade of each wedge represents source concentrations in quartiles (dark = higher concentrations).	78
18. Source contributions to total organic aerosol mass concentrations during the summer focus period (July 29 – August 8).	79
19. Source contributions to total organic aerosol mass concentrations during the fall focus period (November 4 - 14).	79
20. a) Individual organic aerosol source timelines over the summer focus period (July 29 – August 8). b) Diurnal averages for summer organic aerosol sources. Photosynthetic active radiation (PAR) has been included to represent the solar cycle.	80
21. a) Individual organic aerosol source timelines over the fall focus period (November 4 – 14). b) Diurnal averages for fall organic aerosol sources. Photosynthetic active radiation (PAR) has been included to represent the solar cycle.	81
22. Average diurnal concentrations of AMS species over the summer focus period. Total aerosol mass concentrations labeled outside of pie chart ring, and time of day labeled inside of pie chart ring.	82
23. Average diurnal concentrations of AMS species over the fall focus period. Total aerosol mass concentrations labeled outside of pie chart ring, and time of day labeled inside of pie chart ring.	83
24. Average diurnal concentrations of TAG-derived PMF sources over the summer focus period. Total organic aerosol mass concentrations labeled outside of pie chart ring, and time of day labeled inside of pie chart ring.	84
25. Average diurnal concentrations of TAG-derived PMF sources over the fall focus period. Total organic aerosol mass concentrations labeled outside of pie chart ring, and time of day labeled inside of pie chart ring.	85

ABSTRACT

This study was conducted to determine the contribution from various organic aerosol sources downwind of the Los Angeles Air Basin, a region currently out of compliance with air quality standards. Organic marker compounds were measured with hourly time resolution and analyzed by principal component methods to provide hourly source attribution. Measurements were made using an automated, in-situ thermal desorption aerosol gas chromatograph (TAG) with mass spectrometry analysis. The TAG instrument was deployed in Riverside, California during the summer and late fall, 2005. Measurements were made in as part of the Study of Organic Aerosols in Riverside (SOAR). This multi-investigator study, organized through support from Environmental Protection Agency and the California Air Resources Board, brought together many time-resolved aerosol measurements, including the UC San Diego Aerosol Time of Flight Mass Spectrometer and the Aerodyne Aerosol Mass Spectrometer.

The data set produced consists of hourly measurements of 300 compounds, including alkanes, branched alkanes, alkenes, polycyclic aromatic hydrocarbons, branched PAHs, hopanes, acids, phthalates, furanones, guaiacols, syringols, and other oxygenated compounds. The hourly concentration of organic marker compounds measured by TAG, together with the total organic mass from the AMS, were analyzed using positive matrix factorization (PMF).

Major findings of this study include:

1. There are multiple types of secondary organic aerosol (SOA) at Riverside, together creating an average 47% of summertime total organic aerosol mass. Differences between these SOA types likely include particle age and formation mechanism (i.e. heterogeneous chemistry in primary aerosol versus oxidation of gas phase precursors that creates low volatility products favoring the particle phase).
2. The high time resolution obtained by TAG measurements allowed us to observe diurnal changes in aerosol sources. For the first time it was observed that SOA contributes 75% of the organic aerosol mass during average summertime afternoons in this region downwind of Los Angeles.
3. The PMF results make a distinction between local traffic and regional anthropogenic primary sources. There is an indication that hopanes associated with traffic are not long-lived in the atmosphere.
4. In Riverside, regional primary anthropogenic sources contribute approximately 5 times more organic aerosol mass on average than local traffic emissions during the summer, and 15 times more during fall. Overall, however, total SOA sources contribute 2.5 times more organic aerosol mass than the combination of these two primary aerosol sources in summer. In the fall SOA was not completely separable from primary sources. While primary vehicle emissions (local and regional) account for less than 20% of the total organic aerosol mass during both seasons, a significant amount of vehicle emissions have been processed in the atmosphere contributing to the large amounts of observed SOA.
5. Biogenic sources contribute more organic aerosol mass during the summer than in the fall at Riverside, and conversely biomass burning sources contribute a larger fraction of the total organic aerosol mass during the fall.

EXECUTIVE SUMMARY

The concentrations of airborne particulate matter in many regions of California do not meet federal or state air quality standards for Particulate Matter with diameters below 2.5 μm ($\text{PM}_{2.5}$). Organic matter is a major constituent of these airborne particles, comprising 20-50% of the $\text{PM}_{2.5}$ mass in many regions. There are multiple sources, including primary emissions and secondary components. The chemical composition is complex. Many hundreds of organic compounds in $\text{PM}_{2.5}$ have been identified through chromatography and mass spectrometry techniques. This complexity presents a challenge for the characterization of organic particles, but it also provides an opportunity for understanding the origins of these constituents.

A two phase study was conducted to determine the contribution to $\text{PM}_{2.5}$ from various organic aerosol sources in a region downwind of the Los Angeles Air Basin, a region currently out of compliance with air quality standards. The objective of phase I was to demonstrate the ability of the In-situ thermal desorption aerosol gas chromatograph (TAG) instrument to separate and identify organic marker compounds found in atmospheric $\text{PM}_{2.5}$ samples with hourly time resolution. For phase I, we prepared a report (Appendix A) providing evidence that TAG was ready for field measurements in California. The Interim Report also describes the method evaluation and presents initial results for field measurements of atmospheric aerosols in Nova Scotia, Canada. The objective of phase II was to deploy TAG for one month in summer and one month in fall, and to use the observations to resolve the importance of different organic aerosol sources.

Presented here are phase II results in which the concentrations of organic marker compounds were measured with hourly time resolution and analyzed by principal component methods to provide hourly source attribution. Measured compounds included markers for primary emissions, such as combustion sources, as well as secondary products formed from anthropogenic or biogenic precursors. The variation in organic composition throughout each study period, combined with other hourly data sets, were used to identify the relative contributions of local vehicles, regional anthropogenic particulate emissions, biomass burning, biogenic sources and secondary organic matter.

Summary of Measurements

The TAG instrument was deployed in Riverside, California during one month in summer and one month in late fall, 2005 as part of the Study of Organic Aerosols in Riverside (SOAR). This multi-investigator study, organized through support from Environmental Protection Agency and the California Air Resources Board, brought together many time-resolved aerosol measurements, including the UC San Diego Aerosol Time of Flight Mass Spectrometer and the Aerodyne Aerosol Mass Spectrometer.

Data Set

The TAG measurements resulted in a data set of hourly observations for 300 compounds during the summer and winter study periods, identified using mass spectra and retention time matches to authentic standards. Measured compounds include alkanes, branched alkanes, alkenes, polycyclic aromatic hydrocarbons, branched PAHs, hopanes, acids, phthalates, furanones, guaiacols, syringols, and other oxygenated compounds. Of those identified, we report ambient concentrations for 20 compounds based on calibrations derived from authentic liquid standards. For the remaining 280 compounds, relative concentrations are reported.

Source Allocation Results

The hourly concentration of organic marker compounds measured by TAG, together with the total organic mass from the AMS, were analyzed using positive matrix factorization (PMF). Because PMF relies on relative concentrations, it was possible to include identified compounds in the analysis, even though their absolute concentrations were not always known.

During the summer campaign, nine factors (source types) were identified. These included three types of secondary organic aerosols (SOA), all differing in chemical composition and temporal trends. The first two SOA factors exhibited a mid-morning maxima coincident with the break up of the inversion layer, while the third SOA factor peaked in the afternoons, coincident with transport from Los Angeles. Primary organics of anthropogenic origin included those of regional extent, local vehicle traffic, and local food cooking. Biogenic organics were split into three factors: one that was dominantly nonvolatile biogenics, one with semivolatile biogenic compounds, and one including biomass burning.

During the fall campaign, six factors were identified. As in the summer there were two primary anthropogenic factors, one associated with regional sources and one, containing hopanes, associated with local traffic. Two major factors contained markers for both SOA and Food Cooking. Compounds not included in the factor analysis that correlated with these SOA factors included additional acids, ketones and aldehydes. A biogenic factor containing semivolatile terpenes was seen at night, associated with southeast winds, and may have been associated with the nearby agricultural test crops and botanical gardens. This same factor was observed during the summer at higher concentrations. Similarly, a factor associated with biomass burning was more commonly observed at night.

Results of the PMF analysis of TAG data were compared to a mass concentration based classification of single particle types identified by the ATOFMS. These single particles types included two types of aged organics, aged organics containing sulfate, organics containing elemental carbon, organics containing both elemental carbon and sulfate, and elemental carbon alone. The highest correlation between the TAG-defined factors and the ATOFMS-defined clusters were observed during the summer period between the SOA factors identified by TAG and the sulfate containing particles from the ATOFMS.

Major findings of this study include:

1. There are multiple types of SOA at Riverside, together creating an average 47% of summertime total organic aerosol mass. Differences between these SOA types likely include particle age and formation mechanism (i.e. heterogeneous chemistry in primary aerosol versus oxidation of gas phase precursors that creates low volatility products favoring the particle phase).
2. The high time resolution obtained by TAG measurements allowed us to observe diurnal changes in aerosol sources. For the first time it was observed that SOA contributes 75% of the organic aerosol mass during average summertime afternoons in this region downwind of Los Angeles.
3. The PMF results make a distinction between local traffic and regional anthropogenic primary sources. There is an indication that hopanes associated with traffic are not long-lived in the atmosphere.
4. In Riverside, regional primary anthropogenic sources contribute approximately 5 times more organic aerosol mass on average than local traffic emissions during the summer, and 15 times more during fall. Overall, however, total SOA sources contribute 2.5 times more organic aerosol mass than the

combination of these two primary aerosol sources in summer. In the fall SOA was not completely separable from primary sources. While primary vehicle emissions (local and regional) account for less than 20% of the total organic aerosol mass during both seasons, a significant amount of vehicle emissions have been processed in the atmosphere contributing to the large amounts of observed SOA.

5. Biogenic sources contribute more organic aerosol mass during the summer than in the fall at Riverside, and conversely biomass burning sources contribute a larger fraction of the total organic aerosol mass during the fall.

DISCLAIMER

The statements and conclusions in this report are those of the authors from the University of California and Aerosol Dynamics Incorporated and not necessarily those of the California Air Resources Board. The mention of commercial products, their source, or their use in connection with material reported herein is not to be construed as actual or implied endorsement of such products.

Hourly, In-Situ Quantitation of Organic Aerosol Marker Compounds

1. Introduction

1.1 Objectives

The fundamental objective of this work as funded by ARB was to prove the utility of hourly organic aerosol speciation data to identify the origins of PM_{2.5} organic matter. This we proposed to achieve through automated, time-resolved measurements of organic marker compounds in ambient aerosols using our new Thermal desorption Aerosol GC (TAG) system (Williams et al., 2006), combined with source attribution through statistical analysis (Williams et al., 2007; Jaekels et al., 2007). We proposed to deploy TAG for measurements during one fall and one summer field campaign of approximately 1 month duration each in order to investigate seasonal differences in tracers and sources. We proposed to use our hourly observations combined with statistical analysis to identify the major source types, and combine our data with those of collocated gas and aerosol instrumentation to identify and quantify the contribution from different source categories. In our initial proposal, several field sites were considered as possibilities. After the proposal was funded, we worked with ARB personnel to agree on the appropriate field site for our measurements. The collaborative Study of Organic Aerosols in Riverside (SOAR) was then planned including support largely from CARB and EPA, and included a wide variety of research teams (<http://cires.colorado.edu/jimenez-group/Field/Riverside05/>), to address the following major questions:

1. The characterization of the composition and sources of the ambient organic aerosol by a variety of state-of-the-art instrumentation and source apportionment techniques.
2. The intercomparison of multiple organic analysis techniques as a way to better understand both the organic aerosol and the analysis techniques.
3. The field demonstration of some new instruments such as TAG, the high m/z resolution AMS, the Vacuum Ultraviolet Ionization (VUV) AMS, and the dual-channel Sunset EC/OC analyzer.
4. The characterization of the quantification of the organic and total submicron aerosol by combining the data from many different instruments operating on different principles.

Analysis of the broad array of observations made during the SOAR study is ongoing. This report focuses on the objectives from our proposal to ARB, but the work supported by ARB will contribute to all four of the objectives listed above. Specifically, this report provides a detailed description of the TAG system, the calibration of TAG measurements for speciated organics in aerosols, TAG and associated data collected during the SOAR campaign in summer and fall 2005, and the source apportionment of organic aerosols in summer and fall based on those measurements.

1.2 Background

Many urban and rural California air districts are now out of compliance with state and federal air quality standards for particulate matter. The Air Resources Board and Office of Environmental Health Hazard Assessment are currently formulating new 24-hour PM_{2.5} ambient air quality standards for California. Regulatory efforts to conform to PM_{2.5} standards require improvements in our knowledge of the factors controlling the concentration, size and chemical composition of PM_{2.5}. While many advances have been made in measuring and modeling the inorganic ionic species that are found in PM_{2.5}, much less is known

about the organic fraction. Yet organic matter is a major constituent of airborne particles, comprising 20-50% of the PM_{2.5} mass in many regions (e.g. Schauer and Cass, 2000).

The chemical composition of atmospheric organic matter is complex. Many hundreds of organic compounds have been identified through chromatography and mass spectrometry techniques (Rogge et al., 1997a, 1997b, 1998; Schauer et al., 1999; Nolte et al., 1999; Fine et al., 2001). These include alkanes, substituted phenols, alkanals, sugar derivatives, aromatic polycyclic hydrocarbons, mono- and di-carboxylic acids. Some organic compounds are markers for primary emissions, such as combustion sources, while others are secondary products formed from anthropogenic or biogenic precursors. Quantitative knowledge of the composition of PM_{2.5} organic matter is key to tracing its sources and understanding its formation and transformation processes.

1.3 Our Measurement Approach: On-line Thermal desorption Aerosol GC (TAG)

Traditional methods for organic compound identification and quantification involve collection by filtration, with subsequent extraction and analysis by liquid or gas chromatography. Generally, the most complete identification has been by gas chromatography followed by mass spectrometry (GC/MS). While the identified compounds comprise only a fraction of the total organic mass, those that are quantified serve as valuable tracers for sources, and have been used to determine the relative contribution of various source types to primary ambient organic matter (Schauer and Cass, 2000; Fraser et al., 2000). These methods have provided valuable insight and guidance in our understanding of airborne organic matter. However, GC/MS analysis of extract from filters requires large samples, typically milligrams of collected organic material. The cost is high, and generally the time resolution is poor.

TAG was designed for the quantitative, time-resolved measurement of the ambient concentration of specific low-volatility organic compounds in PM_{2.5}. The fundamental principle is collection of ambient PM_{2.5} aerosols onto a passivated surface by means of impaction, immediately followed by thermal desorption onto a GC column, with subsequent GC/MS analysis. TAG combines several proven technologies for the measurement of organic compounds in the solid phase. The impaction collection is a straightforward extension of our existing automated system for measuring particulate nitrate, wherein particles are preconditioned via humidification and then deposited on a metal surface by impaction (Stolzenburg and Hering 2000). Thermal desorption GC/MS has been used successfully for the analysis of time-integrated filter and impactor samples of atmospheric aerosols (Waterman et al, 2000, Neusüss et al, 2000, Falkovich and Rudich, 2001). The automation of the GC/MS is an extension of our well-established work for in-situ measurement of volatile organic compounds in the gas phase (Goldstein et al., 1995; Lamanna and Goldstein, 1999).

Our GC/MS analysis builds on the extensive body of knowledge on the quantification of organic material, and for identification of the origins of organic aerosols (Schauer and Cass, 2000, Fraser et al, 2000; Forstner et al., 1997). Our analytical technique is very similar to that employed by Dr. Schauer. Compounds are separated chromatographically on a column, exactly as used for filter samples, and then identified individually by comparing their mass spectrum fragmentation pattern to the published spectra on the NIST MS data base. In this manner we are able to identify and quantify individual organic compounds. A major difference between filter-based work and our instrument is that TAG provides automated, in-situ analysis with high time resolution, and avoids sample-handling artifacts associated

with filter collection. Unlike filter collection with gas phase sorption techniques, TAG does not efficiently collect ultra-fine particles and the most-volatile component of fine particulates (e.g. TAG was not designed to address gas/particle partitioning). Therefore, some inherent differences between the two sampling approaches are expected to lead to differences in measurements but with the advantage of high time resolution that is necessary for proper source identification.

The particle beam mass spectrometry instruments of Aerodyne (Jayne et al., 2000) and Ziemann and coworkers (Tobias and Ziemann, 1999; Docherty and Ziemann, 2001, Tobias et al, 2002) are fundamentally different than ours because they do not utilize chromatographic separation to differentiate organic compounds prior to mass spectrometric analysis. There are hundreds to thousands of organic compounds in ambient aerosols, and unless they are separated before introducing them to a mass spectrometer it is impossible to specifically identify them. Ziemann's TDPBMS is very elegant, but is tailored for measurement in well-defined situations such as smog chamber studies. His programmed thermal desorption provides some degree of compound separation, but not the same as with the GC chromatographic separation we use. The Aerodyne AMS instrument makes no attempt to separate organic compounds before introducing them to the mass spectrometer, thus they can measure mass fragments which are likely indicative of functional groups. While their instrument offers advantages of time and size resolution, it does not offer quantification at the compound level for individual organic species.

Our in-situ measurements will allow continuous hourly resolution which is currently impossible using the filter collection approach. This enables us to make measurements with much finer time resolution and gain information on sources from the temporal variability of their impact on the total organic aerosol composition.

2. Field Measurement Site

The TAG instrument was deployed in Riverside, California during the summer (July 17 – August 16, 2005) and late fall (October 26 – November 30, 2005). Measurements were made in as part of the Study of Organic Aerosols in Riverside (SOAR). This multi-investigator study, organized through support from Environmental Protection Agency and the California Air Resources Board, brought together many time-resolved aerosol measurements, including the UC San Diego Aerosol Time of Flight Mass Spectrometer and the Aerodyne Aerosol Mass Spectrometer. Additionally, measurements were made of gas phase VOC and standard meteorological parameters.

The SOAR field site was located in Riverside, CA (33°58'18''N, 117°19'17''W) on the University of California campus, which is approximately 80 km to the east-southeast of downtown Los Angeles, CA, and 0.6 km east of interstate highway 215 (Fig. 1). Interstate highway 215 carries an annual average of 173,000 vehicles per day through Riverside, CA as reported in 2002 [*Caltrans*] creating a significant amount of local primary emissions. Riverside is currently classified as one of the most polluted areas in California and the US for short term and long term particulate matter by the American Lung Association.

Riverside is contained within the eastern edge of the greater Los Angeles Basin. Airborne pollutants are routinely trapped within the basin by the surrounding Santa Susanna, Santa Monica, San Gabriel, and San Bernardino Mountains to the north, the Santa Anna Mountains to the south, and the San Jacinto Mountains to the east. The population of the entire Los Angeles Basin (i.e. Los Angeles County, Orange

County, Ventura County, San Bernardino County, and Riverside County) in 2006 was estimated at 17.8 million people [*U.S. Census Bureau*]. The L.A. Basin is home to many industries and has high land, sea, and air traffic, therefore acting as a major aerosol emission region (Fig. 1). The basin is large enough to retain much of the primary aerosols throughout the day, allowing enough time for the aerosols to undergo photochemical and heterogeneous reactions in the atmosphere, as well as photooxidize primary gas phase emissions, creating lower volatility reaction products that favor the particle phase. Turpin and Huntzicker (1991, 1995) and Turpin et al. (1991) provided strong evidence that secondary PM formation occurs during periods of photochemical ozone formation in Los Angeles and that as much as 70% of the organic carbon in ambient PM was secondary in origin during a smog episode in 1987. More recent studies have shown that secondary sources on average contribute 60% of the total organic aerosol mass in the Riverside area during the late summer (Na et al., 2004).

The average daytime wind direction is from west to east (Fig. 2), typically carrying pollutant emissions from Los Angeles to Riverside, and creating a significant amount of regional secondary aerosol in transit. Average nighttime winds typically came from the south at low wind speeds (Fig. 2), bringing locally produced particles to the site. Located directly to the southeast of the site was a large botanical garden, and to the south and southwest was a wide range of test crop groves, providing significant biogenic contributions to our measurements. Exceptions to this typical diurnal wind pattern were observed during the fall, when high pressure systems settled in from the north, forcing dry desert air to move from the east back to the west. These wind patterns are known as the Santa Anna winds.

3. Experimental Methods

3.1 Speciated organics in aerosols measured by Thermal desorption Aerosol GC (TAG)

During SOAR the TAG system operated on 30 and 35 days respectively in the summer and fall study periods, providing hourly measurements of ambient aerosols on an average of 15.5 hours out of every 24-hour period. Field blanks, system zeros and calibration measurements filled the remaining hours. Blanks were collected automatically, interspersed among hourly collection of ambient aerosols. During SOAR the system operated on a 26 hour cycle which included 19 ambient aerosol samples, 5 dynamic blanks, 1 zero air blank and 1 filtered zero air blank. Typically the system was taken off line once each day for manual calibrations with authentic organic standards introduced directly into the collection cell. Details of the calibration procedure are given in Section 3.2.

The TAG instrument is shown in Figure 3 Each of its major components are described below in order from the sample inlet to the detector. TAG has two basic modes of operation: (1) sampling with concurrent GC/MS-FID analysis of the previously collected sample (Fig. 3a), and (2) thermal desorption with sample injection (Fig. 3b). The Thermal Desorption Mode transfers the previously collected sample onto the GC column. During the Sampling/Analysis Mode, the GC analysis is completed while the CTD cell is cooled to room temperature and the next sample is collected. The switching between these modes is determined by the valve and temperature configuration, as described below.

3.1.1 Inlet Precut and Humidity Conditioning

Ambient air is pulled through a BGI sharp cut PM_{2.5} cyclone (SCC, BGI Inc., Waltham, MA) (Kenny et al. 2000), and 3/8" tubing by a vacuum pump to achieve a flow rate of 9 L/min, restricted either by the impaction jet on the sample line or the critical orifice on the bypass line depending on the valve positions. The cyclone excludes particles larger than 1.5 μm in aerodynamic diameter which include crustal materials more prone to particle bounce within the impactor. All components exposed to the

sample (i.e. tubing, fittings, impaction jet) are 316 stainless steel chemically passivated with an Inertium® coating (Advanced Materials Components Express, Lemont, PA). To minimize particle losses, ball valves are used in aerosol sampling lines upstream of the collection cell.

Particles in the sample stream are humidified to increase adhesion and eliminate particle bounce during the following impaction stage (Stein et al. 1994). Particle aerodynamic diameter is essentially unchanged after humidification due to a compensating decrease in particle density with water uptake. The humidifier consists of 10 parallel water semi-permeable Nafion tubes, each with 2.2 mm inner diameter and 30 cm length enclosed in a water jacket. The humidifier (MH-110, PermaPure, Toms River, NJ) with a 9 L/min air stream and an input water vapor content of 20-95 % relative humidity (RH) consistently produces an output value of approximately 65-95 % RH, high enough to minimize particle bounce. Similar humidifiers have been successfully employed in other inertial impaction collection systems (Stolzenburg et al. 2003).

Following humidification, the air stream passes through V6 and is collected, or is diverted to the bypass line through solenoid valve V4. RH and temperature are monitored using an in-line RH&T probe (50y, Vaisala Inc., Woburn, MA) on the bypass line. The critical orifice on the bypass line is equivalent to the critical orifice on the sampling line, which creates a constant flow rate of 9 L/min and ensures a constant RH.

3.1.2 Sampling Modes: Ambient Aerosol / Filtered Ambient Blank / Zero Air Blanks

TAG has four modes of sampling: ambient aerosol, filtered ambient, zero air and filtered zero air. The latter three are different types of field and system blanks. Filtered ambient samples were used to detect any gas phase compounds collected on the walls of the CTD cell. These were performed most frequently, on an average of 5 times every 26 hours. Zero air samples were used to test for within-system contamination (i.e. zero air sample). Filtered zero air passed zero air through the filter used for the filtered ambient, and tested for gas phase desorption from that filter. These two types of zero air samples were performed consecutively, and were done less frequently.

The sampling mode is determined by the configuration of valves V1, V2 and V3. Following the cyclone, the sample stream can be sent directly through valve V2 (Fig. 3) to collect ambient PM_{2.5}, or through V3 and a Teflon membrane filter (Zefluor 2.0 μm, Pall Corp.) before collection in order to achieve a field blank. Clean air is delivered by a pure air generator (737, AADCO, Cleves, OH), and is introduced upstream of the humidifier by opening V1. The filtered ambient “blanks” are used to estimate the extent of gas-phase adsorption to the surfaces heated during thermal desorption, including the multijet impactor, impaction substrate, walls of the CTD cell and the tubing between valves V5 and V6. The particle and hydrocarbon free tests for contamination coming from within the system, such as desorption of chemical build up on the filter and impaction surface.

The system automatically cycles among the three modes of operation, to provide automated collection of each type of system blank interspersed among the ambient samples. SOAR used a 26-hour cycle time, with 5 filtered ambient samples interspersed after 2 to 4 ambient samples, and 1 zero air immediately followed by 1 filtered zero air. The 26-hour cycle was chosen so that the time of day of the filtered blanks varied. This cycle was interrupted for introduction of standards, as described in Section 3.2. For SOAR the compound abundances in clean air samples were below method detection limits. Compound abundances in clean air samples through the filter were kept below method detection limits by periodically replacing the filter used for the filtered ambient blanks.

3.1.3 Collection-Thermal Desorption (CTD) Cell

The CTD cell collects particles and then thermally desorbs them into helium (He) carrier gas that flows into the GC column. Details of the CTD cell have been documented by Williams et al., 2006. In preparation for the SOAR campaign, the CTD cell design was upgraded to facilitate in-situ field calibrations of TAG. A diagram of the new CTD cell can be found in Figure 4.

This new cell differs from that of the original TAG system by the incorporation of an injection port. An Agilent blunt-end microliter syringe is used to deliver liquid standards through a small ~3 mm OD septum in one arm of a 1/8" compression fitting tee. Injected standards are deposited near the impaction region of the CTD on the same kind of passivated surface on which aerosol sample collection occurs. A fixed volume of 5 μ l is used for all injections in order to ensure constant aliquot surface coverage inside the cell and reproducible droplet release from the syringe needle (see inset detail of Figure 4). This direct introduction of standards at the point of ambient sample collection is designed to mimic the complete analysis process including losses during purging of volatiles, surface release, transport through the transfer lines and heated 6-port valve, as well as chromatographic elution characteristics.

Cell injections are performed during the initial vented purge phase of an otherwise normal thermal desorption cycle. This minimizes solvent exposure of the chromatographic column while exactly following the protocol used for ambient sample analysis. During purging, He gas is passively split between three passages leading to the CTD, including the side-arm of the injection port tee. Approximately half of the flow is introduced upstream of the impactor jet to insure a steady stream across an ambient sample while the remainder of the purge flow is nearly equally split between the downstream and injection ports of the cell. Typically, He flow is 50-100 cc/min during the purge before switching to the 2 cc/min carrier gas delivered to the GC column during the thermal desorption phase. System flow path and valve sequencing details can be found in Figure 3.

During in-situ automated sampling, aerosols are typically impacted onto the collection substrate at a temperature of 30 °C for 30 minutes. After collection, the upstream ball valve V6 closes off the input air flow and V5 closes off the output end of the CTD cell. As the CTD cell ramps from 30 °C to 50 °C, solenoid valves V7, V8, and V9 open to purge with He any water vapor adsorbed to surfaces. If a large amount of H₂O entered the GC, then it would interfere with the chromatography. Some of the most volatile compounds (30 °C < boiling point < 100 °C) will be purged along with H₂O. This sets the upper vapor pressure limit for organic compounds analyzed by this technique. However, it is our goal to collect as many marker compounds as possible while maintaining consistent chromatography. To reach this goal, compounds with very low boiling points (i.e. < 100 °C) and extremely high boiling points (i.e. > 500 °C) will not be analyzed.

After approximately 5 min of purging at 50 °C, the 6-port valve (Valco Instruments Co. Inc.) is switched to transfer He through the CTD cell and into the GC column. The organic compounds in the collected sample are desorbed by heating the CTD to 300 °C at a rate of approximately 30-40 °C/min. The sample transfer lines and the 6-port valve are also heated to 300 °C. During desorption, the GC oven is held at 45 °C to refocus the sample onto the head of the column. Following desorption, the system is switched back to the sampling and analysis configuration, simultaneously allowing GC/MS-FID analysis of the current sample, and collection of the subsequent sample to proceed. More information regarding the desorption process is provided in the following *Thermal Desorption and Transfer Efficiency* section.

3.1.4 Gas Chromatographic Separation

Chromatographic separation of the analytes is achieved using a Hewlett-Packard (HP) 6890 GC equipped with a Rtx-5MS column (30 m, 0.25 mm i.d., 0.25 μm film thickness; Restek Corp.). The temperature program for the GC oven starts at 80 °C with an immediate drop to 45 °C and held for 12 minutes during sample injection, increases 8.5 °C/min to 300 °C, and holds at 300 °C for 7 minutes. This GC method is typical of published analytical protocols for speciated organic aerosol analyses (Yue and Fraser 2004a; Fine et al. 2001; Nolte et al. 1999). The oven then returns to 80 °C in preparation for the next run. The GC oven temperature cycle is temporally minimized by starting and ending each run at 80 °C.

Compounds eluting from the column are split between the flame ionization detector (FID) and mass selective detector (MSD) to provide simultaneous mass spectra identification and FID quantification. The carrier He (UHP further purified of oxygen, moisture, and hydrocarbons using traps from Restek Corp.) is kept at a constant head pressure of 25 psi, with a constant 75 % split to the MSD and 25 % to the FID.

3.1.5 Mass Selective Detection (MSD) and Flame Ionization Detection (FID)

A 70 eV electron impact (EI) ionization, quadrupole mass selective detector (5973 MSD, HP) is operated in total ion scan mode (29-550 m/z) to collect full mass spectral signatures for compound identification. Compounds are identified by matching MSD ion fragment patterns for each resolved peak to compounds found in mass spectral databases or to authentic standards when available. A flame ionization detector (FID), widely utilized for its linear detection of organic compounds (e.g. Goldstein et al. 1995), is also used to provide additional quantification capability. Calibration curves for several compound classes (polar and nonpolar) were obtained by manual injection of multi-component standards prepared by the Wisconsin State Laboratory of Hygiene. Examples are presented in the following *Instrument Evaluation* section.

3.1.6 Instrument Automation and Data Acquisition

TAG is fully automated for unattended field operation. Valve array (V6, V7, V8, V9), the 6-port valve, the CTD cell T1 cartridge heater, and T2 heating tape are controlled through the GC via auxiliary output circuitry. The PC controlling the GC is interfaced with a CR10X datalogger (Campbell Scientific Inc.), which is also triggered via GC auxiliary output circuitry at the start of each analysis. Valve array (V1, V2, V3, V4, V5), the CTD cell box cooling fan, and T3 heating tape are switched at the appropriate times during the sampling cycle by a relay module (SDM-CD16AC, Campbell Scientific Inc.) controlled by the datalogger.

All temperature zones are controlled by PID controllers (CN1166 Series, Omega Engineering Inc.) capable of 16 segments of preprogrammed temperatures triggered by the previously mentioned methods. Actual temperatures are measured using K-type thermocouples (Omega Engineering Inc.). Sample flow is monitored using a Mass-Flo Meter (MKS Instruments Inc.), and pressure is monitored downstream of the CTD cell using a pressure transducer (Honeywell Data Instruments). Relevant engineering data (i.e. time, temperatures, flow rates, pressures, etc.) for each sampling interval are recorded by the CR10X datalogger with an AM416 multiplexer (Campbell Scientific Inc.), then uploaded to the PC and stored with the associated chromatographic data.

3.1.7 Data Reduction and Analysis

Chromatogram integrations are done using HP ChemStation (G1701AA Version A.03.00) software.

Mass spectra are identified using the Palisade Complete Mass Spectral Library (600K edition, Palisade Mass Spectrometry, Ithaca, NY) for EI quadrupole mass spectral matching of 495,000 unique compounds using 606,000 available mass spectra. All subsequent data processing and QA/QC is performed using routines created in S-Plus 6.2 (Insightful Corp.) and RS/11 5.3 (Domain Solutions Corp.).

Particle source apportionment was performed using positive matrix factorization (PMF) to separate TAG marker organic compounds into time-covarying groups that represent multiple independent sources or transformation processes of aerosols arriving at the study site. PMF was applied using EPA PMF 1.1, which is based on the multilinear engine ME-2 [Paatero, 1999]. Compound integrations were completed using single ion abundances on the MSD. With a goal of minimizing data uncertainty, drift-corrected relative response timelines were used as the input parameters for PMF analysis.

3.1.8 Instrument Evaluation: Methods

Critical aspects of TAG instrument performance have been evaluated in the laboratory. Here we describe testing methods used for (1) the particle collection efficiency within the CTD cell, and (2) the system reproducibility for collocated sampling.

3.1.8.1 Particle Collection Efficiency

Particle collection efficiencies were measured using monodisperse particles generated by nebulization and mobility selected by means of a high-flow differential mobility analyzer. Upstream particle number concentrations were measured using a TSI 3760 condensation particle counter (CPC). Downstream concentrations were measured using an aerosol electrometer adapted from a TSI Model 3020 EAA, through which all of the flow from the cell was directed. This approach had the advantage of providing a direct measure of the total charge flux associated with aerosol escaping collection, but requires high concentrations and correction for doubly charged aerosol. Efficiency measurements were also made using a pair of Model 3760 CPCs, one upstream and one downstream. The downstream CPC was operated at low pressure, with a bypass flow to account for the difference in impactor and CPC flow rates, and with an auxiliary magnehelic installed in the CPC pressure balance line to ensure that the instrument was not flooded during pump down. For both configurations, the downstream concentration values were compared to that obtained by passing the aerosol through a “bypass” orifice with the same flow rate and a straight path to the downstream particle counter. Simple ball valves directed the flow either through the CTD cell or through the bypass orifice.

3.1.8.2 Reproducibility for Ambient Sampling

Reproducibility for identifying and quantifying individual compounds in ambient aerosol samples was tested using simultaneous off-line collection of multiple ambient aerosol samples in parallel onto glass collection boats. Collection was done in Berkeley, CA in the vicinity of an interstate highway. Following collection, sample boats were sequentially inserted into the CTD cell mounted on the GC/MS-FID for thermal desorption and analysis.

Our sampling configuration consisted of 3 CTD cells operated in parallel with a fourth CTD cell used as a vapor adsorption blank. The fourth cell was immediately preceded by a Teflon filter, but otherwise operated for the entire sample time identical to the other CTD cells. All four cells were mounted downstream of a PM_{2.5} cyclone, and their sampling rates were determined to be within 10 % of each other. Glass sample substrates were prepared by solvent washing and baking in an oven at 400 °C for two hours, then stored and refrigerated in aluminum lined Petri dishes until used for sample collection.

Samples of 1 m³ ambient air were collected. The reproducibility for quantifying individual compounds in ambient air samples can be assessed from these triplicate samples.

3.1.9 Instrument Evaluation: Results

3.1.9.1 Particle Collection Efficiency

Particle collection efficiencies were measured using oleic acid, a non-bouncy liquid particle, and potassium chloride, a solid particle below its deliquescence point of 84 % RH at 25 °C. For the potassium chloride tests the air stream was humidified to 60-70 % RH, as is done in the TAG system under normal operation. Results obtained using a CPC to count particles penetrating the cell are shown in Figure 5. The 12-jet impactor displays a particle size cutpoint (particle size at which 50 % collection efficiency is achieved) of $D_{50} = 0.085 \mu\text{m}$ for oleic particles. This is considerably higher than that obtained with a single-jet impactor of the same diameter, indicating cross-flow interference among the jets. These results led to the design of the 9-jet impactor, with more widely spaced jets. The 9-jet impactor displays a particle size cutpoint of $D_{50} = 0.065 \mu\text{m}$ for oleic particles and $D_{50} = 0.085 \mu\text{m}$ for the more bouncy potassium chloride particles. Particle collection efficiency exceeds 90 % on both impactors for all particles larger than 0.17 μm .

Oleic acid aerosol calibrations were also done using an electrometer for downstream counting. This approach has the advantage of not requiring the flow split below the cell needed for the CPC counting method, but is not sensitive enough for measurements at larger particle sizes where concentrations are small. Calibrations done with the electrometer method yielded similar cutpoints, within 0.05 μm , to those obtained by the CPC counting method.

3.1.9.2 Reproducibility for Ambient Sampling

Figure 6 shows a scatter plot of peak areas for a selection of largely nonvolatile compounds measured between the first of these triplicate samples on the x-axis and the other two on the y-axis. Some variability between the peak areas scales linearly indicating slight differences in sample size, but nearly identical relative responses. Relative standard deviations for measurements of individual compounds in the triplicate samples ranged from 0.04 to 0.33 for 11 selected representative compounds (not present in the vapor adsorption blank) with a pooled standard deviation of 0.12, and reproducibility for the majority of these compounds was better than 10 %.

3.1.10 Instrument Summary

TAG is the first continuously operating automated gas chromatography instrument to be successfully used for measuring hourly in-situ organic aerosol chemical speciation. The sampling and data acquisition process are fully automated, allowing around-the-clock operation. The system efficiently collects particles in the 0.06 to 1.5 μm size range, and efficiently transfers organic compounds via thermal desorption into the GC with quantitatively reproducible results.

While our focus is to use individual organic marker compounds to determine aerosol sources and transformations, and not to characterize the entire chemical makeup of the aerosol, it is still of interest to increase the number of marker compounds measured by TAG. Many of the organic compounds of interest in the ambient aerosol are oxygenated and polar, and are not completely eluted through GC columns. For example, dicarboxylic acids are typically not completely eluted. Often polar compounds are derivatized prior to GC analysis to increase their transmission efficiency through analytical instruments. However, our results show recovery of underivatized monocarboxylic acids and other functionalized compounds in thermally desorbed standards (see Table 2 and Table 1 of Appendix A).

Field measurements with TAG in a variety of environments will provide higher time resolution data than has previously been available for speciated organics in aerosols, opening new windows into the study of their origins, chemistry, fate, and impacts on the environment and human health. TAG's first field deployment occurred as part of the ICARTT 2004 campaign in Nova Scotia, and is described in detail by Williams et al. (2007). Deployment in Riverside as part of the SOAR was TAG's second field campaign.

3.2 Calibration and Quantification

This work includes the extension of TAG measurements into the quantitative realm. During the Riverside field deployment, the TAG system was systematically calibrated with various organic standards mixtures introduced directly into the aerosol collection cell. We address here the protocol used for these calibrations, and how the calibration data are applied to ambient TAG measurements. Our objective in these calibrations was to provide the data necessary to correct for slow drifts in instrument response, and to assess concentration-dependent response factors for a variety of compounds, without overly consuming operational time.

We specifically address the following questions regarding TAG quantification:

- How stable is the TAG system over the period of a multi-week study?
- Can MS detector drift be corrected adequately without an internal standard for each sample?
- What is the precision of measurements with injection based calibrations?
- How can a wide range of compounds be quantified with limited standards?
- How do indicated concentrations compare with the range of published values from prior filter based measurements?

The analysis presented here focuses on n-alkanes and polycyclic aromatic hydrocarbons, two classes of compounds that are regularly generated by primary emission sources (Schauer et al. 1996). PAHs are primarily linked to incomplete vehicular combustion and are of inherent interest because of their suspected mutagenicity and carcinogenicity (EPA, 2002). The aliphatic alkane series is ubiquitous in the atmosphere with both anthropogenic and biogenic sources and the biogenic contribution level is often estimated through the observed odd-carbon number preference (Simoneit and Mazurek 1982). Because of their relatively low polarity, these classes of compounds pose less difficulty for reproducible chromatography than many other classes of observed compounds, and therefore allow simpler data treatments.

3.2.1 Experimental Methods

3.2.1.1 Authentic standards

During the Riverside study, 11 distinct sets of authentic standard mixtures were employed, including more than 200 compounds providing measurable responses. Here we discuss in detail three sets of these standards, as listed in Table 1. These include (1) a tracking standard consisting of a custom multi-class mixture of compounds obtained from the Wisconsin State Laboratory of Hygiene, (2) an n-alkane windowing standard (Alkane) covering the carbon number range of C₈-C₄₀ obtained from Accustandard (#DRH-008S-R1) and (3) a 116-compound semi-volatile aromatic mix (PAH) obtained from Cerilliant (EPA Method 8270c, #ERS-026). Standards were stored at < 0 °C in original sealed ampules until injection samples were prepared by dilution and transferred to amber mini-vials with hard caps for

storage or septa caps for injection use. Injection vials were removed from the freezer approximately 30 minutes prior to each injection to allow thermal equilibration.

Reagent and HPLC grade solvents were obtained from VWR, Sigma-Aldrich and Fisher Scientific at 99.5% to 99.9% purity levels. Because of the initial purging of volatile species, solvent blends were chosen for each standard's dilution to match the solubility of each standard's solvent base but minimize toxicity for field use. Toluene was substituted for benzene in the field preparations for the custom tracking standard and toluene plus acetone replaced methylene chloride plus benzene in the EPA standard. The alkane standard was diluted with chloroform, the original solvent base for this standard. Dilution ratios ranged from a low of 25:1 for an organic acid mix and a high of 6400:1 for the tracking standard during limits of detection measurements. On column mass levels per compound ranged from ten's of nanograms to 10's of picograms, respectively. Reagent grade solvents used do not contain measurable quantities of compounds analyzed during SOAR with 5- μ l injections so that liquid solvent blanks were not necessary. The appearance of cross-contamination between standards is obvious and did not occur during either study period.

3.2.1.2 Assessment of precision and limits of quantitation

Compound precision was measured through four repeated injections of 5 μ l injections of the tracking standard each immediately followed by a normal thermal desorption analysis. The single ion peaks from the MSD were integrated and compared across injections. The resulting relative standard deviation (RSD) of these peak areas is taken as a baseline or minimum precision of the instrument response to sample injections for the representative compounds of the tracking standard.

Limits of quantitation (LOQ) for the tracking standard were obtained by injecting successive dilutions to determine at which point single ion peaks could no longer be distinguished from background noise. The specific dilution factors used were 2, 4, 8, 32 and 64 relative to the standard concentration level used for tracking purposes. A single compound LOQ is defined here as the geometric mean mass of the lowest concentration with an easily quantifiable single ion signal and the next lower dilution level without a quantifiable signal. This operational definition is more stringent than the usual 3-sigma definition of limit of detection based on instrument noise.

3.2.2 Calibration Methodology

The calibration protocol utilized two categories of standards (Table 1): (1) a single tracking standard consisting of a mixture of several compound groups and (2) multiple auxiliary standards, each of which represents a single family of compounds. Importantly, many of the auxiliary standards contained at least one compound also found in the tracking standard. These overlapping compounds determine relative response factors to connect the tracking standard response to the auxiliary standard calibrations.

For the summer (fall) field study a total of 58 (64) distinct standard injections were performed. Of these, approximately one-half were of the tracking standard and the remainder spread across the other standard sets. The tracking standard injections performed on a nearly daily basis were used to drift correct the instrument and provide a time-independent calibration for each study period. The majority (80% in summer, 90% in fall) of these were done at consistent level to gauge changes in instrument response. Multi-point calibrations with the tracking standard were done on 2 days in the summer and 3 days in the fall. Three point calibrations were done with the EPA Method 8270c standard, once in the summer and twice in the fall. The alkane windowing standard was run at two levels in the summer and fall.

The tracking standard (TS) was regularly injected at a fixed concentration level and used for gauging both absolute system response and system drift. On two days in the summer and three days in the fall, the TS was introduced at multiple levels to establish calibration curves and LOQs. Auxiliary standards were used to positively identify compounds by retention times and were injected less frequently. This protocol was designed to maximize the calibration information while minimize the time TAG was not acquiring ambient air samples. For each calibration point, an ambient or field blank data point is missed cutting into the temporal resolution of the instrument.

The quadrupole mass spectrometer was tuned at the outset of each study period using the internal perfluorinated calibrant, PFTBA, and then allowed to run continuously without retuning for the 4-week field campaigns. Re-tuning during the course of a study would have required more extensive calibrations, and would have severely restricted the amount of time available for ambient sampling.

The repeated (near daily) fixed concentration TS injections were used to quantify the long-term drift in system response during each 4-week study period. For each of the compounds found in the TS, all of the data (standards and ambient) were corrected based on the measured change in system response to the fixed concentration TS injection data. We refer to this correction as “de-trending” that provides a system response in the absence of instrument drift.

For each of the two study periods, the de-trended TS data was then used to generate a single, time-independent, multipoint calibration curve for each compound in the TS. These resulting calibration curves were then applied to similarly de-trended raw ambient data. All MSD analyses were performed on single ion peak areas wherein the selected ion mass was chosen for maximum relative abundance and non-interference with co-eluting compounds.

For compounds found only in the auxiliary standards, we assessed the response relative to a compound that is common to the auxiliary and tracking standards. This reference or cross-over compound provides a relative response factor that is applied to the calibration curve for the reference compound, extending quantification to all of the compounds common to both standards. Specifically, the ambient data for compounds found in the auxiliary standard not-present in the TS are de-trended in the same manner as for the cross-over TS compound, and then reduced using the calibration curve for latter multiplied by the relative response factor. This assumes a similar concentration-dependent response for the two compounds. Thus care is taken to use an appropriate concentration level for assessing the relative response factor. Also, we note that the determination of the relative response factors is aided by the fact that all compounds in the auxiliary standard are at the same concentration level. To date we have not fully addressed the quantification of compounds in the auxiliary standards that do not contain a compound common with the tracking standard.

3.2.3 Calibration and Quantification Results

The tracking standard injection data were used to accomplish four important system evaluation and data reduction functions:

- Measure in-situ calibration precision through repeat injections at fixed levels
- Determine limits of quantification by response to serially diluted injections
- Assess MSD drift over time using fixed-level injections approximately 1/day
- Determine time-independent calibrations for select authentic compounds

3.2.3.1 Precision and LOQ

The baseline precision results obtained from four repeated injections of the tracking standard are presented in Table 2. For the non-polar compounds used in this treatment (shown in grey), the relative standard deviations ranged from 1.1% (cholestane) to 3.8% (hexadecane), thus demonstrating the excellent repeatability achievable with the CTD based injection port. For the two least volatile compounds, cholesterol and hexatriacontane, the relative standard deviations were 8.8% and 15%, respectively, indicating that the reduced sensitivity (higher LOQs) of these compounds affected the reproducibility. Lowest precision (23%) was obtained for decanoic acid, a compound known to have poor reproducibility in GC work without derivitization.

LOQs range from 0.02 ng for cholestane to 7 ng for hexatriacontane (right most column of Table 2). This conservative measure of system response is higher than a limit of detection often defined as 3 times noise level and includes non-linear effects of the thermal desorption sample introduction system (i.e. adsorption site density throughout the heated transfer line pathway). Figure 7 demonstrates a linear correlation exists between the precision of repeat injections and the LOQ of individual compounds. Plotted are the RSD values for the less-volatile set of compounds (i.e. excluding those that elute prior to hexadecane) versus the ratio of LOQ to the injection mass level for that compound. For either smaller LOQ or larger injected mass levels or both, the precision improves and the RSD is observed to decrease. The minimum or baseline precision of the injection based calibrations may be inferred from the intercept of the regression line ($R^2=0.99$) to be 1.3%. Conversely, to maintain injection precision below 15% towards calibrating a collected analyte requires a sample size greater than $2.9 \times \text{LOQ}$ for that analyte based on the regression. For example, calibrating octacosane (LOQ=.15 ng) at a baseline precision level of 15% would require an injection mass level of 0.44 ng on column. For a 30-minute sample collection period, this mass corresponds to an ambient concentration of 1.7 ng/m^3 , a reasonable atmospheric level for this compound (see discussion of ambient timeline below).

3.2.3.2 System stability and drift corrections

Temporal trends in TAG response were obtained during the fall study by examining 19 separate injections of the tracking standard that spanned 22 out of the 30 days in the fall period. Figure 8 shows the relative system response for the four TS compounds, cholestane, eicosane, octacosane and chrysene as a function of time for the fall dataset. For purposes of inter-comparison, each compound's single ion peak areas have been normalized by the study average response for that compound. The distinct symbols are results from three different calibration solutions that were used during the course of the fall study.

For all four compounds, the MSD data for the fall show a steady decline in response over the study with total relative response changes ranging from -43% (chrysene) to -54% (cholestane). Notably, eicosane and octacosane exhibited essentially the same study-wide decline of -45% and -46%, respectively, as might be expected given that the same ion (57 m/z) was used for both integrations. Some of the compounds, e.g. chrysene, exhibit much greater variability on a time scale of days that is evidently superimposed on the downward trend observed in all compounds.

In contrast to the MSD data, the FID data for cholestane shows no trend across the study, with a regression slope less than 1/10 that of the MSD, and not significantly different from zero ($R^2=0.079$). The lack of a similar trend with the FID establishes that the main source of change in response for TAG stems from the MS detector itself. Co-elution interferences prevented similar analyses of FID response on the other compounds.

The MSD drift for the fall is assessed by linear fits to the data of Figure 8. Even though systematic changes across all compounds are evident for the individual injections, the density in the time series data permits only a linear regression for the trend analysis. The first set of data (triangles) used a relatively older standards solution with less reliable concentrations and so was excluded from the trend analysis. Results of the linear fits are shown on graphs. Coefficients of determination range from 0.53 (chrysene) to 0.88 (cholestane). These regression lines are used to correct the raw data for the detector drift. This correction or “de-trending” is applied to both the calibration and ambient data, in accordance with the relation:

$$y_s(t) = \frac{y'_s(t)}{G_s(t)} \quad (1)$$

where y'_s is the raw MSD signal (ion area) for compound s in the TS. The de-trending function $G_s(t)$ is given by the linear regression

$$G_s(t) = A \cdot t + B \quad (2)$$

where A and B are the slope and intercept values, respectively, shown in Figure 8 except for a normalization factor applied to the coefficients for presentation purposes. For a given time t , the value of G_s varies with compound with a range relative to each compound mean from near 1.4 at the beginning of each study period to near 0.7 towards the end, or a factor of two decrease in response.

Similar trend results were observed for the summer SOAR data, where 20 TS injections were made over a period of 25 out of 28 days total for that campaign. Figure 9 shows the resulting trends where symbols represent different dilution levels used with the tracking standard (either 200:1 or 100:1 from stock). The 200:1 data during the first week were corrected to a 100:1 level by application of a preliminary calibration curve to the concentration ratio of two (i.e. scalar factor= 2^{b_s} , where b_s is the exponent of the power law, see following section for details). A similar downward trend to that observed with the fall data is detected with the MSD data from the SOAR data, but with a larger range of maximum changes in relative response of -15% (eicosane) to -69% (chrysene). As with the fall dataset, the FID signal for cholestane shows an insignificant decrease in response over the majority of the study period.

One notable difference between the two study periods is in the consistency in alkane trends for the fall relative to the alkane trends in the summer. While the fall dataset possess trend slopes for eicosane and octacosane that are equal to each other, the same trends in the summer differ by nearly a factor of three. This difference may be partly due to the greater scatter in the data and the use of a mixture of two concentration levels with the necessary re-scaling of the more dilute data (triangles). An examination of the more volatile compound hexadecane for the summer showed no downward trend within limits of uncertainty (slope = $-5.1 \times 10^{-5} \pm 4.4 \times 10^{-4}$ with 90% confidence intervals). Therefore, other unidentified factors affecting the overall instrument response beyond the MSD drift were affecting the more volatile alkanes. Treating these compounds on an individual basis is necessary for the summer dataset, whereas the alkanes C_{16} to C_{28} in the fall dataset possess trend slopes that differ at most by 11% and could be corrected similarly.

3.2.3.3 Time-independent, multi-point calibrations

Since TAG is operated near the detection limits for many individual compounds, the use of a non-linear calibration form is required. The functional form of the field calibration F was chosen to be a power law:

$$y_s = F[m_s] = a_s \times m_s^{b_s} \quad (3)$$

where y_s is the instrument response to the injected mass m_s for compound s . The calibration parameters a_s and b_s are obtained from least-squares fitting of the de-trended raw data after transforming to linear form through use of the natural logarithm.

Time-independent calibrations are formed from the de-trended responses to the selected TS compounds injected at multiple concentrations, as illustrated with the summer SOAR data in Figure 10. Here are shown both linear (dotted line) and power law (solid line) fits of the de-trended calibration data to demonstrate that the non-linear form is much better at tracking the data for lower concentrations. The figure insets show with expanded axes that extrapolations of the linear fits always miss the lowest level mass calibration data. In all cases, the R^2 values of the power laws are equal to or greater than the linear fit results. For two compounds, eicosane and chrysene, the linear fits are observed to be slightly closer to the data at the highest injection level but since ambient levels are at or below the 1 ng per sample level, or 4 ng/m³ equivalently, this distinction between the two functional forms at high mass loadings is not important.

The summer TS calibration is comprised of a 3-point set on 7/27, a 5-point set during the LOQ injections on 8/12 and finally a 3-point set on 8/13. The number of datum from the LOQ sequence of injections contributed to a compound's calibration set varies by the individual LOQs. All four of the compounds under discussion were detected at five dilution levels except for cholestane which was only observed at four levels.

The vertical spread in the normalized response data indicate the degree to which de-trending successfully removes systematic changes from detector drift. The highest level injection was made on all three calibration days and shows that points with the lowest response with a 16 day drift correction are comparable to the variation seen in the pair of datum taken 1 day apart. A small systematic under-correction in the de-trended data is detectable at this highest level of mass injection. The 7/27 data differed relative to the average of the data from 8/12 and 8/13 by +0.2%, -11%, -4.6% and -3.8% for cholestane, chrysene, octacosane and eicosane, respectively.

3.2.3.4 Relative response factors for *n*-alkanes and PAHs

Calibrations for compounds not present in the tracking standard were obtained from less frequently applied auxiliary standards (Table 1). Using compounds common to both the tracking standard and the auxiliary standards allows relating the response of all of the auxiliary compounds to that of the overlapping TS compound. A scaling relationship was constructed between the response of the cross-over TS compound within the auxiliary standard, y_s , and the response to the remaining compounds, y_i , as the simple ratio

$$R_{i,s} = y_i / y_s \quad (4)$$

This response factor was constructed to apply to the *n*-alkanes in the range of C₁₅-C₃₂ (Fig. 11) using the reference compound C₂₀. All single ion peak areas were computed for the alkanes using mass fragment $m/z = 57$. For the PAHs in the range of 3-5 fused aromatic rings (e.g. phenanthrene to benz(a)pyrene, Table 3) the response factor was generated using chrysene ($m/z=228$) as the reference compound. In these two standards all compounds were present in equal masses, and therefore it was not necessary to correct for variations in concentrations among compounds within the auxiliary standards.

3.2.3.5 Alkane response factors

Figure 11 shows relative response factors for the *n*-alkane windowing standard for the summer and fall

studies for several concentration levels referenced to eicosane (C_{20}) as a function of carbon number. A similar result would be obtained if boiling point or vapor pressure had been used instead of carbon number. Evident is a similar volatility window observed by TAG for these two periods with a slightly better response for the largest alkanes in the summer. Solid lines are locally-weighted least-squares smoothed (LOWESS) curves to be used for $R_{i,s}$.

The fall data show response factors at 1 ng per compound and at 3 ng per compound. Little difference in response factor is seen for these two injection masses. In the summer, two more-disparate levels were used: 1.3 and 10 ng. These data show a strong mass dependence at high carbon numbers, and a lesser dependence on the low carbon number side, with an overlap for carbon numbers near 20. The 10 ng level standards were done twice, with consistent results, while the 1.3 ng injection was performed only once and was co-injected with another standard at similarly low levels. However, the 1 ng level is closer to the range of concentrations measured in the ambient sample, and co-injection of standards that otherwise do not over-load the column is not expected to change the instrument's response. Also, the 1.3 ng summer data are closest to the 1-3 ng data from the fall. For these reasons we employ the response factor from the 1 ng level for both study periods.

The presence of over-lapping compounds between the TS alkanes and the auxiliary alkanes, allows for an independent measurement of two of the response factors, C_{16} and C_{28} , shown in Figure 11 by grey circles. The range bars represent ± 1 standard deviation of the TS data from the multi-point injection subset for the indicated average mass levels. A consistent discrepancy between these two approaches is observed, with the combined results from both factors from the two studies showing TS values on average smaller relative to the auxiliary standard by $24\% \pm 5\%$. This discrepancy is unresolved, and must be included as an uncertainty in the ambient concentrations derived therefrom.

3.2.3.6 PAH response factors

Response factors for a collection of PAHs present in the EPA method 8270c auxiliary standard were obtained during both study periods, as collected in Table 3. For the normalization, the average of benz(a)anthracene and chrysene was chosen because these compounds elute from the column without sufficient separation to allow consistent independent peak integrations to be performed. Similarly, the response factors for the two isomers benz(b)fluoranthene and benz(k)fluoranthene were combined. Response factors for 1 ng/compound injections are shown in columns three and five with the average responses for the entire range of injections levels given in columns four and six. The ranges of injection levels differed between the two study periods, with 1-8 ng and 1-3 ng employed in the summer and fall, respectively. The uncertainty for the 1 ng level response factors can conservatively be taken to be equal to the standard deviations obtained for the average responses over the stated ranges. As with the alkane response factors, independent information such as expected ambient concentration levels needs to be used to justify using the 1-ng results.

The m/z value for the chrysene analysis ion, 228, falls in the middle of the range of m/z values for the other PAHs listed in Table 3. The chrysene trend with time was used to correct these other compounds because it was observed that the drift dependence on ion mass is smaller than the dependence on compound class. This distinction can be seen by the example compounds shown in Figure 12 and the trends for other compounds not shown.

3.2.3.7 Application of TAG calibration

Application of the calibration results to the ambient aerosol data involves (1) identifying the compound

through mass spectrum and retention time matching, (2) pairing it with a TS reference compound, (3) integrating the single-ion peak area, (4) correcting for the time-dependent MSD drift during the study period according to the de-trending results of the chosen TS compound, (5) applying, if needed, the mass dependent relative response factor selected from the auxiliary standard and (6) using the calibration for the matched TS compound to obtain the absolute sample mass for the desired compound. Here we summarize this procedure in mathematical terms.

With an assumed linear drift in the MSD data, we correct the temporal variation of TS compound s by the linear regression de-trending function of time $G_s(t)$ as described above. The de-trended calibration data, given by Eq. (1), is used to construct a time-independent function of system response and time given by Eq. (3) which can be inverted to obtain mass as a function of system response. If the compound is a member of the auxiliary standards, the relative response factor $R_{i,s}$ given by Eq. (4), is used to convert the expected response to compound i from that of the TS standard s .

To apply the resulting calibration relationship, raw TAG responses for compound i , $y_i(t)$, are first de-trended just as with the calibration data to form $y'_i(t)$. Then the calibrated TAG response for compound i , is obtained from the inverse function F_s^{-1} given by Eq. (3) in conjunction with the scaling response factor $R_{i,s}$ to obtain:

$$m_i(t) = F_s^{-1}[y'_i(t)] = \left(\frac{y'_i(t)}{aR_{i,s}} \right)^{1/b} = \left(\frac{y_i(t)}{aR_{i,s}G_s(t)} \right)^{1/b} \quad (5)$$

When calibrating a compound present in the tracking standard, $s \equiv i$ and $R_{i,s} = 1$ so that the calibration simplifies to:

$$m_s(t) = \left(\frac{y_s(t)}{aG_s(t)} \right)^{1/b} \quad (7)$$

Dividing these quantities, $m_i(t)$ or $m_s(t)$, by the sample volume (typically 0.25 m^3 for a 30 minute sample) gives the resulting ambient mass concentration.

3.2.3.8 Application to Riverside ambient measurements

The analysis of the Riverside measurements focuses on two, two-week periods, July 29 – August 8 (summer) and November 4 – 14 (fall). During each of these periods 300 compounds were identified and tracked with the TAG system. Similarly, the value of the field blanks, associated with gas-phase adsorption, were obtained for each of these 300 compounds throughout the study periods. However, calibration standards described above encompassed only a portion of these compounds. From these calibration standards we are able to assess the MSD drift, as defined by equation (2), for the entire set of 300 compounds, providing drift-corrected, field-blank subtracted relative concentration time lines for the PMF analysis, as described in Section 4.

Ambient mass concentrations (ng/m^3) are reported for those species for which calibration standards, or calibration surrogates were measured. In advance of the field study, it was not possible to identify the entire set of compounds that were to be measured. Nor was it possible to obtain authentic standards for many of the compounds identified. Thus the compounds for which absolute hourly concentration values

are reported is much smaller than the list of compounds for which relative concentrations were obtained. The data set of quantifiable compounds is restricted to those species that (1) were present in the tracking standard or in one of the authentic standards, or quantifiable through a surrogate compound with a known relative response factor, (2) were found at concentration levels spanned by the multipoint calibration curves (3) exhibited a drift in response to standards consistent with a linear decrease in sensitivity of the MSD, and (4) possessed a correctable gas phase contribution. A set of 20 compounds including 13 alkanes (C₁₉-C₃₁) and 7 PAHs (3 to 5 rings) were quantified based on the multipoint calibrations from authentic standards (Table 3), the relative response factor to a surrogate compound in the tracking standard, and the measured MSD drift of that surrogate compound, as measured by the tracking standard. An additional two hopane compounds were quantified based on post-field assessment of the relative response factors to cholestane, a similar compound in the tracking standard. Finally, the data were corrected for the gas phase adsorption based on the data from filtered air blanks interpolated to the time of the ambient measurements.

For each ambient and field blank data point, the uncertainty is calculated by propagation of errors based on the uncertainty in the drift-corrected, multipoint calibration fit factors and the uncertainty in the drift-corrected peak areas. Because the multipoint calibrations span the study period, and because the drift correction is applied prior to the derivation of the multipoint calibration curve, the uncertainties associated with the scale factor and the exponent coefficient in equation (3), implicitly contain the uncertainty associated with the drift correction. Corrections for the field (filtered air) blank were applied after reducing both the field blank and ambient data sets to concentrations values, with a corresponding propagation of the uncertainty values associated with each. The final data set gives the field-blank corrected ambient aerosol concentration and the uncertainty associated with each data value.

Summary statistics for this set of calibrated compounds are given in Table 4 for summer and fall. Shown are the intensive period mean, standard deviation and measured, blank-subtracted, aerosol concentrations. For these compounds, which are generally associated with primary sources, the ambient concentrations were higher during the fall study. Table 4 also shows the mean contribution to the total (gas + particle) TAG signal attributed to gas phase adsorption, as measured by the filtered air blanks. The gas phase signal scales with the compound volatility, but shifts with season. In the summer period the C₂₆-C₃₁ alkanes were seen almost entirely in the aerosol phase, while in the fall the purely aerosol compounds included C₂₄-C₂₅ as well.

Example data for the eleven day period of November 4 to 15, 2005 from the SOAR field study are shown in Figure 12. The octacosane and chrysene data were reduced by direct application of the tracking standard calibrations using Eq. (7) since these compounds are in the tracking standard. The two identified hopanes summed in the time series, 17 β (H)-28-norhopane and 17 α (H), 21 β (H)-hopane, were calibrated using the closest TS compound available, cholestane, with a relative response correction of 1.25 and 0.79, respectively, based on subsequent co-injections of an authentic standard with these hopanes plus 5 α -cholestane.

The data of Figure 12 illustrate the hourly variability in the observed atmospheric concentrations. Diurnal patterns are apparent, especially the morning and evening peaks in all of these primary emission compounds. Note that this variability is on a timescale that would be missed entirely with a 24h integrated sample and greatly obscured with even 6-hour samples. The day to day variability, moreover, is much smaller than the diurnal variability so that the higher time resolution afforded by TAG can lead to improved source apportionment analyses.

The range of values shown in Figure 12 is comparable to previously published values for these compounds. The average concentration of the two hopane sum measured by TAG was $0.2 \pm 0.2 \text{ ng/m}^3$ as compared to the most recent published value of approximately 0.2 ng/m^3 measured in Riverside during a 1-week period in January 2003 (Fine et al. 2004b). The chrysene average measured by TAG was $0.44 \pm 0.43 \text{ ng/m}^3$ as compared to an annual mean value of $0.032 \pm 0.033 \text{ ng/m}^3$ reported for Riverside over the May 2001 – July 2002 period (Eiguren-Fernandez et al. 2004). The octacosane average measured by TAG was $2.3 \pm 1.5 \text{ ng/m}^3$, a reasonable ambient level but for which no recent published values for comparison could be found.

3.2.4 Calibration and Quantification Summary

Because TAG is an on-line instrument, the allotted time used for the analysis of standards must be carefully balanced with the time for ambient measurements. A protocol was therefore devised utilizing a single tracking standard in combination with several auxiliary standards. The tracking standard contains a range of compounds, including several alkanes, aromatic hydrocarbons, a sterane, and several organic acids. This standard was injected at fixed concentration levels on a nearly daily basis, and was used to correct MS and system drift. Additionally, multipoint calibrations with the tracking standard and the most common auxiliary standards were done on one to three days of each one-month study period. Other auxiliary standards were applied less frequently, and at only one or two concentration levels. Analysis of ambient data for compounds in the auxiliary standards was done by evaluating the relative response to a “reference” compound present in both the tracking standard and the auxiliary standard.

Analysis of the tracking standard data show a consistent drift in the system response throughout each study period, that was well-represented by a simple linear fit over time. Comparison of the MSD and FID data for cholestane showed that this drift was attributable to the mass spectrometer. After correcting this linear drift, we find that for each compound a single multipoint calibration curve could be used to represent the system response over the entire study period. Near the detection limit, this response was best represented by a power law. Analysis of an n-alkane windowing standard showed a systematic carbon number dependence for the response relative to C_{20} . Ambient data reduced using these calibrations yield concentrations for alkanes, PAHs and hopanes within the range of that reported by other investigators for this air basin.

For compounds for which appropriate authentic standards were not available, the tracking standards provide a means to correct for MSD drift. Because the observed MSD drift was similar among most compounds measured, this was assumed to apply to other compounds for which standards were not available (see section 4). The removal of instrument drift, an integral part of the calibration procedure, provides a useful advance in itself when compound timelines are to be used in receptor modeling, as described below.

3.3 Gas Phase VOC measurements

The gas phase volatile organic carbon (VOC) measurements were set up to measure a wide a range of compounds. This system has been used in many field campaigns and has been described in the peer reviewed literature (Millet et al., 2005; Millet et al., 2004). The description below is taken directly from Millet et al. (2005). In the SOAR deployment two separate measurement channels were used, equipped with different preconditioning systems, preconcentration traps, chromatography columns, and detectors. Channel 1 was designed for preconcentration and separation of C_3 - C_6 non-methane hydrocarbons,

including alkanes, alkenes and alkynes, on an Rt-Alumina PLOT column with subsequent detection by FID. Channel 2 was designed for preconcentration and separation of oxygenated, aromatic, and halogenated VOCs, NMHCs larger than C₆, and some other VOCs such as acetonitrile and dimethylsulfide, on a DB-WAX column with subsequent detection by quadropole MSD (HP 5971).

Air samples were drawn at 4 sl/min through a 2 micron Teflon particulate filter and 1/4" OD Teflon tubing (FEP fluoropolymer, Chemfluor) mounted on top of the laboratory container. Two 15 scc/min subsample flows were drawn from the main sample line, and through pretreatment traps for removal of O₃, H₂O and CO₂. For 30 minutes out of every hour, ambient air was sampled and the subsamples flowed through 0.03" ID fused silica-lined stainless steel tubing (Silcosteel, Restek Corp) to the sample preconcentration traps where the VOCs were trapped prior to analysis. When sample collection was complete, the preconcentration traps and downstream tubing were purged with a forward flow of UHP helium for 30 seconds to remove residual air. The samples were then injected by switching valves and heating the preconcentration traps rapidly to 200 °C, so the trapped analytes desorbed into the helium carrier gas and were transported to the GC for separation and quantification.

As non-inert surfaces are known to cause artifacts and compound losses for unsaturated and oxygenated species, all surfaces contacted by the sampled airstream prior to the valve array were constructed of teflon (PFA or FEP). All subsequent tubing and fittings, except the internal surfaces of the Valco valves were Silcosteel. The valve array, including all silcosteel tubing, was housed in a temperature controlled box held at 50 °C to prevent compound losses through condensation and adsorption. All flows were controlled using Mass-Flo Controllers (MKS Instruments), and pressures were monitored at various points in the sampling apparatus using pressure transducers (Data Instruments).

In order to reduce the dew point of the sampled airstream, both subsample flows passed through a loop of 1/8" OD teflon tubing cooled thermoelectrically to -25 °C. Following sample collection, the water trap was heated to 105 °C while being purged with a reverse flow of dry zero air to expel the condensed water prior to the next sampling interval. A trap for the removal of carbon dioxide and ozone (Ascarite II, Thomas Scientific) was placed downstream of the water trap in the Rt-Alumina/FID channel. An ozone trap (KI-impregnated glass wool; *Greenberg et al.* [1994]) was placed upstream of the water trap in the other channel leading to the DB-WAX column and the MSD.

Sample preconcentration was achieved using a combination of thermoelectric cooling and adsorbent trapping. The preconcentration traps consisted of three stages (glass beads/Carbopack B/Carboxen 1000 for the Rt-Alumina/FID channel, glass beads/Carbopack B/Carbosieves SIII for the DB-WAX/MSD channel; all adsorbents from Supelco), held in place by DMCS-treated glass wool (Alltech Associates) in a 9 cm long, 0.04" ID fused silica-lined stainless steel tube (Restek Corp). A nichrome wire heater was wrapped around the preconcentration traps, and the trap/heater assemblies were housed in a machined aluminum block that was thermoelectrically cooled to -15 °C. After sample collection and the helium purge, the preconcentration traps were isolated via closing a valve until the start of the next chromatographic run. The traps were small enough to permit rapid thermal desorption (-15 °C to 200 °C in 10 seconds) eliminating the need to cryofocus the samples before chromatographic analysis (following *Lamanna and Goldstein* [1999]). The samples were thus introduced to the individual GC columns, where the components were separated and then detected with the FID or MSD.

Chromatographic separation and detection of the analytes was achieved using an HP 5890 Series II GC. The temperature program for the GC oven was: 35 °C for 5 minutes, 3 °C/minute to 95 °C,

12.5 °C/minute to 195 °C, hold for 6 minutes. The oven then ramped down to 35 °C in preparation for the next run. The carrier gas flow into the MSD was controlled electronically and maintained constant at 1 mL/min. The FID channel carrier gas flow was controlled mechanically by setting the pressure at the column head such that the flow was 4.5 mL/min at an oven temperature of 35 °C. The carrier gas for both channels was UHP (99.999%) helium which was further purified of oxygen, moisture and hydrocarbons (traps from Restek Corp.).

Zero air for blank runs and calibration by standard addition was generated by flowing ambient air over a bed of platinum heated to 370 °C. This system passes ambient humidity, creating VOC free air in a matrix resembling real air as closely as possible. Zero air was analyzed daily to check for blank problems and contamination for all measured compounds.

Compounds measured on the FID channel were quantified by determining their weighted response relative to a reference compound (see *Goldstein et al.* [1995a] and *Lamanna and Goldstein* [1999] for details). Neohexane (5.15 ppm, certified NIST traceable $\pm 2\%$; Scott-Marrin Inc.) was employed as the internal standard for the FID channel, and was added by dynamic dilution to the sampling stream. Compound identification was achieved by matching retention times with those of known standards for each compound (Scott Specialty Gases, Inc.).

The MSD was operated in single ion mode (SIM) for optimum sensitivity and selectivity of response. Ion-monitoring windows were timed to coincide with the elution of the compounds of interest. Calibration curves for all of the individual compounds were obtained by dynamic dilution of multi-component low-ppm level standards (Apel-Riemer Environmental Inc.) into zero air to mimic the range of ambient mixing ratios. A calibration or blank was performed every 6th run. Chromatogram integrations were done using HP Chemstation software. All subsequent data processing and QA/QC was performed using routines created in S-Plus (Insightful Corp.).

3.4 Additional Measurements

A wide range of meteorological, radiation, trace gas and aerosol measurements were made during the SOAR campaign. The majority of data presented below was collected with our Thermal desorption Aerosol Gas chromatography (TAG) system. Our research group also measured a wide range of volatile organic compounds in the gas phase using our automated in-situ GC-MSD-FID instrument [*Millet et al.*, 2006]. Additional data included in this report was collected using an Aerodyne Aerosol Mass Spectrometer (AMS) which measures non-refractory PM₁ aerosol components (NR-PM₁) [*Allan et al.*, 2004; *Jimenez et al.*, 2003; *Jayne et al.*, 2000], and an Aerosol Time-Of-Flight Mass Spectrometer (ATOFMS) which produces detailed mass spectra of individual particles, detecting organic carbon functional groups, elemental carbon, sulfate, nitrate, metals, chlorine, ammonium, and more [*Noble and Prather*, 1996]. Other supporting measurements included: CO measured by nondispersive infrared absorption (TEI, model 48C), ozone measured using a UV photometric O₃ analyzer (Dasibi Inc., model 1008-RS), total organic carbon (OC) and total elemental carbon (EC) measured using an EC/OC monitor (Sunset Labs), photosynthetically active radiation (PAR) measured with a quantum sensor (Li-Cor Inc., model LI-190SZ), wind speed and direction by propeller wind monitor (R.M. Young Co.), and temperature and relative humidity were monitored on an RH&T probe (Campbell Scientific Inc., model HMP45C). For a complete overview of all the gas and particle measurements included in the experiment, please refer to the SOAR website (<http://cires.colorado.edu/jimenez-group/Field/Riverside05/>).

4. SOAR Results

4.1 SOAR Speciated Organic Aerosol Measurements

The data set produced consists of hourly measurements of 300 compounds during the summer and winter study periods. These compounds are identified using mass spectra and retention time matches. They include alkanes, branched alkanes, alkenes, polycyclic aromatic hydrocarbons, branched PAHs, hopanes, acids, phthalates, furanones, guaiacols, syringols, and other oxygenated compounds. Of those identified, we report ambient concentrations for 20 compounds based on calibrations derived from authentic liquid standards. For the remaining 280 compounds, relative concentrations are reported. Automated TAG sampling was set on a 26 hour cycle throughout the study, including 19 ambient aerosol collections, 5 filtered ambient samples, 1 zero air sample, and 1 filtered zero air sample.

4.2 Positive Matrix Factorization

Until recently, PMF has mainly been used for source apportionment analyses using trace elements, EC/OC, and inorganic ions as input [Jaekels *et al.*, 2007]. Organic marker compounds have not typically been used in PMF analyses since PMF requires a significant timeline of observations, which poses significant challenges and is labor intensive when acquiring organic molecular marker observations from quartz filters. Organic marker compounds have now been used in a PMF source apportionment analysis, but it required 2 years to collect the 120 samples used in the analysis [Jaekels *et al.*, 2007]. Over an 11 day focus period, TAG collected 164 ambient samples providing a sufficient timeline to be used in the PMF analysis. In this report we report PMF analysis for two of these focus periods, one in summer and one in fall, in order to explore seasonal differences in organic aerosol composition.

PMF is described briefly here, and a more complete description can be found in [Paatero, 1997]. EPA PMF 1.1 uses constrained, weighted, least-squares to complete a receptor model. The operator determines an appropriate number of sources (p) influencing concentrations at the receptor site, and linear combinations of the factors explain the observed concentrations of different species so that,

$$x_{ij} = \sum_{k=1}^p g_{ik} f_{kj} + e_{ij} \quad (1)$$

where, in our case, x_{ij} is the concentration in Riverside, CA for the j^{th} species during the i^{th} hour of study, g_{ik} is the contribution of factor k to the organic aerosol in Riverside during time i , f_{kj} is the fraction of factor k that is species j , and e_{ij} is the residual for the j^{th} species during the i^{th} hour of study. Here it is assumed that only the x_{ij} 's are known and that the contributions (g_{ik}) and the fractions (or profiles) (f_{kj}) are estimated. The model is constrained by assuming all contributions and mass fractions are non-negative [EPA PMF 1.1 User's Guide].

PMF analysis also requires an estimate of data uncertainty in order to weight profiles to favor data with smaller uncertainty. The user must specify a method detection limit (MDL) and a percentage uncertainty for each parameter included in the analysis. Uncertainty is then defined as:

$$\begin{aligned}
 s_{ij} &\equiv 2 \times MDL_j, \text{ if concentration} \leq MDL \\
 s_{ij} &\equiv \sqrt{(\text{percentage}_j \times x_{ij})^2 + (MDL_j)^2}, \text{ if concentration} > MDL.
 \end{aligned}
 \tag{2}$$

where s_{ij} is the uncertainty in the j^{th} species during the i^{th} hour of study. For the PMF results reported here, a 10% uncertainty for all input parameters [Williams *et al.*, 2006] and a MDL equal to 1/3 times the standard deviation of x_j has been used for each input parameter, creating the most stable model results observed over a range of estimated MDL values.

PMF works to minimize the sum of squares:

$$Q = \sum_{i=1}^n \sum_{j=1}^m \left(\frac{x_{ij} - \sum_{k=1}^p g_{ik} f_{kj}}{s_{ij}} \right)^2.
 \tag{3}$$

Three different Q values can be calculated. Q_{true} is the result of minimizing the sum of squares. Q_{robust} is derived in the robust mode, meaning that outlying values have been reduced to prevent their influence on the fitting of contributions and profiles. Finally, $Q_{\text{theoretical}}$ is calculated as the product of the number of input parameters (j) and the number of hours (i). If the model is appropriate for the input data, then Q_{robust} should be approximately equal to $Q_{\text{theoretical}}$.

EPA PMF also offers a bootstrapping tool combined with a rotational freedom method to estimate uncertainties in model results. The results of this test inform the operator of the robustness of the specific factors (profiles) defined by the original base case model by comparing these profiles to the profiles defined in a series of additional runs (bootstraps). Here, we use 300 bootstraps, all with random starting points, and match only profiles with correlations (r) > 0.6.

Only the particle-phase portion (= ambient – filtered ambient) of TAG compounds has been included in our PMF analyses. Since fewer filtered ambient (gas-phase) samples were taken than ambient (gas + particle) samples, information is potentially lost when interpolating the gas-phase timeline onto the ambient timeline. However, time resolution is lost by interpolating the ambient timeline onto the gas-phase timeline. As a solution, we have interpolated the gas-phase timeline onto the ambient timeline and have only included compounds in PMF analyses that meet the following requirements: compounds must on average be > 35% in the particle phase, to eliminate large subtractions, and each compound's particle-phase timeline must have a correlation > 0.7 with its ambient (gas + particle) timeline, indicating that most of the variability is conserved after subtracting the gas-phase portion.

4.3 Results

4.3.1 Drift Correction

Over the course of focus periods used throughout the remainder of this report, July 29 – August 8 (summer) and November 4 – 14 (fall), the average detector response drifted by approximately -18% during the summer study and -17% during the fall study (Table 5). The MSD drift appears to vary by compound (Table 5). It is estimated that biases introduced by appointing surrogate compounds for those not included in our chemical standards inventory will be larger than biases introduced by assuming a constant detector drift across all compounds. To avoid increasing uncertainty for PMF input data, we make the assumption that detector response drift is constant for all compounds, and apply a correction

for the average detector drift across the seasonal focus periods for all compounds. A sensitivity test using zero detector drift derived the same source types as those derived using seasonal average detector drifts.

4.3.2 Compound Identification

Chromatograms obtained in Riverside, CA consist of the most complex matrix of organic compounds seen by the TAG instrument to date. Many compounds have been identified using mass spectral and retention time matches with authentic standards. Other resolved compounds have been matched to compounds found in the Palisade Complete Mass Spectral Database. There is a high level of compound coelution from the GC column, resulting in difficult-to-identify overlapping compounds. By paying particular attention to background mass spectral subtractions, it is possible to separate overlapping compounds if they display differing mass spectral patterns. By taking advantage of these differences, we have identified approximately 300 individual organic compounds present in ambient Riverside air as measured by TAG. A complete compound list is provided in Table 6. Uncertainty in compound identification generally increases with additional functional groups, with the exception of compounds present in our standard inventory.

Several other useful parameters are included at the bottom of Table 6. One is a parameter used to estimate contributions to n-alkane mass from plant waxes. These waxes display an odd-carbon preference, and can be quantified as:

$$Cwax = \sum_{n=25}^{35} \left[C_n - \frac{(C_{n-1} - C_{n+1})}{2} \right], n = \text{odd integers only} \quad (4)$$

where C is the n-alkane concentration, n is the number of carbons in the n-alkane, and $Cwax$ is the overall contribution to n-alkane mass from plant waxes. This estimate is derived from previous work [Simoneit, 1984].

Also included in this list are parameters serving as a rough estimate of total primary organic aerosol eluting through the GC system, represented by the common m/z 57 ion $C_4H_9^+$, titled “early.57, mid.57, and late.57”. These three parameters represent the sum of all resolved and unresolved m/z 57 ion abundance between the retention times of 18 – 34 minutes, 34 – 40 minutes, and 40 – 59 minutes, respectively.

The final parameters included in this list are indicators of total secondary organic aerosol eluting through the GC system, represented by the common m/z 43 ion ($C_2H_3O^+$), titled “secondary.early43, secondary.mid43, secondary.late43”. These represent the sum of all resolved and unresolved secondary-associated m/z 43 ion abundance between the retention times of 18 – 34 minutes, 34 – 40 minutes, and 40 – 59 minutes, respectively. The secondary portion of m/z 43 is estimated as:

$$Secondary.early43 = \sum_{t=18}^{34 \text{ min}} m/z43 - \left[\left(\frac{m/z43}{m/z57} \right)_{C_{13}-C_{19}} \times \sum_{t=18}^{34 \text{ min}} m/z57 \right] \quad (5)$$

$$Secondary.mid43 = \sum_{t=34}^{40 \text{ min}} m/z43 - \left[\left(\frac{m/z43}{m/z57} \right)_{C_{20}-C_{23}} \times \sum_{t=34}^{40 \text{ min}} m/z57 \right] \quad (6)$$

$$\text{Secondary.late43} = \sum_{t=40}^{59 \text{ min}} m/z43 - \left[\left(\frac{m/z43}{m/z57} \right)_{C_{24}-C_{31}} \times \sum_{t=40}^{59 \text{ min}} m/z57 \right] \quad (7)$$

where the ratios of m/z 43 to m/z 57 as observed in C₁₃-C₁₉ alkanes (0.75), C₂₀-C₂₃ alkanes (0.67), and C₂₄-C₃₁ alkanes (0.61) are multiplied by early.57, mid.57, and late57, and subtracted from the total m/z 43 in order to eliminate the portion of m/z 43 originating from primary hydrocarbons (C₃H₇⁺). The alkanes chosen for m/z 43 to m/z 57 ratios are those present within the corresponding retention time window.

4.4 Source Apportionment

PMF analyses were performed on 124 TAG compounds for the summer period and 141 TAG compounds for the fall period, along with Cwax (summer only), late.57, secondary.late43, and AMS total organic aerosol mass over the focus periods of July 29 – August 8, and November 4 – 14. The summer focus period is very representative of the seasonal meteorological trends (e.g. windspeed, wind direction), atmospheric chemistry (e.g. O₃), and atmospheric composition (e.g. CO, AMS total organic aerosol) observed over the entire summer study (Fig. 13a). However, the fall study was highly influenced by meteorological events (e.g. Santa Anna Winds) [Qin *et al.*, In Prep], while the chosen focus period represents a time with larger urban influence (Fig. 13b), and excludes the period with Santa Ana winds bringing air mainly from the less populated desert region to the East.

The AMS data contained several gaps within the fall focus period due to a glitch in the acquisition software. There was a strong correlation between total PM_{2.5} mass concentration measured by a beta attenuation monitor (BAM) at the California Air Resources Board monitoring station at Rubidoux, CA, located approximately 10 km northwest of the SOAR site and the AMS data collected at Riverside, ($r^2 = 0.65$, slope = 0.17), and this relationship was used to fill the gaps in the AMS data to complete the timeline in the fall focus period.

The variability in the data was best explained by 9 factors for the summer period and 6 factors for the fall period through the PMF analysis using the defined input parameters. Additional factors explain less than 2.1% (3.4%) of the total organic aerosol mass concentrations during the summer (fall), and appear to only further divide major sources into multiple sources of nearly identical composition and diurnal variability, and therefore were not included in the analysis. Separated by season, factor profiles are shown in Figure 14 (summer) and Figure 15 (fall), and only include PMF compounds that clearly load highest into a single factor. A complete list of factor profiles including all PMF parameters is provided in Table 7 (summer) and Table 8 (fall).

Additional gas and particle-phase measurements contribute supporting information to help correctly identify the source of each factor based on their variability and known sources. For example, O₃ is a tracer for aged urban pollution and CO is a tracer of primary combustion. Correlations of selected parameters to the TAG-defined factors are reported in Table 9 (summer) and Table 10 (fall). Included are O₃, CO, H₂O, gas phase VOCs, EC, OC, AMS measurements of aerosol organics, total sulfate, total nitrate, and total ammonium, and ATOFMS-defined clusters (representative of varying sources, and explained in detail by Qin *et al.*, *In Prep.*). These single particles types included two types of aged organics, aged organics containing sulfate, organics containing elemental carbon, organics containing both elemental carbon and sulfate, elemental carbon alone, aged sea salt particles, dust particles, vanadium-rich particles, biomass particles rich in potassium, and particles rich in ammonium nitrate.

We defined particle types for each Factor based on TAG compound matches to known source profiles, VOC and other gas phase compound matches to known source profiles, AMS parameters, and ATOFMS-defined clusters. Meteorological parameters such as wind speed and wind direction aid in defining the source location. For example, during the summer, particle types that arrive at the site only from the west during daytime high winds are being transported from further distances as the boundary layer rises and atmospheric mixing increases, whereas particles arriving to the site at night from a variety of wind directions and at low wind speeds during periods of strong atmospheric stability and a shallow boundary layer, are more locally generated aerosols.

4.4.1 Summer PMF Results

PMF results were reproduced in 30 independent runs, each with random starting points. The Q values, Q_{true} (25,986) and Q_{robust} (24,788), are within 5% of each other, indicating that the impact of outlier values does not have extreme influence in the fitting of the model. Q_{robust} is approximately 34% larger than the theoretical value, $Q_{\text{theoretical}}$ (18,432), well within a reasonable range. Bootstrapping efforts confirm stable model results. Of the 300 bootstraps, and the resulting 2700 factors, only 133 factors did not match the factors defined in our base case.

4.4.1.1 Factors 1, 2, 3: SOA1, SOA2, and SOA3

We define Factor 1 as secondary organic aerosol type 1 (SOA1). This particle type arrives to the site during the daytime from the west as can be seen in Figure 16, and increases with windspeed (correlations shown in Table 9). Compounds loading highest into this PMF factor consist of mostly oxygenated species (Fig. 14, Table 9) along with a few hydrocarbons. Oxygenated compounds associated with this source include several esters of aromatic carboxylic acids (phthalates), two esters of alkanolic acids (hexadecanoic acid, methyl ester and isopropylpalmitate also called hexadecanoic acid, 1-methylethylester), an ester of a resin acid (dehydroabietic acid, methyl ester), two oxygenated nitrogen-containing organics (penoxaline and nitrophenylbenzenamine), and two ketones (heptadecanone and octadecanone). The abundance of large esters present here suggests at least a portion of SOA1 may result from acid catalyzed esterification of primary aerosol.

To gain further insight on factor identification, column 8 of Table 6 lists other particle phase TAG compounds which were not included in the PMF analysis that have their highest correlations with SOA1 aerosol. Some correlations worth mentioning include several other ketones, one of which also contains nitrogen (indoloquinone), and two of which are oxygenated PAHs (anthraquinone and cyclopenta(def)phenanthrenone). There is also another ester of an aromatic carboxylic acid (diisobutylphthalate).

We define Factor 2 as secondary organic aerosol type 2 (SOA2). This particle type also arrives to the site during the daytime from the west (Fig. 16) at elevated windspeeds. Compounds loading highest into this factor consist of almost exclusively oxygenated species (Table 9), including large contributions from phthalic acid and two methylated phthalic acids (3-methylphthalic acid and 4-methylphthalic acid), two oxygenated nitrogen species (4-nitrophenol and phthalimide), three di-ketones (dodecanedione, undecanedione, and dimethylisobenzofurandione), and two ketones (xanthone and methylfuranone). A majority of these compounds are formed through the photooxidation of gas-phase precursors. Other species, not included the PMF analysis, with high correlations to this factor include acids, ketones, and aldehydes (phenylacetic acid, benzoic acid, phenylpentenone, 9H-fluoren-9-one, acetone, methyl ethyl ketone (mek), cinnamaldehyde, propanal) some of which have both secondary and primary origins

(Table 9).

We define Factor 3 as secondary organic aerosol type 3 (SOA3). This particle type also arrives to the site during the daytime from the west (Fig. 16) at very high windspeeds. Chemical species loading highest into this factor are dominantly oxygenated (Fig. 14). There is some overlap between species that are associated with SOA3 and the two previous SOA factors. Overlapping compounds with SOA2 include phthalic acid, dodecanedione, undecanedione, and xanthone. Overlapping compounds with SOA1 include octadecanone, heptadecanone, dehydroabiatic acid-methyl ester, and isopropylpalmitate. However, there are several unique compounds that make SOA3 different. Included in that list are many oxygenated species containing functional groups such as ketones and di-ketones (dioxaspirononanedione, naphthofurandione, d.tetradecalactone, dimethoxydiphenyl-ethanone, dihydro-5-ethyl-2(3H)furanone, dihydro-5-undecyl-2(3H)furanone, and dihydro-5-dodecyl-2(3H)furanone), an alkanolic acid (dodecanoic acid), and oxygenated compounds which contain nitrogen, sulfur, phosphate, and chlorine (5-methyl-2-nitrophenol, butylbenzenesulfonamide, chlorophosphatepropanol, bischloropropylphosphate, and chlorothalonil). Of all 9 factors, SOA3 has the highest correlation with O_3 , and is anticorrelated with CO, indicating this is not a primary aerosol source, but has been formed through secondary formation processes. Based on the compounds associated with SOA3, this aerosol is likely formed through both heterogeneous reactions in primary aerosol (as seen with SOA1) and photooxidation of gas phase precursors (as seen with SOA2). An exact interpretation of the differences between these three SOA sources based on chemical composition alone is limited by the lack in unique source profiles for various secondary sources.

The highest correlations between ATOFMS defined clusters and TAG-defined sources during the summer period are observed for various aged and sulfate-containing submicron and supermicron clusters and these three SOA sources. These two independent methods (ATOFMS clusters and TAG PMF) agree that summertime aerosol is dominated by secondary sources.

The parameters secondary.early43, secondary.mid43, and secondary.late43 all display highest correlations with SOA sources, indicating that these parameters are in fact secondary in nature, dominated by the m/z 43 ion $C_2H_3O^+$. The parameters early.57 and late.57 have highest correlations to LocalVehicle aerosol sources, indicating that these parameters are in fact from primary emissions, dominated by the m/z 57 ion $C_4H_9^+$. The parameter mid.57 correlates highest to SOA1, indicating that the m/z 57 ion abundance in this volatility region may be secondary in nature, dominated by the m/z 57 ion $C_3H_5O^+$.

Phthalic acid has been suggested as a single-species tracer to represent total SOA abundance in the atmosphere [Fine *et al.*, 2004a]. Our results confirm that phthalic acid does indeed load into each of the SOA factors, slightly favoring SOA2 (Fig. 14), and thus additional tracers are needed to differentiate between types of SOA sources. Of the compounds observed here, phthalic acid does appear to remain the best candidate for a single-species tracer of SOA in an urban environment. However, multiple sources of SOA are only derived using less ubiquitous secondary species.

4.4.1.2 Factors 4, 5: *RegionalPrimaryAnthro and LocalVehicle*

We define Factors 4 and 5 respectively as regional primary anthropogenic (RegionalPrimaryAnthro) and local vehicle (LocalVehicle) aerosol. Both particle types arrive to the site from the west, but LocalVehicle particles also arrive to the site from the northwest and east (Fig. 16). RegionalPrimaryAnthro particles arrive at the site throughout the day, whereas LocalVehicle particles

reach a maximum in the morning hours (discussed in more detail below in section titled *Average Diurnal Variations in Organic Aerosol Composition*). The chemical characterization of RegionalPrimaryAnthro particles is dominantly hydrocarbons, including several alkanes, cyclohexanes, and straight and branched PAHs (Fig. 14) along with a few oxygenated species. Other parameters with high correlation to RegionalPrimaryAnthro particles are most notably AMS measurements of total particulate NO_3^- , NH_4^+ , and Chloride (Table 9). The hydrocarbons observed in this particle type are typical of vehicular emissions [Schauer *et al.*, 1999; Schauer *et al.*, 2002; Fraser *et al.*, 1998; Rogge *et al.*, 1993], but do not include the hopanes and steranes often seen from direct vehicle emissions. The particulate NO_3^- and NH_4^+ associated with this factor have various possible sources. The most likely sources found west of Riverside are dairies and agriculture (ammonia) and vehicle emissions (nitrogen oxides) [Sawant *et al.*, 2004].

LocalVehicle particles have high loadings of hopanes (28nor-17 β (H)-hopane and 17- α (H)-21 β (H)-hopane), branched alkanes (2-methyloctadecane, 3-methyloctadecane, and 4-methyloctadecane), and straight chain alkanes, cyclohexanes, and PAHs, all of which are characteristic of vehicle emission profiles [Schauer *et al.*, 1999; Schauer *et al.*, 2002; Fraser *et al.*, 1998; Rogge *et al.*, 1993]. Two other compounds (monostearin and monopalmitin) appear in this factor from a semi-collocated source, meat cooking, however their overall influence is minor since PMF results are unchanged by excluding them from the analysis, whereas excluding the vehicle markers does not introduce a meat cooking source.

LocalVehicle particles include shorter lived compounds such as acephenanthrylene and others that are likely only detectable on the local scale prior to major dilution [Arey *et al.*, 1989]. For example, monostearin and monopalmitin (meat cooking markers) are not typically detectable without chemical derivatization, and therefore must be at high concentrations (not diluted) to allow underivatized TAG detection. This indicates that LocalVehicle represents local vehicle emissions (e.g. on the scale of the immediate Riverside area and interstate highway 215). The presence of hopanes in local vehicle particles, but not in RegionalPrimaryAnthro particles may suggest that hopanes, like acephenanthrylene, have a short atmospheric lifetime. It has been suggested that hopanes can have atmospheric lifetimes as short as 1 day during summer periods [Rudich *et al.*, 2007].

RegionalPrimaryAnthro particles do not display a regular daily maximum, but do have a midweek maximum, similar to particulate NO_3^- and NH_4^+ , suggesting they are representative of vehicular or other primary anthropogenic emissions transported to the site from further away.

Another possible explanation is that RegionalPrimaryAnthro and LocalVehicle sources represent a split between diesel and gasoline vehicle emissions. Since there is a higher emission ratio of elemental carbon (EC) from diesel fuel, EC is often used to differentiate diesel emissions from gasoline emissions. However, it appears that EC has some correlation with each of these sources. EC has clear morning maximums, indicating some local diesel emissions associated with LocalVehicle. However, EC persists throughout the day, unlike LocalVehicle, and has an elevated background concentration during midweek similar to RegionalPrimaryAnthro. EC has a Tuesday maximum ($1.51 \pm 0.44 \mu\text{g m}^{-3}$) and a Sunday minimum ($0.66 \pm 0.12 \mu\text{g m}^{-3}$), as averaged across the entire 4 week study. This is very similar to the trend in RegionalPrimaryAnthro, where there is a Tuesday maximum of $8.4 \mu\text{g m}^{-3}$, and a Saturday minimum of $0.8 \mu\text{g m}^{-3}$. LocalVehicle does not display this trend. LocalVehicle has a Friday maximum and a Sunday minimum. A combination of RegionalPrimaryAnthro and LocalVehicle best explains the trends in EC. It is therefore more likely that the factor split between RegionalPrimaryAnthro and

LocalVehicle is due to emission proximity and not fuel type.

It should be noted that hopanes have been shown to favor the ultrafine aerosol mode (diameters < 180 nm) in Riverside [Fine et al., 2004], and the TAG collection stage does not collect a significant fraction of aerosols < 90 nm in diameter. A portion of the hopane mass is therefore not efficiently collected, and we make the assumption that the portion that is collected maintains the variability of the entire hopane mass.

4.4.1.3 Factor 6: FoodCooking

We define Factor 6 as food cooking aerosol (FoodCooking). This particle type generally reaches the site from many wind directions (Fig. 16) at lower windspeeds, indicating that this is due to a local source. Characteristic TAG compounds loading highest into this factor are alkanolic acids (hexadecanoic acid, octadecanoic acid, and tetradecanoic acid), alkylnitriles (hexadecanenitrile and octadecanenitrile), and nonanal, all molecular tracers for various types of food cooking [Rogge et al., 1991]. While many of these compounds can have secondary sources, this source is not elevated in the afternoon, and is therefore likely a primary emission. All of these compounds have been identified in meat cooking source profiles, but most have also been identified in other food cooking source profiles. There is not enough information here to estimate emissions from specific food types (e.g. beef, pork, chicken, seed oils) and preparation methods (e.g. pan frying, charbroiling). We argue this Factor represents an integration of all food cooking operations.

Marker compounds often used specifically for meat cooking were detected (monostearin and monopalmitin), but their timelines are dominated by extremely elevated concentrations on Friday and Saturday mornings (likely a local source). This is the same day-of-week pattern previously observed in Los Angeles for these compounds [Lough et al., 2006]. By removing these elevated events (all values > 1.5 σ) for monostearin and monopalmitin, there is an increased correlation between these compounds and the food cooking factor. The food cooking source may not fully capture local meat cooking aerosol, or there is another source of these monoglycerides not currently included in source profiles found in the literature.

Several biogenic compounds have high correlations to our identified food cooking aerosols. Three of them are salicylate compounds, which recently have been shown to have high emissions from desert plants, and mesquite in particular [Guenther et al., Submitted]. A fourth biogenic compound is dimethoxydiphenyl-ethanone, which is structurally similar to compounds found in biomass smoke [Simoneit et al., 1993]. This source appears to build up over the weekend periods, with the two maximums both observed on Sunday nights through early the following morning. It is not possible to indicate how representative this is of a seasonal trend, given we are only including two weekends. Nonetheless, with the apparent elevated weekend concentrations and the nature of the correlated compound's known sources, this additional information may point to a significant portion of food cooking particles coming from weekend barbecues.

4.4.1.4 Factor 7: BioParticle+Mixed

We define Factor 7 as particle-phase biogenic plus mixed sources (BioParticle+Mixed). This source arrives at the site from almost every wind direction (Fig. 16). Compounds with high loading into this factor include many biogenic compounds such as chromenes (eupatoriochromene and enecalinal), a sesquiterpene (δ -cadinene), a terpenoid mixture (norabietatetraene-mixture), vanillin, and the parameter Cwax which is used as a marker for plant waxes. It is likely that this factor is dominantly biogenic, but

has contributions from several other sources. Some of these large biogenic compounds could be in the atmosphere from combustion processes, and therefore overlapping with a dominantly biomass burning source that will be described later in this report. This is supported by the presence of retene, a branched PAH found in biomass burning aerosol. Other potential sources associated with this factor are indoor sources, as suggested by the presence of bis(2-ethylhexyl)phthalate and hentriacontane, two compounds found at extremely high concentrations in indoor air [Weschler *et al.*, 1984]. There could also be an additional petroleum-derived component, based on the presence of methyladamantane, several even-numbered alkanes, and cyclohexanes, which are all characteristic of petroleum [Schauer *et al.*, 1999; Schauer *et al.*, 2002; Stout and Douglas, 2004].

4.4.1.5 Factor 8: *BioSemivolatile*

We define Factor 8 as semivolatile biogenic species (BioSemivolatile). Many biogenic compounds load into this factor. Examples of known biogenic compounds are the terpenes p-cymenene, α -phellandrene, δ -3-carene, limonene, and δ -cadinene. Other biogenic compounds with high correlations to this factor include the terpenes cumene, p-cymene, m-cymene, γ -terpinene, α -terpinene, and the oxygenated terpenes pinonaldehyde, nopinone, α -campholenal, and cuminic aldehyde. The majority of these particles arrive to the site from the southeast (Fig. 16) during the night. It is suspected that these biogenic compounds are from local agricultural test crops and botanical gardens found to the south of the University of California, Riverside campus. Unlike the previous biogenic factor (BioParticle+Mixed), a majority of these biogenic compounds favor the gas phase, and are likely condensing into the particle phase at cooler atmospheric temperatures as is indicated by the anticorrelation between this factor and air temperature, and a positive correlation with relative humidity (Table 9).

This factor includes compounds of unknown origin (methyloxadamantane, methoxypyridine, pelletierine, pentylcyclohexanone, and N-[(2-methoxyphenyl)methylene]-benzenamine). Because they are emitted in the same region as the biogenic compounds, we suspect they could also have biogenic origins.

4.4.1.6 Factor 9: *BiomassBurning*

We define Factor 9 (the final factor) as biomass burning aerosol (BiomassBurning). Biomass burning aerosol arrives at the site at highest concentrations from the southeast, but also frequently arrives to the site from the west (Fig. 16). Wildfires were low during SOAR-1 according to MODIS Active Fire Detections database (<http://maps.geog.umd.edu/firms/maps.asp>), therefore the most significant form of biomass burning observed is likely residential wood burning. Compounds that display high loadings into this factor include norabieta.4.8.11.13.tetraene, vanillin, norabietatetraene-mixture, 2-methylpyrene, and benz(de)anthracene, all known biomass burning marker compounds [Fine *et al.*, 2004b; Rogge *et al.*, 1998; Simoneit, 1989]. Additional compounds with high correlations to this particle type are dehydroabietin, abietatriene, precoceneII, and lily aldehyde, all of which are potential markers for biomass burning aerosol due to biogenic origins [Simoneit, 1989]. There are a few nitrogen containing compounds associated with this factor as well. Nitrogen-containing organics have not been reported in biomass burning source profiles, but it is reasonable to assume that there would be some N-containing compounds in biomass burning aerosol. The Carbon to Nitrogen ratio (C:N) is around 100 for woody plants and as low as of 5 for macroalgae [Raven *et al.*, 2004].

Biomass burning aerosol measured by ATOFMS as single particles rich in potassium correlates better with SOA2 than this BiomassBurning source. This could indicate that some of the biomass burning

aerosol has undergone photochemical processing, hence diminishing traditional primary marker compounds such as PAHs. If this is the case, then this BiomassBurning source as defined by TAG compounds is representative of only the unprocessed portion of the biomass burning plume. There may be additional aerosol mass originating from biomass burning sources, but is attributed to SOA2 after undergoing some degree of atmospheric aging.

4.4.2 Fall PMF Results

PMF results were reproduced in 30 independent runs, each with random starting points. The average Q values, Q_{true} (34,928) and Q_{robust} (33,707), are within 5% of each other, indicating that the impact of outlier values does not have extreme influence in the fitting of the model. Q_{robust} is approximately 41% larger than the theoretical value, $Q_{\text{theoretical}}$ (23,904), well within a reasonable range. Bootstrapping efforts confirm stable model results. Of the 300 bootstraps, and the resulting 2700 factors, only 63 factors did not match the factors defined in our base case.

4.4.2.1 Factors 1, 2: SOA+FoodCooking1 and SOA+FoodCooking2

Factor 1 contains many of the same molecular marker compounds as summertime SOA2 and FoodCooking aerosol, and will therefore be referred to as secondary organic aerosol plus food cooking type 1 (SOA+FoodCooking1). This particle type arrives at the site at highest concentrations from the southeast (Fig. 17). Backtrajectories suggest this air mass had traversed San Diego and moved north to Riverside within the past 36 hours [Qin *et al.*, In Prep]. Compounds that display high loadings into this factor include several associated with summertime FoodCooking aerosol (tetradecanoic acid, hexadecanoic acid, octadecanoic acid, and nonanal), and some associated with summertime SOA2 (4-nitrophenol and dodecanedione).

Factor 2 contains many of the same molecular marker compounds as summertime SOA2, SOA3, and FoodCooking aerosol, and will therefore be referred to as secondary organic aerosol plus food cooking type 2 (SOA+FoodCooking2). This particle type arrives at the site at highest concentrations from the southeast and, less frequently, from the west (Fig. 17). Backtrajectories suggest this air mass had also traversed San Diego and moved north to Riverside within the past 36 hours [Qin *et al.*, In Prep.]. Compounds that display high loadings into this factor include several associated with summertime FoodCooking aerosol (hexadecanenitrile and octadecanenitrile), as well as food cooking marker compounds that were not seen to correlate with the summertime FoodCooking source (monostearin and monopalmitin). Other compounds loading into this factor were associated with summertime SOA2 (phthalic acid, 3-methylphthalic acid, 4-methylphthalic acid, and dimethylisobenzofuranone), and with summertime SOA3 (ethylidihydrofuranone, dioxaspirononanedione, and undecanedione).

Other non-PMF parameters display high correlation with these two SOA+FoodCooking sources, including many additional TAG compounds, such as acids, ketones, and aldehydes (Table 6). Many other measurements were highly correlated with these sources including all AMS species, many ATOFMS clusters, CO, and other gas phase VOCs and OVOCs. These two sources appear at similar times of the study, and appear to be an accumulation of various primary and oxygenated compounds. TAG data suggest the primary compounds are dominantly from food cooking operations.

4.4.2.2 Factor 3: RegionalPrimaryAnthro

Factor 3 contains many of the same molecular marker compounds as summertime RegionalPrimaryAnthro aerosol, and will therefore also be referred to as regional primary anthropogenic (RegionalPrimaryAnthro). These particles arrive to the site at high concentrations from the west most

frequently, and less frequently from the southeast (Fig. 17). The chemical characterization of RegionalPrimaryAnthro particles is dominantly hydrocarbons, including several straight and branched alkanes, cyclohexanes, and branched PAHs (Fig. 15) along with a few oxygenated species. The particulate hydrocarbons observed in this aerosol type are typical of vehicular emissions [Schauer *et al.*, 1999; Schauer *et al.*, 2002; Fraser *et al.*, 1998; Rogge *et al.*, 1993], but, as previously observed during the summer period, do not include the hopanes and steranes often seen from direct vehicle emissions.

Other parameters with high correlation to RegionalPrimaryAnthro particles include air temperature, solar radiation (PAR), windspeed, O₃, isoprene, methyl vinyl ketone (mvk), and methacrolein (macr) (Table 10). The compounds mvk and macr are known oxidation products of isoprene [Tuazon and Atkinson, 1990]. There was no observed correlation between this source and particle phase biogenic compounds.

4.4.2.3 Factor 4: LocalVehicle

Factor 4 contains many of the same molecular marker compounds as summertime LocalVehicle aerosol, and will therefore also be referred to as local vehicle (LocalVehicle). These particles have high loadings of hopanes (norhopane and hopane), several alkanes, cyclohexanes, PAHs, and branched PAHs, all of which are characteristic of vehicle emission profiles [Schauer *et al.*, 1999; Schauer *et al.*, 2002; Fraser *et al.*, 1998; Rogge *et al.*, 1993]. LocalVehicle particles arrive to the site most frequently from the west (Fig. 17). Also correlated with this source are the gas phase species CO, o-xylene, benzene, toluene, and small alkanes, alkenes, and alkynes, all of which have known vehicular emissions [Millet *et al.*, 2005; Millet *et al.*, 2006].

4.4.2.4 Factor 5: BioSemivolatile

Factor 5 contains many of the same molecular marker compounds as summertime BioSemivolatile aerosol, and will therefore also be referred to as biogenic semivolatile (BioSemivolatile). Many biogenic compounds load into this factor. Examples of known biogenic compounds are the terpenes α -phellandrene, γ -terpinene, δ -3-carene, β -selinene, methyl chavicol, limonene dioxide 4, and δ -cadinene. These particles arrive to the site from the southeast (Fig. 17) during the night. It is again suspected that these biogenic compounds are from local agricultural test crops and botanical gardens found within the University of California, Riverside campus. They show an anticorrelation with air temperature, and are positive correlated with relative humidity (Table 10).

Included in this factor are the same compounds of unknown origin that were associated with this factor during the summer period (methyloxadamanthane, methoxypyridine, pentylcyclohexanone, and N-[(2-methoxyphenyl)methylene]-benzenamine).

4.4.2.5 Factor 6: BiomassBurning

Factor 6 (final factor for the fall PMF analysis) contains many of the same molecular marker compounds as summertime BiomassBurning aerosol, and will therefore also be referred to as biomass burning (BiomassBurning). Biomass burning aerosol arrives at the site almost exclusively from the southeast (Fig. 17). Compounds that display high loadings into this factor include norabieta-4.8.11.13-tetraene, 8-isopropyl-1,3-dimethylphenanthrene, retene, dehydroabietic acid-methyl ester, norabietatetraene-mixture, and 7-oxodehydroabietic acid-methyl ester, all known biomass burning marker compounds [Fine *et al.*, 2004b; Rogge *et al.*, 1998; Simoneit, 1989]. Additional compounds with high correlations to this particle type are 19-nor-abieta-3,8,11,13-tetraene, dehydroabietin, abietatriene, α -campholenal, lily aldehyde, and pinonaldehyde, all of which are potential markers for biomass burning aerosol.

BiomassBurning aerosol during the fall has a negative correlation with temperature and PAR, meaning higher concentrations during the night, and a positive correlation with atmospheric pressure.

4.4.3 *PMF Residuals*

Gas chromatography as used in the current version of TAG has limitations in terms of the compounds that can be measured and is best suited for measuring the less polar and more volatile compounds in organic aerosols [Williams *et al.*, 2006; Falkovich and Rudich, 2001]. TAG does not detect the most polar and least volatile fraction of the organic aerosol. Here we present two approaches that can be taken to understand how well the elutable fraction (the compounds that pass completely through the TAG system) represents the total organic aerosol mass.

The first insight can be gained by simply looking at the organic aerosol mass that remains unexplained after performing a PMF analysis on elutable TAG compounds. A residual term is calculated (Eqtn. 1, 8), providing a measure of periods where TAG compounds alone can not explain the organic aerosol mass concentrations. Since there is a positive correlation ($r = 0.42$) between our “Residual” PMF factor and the total AMS organic aerosol mass, the elutable TAG compounds do explain a relatively constant fraction of the total mass concentration during the summer.

TAG compounds explain the majority of the total organic aerosol mass concentrations during the fall, but there is one period early in the study (DOY 308-310) where the Residual factor makes up a significant fraction of the organic mass concentrations. However, this is one of the AMS data gaps that had been interpolated using PM_{2.5} data from Rubidoux which is located 10 km away. It is possible there may have been a local source in Rubidoux that contributed to concentrations at that site, but did not influence the SOAR site.

A second method to test whether TAG compounds explain the entirety of the AMS organics variance is to make a direct estimate of TAG total elutable organic mass compared to AMS total organic mass. If this ratio is relatively constant, then it can be assumed that TAG elutable mass is capable of representing the variance seen in the AMS total organic mass. If the ratio is not constant, and in particular, if the ratio of TAG organics to AMS organics becomes very low, then there may be an important fraction of the total organics signal that is not represented by TAG compounds alone.

An estimate of the total organic mass eluting through TAG’s gas chromatography column is made by summing the early.57, mid.57, and late.57 measures of total elutable primary material, scaled to mass concentrations based on appropriate ranges of quantified alkanes. This term is then added to the sum of secondary.early43, secondary.mid43, and secondary.late43 measures of total elutable secondary material, scaled to mass concentrations based on appropriate ranges of quantified alkanic acids.

Since this quantification of TAG total elutable organic mass relies heavily on the assumption of applying surrogate calibrations based on average alkane and alkanic acid responses, this term is ultimately normalized to a value of 1. The same is done for AMS total organics. This provides a qualitative measure of the variability in the TAG organics to AMS organics ratio.

The normalized TAG elutable organics to normalized AMS total organics ratio is fairly constant in the summer (0.88 ± 0.26), with a maximum of 1.61 and minimum of 0.06. This ratio is anticorrelated with the summer Residual factor ($r = -0.35$), meaning that as this ratio decreases, the elutable TAG compounds explain a smaller fraction of the AMS organics, giving rise to Residual mass. Conversely, as

this ratio increases, the Residual factor decreases, meaning the elutable TAG compounds alone can explain the variance in AMS organics. We conclude from this analysis that in summer the PMF Residual factor does in fact report the variance that is not observed by elutable TAG compounds alone.

The normalized TAG elutable organics to normalized AMS total organics ratio is more variable in the fall (1.23 ± 0.78), with a maximum of 4.08 and minimum of 0.27. This ratio is also anticorrelated with the fall Residual factor ($r = -0.40$), meaning that again in the fall, the PMF Residual factor reports the variance not observed by elutable TAG compounds alone.

4.5 Source Contributions to Organic Aerosol Mass

Total organic aerosol mass as measured on the AMS can now be apportioned to our TAG-defined organic aerosol sources. To find the organic mass concentration timeline for the p^{th} factor ($F_p(t)$) we employ the following equation:

$$F_p(t) [\mu\text{g m}^{-3}] = \left[g_{p,\text{contrib.}}(t) \times \frac{f_{p,\text{org,profile}} [\mu\text{g m}^{-3}]}{\sum_{j=1}^{\text{\#PMFcomponents}} f_{p,j,\text{profile}} [\mu\text{g m}^{-3}]} \times f_{p,\text{org,profile}} [\mu\text{g m}^{-3}] \right] \quad (8)$$

where $f_{p,\text{org,profile}}$ is the AMS organic aerosol loading into factor p , and $g_{p,\text{contrib.}}(t)$ is the normalized timeline of factor p (i.e. normalized contribution of factor p to total variance at time t). The ratio of $f_{p,\text{org,profile}}$ divided by the sum of all species contributing to factor p (i.e. sum of $f_{p,j,\text{profile}}$ over all PMF species j) provides a fraction of factor p that is AMS organic aerosol. Multiplying again by $f_{p,\text{org,profile}}$ converts the normalized timeline of factor p to mass concentration of organic aerosol. Any residual mass left unexplained by the PMF analysis is included as an additional “Residual” factor, as discussed in the previous section.

Since the AMS measures $\text{PM}_{1.0}$ and TAG measures $\text{PM}_{2.5}$, the assumption must be made that the organics observed by TAG are dominantly in the $\text{PM}_{1.0}$ size range, and that most of the aerosol mass between $\text{PM}_{1.0}$ and $\text{PM}_{2.5}$ is inorganic. There is evidence from the ATOFMS to suggest that the major sources to aerosol mass in this range are Sea Salt and Dust particles, both high in inorganic mass [Qin *et al.*, In Prep.].

Cumulative mass concentration timelines for summer (fall) organic aerosol sources are shown in Figure 18 (Figure 19), and individual timelines are shown in Figure 20a (Figure 21a). Here, it is clear that there are significant differences between summer and fall organic aerosol contributions, with repeatable daily variations of each source in the summertime, and less repeatable “events” dominating during the fall.

Table 11 reports the average mass concentration contribution from each of the major organic aerosol sources over each focus period. The summer period is dominated by SOA, where the sum of all 3 SOA sources averages $7.6 \mu\text{g m}^{-3}$ of organic aerosol, or 47% of the total organic aerosol mass. The sum of all primary anthropogenic organic aerosol sources (RegionalPrimaryAnthro, LocalVehicle, FoodCooking) averages $4.0 \mu\text{g m}^{-3}$ of organic aerosol, or 25% of the total organic aerosol mass. The combined biogenic sources (BioParticle+Mixed, BioSemivolatile) average $3.3 \mu\text{g m}^{-3}$ of organic aerosol, or 20% of the total organic aerosol mass. BiomassBurning aerosol, potentially a mix of biogenic and anthropogenic sources,

contributes an average 6% and the Residual organic mass contributes only 2% to total organic aerosol loadings on average.

The fall period is dominated by the two SOA+FoodCooking sources (SOA+FoodCooking1, SOA+FoodCooking2), where their sum contributes an average of $6.7 \mu\text{g m}^{-3}$ of organic aerosol, or 69% of the total observed organic aerosol mass. These sources do however include both SOA and markers for primary anthropogenic emissions. Other primary anthropogenic sources (RegionalPrimaryAnthro, LocalVehicle) contribute an additional 16% of the organic aerosol mass. BiomassBurning aerosol contributes a significant amount of organic aerosol mass during the fall (9.5%). Biogenic emissions contribute significantly less than during the summertime, accounting for only 2% of the organic mass, and the Residual sources account for the remaining 3.5%, a larger fraction compared to the summer Residual source.

The following comparisons assume a constant ratio of organic carbon (OC), as has traditionally been measured, to organic matter (OM), as is measured by the AMS. Previous studies have concluded secondary sources dominate all aerosol source contributions in this same region of the L.A. Air Basin. Na et al. [2004] conclude that secondary organic carbon contributes an average of 57% of the total organic carbon during the late summer and fall in Mira Loma, CA (only ~ 16 km west of our field site). This is comparable to our findings.

Sawant et al. [2004] estimate that only a small amount of the total primary emissions of gasoline and diesel particles are from local sources, a finding that is supported by our PMF results. Applying a chemical mass balance model to characteristic OC/EC profiles for various emission types, Na et al. [2004] estimated that an average of approximately 35% of the OC comes from gasoline and diesel primary emissions. Our findings show a smaller fraction (18.5% in summer, 16.1% in fall) comes from primary vehicle emissions. It is possible that we find a smaller vehicular contribution due to the incorporation of several additional sources not accounted for by Na et al. (e.g. biogenic emissions, biomass burning, food cooking). In a recent urban air study, vehicular emissions were determined to contribute an annual average of 14% of total OC emissions [Brook et al., 2007]. This is more similar to our findings.

Hildemann et al., 1989, estimates that up to 20% of total OC in the L.A. Basin can be composed of aerosol derived from food cooking operations. This estimate is above our derived contributions, at least during the summertime. It has recently been shown in other urban regions that food cooking operations can contribute an average of 10% of the total OC [Robinson et al., 2006] which is closer to the summertime food cooking contributions seen here. It should be noted that recent studies have questioned the use of some food cooking molecular marker compounds in the ambient atmosphere due to potential contributions from soil-related sources [Jaekels et al., 2007], although those marker compounds in question are not the only food cooking markers used in our PMF analyses.

Biomass burning aerosol in this region is likely variable from season to season and from year to year. The trend seen here, with a larger fraction of total organic aerosol coming from biomass burning during the fall is predicted to be consistent. Over the entire study period, the average summertime RH was 53.5% with a minimum of 16.9%, and the average fall RH was 48.6% with a minimum of 7.3%, increasing the chances for fires during the drier fall period. To our knowledge, there has not been a previous estimate of biogenic emissions in Riverside, CA.

4.6 Average Diurnal Variations in Organic Aerosol Composition

The diurnal trend, with 2-hour time resolution, of AMS species (Organics, SO_4^{2-} , NO_3^- , NH_4^+ , Chloride), as averaged over the 11 day focus period, is shown using time-of-day pie charts in Figure 22 (Figure 23) for summer (fall).

The total organic aerosol mass concentrations range between $10.0 - 20.8 \mu\text{g m}^{-3}$ during the summer. The fraction of total aerosol mass that is composed of organics during the summer varies throughout the day, with a maximum (59%) between 16:00 – 18:00, a minimum (47%) between 8:00 – 10:00, and a total daily average of $52 \pm 4\%$. Summertime aerosol reaches a maximum mass concentration during the afternoon hours, when photooxidation is high, producing a large quantity of SOA.

The total organic aerosol mass concentrations range between $6.0 - 11.6 \mu\text{g m}^{-3}$ during the fall. The fraction of total aerosol mass that is composed of organics during the fall remains relatively constant throughout the day, with a maximum (44%) between 2:00 – 4:00, a minimum (38%) between 16:00 – 18:00, and a total daily average of $41 \pm 2\%$. In the fall, aerosol concentrations reach a maximum in the morning and evening, when primary emissions are at their highest. Fall data was characterized by the influence from meteorological “events”, while the summer data was characterized by very regular diurnal patterns, thus the fall diurnal averages are less systematic and informative.

To further separate the AMS organic aerosol signal, the 2-hour time resolution diurnal trends of TAG-defined sources, as averaged over the 11 day focus period, are shown using time-of-day pie charts in Figure 24 (Figure 25) for summer (fall), and as continuous timelines in Figure 20b (Figure 21b). These figures offer a more detailed view of diurnal contributions to organic aerosol mass from major sources than has ever before been reported. Only with the high time resolution TAG measurements of speciated organic marker compounds is it possible to view organic aerosol contributions at this high time frequency.

Figures 20b and 24 show that summer local primary emissions (LocalVehicle, FoodCooking, BioParticle+Mixed) tend to reach a maximum during the morning hours, where SOA and regional sources (SOA1, SOA2, SOA3, RegionalPrimaryAnthro) are elevated later in the day, and other sources (BioSemivolatile, BiomassBurning) are at their highest concentrations during the night. There are distinct differences in diurnal variability (as well as chemical composition) between the 3 summertime SOA sources. SOA1 particles appear with the morning sunlight (PAR) and reach a maximum contribution to the total organic aerosol mass between 8:00 and 10:00. SOA2 particles also appear with the morning sunlight and typically reach a maximum between 10:00 and 12:00. However, SOA3 does not appear until later in the morning and reaches a maximum late in the afternoon (14:00 – 16:00). SOA3 is clearly derived through a different process than the other SOA sources, and is likely more representative of an aged regional SOA based on wind speeds and wind directions. Since SOA2 has increased concentrations again in the afternoon, some SOA2 may also be included as regional SOA. The sum of the three summertime SOA sources makes up $74 \pm 3\%$ of the total organic aerosol mass between the hours of 10:00 and 18:00, with a maximum concentration of $15.8 \mu\text{g m}^{-3}$ from 14:00 – 16:00.

In the fall, the major sources of organic aerosol (SOA+FoodCooking1, SOA+FoodCooking2) are episodic and do not display a regular diurnal cycle, while the other sources do have a more regular diurnal cycle. In Figures 21b and 25 it is apparent that RegionalPrimaryAnthro contributes significantly to afternoon organic aerosol at the site. LocalVehicle aerosol has a maximum between 8:00 and 10:00 in

the morning. BiomassBurning and BioSemivolatile both have a maximum contribution to organic aerosol mass during the night, as was also observed in the summer.

5. Implications and Conclusions

The first ever hourly measurements of speciated organic aerosol in an urban region have been successfully obtained. Sampling was completed at Riverside, CA over the summer and fall of 2005. Approximately 300 different organic compounds ranging from nonpolar hydrocarbons to polar acids, aldehydes, and ketones were analyzed in detail over 11 day periods for each season.

Select compounds were used to complete a PMF analysis to identify the major sources of organic aerosol. Similar organic aerosol sources were discovered over both seasons, including three distinct types of SOA sources, food cooking operations, local vehicle emissions, regional primary anthropogenics, particle phase biogenics, semivolatile biogenics, and biomass burning aerosol.

Summertime organic aerosol sources had very regular diurnal contributions, with SOA contributing 75% (average concentrations as high as $15.8 \mu\text{g m}^{-3}$) of the total organic aerosol mass during the afternoon (47% when averaged diurnally), and significant contributions from biogenics and other local anthropogenic emissions during the night. Regional primary anthropogenic particles contributed 15% of the total organic aerosol mass over both seasons. While primary vehicle emissions (local and regional) account for less than 20% of the total organic aerosol mass during both seasons, a significant amount of vehicle emissions have been processed in the atmosphere and are responsible for creating the large amounts of observed SOA. The major sources to organic aerosol in the fall were controlled by episodic events which delivered high mass concentrations of mixed primary and secondary aerosol. Nearly 70% of the fall organic aerosol arrived to the site during these events. The remaining 30% was from primary aerosol sources similar to the summertime. Biogenic sources contributed significantly more total aerosol mass during the summer period compared to the fall. Conversely, biomass burning was found to contribute a larger fraction of the total organic aerosol mass during the fall.

A unique finding during this study was the presence of three separate SOA types during the summer period. An interpretation of the differences between these three SOA types based on chemical composition alone is limited by a lack of source profiles for secondary sources. Here we highlight the need for further SOA source profile studies. However, since many of the oxygenated compounds present in SOA are products of multiple reaction pathways, there will always be a limitation to defining SOA source profiles. Future studies should target unique oxygenated compounds that have only one dominant source.

Pollutants from the L.A. Air Basin have a substantial impact on air quality in Riverside. The majority of the aerosol mass arriving in Riverside, on the eastern edge of the basin, is composed of secondary organic aerosol. This indicates that by the time air masses escape the valley, most of the organic aerosol mass originating in the L.A. Air Basin has undergone some degree of chemical aging, and additional SOA has been created from gas to particle photochemical processes.

6. References

Allan, J.D., Jimenez, J.L., Williams, P.I., Alfarra, M.R., Bower, K.N., Jayne, J.T., Coe, H., Worsnop,

D.R. (2003). Quantitative sampling using an Aerodyne aerosol mass spectrometer 1. Techniques of data interpretation and error analysis, *J. Geophys. Res.*, 108(D3), 4090, doi:10.1029/2002JD002358.

Allan, J.D., Delia, A.E., Coe, H., Bower, K.N., Alfarra, M.R., Jimenez, J.L., Middlebrook, A.M., Drewnick, F., Onash, T.B., Canagaratna, M.R., Jayne, J.T., Worsnop, D.R. (2004). A generalized method for the extraction of chemically resolved mass spectra from Aerodyne aerosol mass spectrometer data, *J. Aerosol Sci.*, 35(7), 909-922.

Arey, J., R. Atkinson, B. Zielinska, and P.A. McElroy (1989). Diurnal Concentrations of Volatile Polycyclic Aromatic Hydrocarbons and Nitroarenes during a Photochemical Air Pollution Episode in Glendora, California, *Environ. Sci. Technol.*, 23, 321-327.

Brook, J.R., L. Graham, J.P. Charland, Y. Cheng, X. Fan, G. Lu, S.M. Li, C. Lillyman, P. MacDonald, G. Caravaggio, J.A. MacPhee (2007). Investigation of the motor vehicle exhaust contribution to primary fine particle organic carbon in the urban air, *Atmospheric Environment*, 41, 119–135.

Caltrans (2007). Traffic Operations Program, Traffic and Vehicle Data Systems website, http://www.interstate-guide.com/i-215_ca.html.

Charlson, R.J., Schwartz, S.E., Hales, J.M., Cess, R.D., Coakley, J.A., Hansen, J.E., Hofmann, D.J. (1992). Climate forcing by anthropogenic aerosols, *Science*, 255(5043), 423– 430.

Christoforou, C.S., Salmon, L.G., Hannigan, M.P., Solomon, P.A., Cass, G.R. (2000). Trends in fine particle concentration and chemical composition in southern California, *J. Air and Waste Management Assoc.*, 50, 43-53.

Chow, J.C., Watson, J.G., Lowenthal, D. H., Solomon, P.A., Magliano, K.L., Ziman, S.D., Richards, L.W. (1993). PM₁₀ and PM_{2.5} compositions in California's San Joaquin Valley, *Aerosol Sci. and Technol.*, 18, 105-128.

Dockery, D.W., Pope, C.A. III, Xu, X., Spengler, J.D., Ware, J.H., Fay, M.E., Ferris, B.G. Jr, Speizer, F.E. (1993). An association between air pollution and mortality in six U.S. cities, *N. Engl. J. Med.*, 329, 1753–1759.

Docherty, K.S., Ziemann P.J. (2001). On-line, inlet-based trimethylsilyl derivatization for gas chromatography of mono- and dicarboxylic acids, *J. Chromat. A.*, 921, 265-275.

Eiguren-Fernandez, A., Miguel, A.H., Froines, J.R., Thurairatnam, S., Avol, E.L. (2004). Seasonal and spatial variation of polycyclic aromatic hydrocarbons in vapor-phase and PM_{2.5} in southern California urban and rural communities, *Aerosol Science & Technology*, 38, 447-455.

EPA (2002). Health Assessment Document for Diesel Engine Exhaust. EPA/600/8-9/057F. Washington, DC: U.S. Environmental Protection Agency.

EPA PMF User's Guide, 1.1; U. S. Environmental Protection Agency: Washington, DC, 2005.

Evershid (1993). R. in K Blau J halket Handbook of Derivatives for Chromatography, Wiley, New

York, p. 53.

Falkovich, A.H., and Rudich, Y. (2001). Analysis of semivolatile organic compounds in atmospheric aerosols by direct sample introduction thermal desorption GC/MS, *Environ. Sci. Technol.* 35, 2326-2333.

Fine, P.M., Cass, G.R., Simoneit, B.R.T. (2001). Chemical characterization of fine particle emissions from fireplace combustion of woods grown in the northeastern United States, *Environ. Sci. Technol.*, 35, 2665-2675.

Fine, P.M., B. Chakrabarti, M. Krudysz, J.J Schauer, and C. Sioutas (2004a). Diurnal variations of individual organic compound constituents of ultrafine and accumulation mode particulate matter in the los angeles basin, *Environmental Science and Technology*, 38, 1296-1304.

Fine, P.M., G.R. Cass, and B.R.T. Simoneit (2004b). Chemical characterization of fine particle emissions from wood stove combustion of prevalent United States tree species, *Environ. Eng. Sci.*, 21, 6, 705-721.

Fraser, M.P., G.R. Cass, and B.R.T. Simoneit (1998). Gas-phase and particle-phase organic compounds emitted from motor vehicle traffic in a Los Angeles roadway tunnel, *Environ. Sci. Technol.*, 32, 2051-2060.

Fraser M.P., M.J. Kleeman, J.J. Schauer, and G.R. Cass (2000). Modeling the Atmospheric Concentrations of Individual Gas-Phase and Particle-Phase Organic Compounds, *Environ. Sci. Technol.*, 34, 1302-1312.

Gard, E., Mayer, J.E., Morrical, B.D., Dienes, T., Fergenson, D.P., Prather, K.A. (1997). Real-time analysis of individual atmospheric aerosol particles: Design and performance of a portable ATOFMS, *Anal. Chem.*, 69, 4083-4091.

Goldstein, A.H., Daube, B.C., Munger, J.W., and Wofsy, S.C. (1995). Automated in-situ monitoring of atmospheric nonmethane hydrocarbon concentrations and gradients, *J. Atmos. Chem.*, 21, 43-59.

Goldstein, A.H., and I.E. Galbally (2007). Known and Unexplored Organic Constituents in the Earth's Atmosphere, *Environmental Science and Technology*, 41, 5, 1514 – 1521.

Greaves, R.C., Bakley, R.M., and Sievers, R.E. (1985). Rapid sampling and analysis of volatile constituents of airborne particulate matter, *Anal. Chem.*, 57, 2807-2815.

Hering, S.V., Appel, B.R., Cadle, S.H., Cahill, T.A., Fitz, D., Howes, J.E., Knapp, K.T., Turpin, B.J. and McMurry, P.H. (1990). Comparisons of sampling methods for carbonaceous aerosols in ambient air, *Aerosol Sci. Technol.*, 12, 200-213.

Hildemann, L.M., G.R. Markowski, and G.R. Cass (1989). Chemical Composition of Emissions from Urban Sources of Fine Organic Aerosol, *Environ. Sci. Technol.*, 25, 744-759.

Jaekels, J.M., M.S. Bae, and J.J. Schauer (2007). Positive Matrix Factorization (PMF) Analysis of

- Molecular Marker Measurements to Quantify the Sources of Organic Aerosols, *Environ. Sci. Technol.*, 41, 5763-5769.
- Jang, M., Ghio, A.J., and Cao, G. (2006). Exposure of BEAS-2B Cells to Secondary Organic Aerosol Coated on Magnetic Nanoparticles, *Chem. Res. Toxicol.*, 19, 8, 1044 - 1050, 10.1021/tx0503597.
- Jayne, J.T., D.C. Leard, X-F. Zhang, P. Davidovits, K.A. Smith, C.E. Kolb, and D.R. Worsnop (2000). Development of an aerosol mass spectrometer for size and composition analysis of submicron particles, *Aerosol Sci. Technol.*, 33, 49-70.
- Jimenez, J.L., Jayne, J.T., Shi, Q., Kolb, C.E., Worsnop, D.R., Yourshaw, I., Seinfeld, J.H., Flagan, R.C., Zhang, X., Smith, K.A., Morris, J., and Davidovits, P. (2003). Ambient Aerosol Sampling with an Aerosol Mass Spectrometer, *J. Geophys. Res. - Atmospheres*, 108(D7), 8425.
- Kanakidou, M., J.H. Seinfeld, S.N. Pandis, I. Barnes, F.J. Dentener, M.C. Facchini, R. van Dingenen, B. Ervens, A. Nenes, C.J. Nielsen, E. Swietlicki, J.P. Putaud, Y. Balkanski, S. Fuzzi, J. Horth, G.K. Moortgat, R. Winterhalter, C.E.L. Myhre, K. Tsigaridis, E. Vignati, E.G. Stephanou, and J. Wilson (2004). Organic aerosol and global climate modelling: a review, *Atmos. Chem. Phys. Discuss.*, 4, 5855–6024.
- Kenny, L.C., Gussman, R.A., Meyer, M. (2000). Development of a Sharp-Cut Cyclone for Ambient Aerosol Monitoring Applications, *Aerosol Sci. Technol.*, 32(4), 338-358,
- Kim, B.M., Teffera, S., Zeldin, M.D. (2000). Characterization of PM_{2.5} and PM₁₀ in the South Coast air basin of southern California: Part I-- spatial variation, *J. Air and Waste Management Assoc.*, 50, 2034-2044.
- Kreisberg, N.M., S.V. Hering, B.J. Williams, A.H. Goldstein (Submitted). Quantitation of Hourly Speciated Organic Compounds in Atmospheric Aerosols, Measured by In-Situ Thermal Desorption Aerosol Gas Chromatography (TAG), *Aerosol Sci. and Technol.*
- Lamanna, M.S., Goldstein, A.H. (1999). In-situ measurements of C₂-C₁₀ VOCs above a Sierra Nevada ponderosa pine plantation, *J. Geophys. Res.*, 104(D17), 21247-21262.
- Lough, G.C., Schauer, J.J., Lawson, D.R. (2006). Day-of-week trends in carbonaceous aerosol composition in the urban atmosphere, *Atmos. Environ.*, 40, 4137-4149.
- Mazurek, M.A. (2002). Molecular identification of organic compounds in atmospheric complex mixtures and relationship to atmospheric chemistry and sources, *Environmental Health Perspectives*, 110, 995-1003.
- Millet, D.B., A.H. Goldstein, J.D. Allan, T.S. Bates, H. Boudries, K.N. Bower, H. Coe, Y. Ma, M. McKay, P.K. Quinn, A. Sullivan, R.J. Weber, and D.R. Worsnop (, 2004). VOC measurements at Trinidad Head, CA during ITCT 2K2: Analysis of sources, atmospheric composition and aerosol residence times, *Journal of Geophysical Research*, 109, D23, D23S16, 10.1029/2003JD004026.
- Millet, D.B., N.M. Donahue, S.N. Pandis, A. Polidori, C.O. Stanier, B.J. Turpin, and A.H. Goldstein

- (2005). Atmospheric VOC measurements during the Pittsburgh Air Quality Study: Results, interpretation and quantification of primary and secondary contributions, *Journal of Geophysical Research*, 110, D07S07, doi:10.1029/2004JD004601.
- Millet, D.B., A.H. Goldstein, R. Holzinger, B.J. Williams, J.D. Allan, J.-L. Jimenez, D.R. Worsnop, J.M. Roberts, A.B. White, R.C. Hudman, I.T. Bertschi, and A. Stohl (2006). Chemical characteristics of North American surface-layer outflow: Insights from Chebogue Point, *Journal of Geophysical Research*, 111, D23S53, doi:10.1029/2006JD007287.
- Molina, M.J., Ivanov, A.V., Trakhtenberg, S., Molina, L.T. (2004). Atmospheric evolution of organic aerosol, *Geophys. Res. Lett.*, 31, L22104, doi:10.1029/2004GL020910.
- Na, K., A.A. Sawant, C. Song, and D.R. Cocker III (2004). Primary and secondary carbonaceous species in the atmosphere of Western Riverside County, California, *Atmos. Environ.*, 38, 1345-1355.
- Neusüss, C., Pelzing, M., Plewka, A., and Herrmann, H. (2000). A new analytical approach for size-resolved speciation of organic compounds in atmospheric aerosol particles: Methods and first results, *J. Geophysical Research*, 105, 4513-4527.
- NARSTO. (2003). Particulate Matter Sciences for Policy Makers, A NARSTO Assessment.
- Noble, C. A., and Prather, K. A. (1996). Real time measurement of correlated size and composition profiles of individual atmospheric aerosol particles, *Environ. Sci. Technol.*, 30, 2667-2680.
- Nolte C.G., Schauer J.J., Cass, G.R., and Simoneit, B.R.T. (1999). Highly polar organic compounds present in meat smoke, *Environ. Sci. Technol.*, 33, 3313-3316.
- Paatero, P. (1997). Least Squares Formulation of Robust Non-Negative Factor Analysis, *Chemometrics and Intelligent Laboratory Systems*, 37, 23-35.
- Paatero, P. (1999). The Multilinear Engine – A Table-Driven, Least Squares Program for Solving Multilinear Problems, Including the n-Way Parallel Factor Analysis Model, *Journal of Computational and Graphical Statistics*, 1, 4, 854-888.
- Qin, X., K.A. Prather, L. Shields (In Prep.). Single Particle Characterization in Riverside, CA during the SOAR 2005 Campaign – Part 1: Seasonal Comparisons, *In Preparation*.
- Ramanathan, V., Crutzen, P.J., Kiehl, J.T., Rosenfeld, D. (2001). Atmosphere—Aerosols, climate, and the hydrological cycle, *Science*, 294(5549), 2119–2124.
- Raven, J.A., Handley, L.L., and M. Andrews (2004). Global aspects of C/N interactions determining plant-environment interactions, *Journal of Experimental Botany*, 55 (394), 11-25.
- Robinson, A.L., R. Subramanian, N.M. Donahue, A. Bernardo-Bricker, and W.F. Rogge (2006). Source Apportionment of Molecular Markers and Organic Aerosol. 3. Food Cooking Emissions, *Environ. Sci. Technol.*, 40, 7820-7827.

- Rogge, W.F., Hildemann, L.M., Mazurek, M.A., Cass, G.R., and Simoneit, B.R.T. (1991). Sources of fine organic aerosol: 1. Charbroilers and Meat Cooking Operations, *Environ. Sci. Technol.*, 25, 1112-1125.
- Rogge, W. F., Mazurek, M. A., Hildemann, L. M., Cass, G. R., and Simoneit, B. R. T. (1993a). Quantification of urban organic aerosols on a molecular level: Identification, abundance and seasonal variation, *Atmos. Environ.*, 27a, 1309-1330.
- Rogge, W.F., Hildemann, L.M., Mazurek, M.A., Cass, G.R., and Simoneit, B.R.T. (1993b). Sources of fine organic aerosol: 2. Noncatalyst and catalyst-equipped automobiles and heavy-duty diesel trucks, *Environ. Sci. Technol.*, 27, 636-651.
- Rogge, W.F., Hildemann, L.M., Mazurek, M.A., Cass, G.R., and Simoneit, B.R.T. (1993c). Sources of fine organic aerosol. 3. Road dust, tire debris, and organometallic brake lining dust: Roads as sources and sinks, *Environ. Sci. Technol.*, 27, 1892-1904.
- Rogge, W.F., Hildemann, L.M., Mazurek, M.A., Cass, G.R., and Simoneit, B.R.T. (1997a). Sources of fine organic aerosol. 7. hot asphalt roofing tar pot fumes, *Environ. Sci. Technol.*, 31, 2726-2730.
- Rogge, W.F., Hildemann, L.M., Mazurek, M.A., Cass, G. R., and Simoneit, B.R.T. (1997b). Sources of fine organic aerosol. 8. boilers burning no. 2 distillate fuel oil, *Environ. Sci. Technol.*, 31, 2731-2737.
- Rogge, W.F., Hildemann, L.M., Mazurek, M.A., and Cass, G.R. (1998). Sources of fine organic aerosol 9: pine oak and synthetic log combustion in residential fireplaces, *Environ. Sci. Techol.*, 32, 13-22.
- Rouf, MA. (1975). Effect of separation distance on the local impingement heat transfer coefficient in the presence of cross-flow. MS thesis, Department of Mechanical Engineering, University of Minnesota.
- Rudich, Y., N.M. Donahue, T.F. Mentel (2007). Aging of Organic Aerosol: Bridging the Gap Between Laboratory and Field Studies, *Annu. Rev. Phys. Chem.*, 58, 321-352.
- Samet, J.M., F. Dominici, F.C. Curriero, I. Coursac, S.L. Zeger (2000). Fine Particulate Air Pollution and Mortality in 20 U.S. Cities, 1987-1994, *New England Journal of Medicine*, 343 (24), 1742-1749.
- Sawant, A.A., K. Na, X. Zhu, and D.R. Cocker III (2004). Chemical characterization of outdoor PM_{2.5} and gas-phase compounds in Mira Loma, California, *Atmos. Environ.*, 38, 5517-5528.
- Schauer, J.J., Rogge, W.F., Hildemann, L.M., Mazurek, M.A., Cass, G.R., Simoneit, B.R.T. (1996). Source apportionment of airborne particulate matter using organic compounds as tracers, *Atmospheric Environment*, 30, 3837-3855.
- Schauer, J.J., M.J. Kleeman, G.R. Cass, and B.R.T. Simoneit, (1999). Measurement of Emissions from Air Pollution Sources. 2. C₁ through C₃₀ Organic Compounds from Medium Duty Diesel Trucks, *Environ. Sci. Technol.*, 33, 1578-1587.
- Schauer, J.J. and Cass, G.R. (2000). Source apportionment of wintertime gas-phase and particle phase air pollutants using organic compounds as tracers, *Environ. Sci. Technol.*, 34, 1821-1832.

Schauer, J.J., M.J. Kleeman, G.R. Cass, and B.R.T. Simoneit, (2002). Measurement of Emissions from Air Pollution Sources. 2. C₁ through C₃₂ Organic Compounds from Gasoline-Powered Motor Vehicles, *Environ. Sci. Technol.*, 36, 1169-1180.

Schwartz, J., Dockery, D.W., Neas, L.M. (1996). Is daily mortality associated specifically with fine particles?, *J. Air Waste Manage. Assoc.*, 46, 927-939.

Schwartz, J., F. Ballester, M. Saez, S. Perez-Hoyos, J. Bellido, K. Cambra, F. Arribas, A. Canada, M.J. Perez-Boillos, and J. Sunyer (2001). The concentration – response relation between air pollution and daily deaths, *Environ. Health Perspect.*, 104(10), 1001-1006.

Simoneit, B.R.T., and Mazurek, M.A. (1982). Organic matter of the troposphere. II-natural background of biogenic lipid matter in aerosols over the rural western United States, *Atmospheric Environment*, 16, 2139-2159.

Simoneit, B.R.T. (1984). Organic matter of the troposphere—III. Characterization and sources of petroleum and pyrogenic residues in aerosols over the western United States, *Atmos. Environ.*, 18, 51-67.

Simoneit, B.R.T. (1985). Application of molecular marker analysis to vehicular exhaust for source reconciliations, *Int. J. Environ. Anal. Chem.*, 22, 203-233.

Simoneit, B.R.T. (1989). Organic Matter of the Troposphere-V. Application of Molecular Marker Analysis to Biogenic Emissions into the Troposphere for Source Reconciliations, *J. Atmos. Chem.*, 8, 251–275.

Simoneit, B.R.T., W.F. Rogge, M.A. Mazurek, L.J. Standley, L.M. Hildemann, G.R. Cass (1993). Lignin Pyrolysis Products, Lignans, and Resin Acids as Specific Tracers of Plant Classes in Emissions from Biomass Combustion, *Environ. Sci. Technol.*, 27, 2533–2541.

Simoneit, B.R.T., Schauer, J.J., Nolte, C.G., Oros, D.R., Elias, V.O., Fraser, M.P., Rogge, W.F., and Cass, G.R. (1999). Levoglucosan, a tracer for cellulose in biomass burning and atmospheric particles, *Atmos. Environ.*, 33, 173-182.

SOAR (2005). <http://cires.colorado.edu/jimenez-group/Field/Riverside05/>

Solomon, S., D. Qin, M. Manning, R.B. Alley, T. Berntsen, N.L. Bindoff, Z. Chen, A. Chidthaisong, J.M. Gregory, G.C. Hegerl, M. Heimann, B. Hewitson, B.J. Hoskins, F. Joos, J. Jouzel, V. Kattsov, U. Lohmann, T. Matsuno, M. Molina, N. Nicholls, J. Overpeck, G. Raga, V. Ramaswamy, J. Ren, M. Rusticucci, R. Somerville, T.F. Stocker, P. Whetton, R.A. Wood and D. Wratt, (2007). Technical Summary. In: *Climate Change 2007: The Physical Science Basis. Contribution of Working Group I to the Fourth Assessment Report of the Intergovernmental Panel on Climate Change* [Solomon, S., D. Qin, M. Manning, Z. Chen, M. Marquis, K.B. Averyt, M. Tignor and H.L. Miller (eds.)]. Cambridge University Press, Cambridge, United Kingdom and New York, NY, USA.

Standley, L.J., and B.R.T. Simoneit (1987). Characterization of Extractable Plant Wax, Resin, and

- Thermally Matured components in Smoke Particles from Prescribed Burns, *Environ. Sci. Technol.*, 21, 163-169.
- Stein, S.W., Turpin, B.J., Cai, X., Huang, P.-F., McMurry, P.H. (1994). Measurements of relative humidity-dependent bounce and density for atmospheric particles using the DMA-Impactor technique. *Atmos. Environ.*, 28, 1739-1746.
- Stolzenburg, M.R., and Hering, S.V. (2000). A new method for the automated measurement of atmospheric fine particle nitrate, *Environ. Sci. Technol.*, 34, 907-914.
- Stolzenburg, M.R., Dutcher, D.D, Kirby, B.W., Hering, S.V. (2003). Automated measurement of the size and concentration of airborne particulate nitrate, *Aerosol Sci. Technol.*, 37, 537-546.
- Stout, S.A., and G.S. Douglas (2004). Diamondoid Hydrocarbons – Application in the Chemical Fingerprinting of Natural Gas Condensate and Gasoline, *Environmental Forensics*, 5, 225-235.
- Subramanian, R., Donahue, N.M., Bernardo-Bricker, A., Rogge, W.F., Robinson, A.L. (2006). Contribution of motor vehicle emissions to organic carbon and fine particle mass in Pittsburgh, Pennsylvania: Effects of varying source profiles and seasonal trends in ambient marker concentrations, *Atmos. Environ.*, 40, 8002-8019.
- Sullivan, A.P., Weber, R.J., Clements, A.L., Turner, J.R., Bae, M.S., Schauer, J.J. (2004). A method for on-line measurements of water-soluble organic carbon in ambient aerosol particles: Results from an urban site, *Geophys. Res. Lett.*, 31, L13105.
- Tobias, H.J., and Ziemann, P.J., (1999). Compound identification in organic aerosols using temperature programmed thermal desorption particle beam mass spectrometry, *Anal. Chem.*, 71, 3428-3435.
- Tobias, H.J., Kooiman, P.M., Docherty, K.S., Ziemann, P.J. (2000). Real time chemical analysis of organic aerosols using a thermal desorption particle beam mass spectrometer, *Aerosol Sci. Technol.*, 33, 170-190.
- Tuazon, E.C., and R. Atkinson (1990). A product study of the gas phase reaction of isoprene with the OH radical in the presence of NO_x, *International Journal of Chemical Kinetics*, 22, 1221–1236.
- Turpin, B.J., Cary, R.A., and Huntzicker, J.J. (1990). An in-situ, time-resolved analyzer for aerosol organic and elemental carbon, *Aerosol Sci. Technol.*, 12(1), 161-171.
- Turpin, B.J., J.J. Huntzicker (1995), Identification of secondary organic aerosol episodes and quantitation of primary and secondary organic aerosol concentrations during SCAQS, *Atmos. Env.*, V29, 3527-3544.
- Turpin, B.J., J.J. Huntzicker (1991), Secondary formation of organic aerosol in the Los Angeles Basin: a descriptive analysis of organic and elemental carbon concentrations. *Atmospheric Environment* **25A**, pp. 207–215.
- Turpin, B.J., J.J. Huntzicker, S.M. Larson and G.R. Cass, (1991), Los Angeles mid-day particulate

carbon: primary and secondary aerosol. *Envir. Sci. Technol.* **25**, pp. 1788–1793.

U.S. Census Bureau (2008). State and County Quickfacts Website.

<http://quickfacts.census.gov/qfd/states/06000.html>

Volkamer et al. (2006). Secondary organic aerosol formation from anthropogenic air pollution: rapid and higher than expected, *Geophysical Research Letters*, 33, L17811, doi:10.1029/2006GL026899.

Waterman, D., Horsfield, B., Leistner, F., Hall, K., and Smith, S. (2000). Quantification of Polycyclic Aromatic Hydrocarbons in the NIST Standard Reference Material (SRM1649A) Urban Dust Using Thermal Desorption GC/MS, *Anal. Chem.*, 72(15), 3563-3567.

Weschler, C.J. (1984). Indoor-Outdoor Relationships for Nonpolar Organic Constituents of Aerosol Particles, *Environ. Sci. Technol.*, 18, 648-652.

Williams, B.J., Goldstein, A.H., Kreisberg, N.M., Hering, S.V. (2006). An in-situ instrument for speciated organic composition of atmospheric aerosols: Thermal desorption aerosol GC/MS-FID (TAG), *Aerosol Science & Technology*, 40, 627-638.

Williams, B.J., Goldstein, A.H., Millet, D.B., Holzinger, R., Kreisberg, N.M., Hering, S.V., White, A.B., Worsnop, D.R., Allan, J.D., Jimenez, J.L. (2007). Chemical speciation of organic aerosol during the International Consortium for Atmospheric Research on Transport and Transformation 2004: Results from in situ measurements, *J. Geophys. Res.*, 112, D10S26, doi:10.1029/2006JD007601.

Yue, Z., and Fraser, M. (2004a). Characterization of non-polar organic fine particulate matter in Houston, Texas, *Aerosol Sci. Tech.*, 38(1), 60-67.

Yue, Z., and Fraser, M.P. (2004b). Polar organic compounds measured in Fine Particulate matter during TexAQS 2000, *Atmos. Environ.*, 38(20), 3253-3261.

Zhang, Q., Alfarra, M.R., Worsnop, D.R., Allan, J.D., Coe, H., Canagaratna, M.R., and Jimenez, J.L. (2005). Deconvolution and quantification of hydrocarbon-like and oxygenated organic aerosols based on aerosol mass spectrometry, *Environ. Sci. Technol.*, 39, 4938-4952.

Table 1. Subset of authentic standards used for TAG calibration during summer and fall Riverside field studies. The tracking standard was injected regularly throughout both study periods while the auxiliary standards were infrequently injected and primarily serve to confirm MS compound identification through retention times.

Description	Compounds	Used herei n	^a Source
<u>Tracking standard</u>			
Quantifies system performance with ~daily injections	C ₁₂ , C ₁₆ , C ₂₀ , C ₂₈ and C ₃₆ n-alkanes	✓	1
	acenaphthene, chrysene	✓	
	Cholestane	✓	
	cholesterol	✓	
	C ₁₀ , C ₁₇ alkanolic acids		
	dimethoxybenzophenone		
	phthalic acid		
	levoglucosan		
<u>Auxiliary standards</u>			
n-alkane windowing standard	Complete series from C ₈ to C ₄₀ phytane, pristane	✓	2
EPA Method 8270c, contains 116 semi- and non-volatile aromatic and polycyclic aromatic hydrocarbons commonly found in the environment	Partial list: phenanthrene (PHE), anthracene (ANT) fluoranthene (FLA), pyrene (PYR) benz(a)anthracene (BaA), Dimethylbenz(a)anthracene (DaA) Benz(b,k)fluoranthene (BbF, BkF) chrysene (CHY), Benz(a)pyrene (BaP)	✓ ✓ ✓ ✓ ✓ ✓	3

^a (1) Custom standard from Wisconsin State Laboratory of Hygiene; (2) Accustandard, catalogue number DRH-008S-R1 ; (3) Cerilliant, catalogue number ERS-026

Table 2. Compounds contained in the Tracking standard.

^a Tracking standard compound	Formula	^b M, ng	^c m/z	^d RSD, %	^e LOQ, ng
Dodecane	C ₁₂ H ₂₆	22	57	3.2	3.9
Phthalic acid	C ₈ H ₆ O ₄	9.2	104	11	3.3
Decanoic acid	C ₁₀ H ₂₀ O ₂	9.0	70	23	3.2
Acenaphthene	C ₁₂ H ₁₀	4.8	154	11	0.11
Hexadecane	C ₁₆ H ₃₄	4.8	57	3.8	0.30
Eicosane	C ₂₀ H ₄₂	3.8	57	2.6	0.059
Dimethoxybenzophenone	C ₁₅ H ₁₄ O ₃	19	235	3.4	1.2
Chrysene	C ₁₈ H ₁₂	3.6	228	2.2	0.056
Octacosane	C ₂₈ H ₅₈	9.8	57	2.0	0.15
Cholestane	C ₂₇ H ₄₈	0.8	217	1.1	0.018
Cholesterol	C ₂₇ H ₄₆ O	20	368	8.8	3.5
Hexatriacontane	C ₃₆ H ₇₄	20	57	15	7.2

^aBold entries are most relevant to this paper.

^bM= on-column mass injection level

^cm/z = single ion mass to charge ratio used for integration analysis

^dRSD= relative standard deviation of repeated injections at level M

^eLOQ= limit of quantitation defined here as the geometric mean of the mass injection level at which a peak integration is well defined and the next more dilute level where the peak is poorly defined but still above the level of noise.

Table 3. Relative response factors for PAHs in the EPA auxiliary standard relative to the tracking standard compound chrysene (CHY), as defined by equation (4). $R_{i,chy}$ is the response at the 1 ng injection level, and $\bar{R}_{i,chy}$ is the average response over a range of injection levels.

Compound	m/z	SOAR (Summer)		SOAR (Fall)	
		$R_{i,chy}$ (1 ng)	^a $\bar{R}_{i,chy}$	$R_{i,chy}$ (1 ng)	^b $\bar{R}_{i,chy}$
PHE	178	1.12	0.83 ± 0.42	^c 0.95	1.03 ± 0.28
ANT	178	1.30	0.98 ± 0.45	^c 0.95	1.16 ± 0.26
FLU	202	1.48	1.23 ± 0.34	1.06	1.25 ± 0.28
PYR	202	1.80	1.41 ± 0.55	1.25	1.39 ± 0.28
^c (BbF + BkF)/2	252	1.34	1.35 ± 0.01	0.60	0.86 ± 0.22
BaP	276	1.17	1.04 ± 0.19	0.72	0.72 ± 0.14

^a Average and standard deviation in the response factor for standard injections of 1 to 8 ng.

^b Range of injections is 1 to 3 ng, except BaP at 3 ng only.

^c Combined response for co-eluting compounds.

Table 4. Summary statistics for aerosol concentrations and gas phase contributions for calibrated compounds during summer and fall intensive study periods.

Compound	SUMMER						FALL					
	Aerosol Conc. (ng/m ³)				Gas Phase Contribution		Aerosol Conc. (ng/m ³)				Gas Phase Contribution	
	Mean	Stdv	Max	Min	Mean	Stdv	Mean	Stdv	Max	Min	Mean	Stdv
nonadecane	1.86	0.72	4.89	1.11	0.69	0.18	4.06	1.06	8.96	2.86	0.80	0.11
eicosane	1.35	0.44	3.57	0.89	0.83	0.16	2.98	0.67	6.84	2.08	0.89	0.14
heneicosane	1.59	0.68	3.19	0.56	0.46	0.16	1.96	0.45	3.76	1.11	0.44	0.12
docosane	1.01	0.40	1.99	0.35	0.49	0.13	1.38	0.38	3.16	0.65	0.42	0.15
tricosane	0.95	0.29	1.63	0.34	0.45	0.12	1.65	0.73	4.27	0.63	0.21	0.14
tetracosane	0.63	0.23	1.60	0.19	0.39	0.19	2.25	1.20	6.19	0.46	0.08	0.09
pentacosane	1.02	0.43	2.69	0.35	0.17	0.14	3.03	1.71	7.97	0.46	0.03	0.03
hexacosane	0.99	0.46	2.48	0.32	0.05	0.14	3.16	1.75	8.00	0.32	0.01	0.01
heptacosane	1.20	0.48	2.48	0.37	0.01	0.01	2.92	1.71	7.34	0.22	0.01	0.01
octacosane	0.97	0.48	2.18	0.06	0.03	0.05	2.29	1.51	6.62	0.12	0.02	0.02
nonacosane	1.14	0.51	2.57	0.06	0.04	0.14	2.08	1.41	6.09	0.10	0.03	0.05
triacontane	0.77	0.44	1.99	0.07	0.03	0.04	1.59	1.21	5.82	0.11	0.04	0.06
hentriacontane	1.08	0.64	2.70	0.08	0.03	0.04	1.65	1.36	6.35	0.14	0.06	0.07
fluoranthene	0.26	0.09	0.55	0.14	0.63	0.13	0.83	0.17	1.29	0.42	0.48	0.12
pyrene	0.19	0.08	0.54	0.11	0.63	0.14	0.86	0.12	1.21	0.67	0.71	0.11
chrysene	0.15	0.10	0.77	0.01	0.03	0.08	0.44	0.43	2.83	0.03	0.05	0.08
benzob.fluorant.	0.02	0.04	0.22	0.01	0.09	0.12	0.11	0.06	0.39	0.03	0.04	0.02
benzok.fluorant.	0.03	0.04	0.24	0.01	0.12	0.22	0.10	0.05	0.34	0.02	0.05	0.02
benzoe.pyrene	0.03	0.04	0.19	0.01	0.15	0.25	0.14	0.09	0.61	0.04	0.05	0.04
benzoea.pyrene	0.02	0.03	0.15	0.01	0.10	0.17	0.12	0.06	0.35	0.03	0.05	0.03
norhopane	0.03	0.04	0.27	0.00	0.08	0.16	0.07	0.08	0.46	0.01	0.03	0.02
hopane	0.06	0.07	0.46	0.01	0.05	0.11	0.10	0.11	0.66	0.01	0.03	0.02

Bold compounds have negligible gas phase contribution. The gas phase contribution is computed using an evenly spaced subset containing 25% of the data, for which minimum interpolation was required.

Table 5. MSD drift over seasonal focus periods July 29 - August 8 (summer) and November 4 - 14 (fall) as measured by daily-run tracking standard.

	SUMMER				FALL			
	slope	intercept	r2	start-finish (%)	slope	intercept	r2	start-finish (%)
Dodecane	4.3E-04	0.84	0.12	+13	-3.1E-04	1.12	0.04	-8
Phthalic acid	3.1E-04	0.98	0.02	+8	-8.7E-04	1.35	0.14	-21
Decanoic acid	-	-	-	-	-3.4E-04	1.14	0.03	-9
Acenaphthene	2.8E-04	0.90	0.11	+8	-8.1E-04	1.32	0.37	-20
Hexadecane	-5.1E-05	1.03	0.00	-1	-1.0E-03	1.41	0.68	-25
Eicosane	-2.3E-04	1.10	0.31	-6	-9.5E-04	1.37	0.87	-23
Heptadecanoic acid	-8.3E-03	6.13	0.38	-61	7.1E-04	0.66	0.06	26
Dimethoxybenzophenone	-2.0E-03	1.84	0.81	-44	-7.4E-04	1.29	0.29	-18
Chrysene	-1.7E-03	1.73	0.89	-40	-8.9E-04	1.35	0.53	-22
Octacosane	-6.8E-04	1.29	0.68	-18	-9.5E-04	1.37	0.77	-23
Cholestane	-9.6E-04	1.40	0.93	-24	-1.1E-03	1.44	0.88	-26
Cholesterol	-1.5E-03	1.65	0.76	-35	-1.3E-03	1.52	0.72	-30
Hexatriacontane	-8.6E-04	1.35	0.16	-22	-	-	-	-
			Drift =	-18%			Drift =	-17%
			s.d. =	23%			s.d. =	15%

Table 6. Compounds observed by TAG during SOAR campaigns.

Compound Name ^a	MW	Formula	CAS#	Major Ions ^b	Summer	Fall	PMF Source ^c with Highest Correlation (r>0.3 only)							
					PMF	PMF	Summer	Fall	Summer	Fall				
Alkanes														
tridecane	184	c13h28	629-50-5	57, 71, 184	-	-	particle	gas+particle	particle	gas+particle				
tetradecane	198	c14h30	629-59-4	57, 71, 198	-	-	FC	BioSemivol	-	LocalVehicle				
pentadecane	212	c15h32	629-62-9	57, 71, 212	-	-	LocalVehicle	FC	-	LocalVehicle				
hexadecane	226	c16h34	544-76-3	57, 71, 226	-	-	LocalVehicle	LocalVehicle	LocalVehicle	LocalVehicle				
heptadecane	240	c17h36	629-78-7	57, 71, 240	-	-	LocalVehicle	SOA1	LocalVehicle	LocalVehicle				
octadecane	254	c18h38	593-45-3	57, 71, 254	-	-	LocalVehicle	LocalVehicle	LocalVehicle	LocalVehicle				
nonadecane	268	c19h40	629-92-5	57, 71, 268	Y	Y	LocalVehicle	LocalVehicle	RPA	RPA				
eicosane	282	c20h42	112-95-8	57, 71, 282	-	-	SOA1	SOA1	RPA	RPA				
heneicosane	296	c21h44	629-94-7	57, 71, 296	Y	Y	SOA1	SOA1	RPA	RPA				
docosane	310	c22h46	629-97-0	57, 71, 310	Y	Y	SOA1	SOA1	LocalVehicle	LocalVehicle				
tricosane	324	c23h48	638-67-5	57, 71, 324	Y	Y	SOA3	SOA3	LocalVehicle	LocalVehicle				
tetracosane	338	c24h50	646-31-1	57, 71, 338	Y	Y	LocalVehicle	LocalVehicle	LocalVehicle	LocalVehicle				
pentacosane	352	c25h52	629-99-2	57, 71, 352	Y	Y	BioPart+Mixed	BioPart+Mixed	LocalVehicle	LocalVehicle				
hexacosane	366	c26h54	630-01-3	57, 71, 366	Y	Y	BioPart+Mixed	BioPart+Mixed	LocalVehicle	LocalVehicle				
heptacosane	380	c27h56	593-49-7	57, 71, 380	Y	Y	BioPart+Mixed	BioPart+Mixed	LocalVehicle	LocalVehicle				
octacosane	394	c28h58	630-02-4	57, 71, 394	Y	Y	BioPart+Mixed	BioPart+Mixed	LocalVehicle	LocalVehicle				
nonacosane	408	c29h60	630-03-5	57, 71, 408	Y	Y	BioPart+Mixed	BioPart+Mixed	LocalVehicle	LocalVehicle				
triacontane	422	c30h62	638-68-6	57, 71, 422	Y	Y	BioPart+Mixed	BioPart+Mixed	LocalVehicle	LocalVehicle				
hentriacontane	436	c31h64	630-04-6	57, 71, 436	Y	Y	BioPart+Mixed	BioPart+Mixed	BB	BB				
Branched Alkanes														
3-methylpentadecane	226	c16h34	2882-96-4	57, 43, 71, 85, 99, 113, 197	-	-	-	BioPart+Mixed	-	LocalVehicle				
4-methylhexadecane	240	c17h36	25117-26-4	57, 43, 71, 85, 113, 197	-	-	BioSemivol	LocalVehicle	SOA+FC1	LocalVehicle				
2-methylhexadecane	240	c17h36	1560-92-5	57, 43, 71, 85, 113, 197	-	-	LocalVehicle	LocalVehicle	-	LocalVehicle				
3-methylhexadecane	240	c17h36	6418-43-5	57, 43, 71, 85, 113, 211	-	-	LocalVehicle	LocalVehicle	LocalVehicle	LocalVehicle				
4-methylheptadecane	254	c18h38	26429-11-8	57, 43, 71, 85, 113, 211	-	-	LocalVehicle	LocalVehicle	LocalVehicle	LocalVehicle				
2-methylheptadecane	254	c18h38	1560-89-0	57, 43, 71, 85, 113, 211	-	-	LocalVehicle	LocalVehicle	LocalVehicle	LocalVehicle				
3-methylheptadecane	254	c18h38	6418-44-6	57, 71, 85, 113, 225	-	-	LocalVehicle	LocalVehicle	LocalVehicle	LocalVehicle				
4-methyloctadecane	268	c19h40	10544-95-3	57, 43, 71, 85, 113, 225	Y	Y	LocalVehicle	LocalVehicle	LocalVehicle	LocalVehicle				
2-methyloctadecane	268	c19h40	1560-88-9	57, 43, 71, 85, 113, 225	Y	Y	LocalVehicle	LocalVehicle	LocalVehicle	LocalVehicle				
3-methyloctadecane	268	c19h40	6561-44-0	57, 43, 71, 85, 113, 239	Y	Y	LocalVehicle	LocalVehicle	LocalVehicle	LocalVehicle				
pristane	268	c19h40	1921-70-6	57, 71, 43, 85, 113, 183, 268	-	-	LocalVehicle	LocalVehicle	LocalVehicle	LocalVehicle				
phytane	282	c20h42	638-36-8	57, 71, 127, 183, 197	-	-	LocalVehicle	LocalVehicle	LocalVehicle	LocalVehicle				
Alkenes (straight and branched)														
1-tetradecene	196	c14h28	1120-36-1	41, 55, 97, 83, 111, 196	-	-	BioSemivol	BioSemivol	SOA+FC2	LocalVehicle				
1-pentadecene	210	c15h30	13360-61-7	43, 55, 97, 83, 69, 111, 125, 210	Y	Y	SOA2	FC	SOA+FC2	SOA+FC2				
1-hexadecene	224	c16h32	629-73-2	43, 55, 97, 83, 69, 111, 125, 224	-	-	LocalVehicle	BioPart+Mixed	SOA+FC2	LocalVehicle				
1-heptadecene	238	c17h34	6765-39-5	43, 55, 97, 83, 69, 111, 125, 238	-	-	LocalVehicle	SOA1	SOA+FC2	SOA+FC2				
3-heptene, 2,2,4,6,6-pentamethyl-	168	c12h24	123-48-8	97, 168, 57	-	-	-	BioSemivol	-	-				
Alkynes														
3-tetradecyne	194	c14h26	60212-32-0	67, 81, 95, 109, 55, 43	-	-	LocalVehicle	LocalVehicle	BioSemivol	BioSemivol				
2-decyne	138	c10h18	2384-70-5	95, 109, 81, 67, 55, 43	-	-	BioSemivol	BioSemivol	SOA+FC1	BioSemivol				
Polycyclic Aromatic Hydrocarbons (PAH)														
naphthalene	128	c10h8	91-20-3	128	-	-	FC	BioSemivol	LocalVehicle	LocalVehicle				
fluorene	166	c13h10	86-73-7	166, 165	-	-	-	BioPart+Mixed	BB	LocalVehicle				
phenanthrene	178	c14h10	85-01-8	178, 179, 89, 76, 152	-	-	FC	BioPart+Mixed	LocalVehicle	LocalVehicle				
anthracene	178	c14h10	120-12-7	178, 89, 76, 152	Y	Y	LocalVehicle	LocalVehicle	LocalVehicle	LocalVehicle				
fluoranthene	202	c16h10	206-44-0	202, 101	Y	Y	LocalVehicle	SOA1	LocalVehicle	LocalVehicle				
acephenanthrylene	202	c16h10		202, 101	Y	Y	LocalVehicle	LocalVehicle	LocalVehicle	LocalVehicle				
pyrene	202	c16h10	129-00-0	202, 101	Y	Y	LocalVehicle	LocalVehicle	LocalVehicle	LocalVehicle				
11H-benzo[b]fluorene	216	c17h12	243-17-4	216, 215	Y	Y	SOA2	SOA1	LocalVehicle	BB				
7H-benz[de]anthracene	216	c17h12	199-94-0	216, 215	Y	Y	BB	SOA1	LocalVehicle	BB				
benzo[a]anthracene	228	c18h12	56-55-3	228	Y	Y	LocalVehicle	LocalVehicle	LocalVehicle	LocalVehicle				
cyclopenta[cd]pyrene	226	c18h10	27208-37-3	226, 113	Y	Y	LocalVehicle	LocalVehicle	LocalVehicle	LocalVehicle				
chrysene	228	c18h12	218-01-9	228, 226	Y	Y	FC	FC	LocalVehicle	LocalVehicle				
benzo[fluoranthenes + pyrenes]	252	c20h12		252, 126	-	-	FC	FC	LocalVehicle	LocalVehicle				
Branched PAH's														
naphthalene, 1-methyl-	142	c11h10	90-12-0	142, 141, 115	-	-	BioSemivol	BioSemivol	LocalVehicle	LocalVehicle				
naphthalene, 2-methyl-	142	c11h10	91-57-6	142, 141, 115	-	-	FC	BioSemivol	LocalVehicle	LocalVehicle				
dimethyl(naphthalenes)	156	c12h12	581-40-8	156, 141, 115	-	-	FC	BioPart+Mixed	LocalVehicle	LocalVehicle				
trimethyl(naphthalenes)	170	c13h14	2131-41-1	170, 155	-	-	BioPart+Mixed	BioPart+Mixed	BB	LocalVehicle				
naphthalene, 2-phenyl-	204	c16h12	612-94-2	204, 202, 101	-	Y	LocalVehicle	LocalVehicle	SOA+FC2	SOA+FC2				
phenanthrene, 1-methyl	192	c15h12	832-69-9	192, 191	Y	Y	LocalVehicle	LocalVehicle	LocalVehicle	LocalVehicle				
phenanthrene, 2-methyl	192	c15h12	2531-84-2	192, 191	-	Y	LocalVehicle	LocalVehicle	LocalVehicle	LocalVehicle				
anthracene, 1-methyl	192	c15h12	610-48-0	192, 191	-	Y	LocalVehicle	LocalVehicle	LocalVehicle	LocalVehicle				
anthracene, 2-methyl	192	c15h12	613-12-7	192, 191	Y	-	LocalVehicle	LocalVehicle	BB	LocalVehicle				
dimethyl(phenanthrenes+anthracenes)	206	c16h14		206, 191	Y	Y	LocalVehicle	LocalVehicle	LocalVehicle	LocalVehicle				
pyrene, 1-methyl-	216	c17h12	2381-21-7	216, 215	Y	Y	LocalVehicle	BioPart+Mixed	LocalVehicle	BB				
pyrene, 2-methyl-	216	c17h12	3442-78-2	216, 215	Y	Y	LocalVehicle	BioPart+Mixed	BB	BB				
retene	234	c18h18	483-65-8	219, 234, 204	Y	Y	BioPart+Mixed	BioPart+Mixed	BB	BB				
simonellite	252	c19h24		237, 252	Y	-	LocalVehicle	LocalVehicle	BB	BB				
8-isopropyl-1,3-dimethylphenanthrene	248	c19h20	135886-06-5	233, 248, 218	Y	Y	BioPart+Mixed	BioPart+Mixed	BB	BB				
rimuene	272	c20h32	1686-67-5	257, 272	Y	Y	SOA3	SOA3	SOA+FC2	SOA+FC2				
trans-4a,4b, 8,8,2-pentamethyl-1-butylperhydrophenanthrene	318	c23h42	91548-78-6	191, 137, 303, 318	-	-	SOA3	SOA1	RPA	RPA				
Hopanes														
28-nor-17.beta.(H)-hopane	398	c29h50	36728-72-0	191, 177, 109, 123, 137, 217, 398	Y	Y	LocalVehicle	LocalVehicle	LocalVehicle	LocalVehicle				
(17.alpha.H,21.beta.H)-hopane	412	c30h52	471-67-0	191, 412, 397, 206	Y	Y	LocalVehicle	LocalVehicle	LocalVehicle	LocalVehicle				

Table 6 (Continued). Compounds observed by TAG during SOAR campaigns.

Compound Name ^a	MW	Formula	CAS#	Major Ions ^b	Summer	Fall	PMF Source ^c with Highest Correlation (r>0.3 only)			
					PMF	PMF	Summer		Fall	
Cyclohexanes										
n-nonylcyclohexane	210	c15h30	359071	<u>83</u> , <u>82</u> , 55, 41, 67, <u>210</u>	-	-	BioSemivol	BioPart+Mixed	SOA+FC1	LocalVehicle
n-decylcyclohexane	224	c16h32	1795-16-0	<u>83</u> , <u>82</u> , 55, 41, <u>224</u>	-	-	FC	LocalVehicle	LocalVehicle	LocalVehicle
undecylcyclohexane	238	c17h34	54105-66-7	<u>83</u> , <u>82</u> , 55, 97, <u>238</u>	-	-	FC	BioPart+Mixed	LocalVehicle	LocalVehicle
dodecylcyclohexane	252	c18h36	1795-17-1	<u>83</u> , <u>82</u> , 55, 97, <u>252</u>	-	-	LocalVehicle	LocalVehicle	-	LocalVehicle
n-tridecylcyclohexane	266	c19h38	6006-33-3	<u>83</u> , <u>82</u> , 55, 41, <u>266</u>	-	-	LocalVehicle	LocalVehicle	LocalVehicle	LocalVehicle
n-tetradecylcyclohexane	280	c20h40	1795-18-2	<u>83</u> , <u>82</u> , 55, 41, <u>280</u>	Y	Y	SOA1	SOA1	RPA	RPA
n-pentadecylcyclohexane	294	c21h42	6006-95-7	<u>83</u> , <u>82</u> , 55, 41, <u>294</u>	Y	Y	SOA1	SOA1	RPA	LocalVehicle
n-hexadecylcyclohexane	308	c22h44		<u>83</u> , <u>82</u> , 55, 41, <u>308</u>	Y	Y	SOA1	SOA1	LocalVehicle	LocalVehicle
n-heptadecylcyclohexane	322	c23h46	19781-73-8	<u>83</u> , <u>82</u> , 55, 41, <u>322</u>	Y	Y	SOA1	SOA1	LocalVehicle	LocalVehicle
n-octadecylcyclohexane	336	c24h48	929696	<u>83</u> , <u>82</u> , 55, 41, <u>336</u>	Y	Y	LocalVehicle	LocalVehicle	LocalVehicle	LocalVehicle
n-nonadecylcyclohexane	350	c25h50	22349-03-7	<u>83</u> , <u>82</u> , 55, 41, <u>350</u>	Y	Y	LocalVehicle	LocalVehicle	LocalVehicle	LocalVehicle
n-eicosylcyclohexane	364	c26h52	4443-55-4	<u>83</u> , <u>82</u> , 55, 41, <u>364</u>	Y	Y	LocalVehicle	LocalVehicle	LocalVehicle	LocalVehicle
Acids										
heptanoic acid	130	c7h14o2	111-14-8	<u>60</u> , <u>73</u> , 87, 43, 101, <u>130</u>	-	-	FC	FC	SOA+FC2	SOA+FC2
octanoic acid	144	c8h16o2	124-07-2	<u>60</u> , <u>73</u> , 43, 101, 115, <u>144</u>	-	-	FC	FC	SOA+FC2	SOA+FC2
nonanoic acid	158	c9h18o2	112-05-0	<u>60</u> , <u>73</u> , 115, 129, <u>158</u>	-	-	BB	FC	SOA+FC1	SOA+FC1
decanoic acid	172	c10h20o2	334-48-5	<u>60</u> , <u>73</u> , 129, 41, <u>172</u>	-	-	SOA1	FC	SOA+FC1	SOA+FC1
undecanoic acid	186	c11h22o2	112-37-8	<u>60</u> , <u>73</u> , 43, 129, 143, <u>186</u>	-	-	SOA3	SOA2	SOA+FC1	SOA+FC1
dodecanoic acid	200	c12h24o2	143-07-7	<u>73</u> , <u>60</u> , 43, 129, 200, <u>157</u>	Y	Y	SOA3	SOA2	SOA+FC1	SOA+FC1
tetradecanoic acid	228	c14h28o2	544-63-8	<u>73</u> , <u>60</u> , <u>129</u> , 185, <u>228</u>	Y	Y	FC	FC	SOA+FC1	SOA+FC1
hexadecanoic acid	256	c16h32o2	57-10-3	43, 73, <u>60</u> , 129, 213, <u>256</u>	Y	Y	FC	FC	SOA+FC1	SOA+FC1
octadecanoic acid	284	c18h36o2	57-11-4	<u>73</u> , 43, <u>60</u> , 129, <u>284</u> , 241, 185	Y	Y	FC	FC	SOA+FC1	SOA+FC1
benzoic acid	122	c7h6o2	65-85-0	<u>105</u> , <u>77</u> , <u>122</u> , 51	-	Y	SOA2	SOA2	SOA+FC2	SOA+FC2
phenylacetic acid	136	c8h8o2	103-82-2	<u>91</u> , <u>136</u> , 65	-	Y	SOA2	SOA2	SOA+FC1	SOA+FC2
propanoic acid, 2-methyl-, 3-hydroxy-2,4,4-trimethylpentyl ester	286	c16h30o4	74381-40-1	<u>71</u> , <u>43</u> , <u>243</u> , 159, 111, 56	-	-	LocalVehicle	BioSemivol	SOA+FC1	SOA+FC2
oleic acid	282	c18h34o2	112-80-1	55, 69, <u>41</u> , 97, 111, <u>264</u> , 282	Y	Y	LocalVehicle	FC	LocalVehicle	LocalVehicle
phthalic acid	166	c8h6o4	88-99-3	<u>104</u> , <u>148</u>	Y	Y	SOA2	SOA2	SOA+FC2	SOA+FC2
3-methylphthalic acid	162	c9h8o4	4792-30-7	<u>90</u> , 89, <u>162</u> , 118, 63, 134	Y	Y	SOA2	SOA2	SOA+FC2	SOA+FC2
4-methylphthalic acid	162	c9h8o4	19438-61-0	118, <u>90</u> , 89, 63, <u>162</u>	Y	Y	SOA2	SOA2	SOA+FC2	SOA+FC2
Phthalates										
dimethyl phthalate	194	c10h10o4	131-11-3	<u>163</u> , <u>194</u>	-	-	LocalVehicle	BioPart+Mixed	SOA+FC2	SOA+FC2
diethyl phthalate	222	c12h14o4	84-66-2	<u>149</u> , <u>177</u> , 105, 222	-	-	LocalVehicle	FC	SOA+FC2	SOA+FC2
diisobutyl phthalate	278	c16h22o4	84-69-5	<u>149</u> , 205, 278, 104	-	-	SOA1	SOA1	-	SOA+FC2
dibutyl phthalate	278	c16h22o4	84-74-2	<u>149</u> , <u>223</u> , 205, 104, 278	-	-	SOA3	SOA3	SOA+FC2	SOA+FC2
1,8-naphthalic anhydride	198	c12h6o3	81-84-5	<u>198</u> , <u>154</u> , <u>126</u> , 63	Y	Y	SOA2	SOA2	SOA+FC2	SOA+FC2
benzyl butyl phthalate	312	c19h20o4	85-68-7	<u>149</u> , 91, <u>206</u> , 104, 123, 132	Y	Y	SOA1	SOA1	SOA+FC2	SOA+FC2
bis(2-ethylhexyl)phthalate	390	c24h38o4	117-81-7	<u>149</u> , <u>167</u> , 57, 279, 113	Y	Y	FC	FC	LocalVehicle	LocalVehicle
dioctyl phthalate	390	c24h38o4	117-84-0	<u>149</u> , <u>167</u> , 279, 57, 70	Y	Y	SOA1	SOA1	LocalVehicle	LocalVehicle
dinonyl phthalate	418	c26h42o4	84-76-4	149, 293	Y	Y	SOA1	SOA1	LocalVehicle	LocalVehicle
Furanones										
2(3H)-furanone, dihydro-5-ethyl-	114	c6h10o2	695-06-7	<u>85</u>	Y	Y	SOA3	SOA3	SOA+FC2	SOA+FC2
2(3H)-furanone, dihydro-5-propyl-	128	c7h12o2	105-21-5	<u>85</u>	-	-	SOA3	SOA3	SOA+FC2	SOA+FC2
2(3H)-furanone, dihydro-5-butyl-	142	c8h12o2	104-50-7	<u>85</u>	-	-	SOA2	SOA2	SOA+FC2	SOA+FC2
2(3H)-furanone, dihydro-5-pentyl-	156	c9h16o2	104-61-0	<u>85</u>	-	-	SOA3	FC	SOA+FC2	SOA+FC2
2(3H)-furanone, dihydro-5-hexyl-	170	c10h18o2	706-14-9	<u>85</u>	-	-	SOA2	FC	SOA+FC2	SOA+FC2
2(3H)-furanone, dihydro-5-heptyl-	184	c11h20o2	104-67-6	<u>85</u>	-	-	SOA3	SOA2	SOA+FC2	LocalVehicle
2(3H)-furanone, dihydro-5-octyl-	198	c12h22o2	2305-05-7	<u>85</u>	-	-	SOA3	SOA3	SOA+FC2	SOA+FC2
2(3H)-furanone, dihydro-5-decyl-	226	c14h26o2		<u>85</u>	Y	Y	SOA3	SOA3	SOA+FC2	SOA+FC2
2(3H)-furanone, dihydro-5-undecyl-	240	c15h28o2		<u>85</u>	Y	Y	SOA3	SOA3	SOA+FC2	SOA+FC2
2(3H)-furanone, dihydro-5-dodecyl-	256	c16h30o2	730-46-1	<u>85</u> , <u>236</u>	Y	Y	SOA1	SOA1	SOA+FC2	SOA+FC2
2(3H)-furanone, dihydro-5-tridecyl-	272	c17h32o2		<u>85</u>	Y	Y	SOA1	SOA1	LocalVehicle	LocalVehicle
2(3H)-furanone, dihydro-5,5-dimethyl-4-(3-oxobutyl)-	184	c10h16o3	004436-81-1	43, <u>166</u> , <u>98</u> , 111, 151	-	Y	SOA3	SOA3	LocalVehicle	LocalVehicle
2(3H)-furanone, 5-methyl-	98	c5h6o2	591-12-8	<u>98</u> , <u>55</u> , 43	Y	Y	BioSemivol	BioSemivol	SOA+FC2	SOA+FC2
Substituted Guaiacols and Syringols										
vanillin	152	c8h8o3	121-33-5	<u>151</u> , <u>152</u>	Y	Y	BioPart+Mixed	BioPart+Mixed	LocalVehicle	LocalVehicle
syringaldehyde	182	c9h10o4	000134-96-3	<u>182</u> , <u>181</u> , 111, 93	-	-	FC	BioPart+Mixed	SOA+FC2	SOA+FC1
Other Oxygenated Compounds										
nonanal	142	c9h18o	124-19-6	<u>57</u> , <u>98</u>	Y	Y	FC	FC	SOA+FC1	SOA+FC1
tetradecanal	212	c14h28o	124-25-4	<u>57</u> , <u>82</u> , <u>96</u>	-	-	-	SOA1	-	LocalVehicle
cinnamaldehyde	132	c9h8o	104-55-2	<u>132</u> , <u>131</u> , <u>103</u>	-	Y	SOA1	SOA2	SOA+FC2	SOA+FC2
hexyl cinnamic aldehyde	216	c15h20o	101-86-0	<u>117</u> , <u>129</u> , <u>91</u> , <u>216</u>	-	-	BB	BioPart+Mixed	BB	LocalVehicle
levoglucosone	126	c6h6o3	37112-31-5	<u>98</u> , <u>96</u> , 39, 53, 68	Y	Y	FC	FC	BB	BB
2,5-cyclohexadiene-1,4-dione, 2,6-bis(1,1-dimethylethyl)-	220	c14h20o2	719-22-2	<u>177</u> , 135, 149, <u>220</u> , 163	-	-	RPA	BioPart+Mixed	SOA+FC2	SOA+FC2
2-decanone	156	c10h20o	693-54-9	<u>58</u> , <u>156</u>	-	-	-	FC	SOA+FC2	SOA+FC1
2-undecanone	170	c11h22o	112-12-9	<u>58</u> , <u>170</u>	-	-	-	FC	SOA+FC2	SOA+FC2
2-dodecanone	184	c12h24o	6175-49-1	<u>58</u> , <u>184</u>	-	-	FC	FC	SOA+FC1	SOA+FC1
2-undecanone, 6,10-dimethyl-	198	c13h26o	1604-34-8	<u>58</u> , 43, 71, 85, <u>109</u> , <u>180</u> , 198	-	-	-	BioSemivol	-	SOA+FC1
2-tridecanone	198	c13h26o	593-08-8	<u>58</u> , <u>198</u>	-	-	-	BioSemivol	SOA+FC1	SOA+FC1
2-tetradecanone	212	c14h28o	2345-27-9	<u>58</u> , <u>212</u>	-	-	-	-	-	-
2-pentadecanone	226	c15h30o	2345-28-0	<u>58</u> , <u>226</u>	-	-	BioPart+Mixed	BioPart+Mixed	-	LocalVehicle
2-hexadecanone	240	c16h32o	18787-63-8	<u>58</u> , <u>240</u>	-	Y	SOA1	SOA1	SOA+FC2	SOA+FC2
2-heptadecanone	254	c17h34o	2922-51-2	<u>58</u> , <u>254</u>	Y	Y	SOA1	SOA1	LocalVehicle	LocalVehicle
2-octadecanone	268	c18h36o	7373-13-9	<u>58</u> , <u>268</u>	Y	Y	SOA3	SOA1	LocalVehicle	LocalVehicle
2-Pentadecanone,6,10,14-trimethyl	268	c18h36o	502-69-2	<u>58</u> , <u>250</u>	-	-	SOA1	SOA1	LocalVehicle	LocalVehicle
.delta.-octalactone	142	c8h14o2	698-76-0	<u>99</u> , 71, <u>42</u> , 55, <u>114</u>	-	Y	SOA3	SOA2	SOA+FC2	SOA+FC2
.delta.nonalactone	156	c9h16o2	3301-94-8	<u>99</u> , 71, <u>42</u> , 55, <u>114</u>	-	Y	SOA3	SOA2	SOA+FC2	SOA+FC2
.delta.decalactone	170	c10h18o2	705-86-2	<u>99</u> , 71, 43, 55, <u>149</u>	-	Y	FC	FC	SOA+FC2	SOA+FC2
.delta.-dodecalactone	198	c12h22o2	713-95-1	<u>99</u> , 42, 55, 71, <u>114</u>	Y	Y	-	SOA2	BioSemivol	BioSemivol
.delta.tetradecalactone	226	c14h26o2	2721-22-4	<u>99</u> , <u>114</u> , 43, 41, 69, 70	Y	Y	SOA3	SOA3	SOA+FC2	SOA+FC2
2,5-undecanedione	184	c11h20o2	7018-92-0	<u>114</u> , <u>99</u> , 71, <u>53</u>	Y	Y	SOA3	SOA3	SOA+FC2	SOA+FC2
6,7-dodecanedione	198	c12h22o2	13757-90-9	<u>99</u> , 71, 43, 55, <u>198</u>	Y	Y	SOA3	SOA2	SOA+FC1	SOA+FC1

Table 6 (Continued). Compounds observed by TAG during SOAR campaigns.

Compound Name ^a	MW	Formula	CAS#	Major Ions ^b	Summer	Fall	PMF Source ^c with Highest Correlation (>0.3 only)			
					PMF	PMF	Summer		Fall	
Other Oxygenated Compounds (Continued)										
9H-fluoren-9-one	180	c13h8o	486-25-9	<u>180</u> , <u>152</u> , <u>76</u>	-	-	SOA2	SOA2	SOA+FC2	SOA+FC2
9H-fluoren-9-ol	182	c13h10o	001689-64-1	<u>181</u> , <u>182</u> , <u>152</u> , <u>76</u>	-	-	BioSemivol	BioSemivol	-	LocalVehicle
benzophenone	182	c13h10o	119-61-9	<u>105</u> , <u>77</u> , <u>182</u> , <u>51</u>	-	Y	LocalVehicle	FC	SOA+FC2	SOA+FC2
anthraquinone	208	c14h8o2	84-65-1	<u>208</u> , <u>180</u> , <u>152</u> , <u>76</u>	Y	Y	SOA1	SOA1	SOA+FC2	SOA+FC2
tetrahydroquinone	112	c6h8o2	637-88-7	<u>112</u> , <u>56</u> , <u>42</u>	-	-	-	BioPart+Mixed	-	LocalVehicle
benzaldehyde	106	c7h6o	100-52-7	<u>106</u> , <u>77</u>	-	-	BioSemivol	BioSemivol	BioSemivol	BioSemivol
benzeneacetaldehyde	120	c8h8o	122-78-1	<u>91</u> , <u>120</u>	-	-	LocalVehicle	LocalVehicle	BioSemivol	BioSemivol
acetophenone	120	c8h8o	98-86-2	<u>105</u> , <u>120</u>	-	Y	BioSemivol	BioSemivol	SOA+FC2	SOA+FC2
p-methylacetophenone	134	c9h10o	122-00-9	<u>119</u> , <u>91</u> , <u>134</u>	-	Y	BioSemivol	BioSemivol	SOA+FC2	SOA+FC2
sabina ketone	138	c9h14o	513-20-2	<u>81</u> , <u>96</u> , <u>95</u> , <u>41</u> , <u>67</u> , <u>55</u> , <u>123</u> , <u>138</u>	Y	Y	BioSemivol	FC	SOA+FC2	SOA+FC2
methyl chavicol	148	c10h12o	140-67-0	<u>148</u> , <u>121</u> , <u>133</u> , <u>91</u> , <u>105</u>	-	Y	-	BioSemivol	BioSemivol	BioSemivol
2-pentylcyclohexanone	168	c11h20o	32362-97-3	<u>98</u> , <u>71</u> , <u>43</u> , <u>55</u> , <u>83</u> , <u>168</u>	Y	Y	BioSemivol	BioSemivol	BioSemivol	BioSemivol
triacetin	218	c9h14o6	102-76-1	<u>43</u> , <u>103</u> , <u>145</u>	-	-	SOA3	SOA3	SOA+FC2	-
1,6-dioxaspiro[4,4]nonane-2,7-dione	156	c7h8o4	3505-67-7	<u>112</u> , <u>56</u> , <u>84</u>	Y	Y	SOA3	SOA3	SOA+FC2	SOA+FC2
1,4-dioxaspiro[5,5]undecan-3-one	170	c9h14o3		<u>98</u> , <u>170</u> , <u>69</u> , <u>55</u> , <u>41</u> , <u>140</u> , <u>127</u>	Y	Y	BioSemivol	BioSemivol	SOA+FC1	SOA+FC1
2(4H)-benzofuranone, 5,6,7,7a-tetrahydro-4,4,7a-trimethyl-	180	c11h16o2	15356-74-8	<u>111</u> , <u>137</u> , <u>267</u> , <u>180</u>	-	Y	-	BioSemivol	SOA+FC2	SOA+FC2
naphtho[1,2-c]furan-1,3-dione	198	c12h6o3	005343-99-7	<u>198</u> , <u>154</u> , <u>126</u>	Y	Y	SOA2	SOA1	SOA+FC2	SOA+FC2
1,3-isobenzofurandione, 4,7-dimethyl-	176	c10h8o3	005463-50-3	<u>176</u> , <u>104</u> , <u>132</u> , <u>148</u>	Y	Y	SOA2	SOA2	SOA+FC2	SOA+FC2
3,5-di-tert-Butyl-4-hydroxybenzaldehyde	234	c15h22o2	1620-98-0	<u>219</u> , <u>191</u> , <u>234</u> , <u>57</u>	-	-	LocalVehicle	BioPart+Mixed	BB	BB
7,9-di-tert-butyl-1-oxaspiro(4,5)deca-6,9-diene-2,8-dione	276	c17h24o3	82304-66-3	<u>205</u> , <u>217</u> , <u>57</u> , <u>175</u> , <u>189</u> , <u>261</u>	-	Y	-	RPA	SOA+FC1	-
ethanedione, diphenyl-	210	c14h10o2	134-81-6	<u>105</u> , <u>77</u> , <u>51</u> , <u>210</u>	Y	Y	LocalVehicle	LocalVehicle	SOA+FC2	SOA+FC2
1-penten-3-one, 1-phenyl-	160	c11h12o	3152-68-9	<u>131</u> , <u>103</u> , <u>160</u> , <u>77</u>	-	Y	SOA1	SOA2	SOA+FC2	SOA+FC1
ethanone, 2,2-dimethoxy-1,2-diphenyl-	256	c16h16o3	24650-42-8	<u>151</u> , <u>105</u> , <u>77</u> , <u>91</u> , <u>225</u>	Y	Y	SOA3	SOA1	-	-
anthrone	194	c14h10o	90-44-8	<u>194</u> , <u>165</u>	-	Y	BB	LocalVehicle	SOA+FC2	LocalVehicle
xanthon	196	c13h8o2	90-47-1	<u>196</u> , <u>168</u> , <u>139</u>	Y	Y	SOA2	SOA3	SOA+FC2	SOA+FC2
cyclopenta(DEF)phenanthrene	204	c15h8o	5737-13-3	<u>204</u> , <u>176</u>	Y	Y	LocalVehicle	SOA1	SOA+FC2	SOA+FC2
chrysanthenone	150	c10h14o	473-06-3	<u>107</u> , <u>91</u> , <u>122</u> , <u>105</u> , <u>150</u> , <u>79</u>	-	Y	-	BioSemivol	BioSemivol	BioSemivol
Other Esters										
ethylhexyl benzoate	234	c15h22o2	5444-75-7	<u>105</u> , <u>70</u> , <u>112</u>	-	-	-	FC	-	SOA+FC2
benzyl benzoate	212	c14h12o2	120-51-4	<u>105</u> , <u>91</u> , <u>212</u> , <u>77</u> , <u>194</u>	-	Y	BB	FC	SOA+FC1	SOA+FC1
2-ethylhexyl salicylate	250	c15h22o3	118-60-5	<u>120</u> , <u>138</u> , <u>250</u>	-	Y	BB	FC	SOA+FC1	SOA+FC1
isopropyl myristate	270	c17h34o2	110-27-0	<u>43</u> , <u>60</u> , <u>102</u> , <u>228</u> , <u>211</u>	-	-	LocalVehicle	FC	-	LocalVehicle
homomenthyl salicylate	262	c16h22o3	000118-56-9	<u>138</u> , <u>109</u> , <u>120</u> , <u>69</u> , <u>262</u>	Y	Y	FC	FC	SOA+FC1	SOA+FC1
n-hexyl salicylate	222	c13h18o3	6259-76-3	<u>120</u> , <u>138</u> , <u>92</u> , <u>43</u> , <u>222</u>	-	-	-	FC	SOA+FC1	SOA+FC1
hexadecanoic acid, methyl ester	270	c17h34o2	112-39-0	<u>74</u> , <u>87</u> , <u>143</u> , <u>270</u>	Y	Y	SOA1	SOA1	SOA+FC2	SOA+FC2
isopropyl palmitate	298	c19h38o2	142-91-6	<u>256</u> , <u>102</u> , <u>43</u> , <u>60</u> , <u>239</u>	Y	Y	SOA1	SOA1	LocalVehicle	LocalVehicle
dehydroabietic acid, methyl ester	314	c21h30o2	1235-74-1	<u>239</u> , <u>314</u> , <u>299</u>	Y	Y	SOA3	SOA1	BB	BB
hexanedioic acid, bis(2-ethylhexyl)ester	370	c22h42o4	103-23-1	<u>129</u> , <u>112</u> , <u>147</u> , <u>57</u> , <u>70</u> , <u>241</u> , <u>259</u>	Y	Y	LocalVehicle	LocalVehicle	LocalVehicle	LocalVehicle
7-oxodehydroabietic acid, methyl ester	328	c21h28o3	110936-78-2	<u>253</u> , <u>328</u> , <u>313</u> , <u>269</u>	Y	Y	-	-	BB	BB
methylidihydrojasmonate	226	c13h22o3	24851-98-7	<u>83</u> , <u>153</u> , <u>156</u>	-	-	LocalVehicle	FC	LocalVehicle	LocalVehicle
Other Phenyls										
biphenyl	154	c12h10	92-52-4	<u>154</u> , <u>153</u>	-	-	FC	FC	SOA+FC2	LocalVehicle
terphenyl	230	c18h14	26140-60-3	<u>230</u> , <u>115</u>	Y	Y	SOA2	SOA1	SOA+FC2	SOA+FC2
p-methylbiphenyl	168	c13h12	644-08-6	<u>168</u> , <u>167</u> , <u>152</u> , <u>153</u>	-	-	FC	BioPart+Mixed	LocalVehicle	LocalVehicle
3,3'-dimethylbiphenyl	182	c14h14	612-75-9	<u>182</u> , <u>167</u> , <u>165</u> , <u>89</u>	-	-	LocalVehicle	BioPart+Mixed	LocalVehicle	LocalVehicle
2,2'-diethylbiphenyl	210	c16h18	013049-35-9	<u>181</u> , <u>210</u> , <u>165</u>	-	-	LocalVehicle	FC	-	LocalVehicle
4,4'-diisopropylbiphenyl	238	c18h22	18970-30-4	<u>223</u> , <u>238</u> , <u>43</u> , <u>165</u> , <u>178</u> , <u>104</u>	-	-	BioPart+Mixed	BioPart+Mixed	-	LocalVehicle
3,4'-diisopropylbiphenyl	238	c18h22	61434-46-6	<u>223</u> , <u>238</u>	-	-	LocalVehicle	BioPart+Mixed	-	LocalVehicle
1-pentylheptylbenzene (6-phenyl)decane)	246	c18h30	2719-62-2	<u>91</u> , <u>161</u> , <u>175</u> , <u>246</u>	-	-	-	BioPart+Mixed	-	LocalVehicle
1-methylundecylbenzene (2-phenyl)decane)	246	c18h30	2719-61-1	<u>105</u> , <u>246</u>	-	-	BioPart+Mixed	BioPart+Mixed	-	LocalVehicle
methylbis(phenylmethyl)benzene	272	c21h20		<u>181</u> , <u>272</u> , <u>91</u> , <u>165</u>	Y	Y	-	-	BB	BB
Terpenes and Terpenoids										
cumene	120	c9h12	98-82-8	<u>105</u> , <u>120</u>	-	-	FC	BioSemivol	-	LocalVehicle
p-cymene	134	c10h14	99-87-6	<u>119</u> , <u>134</u> , <u>91</u>	-	-	BioSemivol	BioSemivol	-	BioSemivol
limonene	136	c10h16	138-86-3	<u>68</u> , <u>67</u> , <u>93</u> , <u>79</u> , <u>53</u> , <u>121</u> , <u>107</u>	Y	-	BioPart+Mixed	BioPart+Mixed	-	LocalVehicle
m-cymene	119	c10h14	535-77-3	<u>119</u> , <u>134</u> , <u>91</u>	-	-	LocalVehicle	BioSemivol	SOA+FC2	SOA+FC2
p-cymenene	132	c10h12	1195-32-0	<u>132</u> , <u>117</u> , <u>115</u> , <u>91</u>	Y	-	BioSemivol	BioSemivol	BioSemivol	BioSemivol
.alpha.-phellandrene	136	c10h16	99-83-2	<u>93</u> , <u>91</u> , <u>77</u>	Y	Y	BioSemivol	BioSemivol	BioSemivol	BioSemivol
.gamma.-terpinene	136	c10h16	99-85-4	<u>93</u> , <u>91</u> , <u>77</u> , <u>79</u> , <u>136</u>	-	Y	BioSemivol	BioSemivol	BioSemivol	BioSemivol
.delta.3-carene	136	c10h16	13466-78-9	<u>93</u> , <u>91</u> , <u>79</u> , <u>136</u>	Y	Y	BioSemivol	BioSemivol	BioSemivol	BioSemivol
.alpha.-terpinene	136	c10h16	99-86-5	<u>121</u> , <u>136</u> , <u>93</u> , <u>106</u>	-	-	BioSemivol	BioSemivol	SOA+FC1	BB
.beta.-selinene	204	c15h24	17066-67-0	<u>93</u>	-	Y	-	FC	BioSemivol	BioSemivol
cis-.alpha.-bisabolene	204	c15h24	17627-44-0	<u>93</u> , <u>109</u>	Y	Y	BioPart+Mixed	BioPart+Mixed	SOA+FC1	LocalVehicle
.delta.-cadinene	204	c15h24	483-76-1	<u>161</u> , <u>204</u> , <u>134</u> , <u>119</u> , <u>105</u>	Y	Y	BioPart+Mixed	BioPart+Mixed	LocalVehicle	LocalVehicle
calamenene	202	c15h22	483-77-2	<u>159</u> , <u>160</u> , <u>144</u> , <u>202</u>	-	-	-	BioPart+Mixed	-	LocalVehicle
cycloisolongifolene	204	c15h24	28380-07-6	<u>91</u> , <u>105</u> , <u>133</u> , <u>204</u> , <u>161</u> , <u>41</u>	-	-	-	LocalVehicle	SOA+FC2	LocalVehicle
sesquiterpenes	204	c15h24		<u>204</u>	-	-	-	BioPart+Mixed	LocalVehicle	LocalVehicle
eudalene	184	c14h16	490-65-3	<u>169</u> , <u>184</u>	-	-	-	BioPart+Mixed	-	LocalVehicle
cadalene	198	c15h18	483-78-3	<u>183</u> , <u>198</u> , <u>168</u> , <u>153</u>	-	-	FC	BioPart+Mixed	-	LocalVehicle
19-nor-abieta-3,8,11,13-tetraene	254	c19h26		<u>239</u> , <u>254</u> , <u>240</u> , <u>195</u> , <u>178</u> , <u>224</u>	-	-	LocalVehicle	LocalVehicle	BB	BB
19-nor-abieta-4,8,11,13-tetraene + 18-nor-abieta-3,8,11,13-tetraene (mixture)	254	c19h26	23963-75-9	<u>197</u> , <u>239</u> , <u>254</u>	Y	Y	BioPart+Mixed	BioPart+Mixed	BB	BB
19-nor-abieta-4,8,11,13-tetraene	254	c19h26		<u>239</u> , <u>254</u> , <u>199</u> , <u>159</u>	Y	Y	BB	BB	BB	BB
18-norabieta-8,11,13-triene (dehydroabietin)	256	c19h28		<u>159</u> , <u>241</u> , <u>185</u> , <u>256</u>	-	-	BB	BioPart+Mixed	BB	BB
19-nor-abieta-8,11,13-triene	256	c19h28	19407-18-2	<u>159</u> , <u>241</u> , <u>185</u> , <u>256</u>	-	-	BB	BioPart+Mixed	BB	BB
abietatriene (dehydroabietane)	270	c20h30	019407-28-4	<u>255</u> , <u>270</u>	-	-	BB	BB	BB	SOA+FC1
Oxygenated Terpenes										
.alpha.-campholenal	152	c10h16o	4501-58-0	<u>108</u> , <u>93</u> , <u>95</u> , <u>41</u> , <u>67</u> , <u>81</u> , <u>55</u>	-	-	BioSemivol	BioSemivol	BB	BB
cuminic aldehyde	148	c10h12o	122-03-2	<u>133</u> , <u>148</u> , <u>105</u>	-	Y	BioSemivol	BioSemivol	SOA+FC2	SOA+FC2
limonene dioxide 4	168	c10h16o2		<u>43</u> , <u>107</u> , <u>67</u> , <u>55</u> , <u>79</u> , <u>95</u>	-	-	-	BB	BioSemivol	BioSemivol
lily aldehyde	204	c14h20o	80-54-6	<u>189</u> , <u>147</u> , <u>131</u> , <u>204</u>	-	-	-	BioPart+Mixed	BB	BB
nopinone	138	c9h14o	38651-65-9	<u>83</u> , <u>55</u> , <u>109</u>	-	Y	BioSemivol	BioSemivol	SOA+FC1	SOA+FC1
pinonaldehyde	168	c10h16o2		<u>43</u> , <u>83</u> , <u>69</u> , <u>98</u> , <u>109</u>	-	Y	BioSemivol	BioSemivol	BB	BB

Table 6 (Continued). Compounds observed by TAG during SOAR campaigns.

Compound Name ^a	MW	Formula	CAS#	Major Ions ^b	Summer	Fall	PMF Source ^c with Highest Correlation (r>0.3 only)			
					PMF	PMF	Summer		Fall	
Chromenes										
galaxolide 1	258	c18h26o		243, 258, 213	-	-	BioPart+Mixed	BioPart+Mixed	BB	BB
galaxolide 2	258	c18h26o		243, 258, 213	-	-	LocalVehicle	BioPart+Mixed	-	LocalVehicle
precocene I	190	c12h14o2	17598-02-6	175, 190	-	-	SOA1	SOA1	-	BB
precocene II	220	c13h16o3	644-06-4	205, 220, 191, 41, 95, 123, 177	-	-	BB	BB	BB	BB
eupatoriochromene	218	c13h14o3	19013-03-7	203, 218, 185	Y	Y	BioPart+Mixed	BioPart+Mixed	LocalVehicle	LocalVehicle
encecalin	232	c14h16o3	20628-09-5	217, 232	Y	-	BioPart+Mixed	BioPart+Mixed	LocalVehicle	LocalVehicle
Nitrogen and Sulfur Containing Compounds										
hexadecanenitrile	237	c16h31n	629-79-8	41, 43, <u>97</u> , 57, 110 , 111, <u>180</u> , 222	Y	Y	FC	FC	SOA+FC2	SOA+FC2
octadecanenitrile	265	c18h35n	638-65-3	41, 43, <u>97</u> , 57, 110 , 111, <u>222</u>	Y	Y	FC	FC	SOA+FC2	SOA+FC2
4-nitrophenol	139	c6h5no3	100-02-7	139, 65, 109, 39, 81, 93	Y	Y	SOA2	SOA2	SOA+FC1	SOA+FC1
5-methyl-2-nitrophenol	153	c7h7no3	700-38-9	153, 77, 123	Y	-	SOA3	SOA3	-	-
2,6-di-tert-butyl-4-nitrophenol	251	c14h21no3	728-40-5	236, 208, 251	Y	-	BB	BB	BB	BB
diethyltoluamide	191	c12h17no	134-62-3	119, 91, 190	-	-	-	RPA	-	LocalVehicle
p-aminobenzaldehyde	212	c13h12no2	017625-83-1	212, 105, 77	-	Y	BB	LocalVehicle	LocalVehicle	LocalVehicle
phthalimide	147	c8h5no2	85-41-6	147, 76, 104, 50	Y	Y	SOA2	SOA2	SOA+FC2	SOA+FC2
diphenylamine	169	c12h11n	122-39-4	169, 168	Y	-	BioPart+Mixed	BioPart+Mixed	BB	LocalVehicle
6-tert-butyl-2,3-naphthalenedicarbonitrile	234	c16h14n2	32703-82-5	219, 191, 234, 41	Y	-	-	SOA1	BB	BB
benzenamine, 2-nitro-N-phenyl-	214	c12h10n2o2	119-75-5	214, 167, 180, 77	Y	Y	SOA1	SOA1	SOA+FC1	SOA+FC1
penoxaline	281	c13h19n3o4	40487-42-1	252, 281, 191, 162	Y	Y	SOA1	SOA1	SOA+FC1	SOA+FC1
11H-indolo[3,2-c]quinoline	218	c15h10n2	239-09-8	218, 202	Y	Y	SOA1	SOA1	LocalVehicle	LocalVehicle
1,4-benzenediamine, N-(1,3-dimethylbutyl)-N'-phenyl-	268	c18h24n2	793-24-8	211, 268, 183, 253	Y	Y	BioPart+Mixed	BioPart+Mixed	BB	BB
benzenamine, N-[(2-methoxyphenyl)methylene]-	211	c14h13no	369-37-7	93, 119, 91, 77, 211	Y	Y	BioSemivol	BioSemivol	BioSemivol	BioSemivol
4-methoxypyridine	109	c6h7no	620-08-6	109, 79, 52	Y	Y	BioSemivol	BioSemivol	BioSemivol	BioSemivol
pelletierine	141	c8h15no	911650	84, 43, 55, 141	Y	Y	BioSemivol	BioSemivol	SOA+FC1	SOA+FC1
benzenesulfonamide, N-butyl-	213	c10h15no2s	3622-84-2	170, 141, 77, 213	Y	-	SOA3	SOA3	-	-
benzothiazole	135	c7h5ns	95-16-9	135, 108	-	-	-	BioSemivol	BioSemivol	BioSemivol
dibenzothiophene	184	c12h8s	132-65-0	184	-	-	-	BioPart+Mixed	SOA+FC2	SOA+FC2
Chlorine, Fluorine, and Phosphorus Containing Compounds										
trifluralin	335	c13h16f3n3o4	1582-09-8	306, 264, 335, 290	-	-	BioPart+Mixed	BioPart+Mixed	-	-
chlorothalonil	264	c8cl4n2	1897-45-6	266, 264, 268	Y	Y	SOA3	SOA3	LocalVehicle	LocalVehicle
dcpa	330	c10h6cl4o4	1861-32-1	301, 332	-	-	SOA3	SOA3	-	LocalVehicle
2-propanol, 1-chloro-, phosphate (3:1)	326	c9h18cl3o4p	13674-84-5	125, 99, 277, 201, 157, 117, 175	Y	-	SOA3	SOA2	BioSemivol	BioSemivol
bis(1-chloro-2-propyl)(3-chloro-1-propyl)phosphate	326	c9h18cl3o4p	137909-40-1	99, 125, 157, 41, 117, 175, 277	Y	-	SOA3	SOA2	LocalVehicle	LocalVehicle
tris(3-chloropropyl)phosphate	326	c9h18cl3o4p	1067-98-7	99, 43, 157, 175, 117, 277, 291	-	-	BioSemivol	FC	-	-
Siloxanes										
cyclotetrasiloxane, octamethyl-	296	c8h24o4si4	556-67-2	281, 207	-	-	FC	FC	-	-
cyclopentasiloxane, decamethyl-	370	c10h30o5si5	541-02-6	355, 267, 73	-	-	FC	FC	-	SOA+FC2
Other Compounds										
allopregnanone	288	c21h36	000641-85-0	218, 217, 109, 273, 288, 149	-	-	-	SOA1	-	LocalVehicle
1-methyl-2-oxaadamantane	152	c10h16o	6508-22-1	95, 94, 152, 43, 109	Y	Y	BioSemivol	BioSemivol	BioSemivol	BioSemivol
1-methyldiamantane	202	c15h22	26460-76-4	187, 202	Y	Y	BioPart+Mixed	BioPart+Mixed	LocalVehicle	LocalVehicle
furan, 2-ethyl-5-methyl-	110	c7h10o	1703-52-2	95, 110, 43, 67	Y	Y	FC	FC	BioSemivol	BioSemivol
dibenzofuran	168	c12h8o	132-64-9	168, 139	-	-	BioSemivol	FC	SOA+FC2	SOA+FC2
monopalmitin	330	c19h38o4	542-44-9	112, 57, 71, 256, 239, 257	Y	Y	LocalVehicle	LocalVehicle	-	-
monostearin	358	c21h42o4	123-94-4	112, 57, 71, 284, 267, 285	Y	Y	LocalVehicle	LocalVehicle	SOA+FC2	SOA+FC2
Other Parameters										
early.57	Total m/z 57 in high volatility mode (resolved+UCM)				-	-	LocalVehicle	LocalVehicle	LocalVehicle	LocalVehicle
mid.57	Total m/z 57 in mid volatility mode (resolved+UCM)				-	-	SOA1	SOA1	LocalVehicle	LocalVehicle
late.57	Total m/z 57 in low volatility mode (resolved+UCM)				Y	Y	LocalVehicle	LocalVehicle	LocalVehicle	LocalVehicle
secondary.early43	Total 2 ^o m/z 43, high volatility (resolved+UCM)				-	-	SOA2	SOA2	SOA+FC2	SOA+FC2
secondary.mid43	Total 2 ^o m/z 43, mid volatility (resolved+UCM)				-	-	SOA1	SOA2	SOA+FC2	SOA+FC2
secondary.late43	Total 2 ^o m/z 43, low volatility (resolved+UCM)				Y	Y	SOA1	SOA2	SOA+FC2	SOA+FC2
cwax	Excess Odd Carbon from C25-C31 Alkanes				Y	-	BioPart+Mixed	BioPart+Mixed	-	SOA+FC1
ORG	AMS Total Organics				Y	Y	SOA2	SOA2	SOA+FC2	SOA+FC2
PMF parameters										
				AMS	1	1				
				TAG features	3	2				
				TAG compounds	124	141				
				Total	128	144				

^aAmbient compounds in bold print are present in chemical standards inventory.

^bMajor ions in bold have been used as MSD integration ion. Major ions with an underline have been used as additional identification during integrations.

^cAbbreviated Source Names: RPA = Regional Primary Anthropogenic; FC = Food Cooking; BioPart+Mixed = Biogenic Particle + Mixed; BioSemivol = Biogenic Semivolatile; BB = Biomass Burning; SOA+FC1 = SOA + Food Cooking type 1; SOA+FC2 = SOA + Food Cooking type 2.

Table 7. PMF profiles. Summer Factor Contributions to PMF Parameter Concentrations. Reported in Percent of Average Concentration.

Compound	SOA1	SOA2	SOA3	Regional Primary Anthro	Local Vehicle	Food Cooking	BioParticle+Mi xed	Bio Semi- volatile	Biomass Burning	Residual
	(%)	(%)	(%)	(%)	(%)	(%)	(%)	(%)	(%)	(%)
nonadecane	11.5	8.1	0.0	31.2	35.4	9.2	2.7	4.6	0.0	-2.7
heneicosane	30.0	14.1	18.3	20.0	10.2	0.0	3.5	3.3	0.2	0.4
docosane	25.6	11.2	26.7	15.3	6.7	0.7	6.0	2.6	4.0	1.2
tricosane	17.3	3.5	27.3	18.8	7.6	4.5	9.6	3.5	6.1	1.8
tetracosane	4.7	6.5	10.6	29.7	14.1	5.6	16.8	3.8	4.4	3.8
pentacosane	6.1	4.5	2.6	24.8	16.5	7.1	27.1	4.5	6.5	0.3
hexacosane	11.9	4.4	0.0	21.9	15.6	8.4	32.5	0.3	5.6	-0.6
heptacosane	16.1	9.3	0.0	14.1	7.1	6.3	32.2	2.7	11.2	1.0
octacosane	19.5	4.5	0.0	11.8	8.4	7.9	34.7	0.0	11.3	1.8
nonacosane	22.2	7.8	6.7	5.0	5.6	5.0	32.8	0.8	13.3	0.8
triacontane	21.6	1.9	2.3	4.2	13.2	4.5	37.7	2.6	11.9	0.0
hentriacontane	25.2	6.1	1.2	0.0	11.2	6.4	33.0	0.0	17.6	-0.6
dodecanoic.acid	17.6	8.7	27.8	16.0	1.1	6.2	5.8	9.3	5.8	1.8
tetradecanoic.acid	15.0	16.1	23.9	2.6	0.0	28.4	13.4	3.7	0.0	-3.2
hexadecanoic.acid	20.3	4.7	2.8	0.0	0.3	50.0	27.2	0.0	0.0	-5.3
octadecanoic.acid	36.5	3.0	0.0	0.0	0.0	49.0	41.0	0.0	0.0	-29.5
oleic.acid	26.7	10.0	21.7	0.0	28.3	0.0	20.0	10.0	21.7	-38.3
phthalic.acid	15.3	40.0	28.5	9.8	0.0	4.5	0.0	0.0	1.0	1.0
3-methylphthalic.acid	10.0	44.7	17.5	7.8	3.8	9.4	0.0	4.4	3.4	-0.9
4-methylphthalic.acid	16.9	42.8	17.2	7.2	0.0	0.0	1.1	4.7	8.9	1.1
1,8-naphthalicanhydride	13.8	22.0	21.3	0.0	10.0	10.7	8.0	17.6	0.0	-3.3
benzylbutylphthalate	16.1	14.9	21.8	11.8	0.6	12.0	10.2	7.6	3.1	1.8
bis(2ethylhexyl)phthalate	0.0	5.0	0.0	20.0	11.7	18.3	25.0	8.3	0.0	11.7
dioctylphthalate	33.6	21.6	0.0	17.6	3.6	0.0	26.8	0.0	0.0	-3.2
dinonylphthalate	63.9	5.6	21.7	6.7	1.7	0.0	10.6	0.0	0.0	-10.0
dihydro-5-ethyl-2(3H)furanone	3.1	23.4	45.9	6.2	0.0	1.7	0.7	4.8	14.5	-0.3
dihydro-5-decyl-2(3H)furanone	11.4	11.0	20.9	15.5	3.4	9.3	4.8	11.6	10.9	1.2
dihydro-5-undecyl-2(3H)furanone	11.3	9.5	29.7	8.4	0.8	14.2	10.3	7.4	5.0	3.4
dihydro-5-dodecyl-2(3H)furanone	16.0	11.5	26.7	9.2	2.9	15.6	10.4	6.9	0.2	0.6
dihydro-5-tridecyl-2(3H)furanone	22.1	11.4	23.6	10.5	8.3	1.4	5.5	6.2	7.4	3.6
pentadecene	9.8	22.0	3.8	18.8	3.5	8.5	3.3	29.0	0.0	1.5
hexadecanenitrile	4.0	4.5	7.9	23.0	0.9	36.8	10.0	9.6	3.0	0.4
octadecanenitrile	3.4	2.1	8.2	23.2	0.8	44.5	12.9	7.1	0.0	-2.1
tetradecylcyclohexane	25.8	9.7	0.9	24.8	17.3	9.1	3.6	0.0	6.7	2.1
pentadecylcyclohexane	29.5	9.7	15.1	21.4	8.9	4.9	1.9	3.0	3.5	2.2
hexadecylcyclohexane	24.5	17.1	15.3	13.4	6.8	2.6	6.8	8.4	3.2	1.8
heptadecylcyclohexane	24.1	4.4	19.7	11.5	14.7	0.0	11.5	2.6	7.6	3.8
octadecylcyclohexane	14.6	0.0	6.7	16.7	32.5	2.1	21.7	0.0	1.7	4.2
nonadecylcyclohexane	9.5	0.0	0.0	20.0	35.8	0.0	31.6	0.0	8.4	-5.3
eicosylcyclohexane	15.8	0.0	1.1	11.1	31.6	0.0	28.4	0.5	11.1	0.5
nonanal	9.7	1.8	0.0	3.3	0.0	28.5	16.7	19.2	20.3	0.5
levoglucosenone	0.0	18.3	0.0	5.0	26.7	25.0	3.3	20.0	1.7	0.0
2-heptadecanone	33.0	0.0	28.4	9.7	6.2	5.7	0.0	5.1	9.7	2.2
anthraquinone	16.8	19.0	22.8	6.8	6.5	12.3	11.3	2.5	1.5	0.8
homomenthylsalicylate	0.0	0.0	3.7	13.0	9.3	23.7	0.0	20.0	28.7	1.5
hexadecanoic.acid-methylester	33.7	7.1	0.0	17.1	13.7	17.7	1.4	0.0	8.9	0.3
isopropylpalmitate	29.1	19.1	28.2	15.3	3.8	1.2	2.6	0.0	2.4	-1.8
dehydroabietic.acid-methylester	25.0	0.0	31.3	5.0	1.3	4.2	13.8	0.8	14.2	4.6
1-methylphenanthrene	0.0	0.0	11.5	19.1	26.7	14.2	4.5	3.0	19.7	1.2
2-methylanthracene	0.0	7.4	12.2	33.0	20.9	7.8	15.2	0.0	11.7	-8.3
fluoranthene	15.9	7.4	5.1	24.6	17.2	8.7	2.8	0.0	15.6	2.6
acephenanthrylene	26.2	9.6	2.3	0.4	25.4	1.2	30.8	0.0	6.5	-2.3
pyrene	10.4	6.3	2.2	19.6	29.3	6.3	8.1	0.0	17.8	0.0
retene	19.1	2.3	11.4	8.9	6.3	8.9	26.0	4.6	11.7	0.9
benzo(a)anthracene	19.4	0.0	17.8	0.0	20.6	4.4	20.6	0.0	15.6	1.7
cyclopenta(cd)pyrene	21.7	11.3	7.1	0.4	32.1	5.0	21.3	0.0	1.7	-0.4
chrysene	7.2	18.3	8.9	0.0	13.3	19.4	15.6	14.4	0.0	2.8
norhopane	1.3	0.0	0.0	23.8	67.5	2.5	7.5	0.0	3.8	-6.3
hopane	0.0	11.0	0.0	4.0	63.0	0.0	13.0	0.0	14.0	-5.0
d-cadinene	0.0	0.0	0.0	0.0	0.0	5.4	67.7	27.7	14.6	-15.4
4-nitrophenol	8.2	50.0	12.4	0.0	0.0	17.1	12.4	4.7	0.0	-4.7
diphenylamine	0.0	0.0	0.6	11.2	11.8	7.6	20.6	14.1	35.9	-1.8
dimethylisobenzofurandione	18.7	34.6	1.8	1.8	6.2	0.0	0.0	18.5	16.4	2.1
naphthofurandione	10.5	21.4	23.6	2.5	10.5	12.5	1.6	4.1	10.7	2.7
methylfuranone	9.0	24.6	5.0	6.5	2.1	2.5	1.3	39.0	8.5	1.7
octadecanone	26.5	8.8	34.4	2.6	2.9	4.7	8.2	4.1	7.1	0.6
d-dodecalactone	10.4	6.2	23.8	16.9	8.1	16.9	0.0	13.5	7.3	-3.1
d-tetradecalactone	18.8	3.8	41.6	13.1	2.8	1.6	0.0	8.4	8.8	1.2

Table 7 (Continued). PMF profiles. Summer Factor Contributions to PMF Parameter Concentrations. Reported in Percent of Average Concentration.

Compound	SOA1	SOA2	SOA3	Regional Primary Anthro	Local Vehicle	Food Cooking	BioParticle+Mi xed	Bio Semi- volatile	Biomass Burning	Residual
	(%)	(%)	(%)	(%)	(%)	(%)	(%)	(%)	(%)	(%)
sabina.ketone	14.4	3.1	15.3	2.2	3.1	9.4	0.0	30.6	17.5	4.4
pentylcyclohexanone	4.0	10.0	0.0	10.0	3.7	15.7	2.7	57.0	0.0	-3.0
dioxaspirononanedione	4.7	17.9	38.9	3.2	0.0	10.8	5.0	9.7	7.4	2.4
dioxaspiroundecanone	12.6	18.4	0.0	0.0	2.4	5.3	2.9	50.5	7.6	0.3
diphenyl.ethanedione	0.0	2.2	8.3	26.7	20.0	0.0	0.0	15.0	20.6	7.2
dimethoxydiphenyl.ethanone	13.1	0.0	32.3	0.4	1.9	31.9	4.6	5.8	18.1	-8.1
xanthone	14.0	27.6	24.7	9.8	0.0	7.1	0.0	8.7	8.0	0.2
cyclopenta(def)phenanthrenone	9.6	20.6	1.5	18.3	11.3	9.2	0.0	6.7	21.7	1.2
hexanedioic.acid-bisethylhexylester	8.1	0.0	11.4	18.6	12.1	6.3	9.3	12.1	18.6	3.5
7-oxodehydroabietic.acid-methylester	18.6	3.6	1.4	10.7	8.6	10.7	10.0	6.4	32.9	-2.9
dimethyl(phenanthrenes+anthracenes)	5.0	1.1	20.3	12.9	20.0	3.9	9.7	3.4	20.8	2.9
isopropyl-dimethylphenanthrene	7.8	0.0	1.1	31.1	3.3	11.1	26.7	0.0	20.0	-1.1
benzo(b)fluorene	6.8	19.1	15.5	0.0	10.9	14.8	8.9	8.9	13.4	1.8
benz(de)anthracene	8.1	10.7	13.6	5.0	9.1	7.4	7.1	8.1	27.9	2.9
1-methylpyrene	7.9	16.7	15.4	0.0	14.6	10.8	15.8	9.6	9.2	0.0
2-methylpyrene	5.5	6.6	14.9	5.3	14.7	4.0	3.2	10.9	31.5	3.4
anthracene	0.0	1.4	8.1	15.7	38.6	12.4	21.4	0.0	5.2	-2.9
simonellite	21.0	0.0	11.0	8.0	19.0	0.0	10.0	30.0	12.0	-11.0
vanillin	0.0	0.0	0.4	0.0	8.5	0.0	41.9	19.2	39.6	-9.6
ethylmethylfuran	13.5	6.0	15.1	11.2	1.6	16.5	3.7	30.0	0.0	2.3
limonene	0.0	0.0	0.0	8.0	9.0	17.0	25.0	40.0	29.0	-28.0
p-cymene	0.0	0.0	0.0	5.5	5.5	18.2	0.5	62.3	11.8	-3.6
a-phellandrene	3.8	0.0	0.0	3.1	0.0	10.3	1.4	55.9	25.9	-0.3
d-3-carene	3.0	3.9	1.2	7.0	0.0	1.5	2.7	60.0	25.2	-4.5
cis-a-bisabolene	12.1	0.0	16.1	9.7	0.0	2.4	19.1	21.2	15.8	3.6
eupatoriochromene	0.0	0.0	0.0	0.0	0.0	0.0	90.0	18.6	0.0	-8.6
encecalin	11.0	0.0	0.0	3.0	36.0	0.0	58.0	14.0	0.0	-22.0
norabietatetraene-mixture	18.2	9.1	0.0	9.1	0.5	1.8	28.2	0.0	34.1	-0.9
norabieta.4.8.11.13.tetraene	22.6	2.1	0.0	18.9	2.1	0.0	14.2	0.0	46.3	-6.3
rimuene	11.1	0.0	28.1	11.6	10.0	7.6	0.0	16.5	12.4	2.7
5-methyl-2-nitrophenol	16.7	0.0	117.8	0.0	0.0	0.0	0.0	0.0	0.0	-34.4
di.tert.butylnitrophenol	28.7	0.0	0.0	0.0	23.3	0.0	6.0	2.0	56.0	-16.0
butylbenzenesulfonamide	18.7	5.6	36.4	9.2	2.3	0.0	8.5	6.7	11.3	1.3
phthalimide	5.1	24.9	19.2	24.3	2.2	12.7	0.0	9.5	0.3	1.9
tert.butylnaphthalenedicarbonitrile	22.4	9.5	20.5	15.2	0.0	0.0	21.4	11.0	13.3	-13.3
nitrophenylbenzenamine	29.7	10.9	5.6	0.0	11.6	5.6	1.9	4.4	28.1	2.2
penoxaline	58.4	0.0	27.9	10.5	5.3	0.0	4.7	0.0	0.0	-6.8
indoloquinoline	12.8	12.3	14.7	9.6	8.5	13.2	11.9	5.5	9.2	2.3
dimethylbutylphenyl.benzenediamine	27.6	0.0	2.4	1.6	0.0	11.6	30.8	0.0	26.4	-0.4
methoxyphenylmethylene.benzenamine	2.4	0.0	0.6	2.7	0.0	11.8	0.0	55.8	27.0	-0.3
methoxypyridine	0.0	0.0	3.7	13.0	2.2	15.6	0.0	67.8	0.0	-2.2
pelletierine	2.2	16.9	0.6	0.0	0.3	13.3	1.7	63.6	0.3	1.1
terphenyl	10.0	17.8	11.4	13.5	6.5	12.4	7.8	7.8	10.2	2.7
methylbisphenylmethyl.benzene	0.7	9.3	17.3	8.7	16.0	12.0	2.0	14.0	21.3	-1.3
chlorothalonil	0.0	0.0	24.0	18.1	0.0	0.0	2.3	24.9	27.2	3.4
chlorophosphatepropanol	11.8	10.8	30.3	16.0	0.0	10.8	5.5	11.8	2.0	1.3
bis.13.chloropropylphosphate	11.3	13.5	28.8	15.0	0.3	8.5	5.3	14.0	1.3	2.3
undecanedione	1.3	31.3	37.5	17.9	0.0	1.3	2.5	12.5	0.8	-5.0
dodecanedione	0.0	36.8	45.6	7.2	0.0	0.0	0.0	17.2	4.4	-11.2
methyloxadamantane	0.0	0.0	0.0	7.1	2.1	10.7	1.1	72.9	7.9	-1.8
methyldiamantane	0.0	0.0	0.0	0.0	0.0	20.0	85.0	17.5	0.0	-22.5
monopalmitin	14.0	0.0	0.0	0.0	38.0	0.0	20.0	26.0	0.0	2.0
monostearin	21.7	0.0	0.0	0.0	35.0	0.0	21.7	20.0	0.0	1.7
late.57	11.0	1.5	0.0	14.0	39.0	6.0	27.0	0.0	1.5	0.0
secondary.late43	17.5	18.5	19.5	6.5	6.0	12.0	12.0	7.5	0.0	0.5
cwax	16.8	12.6	7.4	1.5	2.4	3.5	27.6	6.8	16.5	5.0
4-methyloctadecane	0.0	5.4	0.0	19.2	54.6	30.8	0.0	6.9	0.0	-16.9
2-methyloctadecane	0.0	2.1	1.1	25.8	44.2	22.6	0.0	8.9	5.8	-10.5
3-methyloctadecane	0.0	0.0	0.0	16.7	46.7	25.0	1.7	18.3	3.9	-12.2
AMS.Organics	10.0	18.9	18.0	15.0	3.5	6.2	6.8	13.5	6.1	2.1

Table 8. PMF profiles. Fall Factor Contributions to PMF Parameter Concentrations. Reported in Percent of Average Concentration.

Compound	SOA+		Regional Primary			Biomass		Residual
	FoodCooking1 (%)	FoodCooking2 (%)	Anthro (%)	Local Vehicle (%)	Bio Semivolatile (%)	Burning (%)		
nonadecane	0.0	4.2	71.7	34.2	0.0	0.0	-10.0	
heneicosane	1.1	12.9	56.3	18.0	8.0	0.0	3.7	
docosane	0.0	14.3	32.3	31.7	9.0	9.3	3.3	
tricosane	0.0	20.3	15.9	32.8	9.3	19.3	2.4	
tetracosane	0.0	25.6	5.6	30.0	8.5	27.0	3.3	
pentacosane	2.1	26.1	0.0	32.9	9.6	27.5	1.8	
hexacosane	4.0	35.3	0.0	24.0	8.0	27.7	1.0	
heptacosane	12.2	30.0	0.0	23.4	6.6	28.8	-0.9	
octacosane	11.9	29.2	0.0	25.8	3.1	34.2	-4.2	
nonacosane	17.7	24.2	0.0	30.8	2.7	29.6	-5.0	
triacontane	16.8	20.0	0.0	37.4	0.5	32.6	-7.4	
hentriacontane	33.2	8.9	0.0	30.0	0.0	30.5	-2.6	
dodecanoic.acid	30.0	16.3	26.3	10.0	11.9	9.7	-4.1	
tetradecanoic.acid	48.0	2.0	7.3	22.0	14.7	9.3	-3.3	
hexadecanoic.acid	42.5	0.0	0.0	30.8	8.3	17.5	0.8	
octadecanoic.acid	55.6	0.0	0.0	32.2	0.0	31.1	-18.9	
oleic.acid	50.0	0.0	0.0	50.0	0.0	43.3	-43.3	
phthalic.acid	15.2	57.1	24.8	0.0	1.7	0.0	1.2	
3-methylphthalic.acid	17.2	58.1	20.6	0.9	0.3	2.5	0.3	
4-methylphthalic.acid	24.4	45.1	30.5	1.5	0.0	0.0	-1.5	
1,8-naphthalicanhydride	30.5	56.8	0.0	22.1	0.0	0.0	-9.5	
benzylbutylphthalate	11.7	42.4	0.0	23.4	20.0	8.6	-6.2	
bis(2ethylhexyl)phthalate	3.0	39.0	0.0	36.0	11.0	8.0	3.0	
dioctylphthalate	20.0	1.0	9.0	63.0	0.0	6.0	1.0	
dinonylphthalate	6.3	3.8	28.8	35.0	8.8	18.8	-1.2	
dihydro-5-ethyl-2(3H)furanone	13.7	63.3	17.0	0.0	5.7	0.0	0.3	
dihydro-5-decyl-2(3H)furanone	16.8	45.8	14.2	17.7	6.1	0.0	-0.6	
dihydro-5-undecyl-2(3H)furanone	15.9	27.7	29.5	15.0	4.1	1.8	5.9	
dihydro-5-dodecyl-2(3H)furanone	16.5	55.4	5.0	15.4	0.0	5.0	2.7	
dihydro-5-tridecyl-2(3H)furanone	7.9	17.5	21.8	37.1	8.9	6.4	0.4	
pentadecene	4.5	70.0	0.0	13.6	2.3	10.0	-0.5	
hexadecanenitrile	3.8	78.1	0.0	9.0	14.3	0.0	-5.2	
octadecanenitrile	5.0	86.5	0.0	10.5	15.0	0.0	-17.0	
tetradecylcyclohexane	6.1	20.4	53.2	10.0	6.1	0.0	4.3	
pentadecylcyclohexane	0.9	17.2	51.3	14.7	9.7	3.1	3.1	
hexadecylcyclohexane	0.2	19.5	29.5	24.3	13.6	9.0	3.8	
heptadecylcyclohexane	0.0	18.0	12.4	52.8	10.8	6.0	0.0	
octadecylcyclohexane	0.0	12.7	0.0	68.7	7.3	6.7	4.7	
nonadecylcyclohexane	0.0	10.7	0.0	66.4	9.3	10.7	2.9	
eicosylcyclohexane	0.0	15.7	0.0	67.9	4.3	13.6	-1.4	
nonanal	32.7	33.2	7.7	0.0	6.8	16.8	2.7	
levoglucosenone	5.5	32.9	4.7	9.7	10.3	33.7	3.2	
hexadecanone.2	17.4	34.8	38.1	11.1	0.0	2.2	-3.7	
heptadecanone.2	15.9	28.8	25.3	13.2	8.8	7.9	0.0	
anthraquinone	20.0	52.9	0.0	27.5	1.8	7.5	-9.6	
homomenthylsalicylate	27.1	14.1	22.9	13.5	5.3	11.8	5.3	
benzylbenzoate	35.5	43.4	5.2	10.7	4.5	3.1	-2.4	
ethylhexylsalicylate.2	11.5	12.9	40.0	4.6	10.5	14.1	6.3	
hexadecanoic.acid-methylester	3.2	31.1	35.0	9.1	10.0	10.7	0.9	
isopropylpalmitate	4.0	13.3	34.0	23.8	19.3	4.5	1.3	
dehydroabietic.acid-methylester	13.6	0.9	0.9	10.0	0.0	70.9	3.6	
1-methylphenanthrene	13.1	9.7	29.7	36.6	6.6	8.6	-4.1	
2-methylphenanthrene	12.4	7.2	34.1	36.6	11.4	3.8	-5.5	
1-methylanthracene	3.6	1.2	44.0	30.4	12.4	10.4	-2.0	
fluoranthene	5.3	26.8	33.2	18.4	10.8	5.3	0.3	
acephenanthrylene	18.8	0.0	6.3	80.0	0.0	5.0	-10.0	
pyrene	7.1	3.9	33.9	41.6	9.7	1.3	2.6	
retene	0.0	4.3	15.7	1.4	5.7	77.1	-4.3	
benzo(a)anthracene	18.3	20.8	0.0	40.8	2.5	17.5	0.0	
cyclopenta(cd)pyrene	16.9	0.0	1.5	82.3	3.1	0.0	-3.8	
chrysene	20.9	9.1	0.0	54.5	0.0	14.5	0.9	
norhopane	2.5	9.2	0.0	82.5	0.0	0.0	5.8	
hopane	4.5	6.4	0.0	87.3	0.0	0.0	1.8	
d-cadinene	4.3	5.7	21.4	28.6	27.1	24.3	-11.4	
4-nitrophenol	38.8	12.5	8.8	16.3	1.3	18.8	3.8	
benzoic.acid	11.6	52.9	18.0	0.0	14.7	2.0	0.9	
phenylacetic.acid	26.6	38.6	22.0	0.0	10.0	2.0	0.9	
dimethylisobenzofurandione	24.0	45.8	19.5	6.3	0.0	4.3	0.3	
naphthofurandione	21.0	68.6	0.0	18.1	0.0	0.0	-7.6	
dihydrodimethylxobutylfuranone	2.6	20.6	28.1	18.7	20.0	14.8	-4.8	
methylfuranone	20.5	54.9	14.3	0.0	10.3	2.2	-2.2	
pinonaldehyde	7.6	0.0	18.0	0.0	18.4	57.6	-1.6	
nopinone	22.1	15.8	30.4	0.0	4.2	28.8	-1.3	
octadecanone	18.1	20.6	30.6	25.6	0.0	13.1	-8.1	
d-octalactone	17.9	63.4	15.9	0.0	0.7	5.2	-3.1	

Table 8 (Continued). PMF profiles. Fall Factor Contributions to PMF Parameter Concentrations. Reported in Percent of Average Concentration.

Compound	SOA+	SOA+	Regional	Local Vehicle	Bio Semivolatile	Biomass	Residual
	FoodCooking1	FoodCooking2	Primary Anthro				
	(%)	(%)	(%)	(%)	(%)	(%)	(%)
d-nonalactone	22.6	63.0	9.1	0.0	6.1	0.4	-1.3
d-decalactone	15.6	49.3	19.3	0.0	13.3	2.6	0.0
d-dodecalactone	7.1	4.3	25.7	11.4	51.4	4.3	-4.3
d.tetradecalactone	11.0	41.9	16.5	14.8	11.6	2.6	1.6
benzophenone	3.1	38.1	27.6	0.0	11.7	15.9	3.5
acetophenone	6.5	40.0	16.8	0.0	25.8	8.1	2.9
sabina.ketone	10.3	57.6	10.0	0.0	17.9	6.5	-2.4
methylacetophenone	7.0	47.7	3.7	1.3	32.3	5.0	3.0
methyl.chavicol	1.0	37.6	4.8	4.3	30.0	24.8	-2.4
chrysanthenone	0.0	15.3	28.9	1.6	46.3	18.9	-11.1
pentylcyclohexanone	23.5	23.9	5.7	4.3	40.9	4.8	-3.0
dioxaspirononanedione	22.6	47.8	12.2	0.0	20.9	0.0	-3.5
tetrahydrotrimethylbenzofuranone	0.0	46.4	26.4	0.4	16.8	9.3	0.7
cinnamaldehyde	18.1	33.7	30.0	7.4	11.1	0.4	-0.7
phenylpentenone	20.6	36.2	39.4	0.0	6.5	0.0	-2.6
dioxaspirodecaneone	34.0	30.0	8.3	2.0	14.0	13.0	-1.3
diphenyl.ethanedione	18.5	34.4	24.4	19.6	18.9	0.0	-15.9
anthrone	14.5	34.0	16.0	19.3	11.2	5.0	0.0
dimethoxydiphenyl.ethanone	0.0	26.7	38.8	7.5	10.0	14.6	2.5
di.tert.butylloxaspirodecadienedione	21.1	30.0	33.3	1.1	14.4	14.4	-14.4
xanthone	26.5	71.8	0.0	15.3	0.0	0.0	-13.5
cyclopenta(def)phenanthrenone	13.5	58.5	0.0	33.5	0.0	0.0	-5.5
hexanedioic.acid-bisethylhexylester	4.3	45.7	0.0	34.3	16.4	7.9	-8.6
7-oxodehydroabietic.acid-methylester	15.0	11.7	7.5	0.0	0.0	66.7	-0.8
phenylnaphthalene	16.5	34.9	18.6	17.0	9.3	8.8	-5.1
dimethyl(phenanthrenes+anthracenes)	5.9	0.0	32.6	36.7	11.9	18.1	-5.2
isopropyl.dimethylphenanthrene	0.0	9.3	0.0	6.7	10.7	86.0	-12.7
benzo(b)fluorene	19.6	0.0	18.2	31.4	5.0	26.1	-0.4
benz(de)anthracene	16.7	0.0	21.1	32.2	5.2	25.6	-0.7
1-methylpyrene	26.5	0.0	15.5	47.0	1.5	15.0	-5.5
2-methylpyrene	8.2	0.0	31.4	21.4	8.6	35.0	-4.5
anthracene	10.0	5.9	21.2	52.4	10.0	8.2	-7.6
vanillin	7.6	31.0	25.2	18.6	6.7	21.9	-11.0
ethylmethylfuran	7.3	10.0	0.0	5.3	68.0	12.7	-3.3
a-phellandrene	15.4	0.0	13.1	0.8	71.5	8.5	-9.2
d-3-carene	5.5	44.1	0.0	4.1	41.4	9.1	-4.1
g-terpinene	11.8	1.8	8.2	4.5	66.4	12.7	-5.5
cuminic.aldehyde	2.3	52.3	14.3	0.0	20.3	7.0	3.7
limonene.dioxide.4	0.0	0.0	34.4	0.0	30.0	43.3	-7.8
b-selinene	0.0	5.0	41.3	0.0	43.8	36.3	-26.3
cis-a-bisabolene	18.9	15.8	18.9	17.9	14.2	15.8	-1.6
eupatoriochromene	0.0	0.0	21.4	72.9	0.0	45.7	-40.0
norabietatetraene-mixture	3.1	16.3	0.0	10.0	1.9	74.4	-5.6
norabieta.4.8.11.13.tetraene	3.1	3.1	0.0	9.2	0.8	86.9	-3.1
rimuene	0.0	61.4	14.1	2.1	17.9	5.5	-1.0
p.aminobenzaldehyde	7.4	20.5	35.0	19.0	12.9	7.1	-1.9
phthalimide	9.5	93.2	1.4	0.0	0.0	0.0	-4.1
nitrophenylbenzenamine	74.5	0.0	0.0	42.7	0.0	30.0	-47.3
penoxaline	22.2	18.3	30.0	0.0	8.1	18.3	3.1
indoloquinoline	10.7	30.7	7.3	28.0	11.0	12.0	0.3
dimethylbutylphenyl.benzenediamine	12.6	25.8	0.0	3.2	7.4	60.0	-8.9
methoxyphenylmethylene.benzenamine	10.0	3.1	9.2	1.5	79.2	0.8	-3.8
methoxypyridine	12.2	33.9	0.0	4.4	47.8	2.2	-0.6
pelletierine	47.0	37.4	0.0	0.0	14.1	3.3	-1.9
terphenyl	18.2	43.0	3.0	20.3	15.2	5.8	-5.5
methylbisphenylmethyl.benzene	11.7	0.0	32.6	16.5	9.6	38.7	-9.1
chlorothalonil	17.6	21.2	49.4	32.4	0.6	3.5	-24.7
undecanedione	16.3	73.2	4.2	0.0	6.8	3.2	-3.7
dodecanedione	41.3	40.0	20.0	0.0	4.7	0.0	-6.0
methylxoadamantane	5.9	38.8	0.0	0.0	52.4	7.6	-4.7
methyldiamantane	3.5	13.0	7.4	32.2	14.8	28.7	0.4
monopalmitin	0.0	66.7	0.0	0.0	53.3	0.0	-20.0
monostearin	0.0	125.0	0.0	0.0	32.5	0.0	-57.5
late.57	6.3	6.9	0.0	76.3	4.4	5.6	0.6
secondary.late43	10.9	43.6	5.8	28.8	3.6	5.5	1.8
4-methyloctadecane	0.0	1.5	61.9	18.1	7.4	21.5	-10.4
2-methyloctadecane	14.0	0.0	59.3	20.7	6.7	10.7	-11.3
3-methyloctadecane	6.9	2.5	50.6	36.3	3.8	8.1	-8.1
AMS.Organics	12.9	56.2	15.1	1.2	1.9	9.4	3.3

Table 9. Correlations ($-0.3 > r > 0.3$) between TAG-Defined Summer Factors and Other Relevant Parameters.

	F1 SOA1		F2 SOA2		F3 SOA3		F4 Regional PrimaryAnthro		F5 LocalVehicle		F6 FoodCooking		F7 BioParticle +Mixed		F8 BioSemivolatile		F9 Biomass Burning		Residual	
	gas	particle	g	p	g	p	g	p	g	p	g	p	g	p	g	p	g	p	g	p
Gas Phase Parameters																				
O ₃	-	-	0.34	-	0.85	-	-	-	-0.31	-	-	-0.42	-	-0.45	-	-	-	-	-	-
CO	0.33	-	-	-	-0.46	-	-	-	0.73	-	0.37	0.54	-	-	-	-	-	-	-	-
H ₂ O	-	-	-	-	-	-	-	-	-	-	0.53	0.33	-	0.37	-	-	-0.44	-	-	-
GC-MSD-FID																				
mtbe	-	-	-	-	-	-	-	-	-	-	0.61	0.56	-	-	-	-	-	-	-	-
oxylene	-	-	-	-	-0.62	-	-	-	0.45	-	0.41	0.59	-	-	-	-	-	-	-	-
benzene78	-	-	-	-	-0.45	-	-	-	0.50	-	0.49	0.59	-	-	-	-	-	-	-	-
toluene91	-	-	-	-	-0.53	-	-	-	0.44	-	0.37	0.60	-	-	-	-	-	-	-	-
propane	-	0.36	-	-	-	-	-	-	0.47	-	0.36	0.32	-	-	-	-	-	-	-	-
hexane	-	-	-	-	-0.38	-	-	-	0.53	-	-	0.48	-	-	-	-	-	-	-	-
propene	-	-	-	-	-0.58	-	-	-	0.51	-	0.33	0.54	-	-	-	-	-	-	-	-
butene	-	-	-	-	-0.57	-	-	-	0.43	-	0.40	0.59	-	-	-	-	-	-	-	-
propyne	-	-	-	-	-0.41	-	-	-	0.52	-	0.34	0.45	-	-	-	-	-	-	-	-
methylpentane	-	-	-	-	-0.41	-	-	-	0.55	-	0.47	0.47	-	-	-	-	-	-	-	-
methylpropanal	-	-	-	-	-0.43	-	-	-	-	-	0.43	0.65	-	0.44	-	-	-	-	-	-
mf	-	-	-	-	-0.44	-	-	-	0.45	-	0.45	-	-	-	-	-	-	-	-	-
iproh	-	-	-	-	-0.38	-	-	-	0.37	-	-	0.42	-	-	-	-	-	-	-	-
ch3cn	-	-	-	-	-0.33	-	-	-	0.37	-	-	0.54	-	-	-	-	-	-	-	-
propanal	0.33	-	0.48	-	-	-	-	-	-	-	0.44	-	-	-	-	-	-	-	-	-
acetone58	0.33	-	0.60	-	-	-	-	-	-	-	-	-	-	-	-	-	-	-0.43	-	-
mek	0.38	-	0.66	-	0.41	-	-	-	-	-	-	-	-	-	-	-	-	-0.42	-	-
pentanal	-	-	-	-	0.54	-	-	-	-	-	-0.37	-	-	-	-	-	-	-	-	-
isoprene67	0.41	-	0.39	-	0.67	-	-	-	-	-	-0.31	-	-	-	-0.54	-	-	-	-	-
macr	0.38	-	0.42	-	0.74	-	-	-	-	-	-	-	-	-	-0.53	-	-	-	-	-
mvk	0.36	-	0.36	-	0.79	-	-	-	-	-	-0.32	-	-	-	-0.53	-	-	-	-	-
apinene	-	-	-	-	-0.40	-	-	-	-	-	-	0.77	-	-	-	-	-	-	-	-
bpinene	-	-	-	-	-0.40	-	-	-	0.31	-	-	0.61	-	-	-	-	-	-	-	-
Particle Phase Parameters																				
OC	-	-	0.66	-	0.37	-	-	-	-	-	0.38	-	-	-	-	-	-	-0.54	-	-
EC	0.31	-	-	-	-0.31	-	-	-	0.79	-	-	-	-	-	-	-	-	-	-	-
AMS																				
Organics	0.41	-	0.64	-	0.41	-	-	-	-	-	-	-	-	-	-	-	-	-0.50	-	0.42
SO ₄ ²⁻	-	-	-	-	-	-	-	-	-	-	-	-	-	-	-	-	-	-	-	0.34
NO ₃	-	-	0.51	-	-	-	0.55	-	-	-	-	-	-	-	-	-	-	-	-	-0.62
NH ₄ ⁺	-	-	0.53	-	-	-	0.49	-	-	-	-	-	-	-	-	-	-	-	-	-0.62
Chloride	-	-	-	-	-0.30	-	0.49	-	-	-	0.39	-	-	-	-	-	-	-	-	-0.39
ATOFMS																				
< 1 um																				
subAgedOC1	-	-	-0.31	-	-0.41	-	0.57	-	-	-	0.33	-	-	-	-	-	-	-	-	-
subAgedOCSO4	0.39	-	0.83	-	-	-	-	-	-	-	-	-0.33	-	-	-	-	-	-0.48	-	-
subAgedOC2	-	-	-	-	-	-	-	-	-	-	-	-	-	-	-	-	-	-	-	-
subECOCSO4	-	-	0.71	-	-	-	0.43	-	-	-	-	-	-	-	-	-	-	-0.59	-	-
subECOC	-	-	-	-	-0.36	-	0.41	-	-	-	0.38	-	-	-	-	-	-	-	-	-
subEC	-	-	0.36	-	-	-	-	-	-	-	0.32	-	-	-	-	-	-	-0.59	-	-
subAmine	-	-	-	-	-	-	-	-	-	-	-	-	-	-	-	-	-	-	-	-
subV	-	-	0.76	-	-	-	-	-	-	-	-	-	-0.37	-	-0.46	-	-	-0.45	-	-
subBiomass	0.37	-	0.60	-	0.36	-	-	-	-	-	-	-	-	-	-	-	-	-0.38	-	-
subAgedSS	-	-	0.52	-	0.65	-	-	-	-	-	-	-	-0.36	-	-0.44	-	-	-	-	-
subDust	-	-	0.42	-	-	-	0.49	-	0.34	-	-	-	-	-	-	-	-	-0.37	-	-
subNH4NO3	-	-	-	-	-	-	-	-	-	-	-	-	-	-	-	-	-	-	-	-
subOther	-	-	0.41	-	-	-	0.31	-	-	-	0.33	-	-	-	-	-	-	-0.67	-	-
> 1 um																				
superAgedOC1	-	-	-	-	-0.37	-	-	-	-	-	0.47	-	-	-	0.30	-	-	-	-	-
superAgedOCSO4	0.41	-	0.86	-	-	-	-	-	-	-	-	-	-	-	-	-	-	-0.48	-	-
superAgedOC2	-	-	-	-	-	-	-0.36	-	-	-	-	-	-	-	-	-	-	-	-	-
superECOCSO4	-	-	0.60	-	-	-	0.46	-	-	-	-	-	-	-	-	-	-	-0.57	-	-
superECOC	-	-	-	-	-	-	-	-	-	-	0.42	-	-	-	-	-	-	-	-	-
superEC	-	-	-	-	-0.45	-	-	-	-	-	0.42	0.33	-	0.33	0.33	-	-	-0.44	-	-
superAmine	-	-	-	-	-	-	-	-	-	-	-	-	-	-	-	-	-	-	-	-
superV	-	-	0.60	-	-	-	0.43	-	-	-	-	-	-	-	-	-	-	-0.49	-	-
superBiomass	0.44	-	0.76	-	-	-	-	-	-	-	-	-	-	-	-0.33	-	-	-0.41	-	-
superAgedSS	0.45	-	-	-	0.43	-	-	-	-	-	-	-	-	-	-	-	-	-	-	-
superDust	0.46	-	0.59	-	-	-	-	-	-	-	-	-	-	-	-	-	-	-0.35	-	-
superNH4NO3	-	-	0.43	-	-	-	-	-	-	-	-	-	-	-	-	-	-	-	-	-
superOther	-	-	-	-	-0.49	-	-	-	-	-	0.48	0.49	-	-	-	-	-	-	-	-
Other Parameters																				
air temperature	0.36	-	0.42	-	0.78	-	-	-	-	-	-	-0.43	-	-0.54	-	-	-	-	-	-
par	0.61	-	0.55	-	0.52	-	-	-	-	-	-	-	-	-0.47	-	-	-	-0.39	-	-
windspeed	0.33	-	0.36	-	0.75	-	-	-	-	-	-	-0.39	-	-0.53	-	-	-	-	-	-
relative humidity	-	-	-0.37	-	-0.68	-	-	-	-	-	0.39	0.49	-	0.57	-	-	-	-	-	-
atmos. pressure	0.31	-	-	-	-0.42	-	-	-	-	-	-	-	-	-	-	-	-	-	-	-

Table 10. Correlations ($-0.3 > r > 0.3$) between TAG-Defined Fall Factors and Other Relevant Parameters.

	F1 SOA+		F2 SOA+		F3 Regional		F4 LocalVehicle		F5 BioSemivolatile		F6 BiomassBurning		Residual	
	FoodCooking1		FoodCooking2		PrimaryAnthro									
	gas	particle	g	p	g	p	g	p	g	p	g	p	g	p
Gas Phase Parameters														
O ₃	-	-	-	-	0.49	-	-0.49	-	-0.32	-	-0.41	-	-	-
CO	-	-	0.65	-	-0.37	-	0.72	-	-	-	-	-	-	-
H ₂ O	-	-	0.39	-	-	-	-	-	-	-	-	-	-	-
GC-MSD-FID														
mtbe	-	-	0.80	-	-0.32	-	-	-	-	-	-	-	-	-
oxylene	-	-	0.58	-	-0.32	-	0.71	-	-	-	-	-	-	-
benzene78	-	-	0.69	-	-0.34	-	0.59	-	-	-	-	-	-	-
toluene91	-	-	0.62	-	-	-	0.64	-	-	-	-	-	-	-
propane	-	-	0.75	-	-	-	0.47	-	-	-	-	-	-	-
hexane	-	-	0.73	-	-0.35	-	0.57	-	-	-	-	-	-	-
propene	-	-	0.45	-	-0.37	-	0.73	-	-	-	-	-	-	-
butene	-	-	-	-	-	-	0.64	-	-	-	0.30	-	-	-
propyne	-	-	-	-	-	-	0.79	-	-	-	0.36	-	-	-
methylpentane	-	-	0.72	-	-0.32	-	0.55	-	-	-	-	-	-	-
methylpropanal	0.43	-	0.63	-	-	-	-	-	-	-	-	-	-	-
mf	-	-	-	-	-	-	0.64	-	-	-	-	-	-	-
iproh	-	-	-	-	-	-	0.35	-	-	-	-	-	-	-
ch3cn	0.34	-	0.32	-	-	-	0.53	-	-	-	-	-	-	-
propanal	0.47	-	0.54	-	-	-	-	-	-	-	-0.35	-	-	-
acetone58	-	-	0.57	-	-	-	0.31	-	-	-	-	-	-	-
mek	0.41	-	0.63	-	-	-	-	-	-	-	-0.33	-	-	-
pentanal	-	-	0.68	-	-	-	-	-	-	-	-0.34	-	-	-
isoprene67	-	-	-	-	0.61	-	-	-	-	-	-	-	-	-
macr	0.48	-	-	-	0.44	-	-	-	-	-	-0.30	-	-	-
mvk	0.51	-	-	-	0.49	-	-	-	-	-	-	-	-	-
apinene	-	-	0.33	-	-0.40	-	0.72	-	-	-	0.33	-	-	-
bpinene	-	-	0.35	-	-0.35	-	0.70	-	-	-	-	-	-	-
Particle Phase Parameters														
AMS														
Organics	-	-	0.84	-	-0.42	-	-	-	-	-	-	-	-	-
SO ₄ ²⁻	-	-	0.84	-	-0.39	-	-	-	-	-	-	-	-	-
NO ₃ ⁻	-	-	0.83	-	-0.35	-	-	-	-	-	-	-	-	-
NH ₄ ⁺	-	-	0.85	-	-0.35	-	-	-	-	-	-	-	-	-
Chloride	-	-	0.82	-	-0.32	-	-	-	-	-	-	-	-	-
ATOFMS														
< 1um														
subAgedOC1	-	-	0.74	-	-0.39	-	-	-	-	-	-0.31	-	-	-
subAgedOCSO4	-	-	0.72	-	-0.39	-	-	-	-	-	-	-	-	-
subAgedOC2	-	-	-	-	-0.36	-	-	-	-	-	0.33	-	-	-
subECOCSO4	-	-	0.87	-	-0.37	-	-	-	-	-	-	-	-	-
subECOC	-	-	0.55	-	-	-	-	-	-	-	-0.33	-	-	-
subEC	-	-	0.83	-	-0.38	-	-	-	-	-	-	-	-	-
subAmine	0.39	-	-	-	-	-	-	-	-	-	-	-	-	-
subV	-	-	0.89	-	-	-	-	-	-	-	-0.39	-	-	-
subBiomass	-	-	0.63	-	-	-	-	-	-	-	-	-	-	-
subAgedSS	-	-	-	-	-	-	-	-	-	-	-	-	-	-
subDust	-	-	0.40	-	-	-	0.38	-	-	-	-	-	-	-
subNH4NO3	-	-	-	-	-	-	-	-	-	-	-	-	-	-
subOther	-	-	0.85	-	-0.38	-	-	-	-	-	-	-	-	-
> 1um														
superAgedOC1	-	-	0.78	-	-0.43	-	-	-	-	-	-	-	-	-
superAgedOCSO4	-	-	0.77	-	-0.34	-	-	-	-	-	-	-	-	-
superAgedOC2	-	-	-	-	-	-	-	-	-	-	-	-	-	-
superECOCSO4	-	-	0.88	-	-0.36	-	-	-	-	-	-	-	-	-
superECOC	-	-	0.59	-	-0.32	-	-	-	-	-	-	-	-	-
superEC	-	-	0.80	-	-0.34	-	-	-	-	-	-0.34	-	-	-
superAmine	0.34	-	-	-	-	-	-	-	-	-	-	-	-	-
superV	-	-	0.33	-	-	-	-	-	-	-	-	-	-	-
superBiomass	-	-	0.73	-	-	-	-	-	-	-	-0.33	-	-	-
superAgedSS	-0.32	-	0.39	-	-	-	-	-	-	-	-	-	-	-
superDust	-	-	0.38	-	-	-	0.61	-	-	-	-	-	-	-
superNH4NO3	-	-	-	-	-	-	-	-	-	-	-	-	-	-
superOther	-	-	0.78	-	-0.39	-	0.43	-	-	-	-	-	-	-
Other Parameters														
air temperature	-	-	-	-	0.72	-	-	-	-0.40	-	-0.44	-	-	-
par	-	-	-	-	0.50	-	-	-	-0.32	-	-0.30	-	-	-
windspeed	-	-	-	-	0.50	-	-	-	-0.35	-	-	-	-	-
relative humidity	-	-	0.34	-	-0.57	-	-	-	0.45	-	-	-	-	-
atmos. pressure	-	-	-0.48	-	-	-	-	-	-	-	0.46	-	-	-

Table 11. Average Source Concentrations and Contributions to Total OA during SOAR 2005.

SUMMER			FALL		
	Average Concentration (ug m-3)	Contribution to Total Organics (%)		Average Concentration (ug m-3)	Contribution to Total Organics (%)
SOA1	1.61	9.9	SOA+FoodCooking1	1.26	13.0
SOA2	3.06	18.9	SOA+FoodCooking2	5.47	56.3
SOA3	2.92	18.0	RegionalPrimaryAnthro	1.46	15.0
RegionalPrimaryAnthro	2.43	15.0	LocalVehicle	0.11	1.1
LocalVehicle	0.57	3.5	BioSemivolatile	0.18	1.9
FoodCooking	1.01	6.2	BiomassBurning	0.91	9.4
BioParticle+Mixed	1.10	6.8	Residual	0.33	3.4
BioSemivolatile	2.18	13.5			
BiomassBurning	0.98	6.0			
Residual	0.34	2.1			

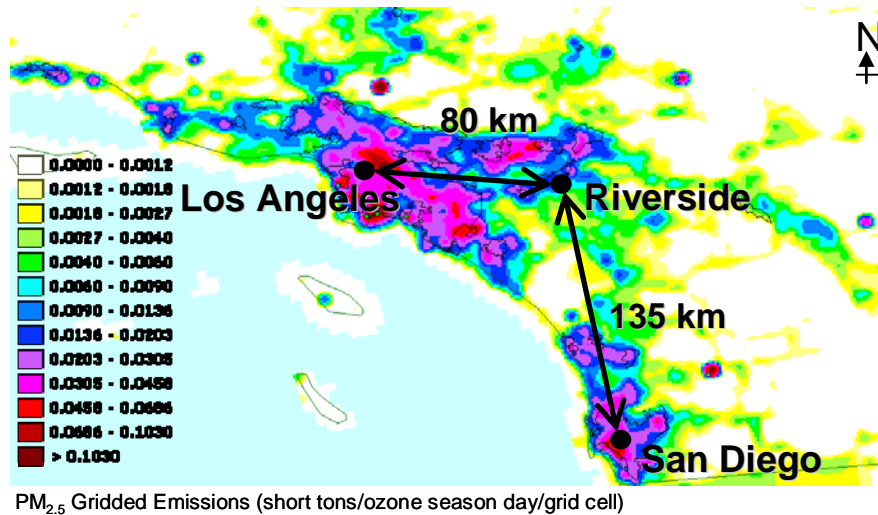


Figure 1. View of the ground-based field site at Riverside, CA (33°58'18"N, 117°19'17"W). Shown are anthropogenic PM_{2.5}-PRI emissions in short tons/ozone season day/grid cell, plotted on a 4-km Lambert-Conformal grid. This emission map was created using the NOAA-NESDIS/OAR Emission Inventory Mapviewer found at: (<http://map.ngdc.noaa.gov/website/al/emissions/viewer.htm>), maintained by Gregory Frost, NOAA.

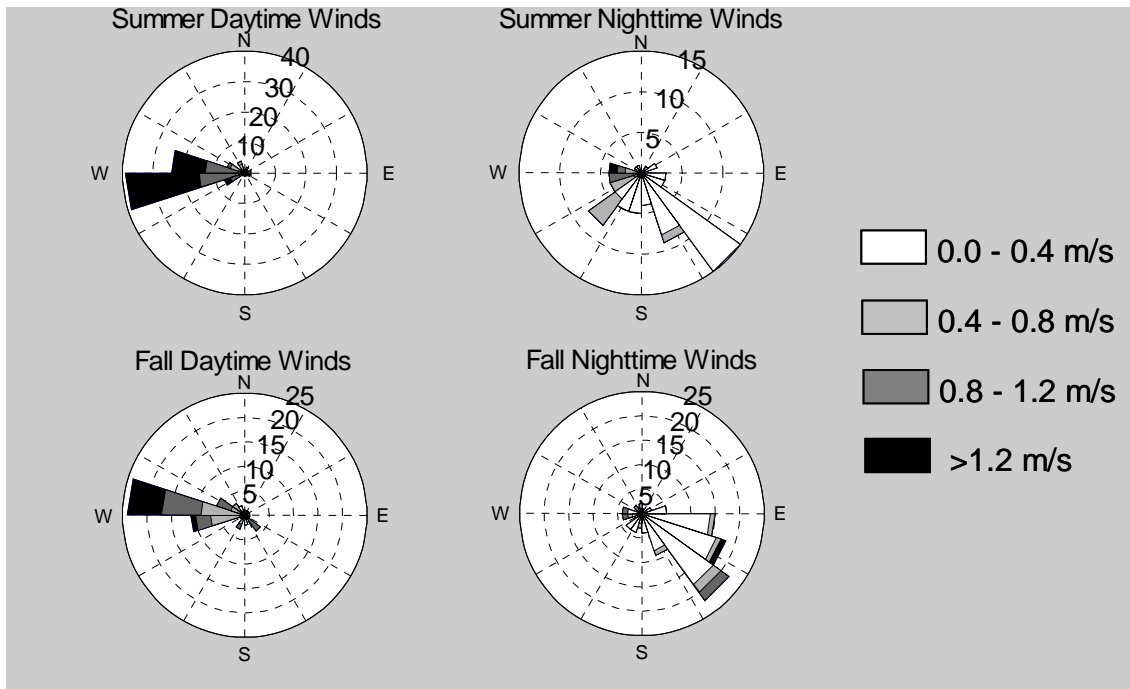


Figure 2. Average daytime and nighttime winds for SOAR focus periods, separated by summer (July 29 – August 8) and fall (November 4 – 14) 2005. Concentric rings represent frequency of observations.

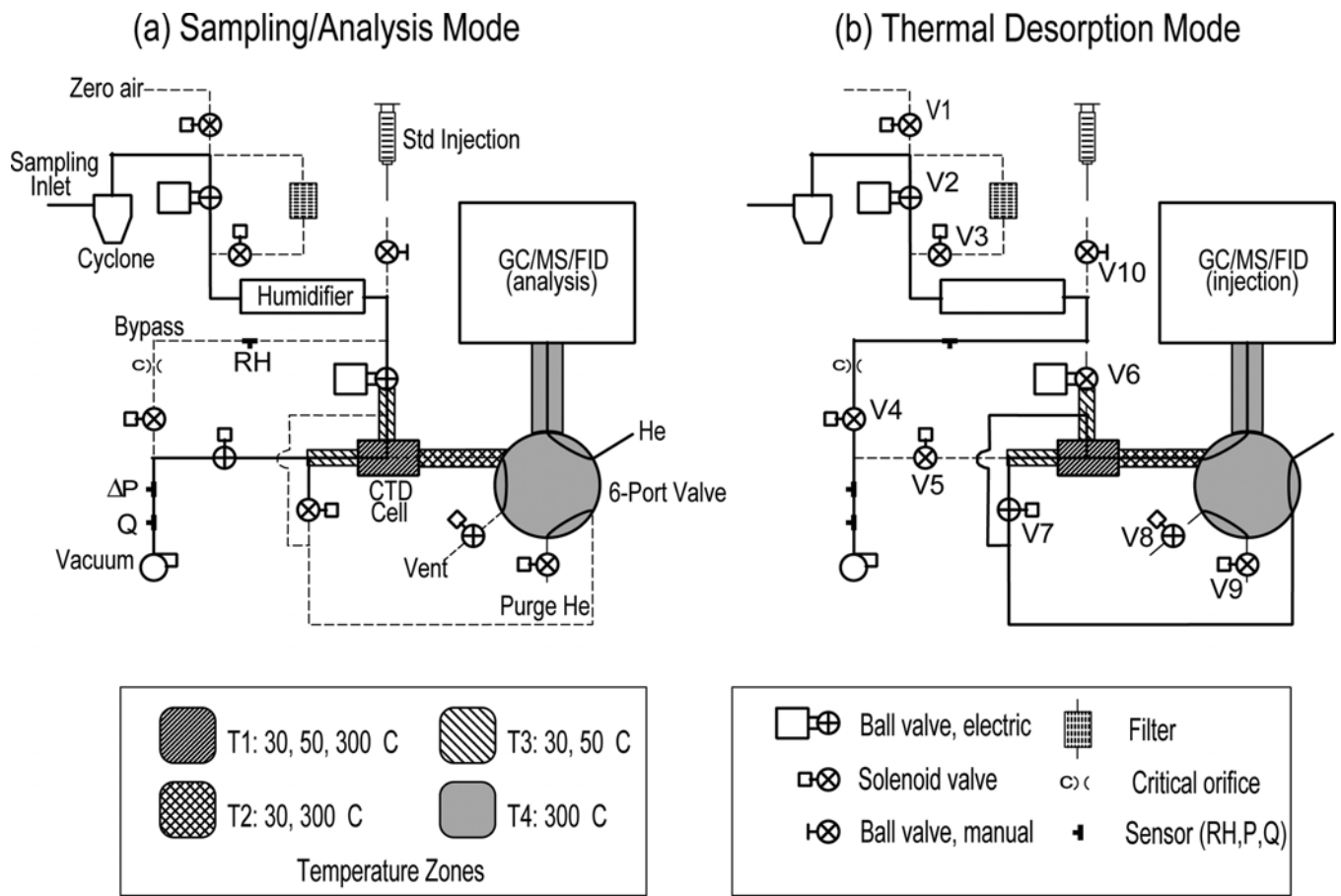


Figure 3. Schematic of the TAG system, showing flow configuration for two modes of operation: (a) concurrent sampling and analysis, and (b) thermal desorption. The thermal desorption mode is used for transfer of collected sample onto the chromatography column.

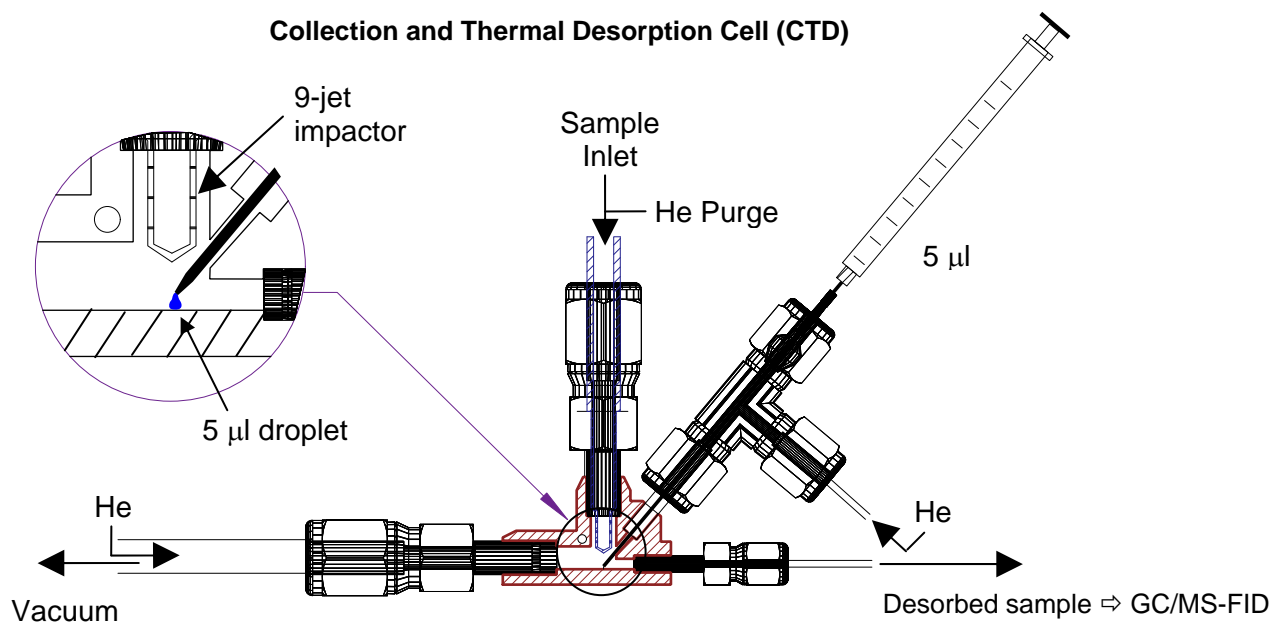


Figure 4. Current design of the collection and thermal desorption (CTD) cell provides in-situ calibrations of TAG via an integrated injection port. Fixed-volume injections of varying concentrations of authentic standards in solution are deposited near the impaction region of the collection cell on the same passivated surface as used for aerosol collection.

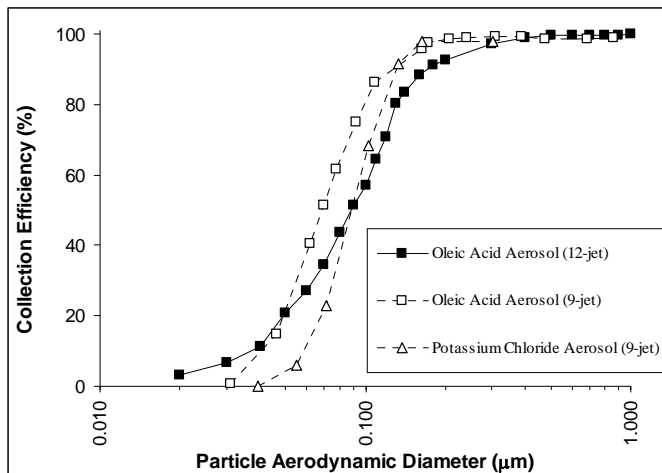


Figure 5. Collection efficiency curves for 9 and 12-jet impactors. The oleic aerosol is a nonhygroscopic oil, while potassium chloride aerosol is a solid particle (84% deliquescence), which was introduced to the cell at 60-70% RH. Data were obtained using the CPC counting method (see text).

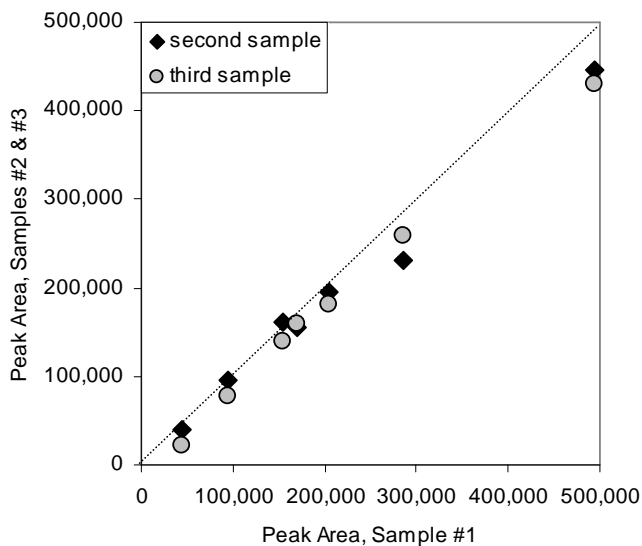


Figure 6. Comparison of peak areas for independent, collocated samples of ambient air in Berkeley California. Line shows 1:1 correspondence.

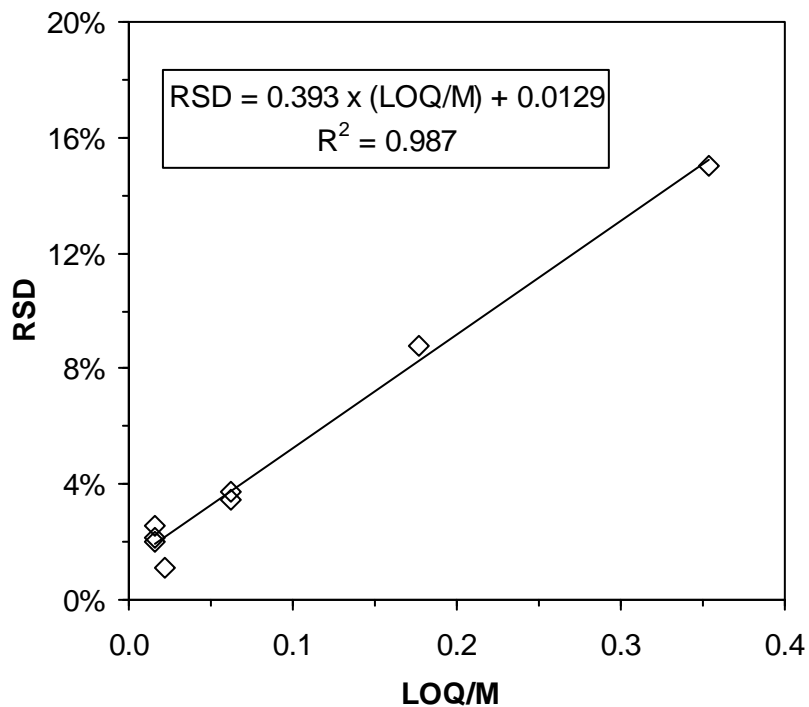


Figure 7. Relationship of injection repeatability (RSD) versus the ratio of LOQ to the individual compound injection mass level M. Compounds that elute before hexadecane (i.e. those listed above the shaded region of Table 2) were excluded. For these less-volatile species, the baseline precision for calibration standards can be taken as the limit of $LOQ/M \rightarrow 0$, which is the intercept of the regression line = 1.3% RSD.

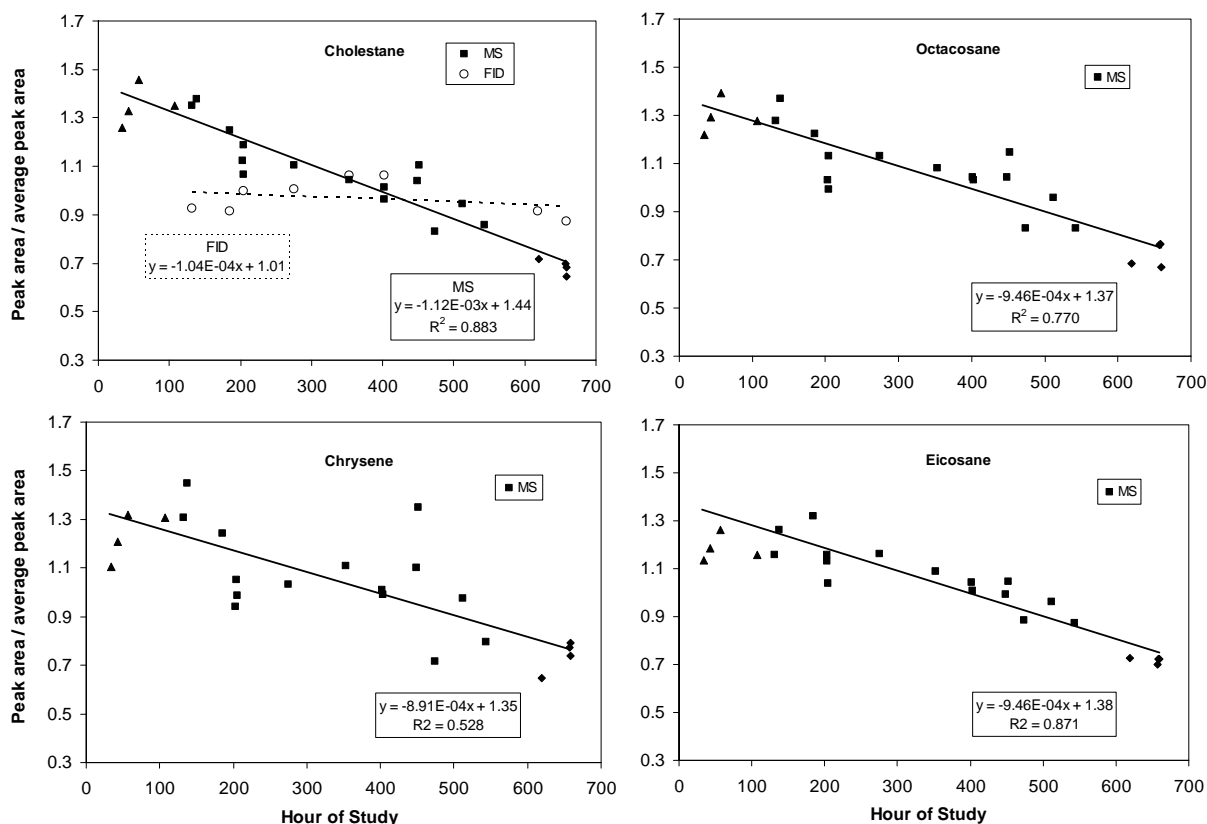


Figure 8. Fall instrument response trends are shown for four selected tracking standard compounds used in this analysis. Plotted is the detector peak area divided by each compound's average response versus hour of study. Mean single ion areas are 6.7×10^5 (cholestane), 4.0×10^6 (chrysene), 2.2×10^6 (eicosane) and 4.2×10^6 (octacosane). These compounds demonstrate a consistent, downward trend in MSD response as a function of time. For a uniformly distributed subset of the tracking standard data, the cholestane FID data show no significant trend. Different filled symbols indicate distinct standard solutions. Drift regressions shown exclude the first set of standard solutions (triangles) due to uncertainty in that standard's concentrations.

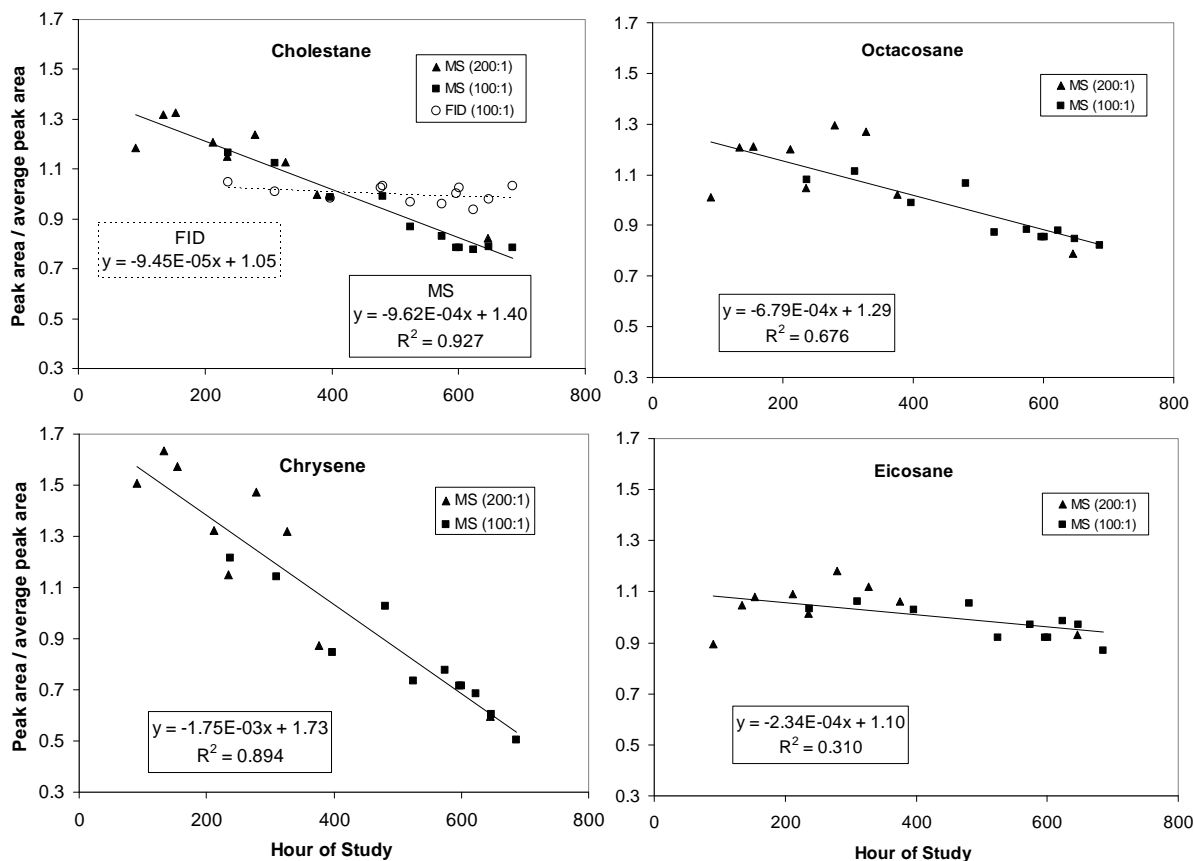


Figure 9. Summer instrument response trends are shown for four selected tracking standard compounds used in this analysis. Plotted is the detector peak area divided by each compound's average response versus hour of study. Mean single ion areas are 8.4×10^5 (cholestane), 6.3×10^6 (chrysene), 2.6×10^6 (eicosane) and 5.6×10^6 (octacosane). These compounds demonstrate a consistent, downward trend in MSD response as a function of time. For a uniformly distributed subset of the tracking standard data, the cholestane FID data shows no significant trend. Different filled symbols are for two standard concentration levels with the indicated stock dilution ratio. The more dilute response data was scaled up to the more concentrated level by application of a preliminary calibration using the more concentrated subset of data.

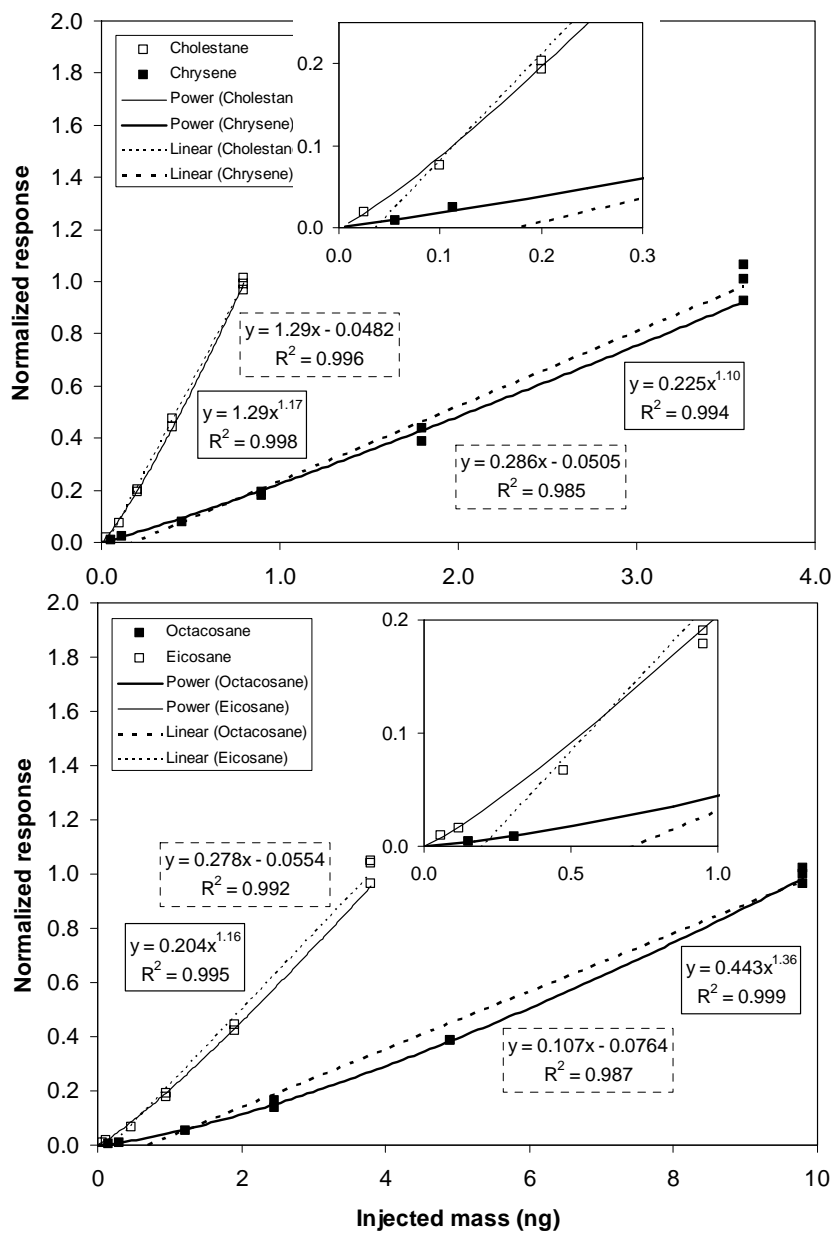


Figure 10. Time-independent calibration of TAG for four of the tracking standard compounds for the Summer SOAR study. Non-linear fits (solid lines) are shown to be superior to linear fits (broken lines) for all four compounds, especially near the limits of detection of the instrument (insets). Vertical spread in calibration points indicates residual variation of data after de-trending.

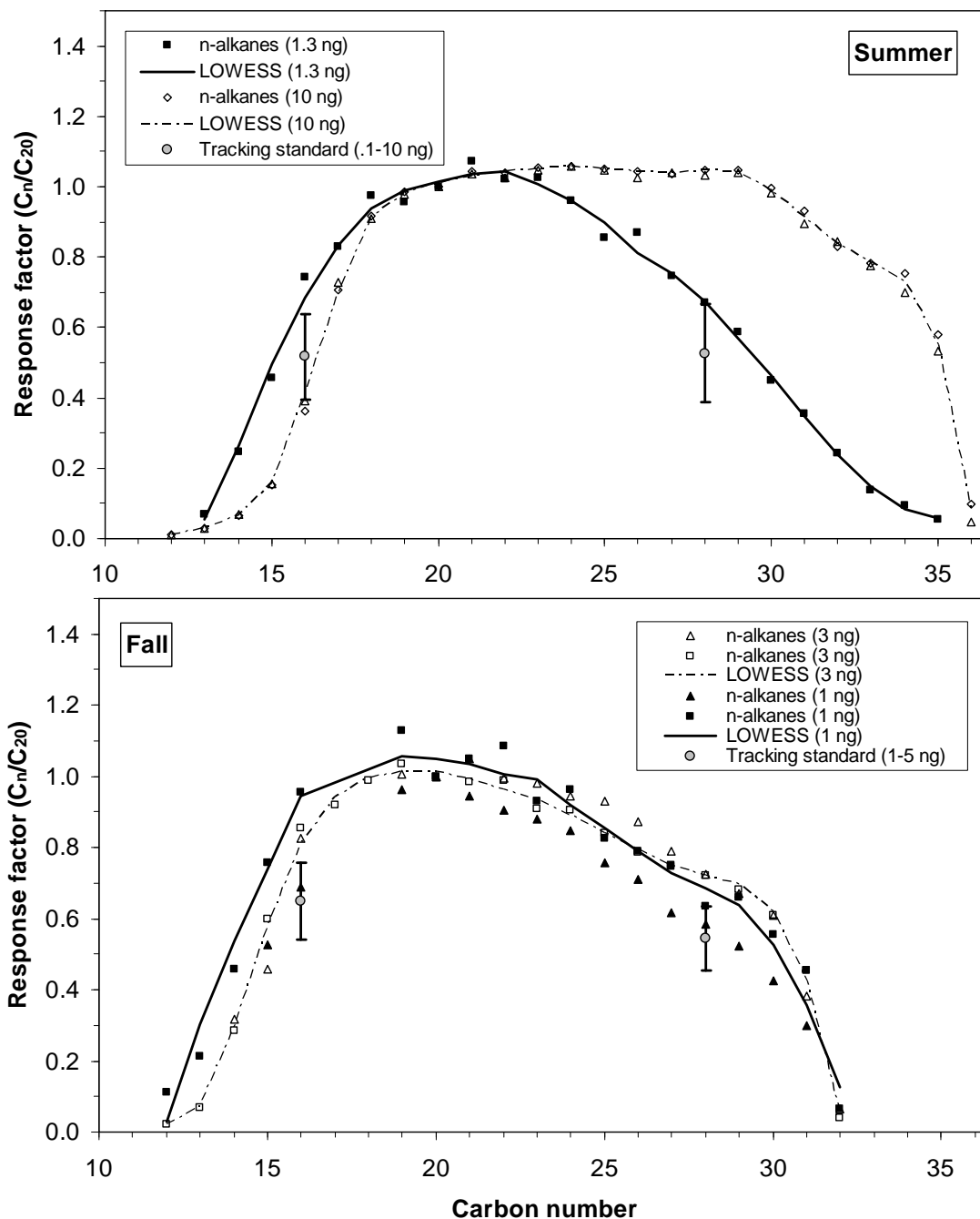


Figure 11. Relative response factors for n-alkanes defined as the ratio of the single ion peak areas (57 m/z) for compound C_n to the reference compound eicosane (C_{20}) for summer and fall periods. Sensitivity to mass level is indicated at both the low and high volatility ends of the carbon number spectrum. Response factors from the alkane auxiliary standard (triangles, squares) provide the complete range of response for TAG and are in general agreement with similar ratios obtained from the multipoint calibration data using C_{16} , C_{20} and C_{28} in the tracking standard (circles), shown with $1-\sigma$ error bars, over the indicated mass injection levels.

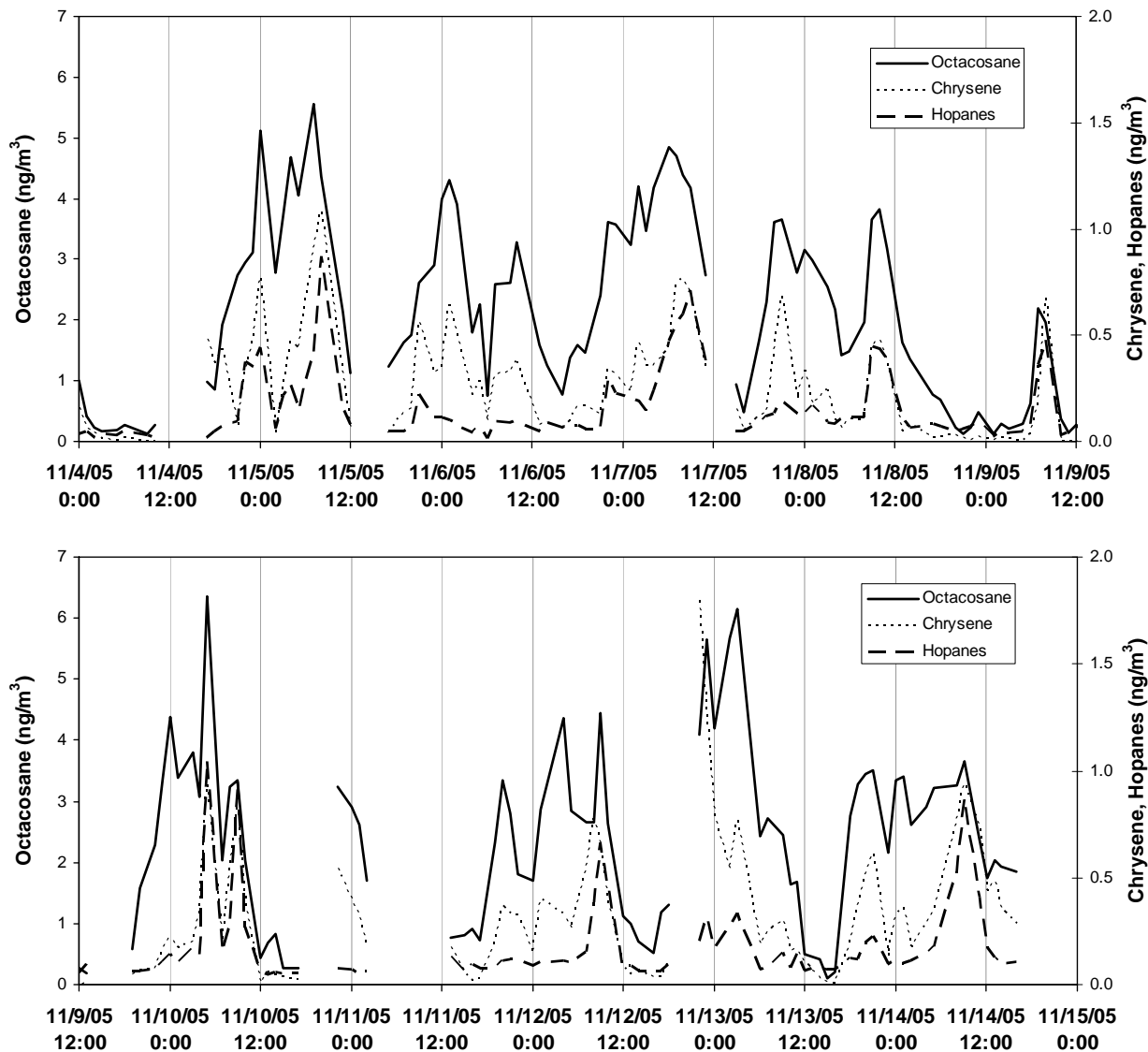


Figure 12. Calibrated TAG response for octacosane, chrysene and the sum of two hopanes, during the fall study. The calibration for the tracking standard cholestane was applied to each of the hopane responses with a relative response factor prior to summing. Gaps greater than 2 hours are shown with line breaks indicating when calibrations or other interruptions of normal operation occurred.

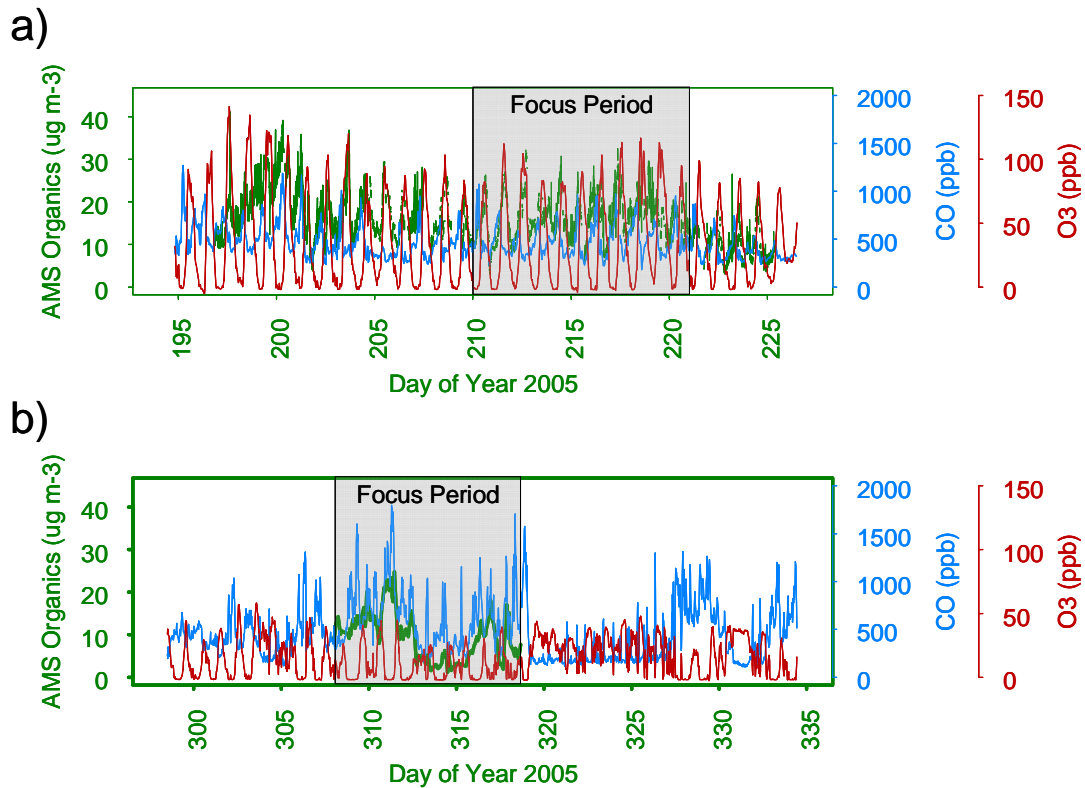


Figure 13. AMS total organics, carbon monoxide (CO), and ozone (O₃) concentrations during SOAR 2005. a) The summer period (July 29 – August 8) displays regular diurnal patterns, with very high O₃ concentrations every afternoon. The summer focus period (outlined in grey) is consistent with the general trend of the entire summer study. b) The fall period (November 4 - 14) is dominated by meteorological “events”, with lower O₃ concentrations than observed in summer. The fall focus period (outlined in grey) is representative of a period high in particulate concentrations and CO concentrations.

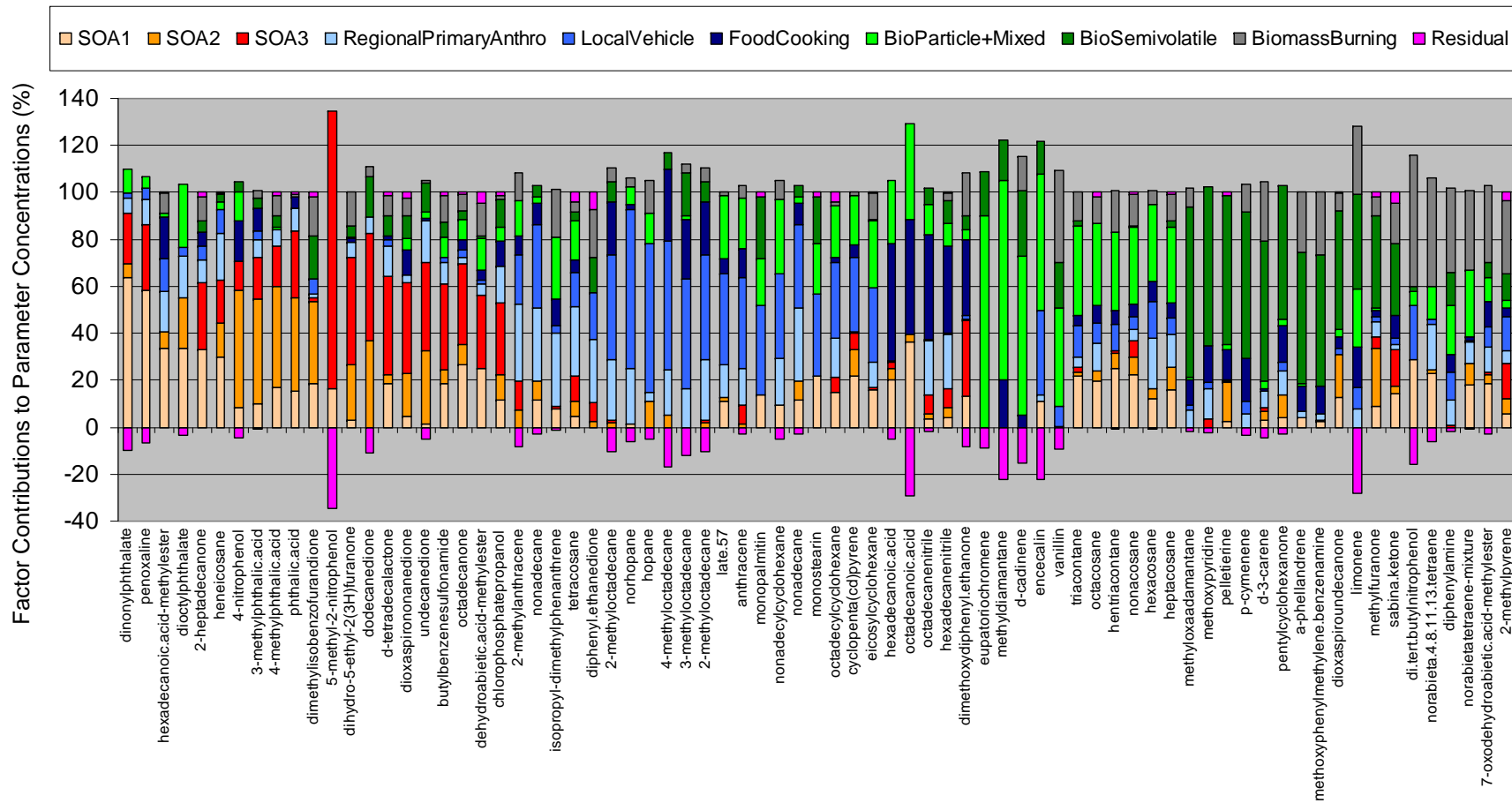


Figure 14. Summer PMF profiles. Only compounds with loadings of at least 30% into a single source are displayed (at least 25% for RegionalPrimaryAnthro).

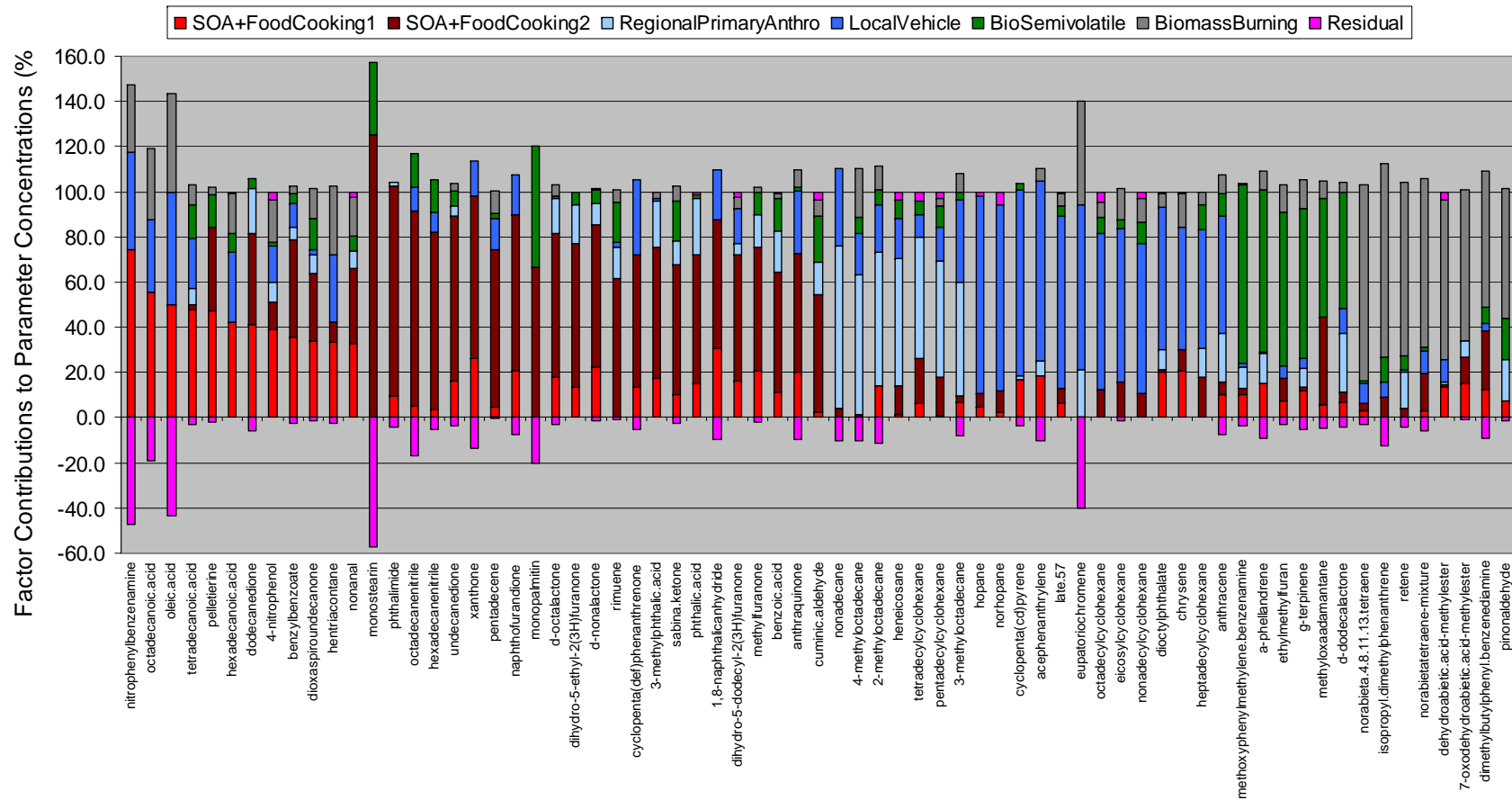


Figure 15. Fall PMF profiles. Only compounds with loadings of at least 50% into a single source are displayed (at least 33% for SOA+FoodCooking1).

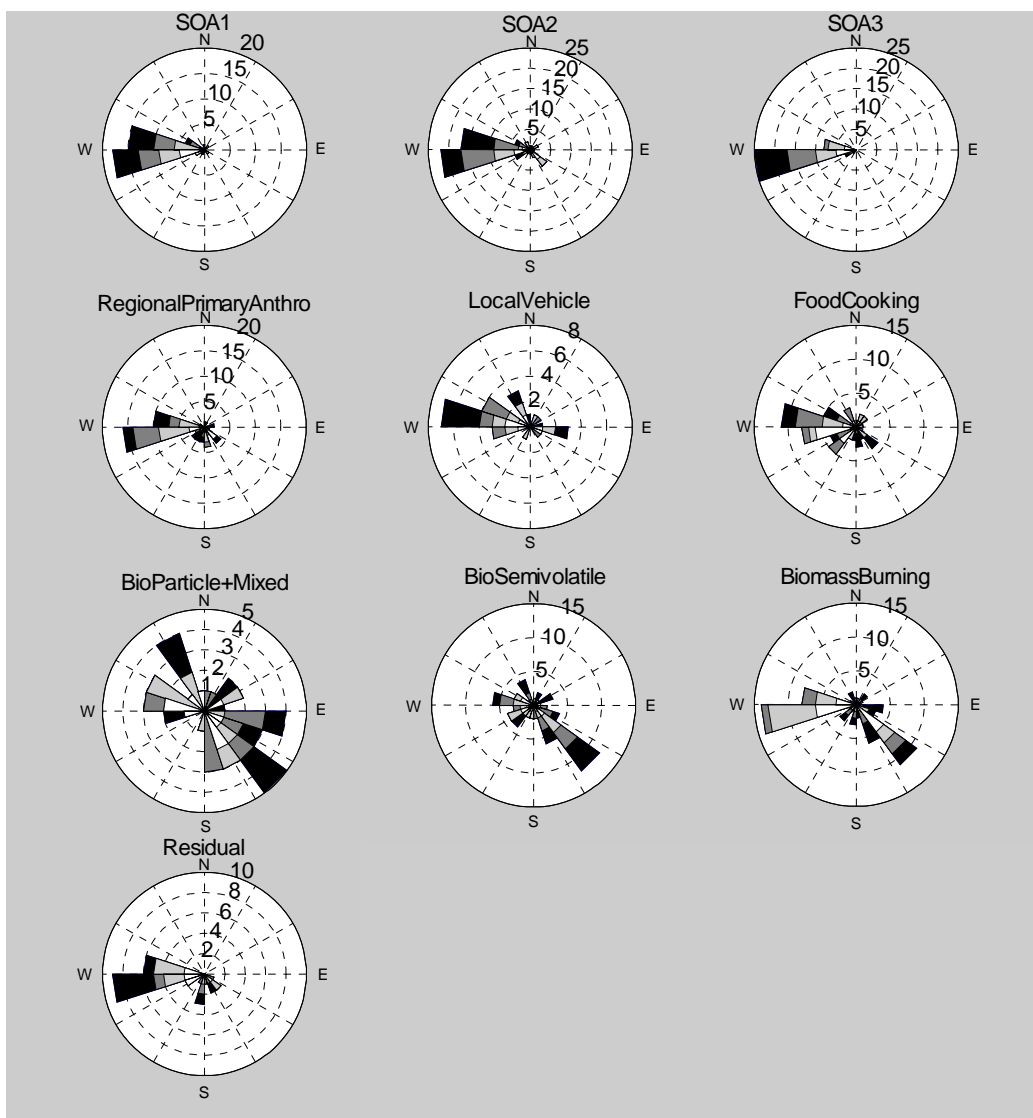


Figure 16. Rose plots of the 9 summer aerosol sources (plus the Residual factor) using only concentrations > 1 standard deviation to emphasize dominant source directions. Frequency of observations are represented by the length of each wedge, and labeled by concentric rings. The shade of each wedge represents source concentrations in quartiles (dark = higher concentrations).

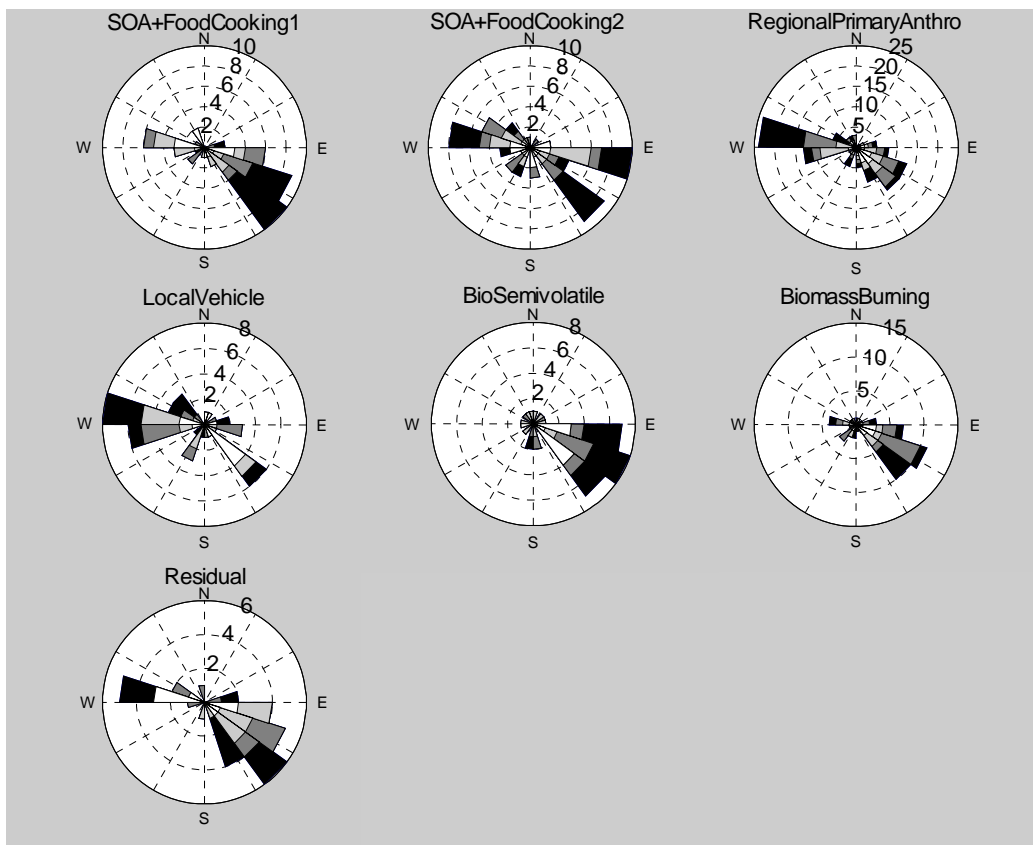


Figure 17. Rose plots of the 6 fall aerosol sources (plus the Residual factor) using only concentrations > 1 standard deviation to emphasize dominant source directions. Frequency of observations are represented by the length of each wedge, and labeled by concentric rings. The shade of each wedge represents source concentrations in quartiles (dark = higher concentrations).

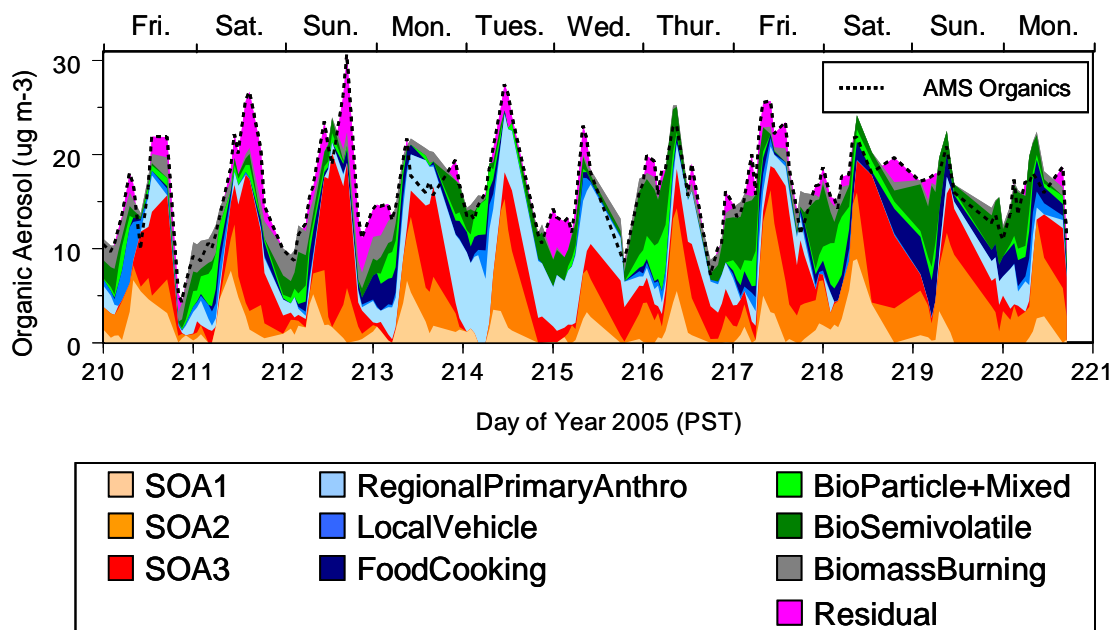


Figure 18. Source contributions to total organic aerosol mass concentrations during the summer focus period (July 29 – August 8).

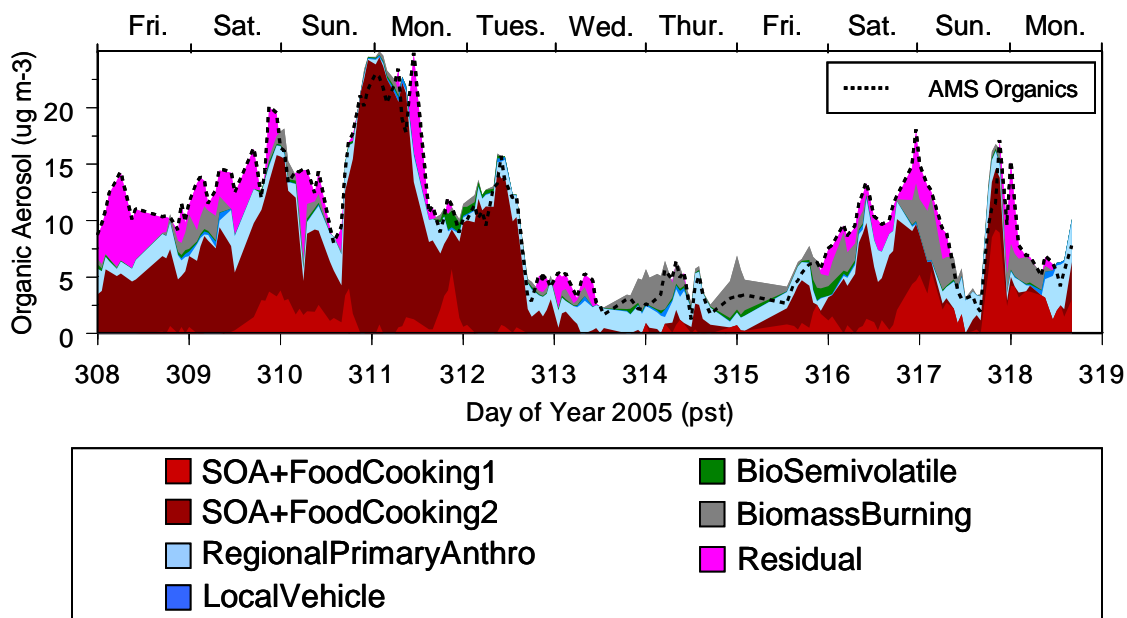


Figure 19. Source contributions to total organic aerosol mass concentrations during the fall focus period (November 4 - 14).

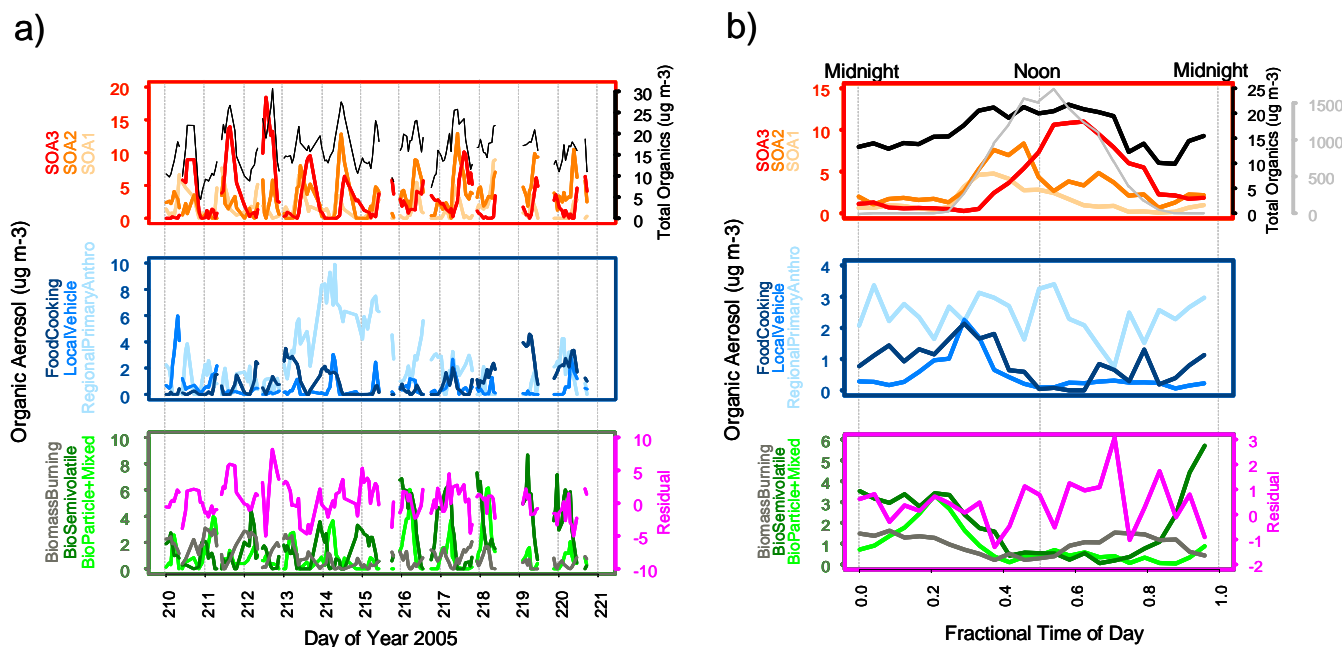


Figure 20. a) Individual organic aerosol source timelines over the summer focus period (July 29 – August 8). b) Diurnal averages for summer organic aerosol sources. Photosynthetic active radiation (PAR) has been included to represent the solar cycle.

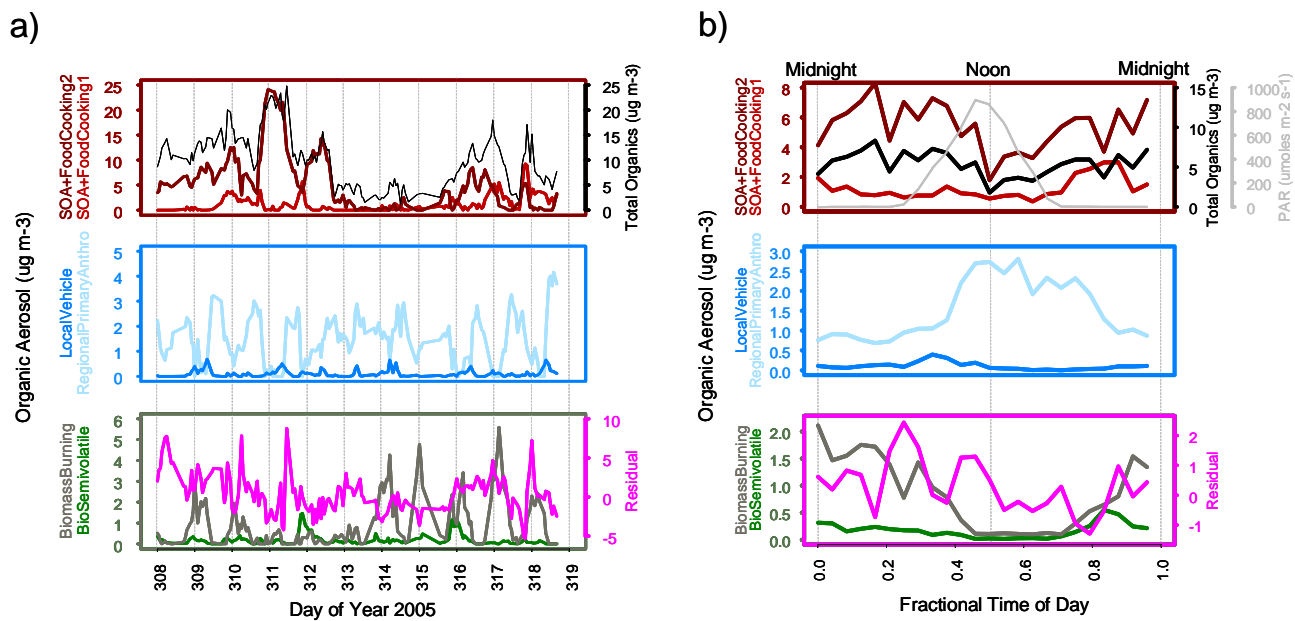
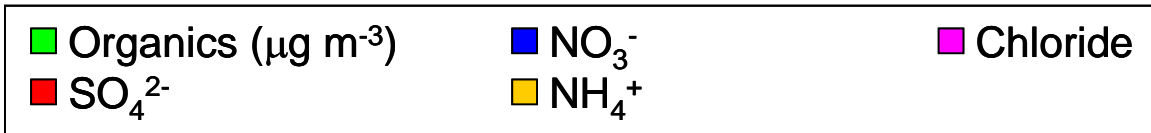
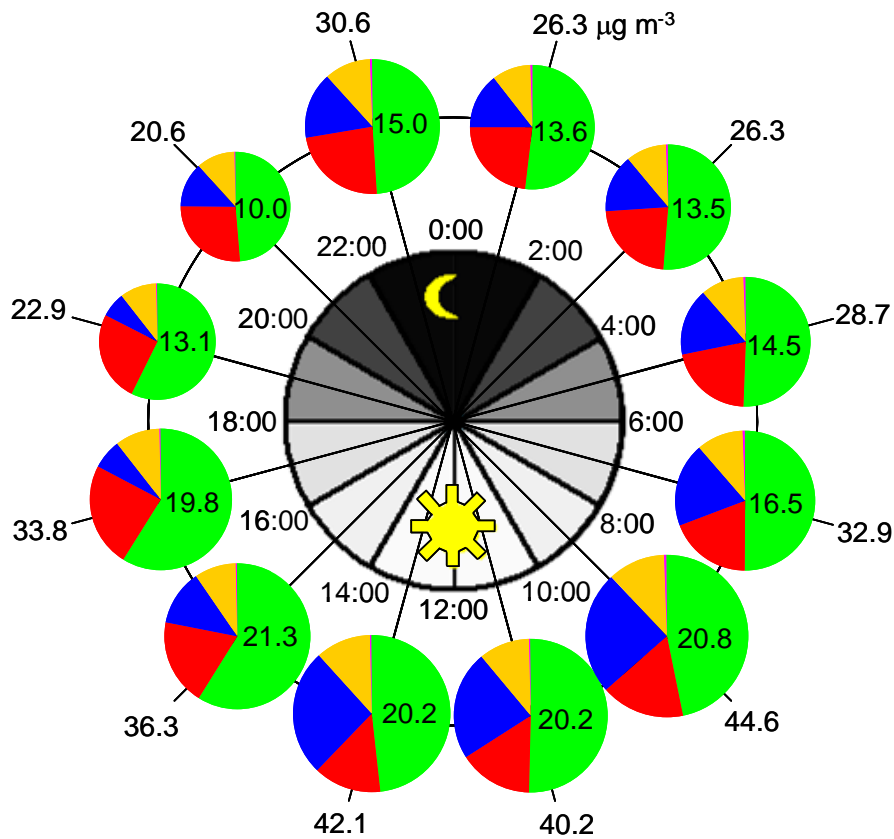
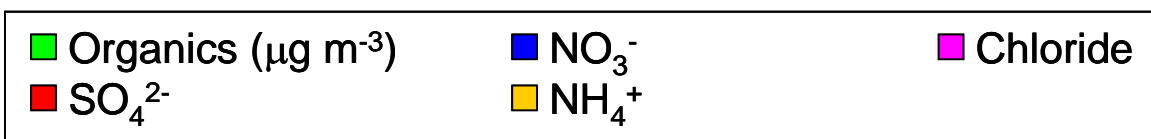
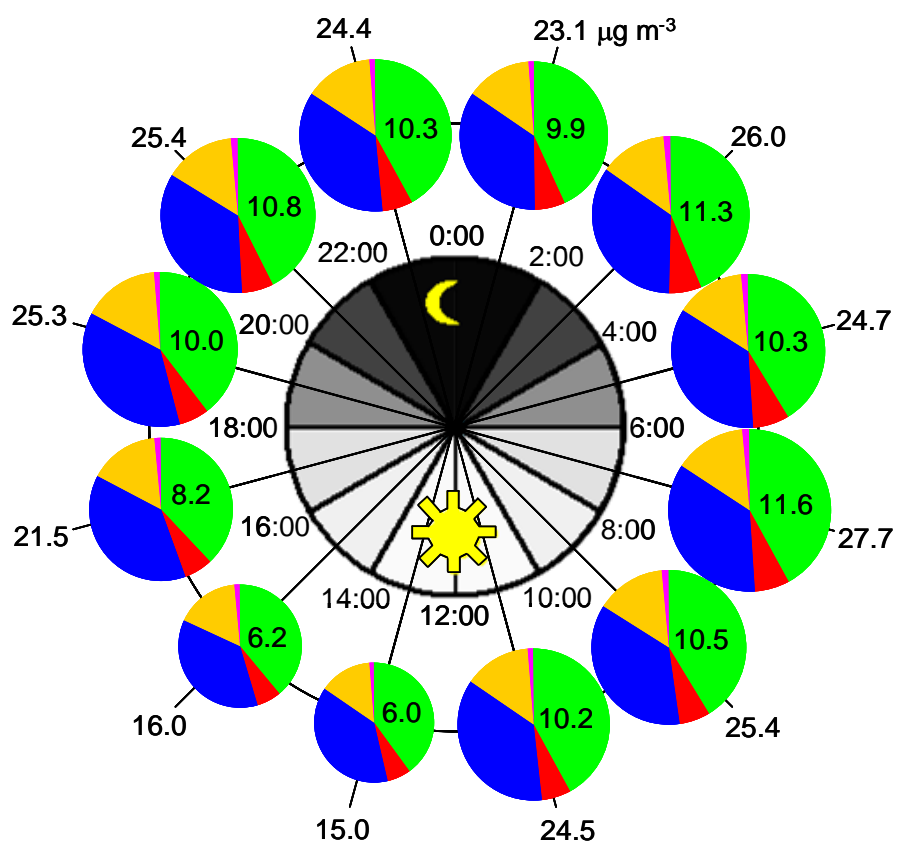


Figure 21. a) Individual organic aerosol source timelines over the fall focus period (November 4 – 14). b) Diurnal averages for fall organic aerosol sources. Photosynthetic active radiation (PAR) has been included to represent the solar cycle.



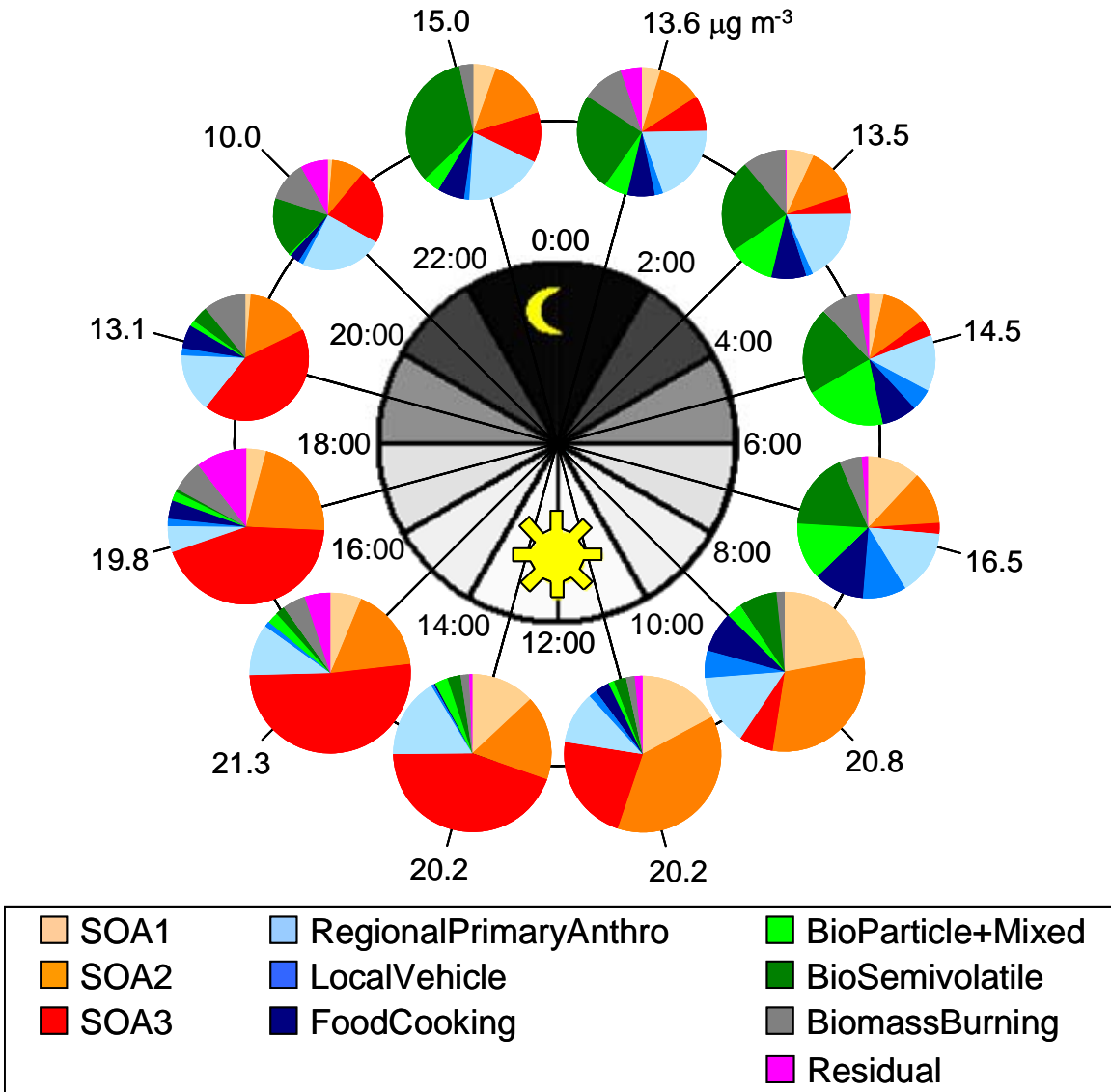
AMS Total Organic Aerosol = 10.0 - 20.8 $\mu\text{g m}^{-3}$

Figure 22. Average diurnal concentrations of AMS species over the summer focus period. Total aerosol mass concentrations labeled outside of pie chart ring, and time of day labeled inside of pie chart ring.



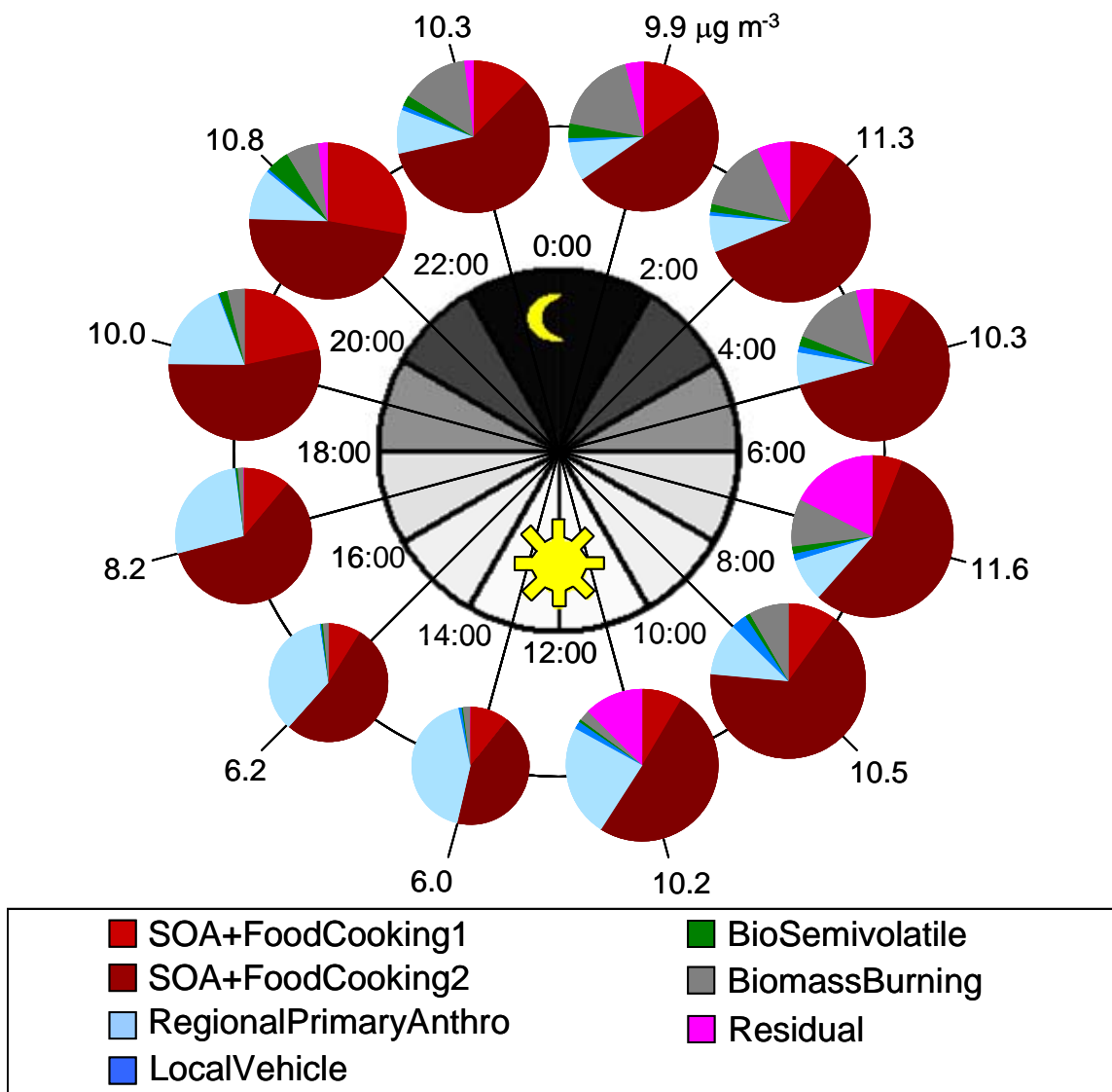
AMS Total Organic Aerosol = 6.0 – 11.6 $\mu\text{g m}^{-3}$

Figure 23. Average diurnal concentrations of AMS species over the fall focus period. Total aerosol mass concentrations labeled outside of pie chart ring, and time of day labeled inside of pie chart ring.



AMS Total Organic Aerosol = 10.0 - 20.8 $\mu\text{g m}^{-3}$

Figure 24. Average diurnal concentrations of TAG-derived PMF sources over the summer focus period. Total organic aerosol mass concentrations labeled outside of pie chart ring, and time of day labeled inside of pie chart ring.



AMS Total Organic Aerosol = 6.0 – 11.6 µg m⁻³

Figure 25. Average diurnal concentrations of TAG-derived PMF sources over the fall focus period. Total organic aerosol mass concentrations labeled outside of pie chart ring, and time of day labeled inside of pie chart ring.

Interim Report

Hourly, In-situ Quantitation of Organic Aerosol Marker Compounds (Contract # 03-324)

Prepared for:
State of California Air Resources Board
Research Division
P.O. Box 2815
Sacramento, CA 95812

Principle Investigator:
Professor Allen Goldstein
Department of Environmental Science, Policy, and Management
College of Natural Resources
151 Hilgard Hall
University of California
Berkeley, CA 94720-3110
(510) 643-2451 tel
(510) 643-5098 fax
ahg@nature.berkeley.edu

Subcontract Co-Investigator
Dr. Susanne V. Hering
Aerosol Dynamics Inc.
Berkeley, CA

Contact for Contractual Matters:
David Garcia
Acting Assistant Director
Sponsored Project Office
University of California
336 Sproul Hall
Berkeley, CA 94720-5940
(510) 510-642-8114
(510) 642-8236 fax
email: dgarcia@uclink.berkeley.edu

January 10, 2005

Abstract

The objective of this work is to identify the origins of PM_{2.5} organic matter within a region in California that is currently out of compliance with PM air quality standards. This we have contracted with ARB to achieve through automated, time-resolved measurements of organic marker compounds in ambient aerosols, combined with source attribution through factor analysis.

The contract with ARB was written to have two phases. The objective of Phase II is to perform field measurements in California during summer and winter in the Fresno area at a site to be determined in coordination with ARB staff. These field experiments will provide measurements of speciated organic composition of PM_{2.5}, with minimal interruption over two periods of one month each, defining daily cycles and seasonal differences with hourly time resolution. The comprehensive hourly time resolution data sets will be suitable for using factor analysis to resolve major sources of organic species in aerosols

The objective of Phase I is to prove our ability to measure atmospheric PM_{2.5} samples with separation and identification of organic compounds at the molecular level. For Phase I we were contracted to prepare the brief written report that we are hereby submitting to the ARB providing evidence that our new instrumentation is ready for field measurements in California. The report is based on evaluation in our laboratory in Berkeley, and on our 6-week summer 2004 field campaign in Nova Scotia. We present our data with comparisons to other on site measurements where possible, and include factor analysis of the measurements to indicate the suitability of hourly data for source attribution of organic particulate matter. This report is to be taken by ARB staff to the Research Screening Committee to get approval for the Phase II field studies in California which were described in our original proposal.

This interim report clearly addresses the concerns of ARB. We show that our new in-situ **T**hermal desorption **A**erosol **G**C/MS-FID (now named **TAG**) can indeed provide time-resolved data for atmospheric PM_{2.5} organics under field conditions. We provide initial results showing how our data set of hourly concentrations of marker compounds provides a new means of determining contributions of sources using factor analysis.

Subsequent to our initial contract, we have been asked by ARB staff (Nehzat Motallebi and Eileen McCauley) to supplement this project by including time resolved gas-phase VOC measurements with a second automated in-situ GC/MS/FID instrument built in our laboratory. These gas phase measurements are to be done alongside the particle phase measurements during both summer and winter in order to provide supporting information for resolution of aerosol source types. Justification for addition of these gas phase measurements is included in our interim report.

Table of Contents

Abstract

- 1. Statement of Significance**
- 2. Measurement and Data Analysis Approach**
- 3. Experimental Methods**
- 4. Laboratory Evaluation**
- 5. Atmospheric Aerosol Measurements in Berkeley, CA**
- 6. Field Campaign in Nova Scotia**
- 7. Gas Phase VOC Measurements**
- 8. Comparison between Berkeley, California and Nova Scotia**
- 9. Conclusion**
- 10. References**

1. Statement of Significance

Many urban and rural California air districts are now out of compliance with state and federal air quality standards for particulate matter. The Air Resources Board and Office of Environmental Health Hazard Assessment are currently formulating new 24-hour PM_{2.5} ambient air quality standards for California. Regulatory efforts to conform to PM_{2.5} standards require improvements in our knowledge of the sources, concentration, and chemical composition of PM_{2.5}.

Organic matter is a major constituent of airborne particles, comprising 20-50% of the PM_{2.5} mass in many regions (e.g. Schauer J. J. and Cass G. R., 2000; Kim, et al., 2000; Christoforou et al, 2000; Chow et al., 1993; NARSTO,2003). Its chemical composition is complex, and largely not understood. Many hundreds of organic compounds have been identified through chromatography and mass spectrometry techniques (Rogge et al., 1997a, 1997b, 1998; Schauer et al., 1999; Nolte et al., 1999; Fine et al., 2001). These include alkanes, substituted phenols, alkanals, sugar derivatives, aromatic polycyclic hydrocarbons, mono- and di-carboxylic acids. Some organic compounds are markers for primary emissions, such as combustion sources, while others are secondary products formed from anthropogenic or biogenic precursors.

Quantitative knowledge of the composition of PM_{2.5} organic matter is a key to tracing its sources and understanding its formation and transformation processes. While the compounds which have been identified comprise only a fraction of the total organic mass, those that are quantified serve as valuable markers for sources. Hopanes, which are remnants of the biological material from which petroleum originated, serve as a unique tracer for fossil fuel combustion. Levoglucosan is a product of the breakdown of cellulose, and is a unique tracer for wood combustion. Biogenic alkanes are distinguished from fossil-derived alkanes through a carbon preference number that reflects the predominance of odd-carbon number alkanes in plant waxes. These differences in organic compound composition have been used to determine the relative contribution of various source types to primary ambient organic matter (Schauer and Cass 2000; Fraser et al 2000; Fine et al 2001; Yue and Fraser 2003a, 2003b).

A substantial limitation in the use of organic marker compounds for source identification is the difficulty of the analyses. To date, the most extensive work on the identification of organic compounds in ambient aerosols has been by filter collection, with laboratory extraction, chromatographic separation and mass spectrometric analyses. Generally large samples are required, and analyses are time-consuming and expensive. These methods have provided valuable insight and guidance in the understanding of airborne organic matter, but are limited by the intensity of manual efforts, cost and by their poor time resolution.

In this report we present a new method for organic characterization, and its application to organic aerosol source resolution. Our measurement approach, the In-situ Thermal Desorption Aerosol GC/MS-FID (TAG) provides hourly time resolution for organic marker compounds. Our source attribution approach uses the time resolution afforded by our new measurement method to resolve sources based on factor analysis. This interim report describes our method, and presents initial results for measurements of atmospheric aerosols in Berkeley, California and Nova Scotia, Canada. Our instrument development and testing efforts described here have been supported through the US DOE. Our 6-week deployment in Canada was conducted as part of the NENA-2004 campaign (North-East North-Atlantic experiment) with additional support provided by NOAA.

2. Measurement and Data Analysis Approach

Hourly Measurement of Organic Marker Compounds. Our in-situ Thermal Desorption Aerosol GC/MS (TAG) is designed for the quantitative, time-resolved measurement of the ambient concentration of specific organic compounds in PM_{2.5}. It is based on the general analytical approach used for many years in laboratory analysis of filter samples. The difference is that samples are collected by impaction, and analyses are performed in-situ immediately after sample collection. The method is automated, allowing around-the-clock operation, with hourly time resolution.

The TAG system collects ambient PM_{2.5} aerosols onto an inert substrate by means of impaction, immediately followed by thermal desorption onto a GC column, with subsequent GC/MS-FID analysis. The interface between the GC/MS and ambient aerosol is provided by a collection and thermal desorption (CTD) cell that provides both sample collection, and subsequent sample transfer to the GC column. Once

on the column compounds are separated using standard chromatographic methodology, and detected by a mass spectrometer or flame ionization detector, or both. The method is semi-continuous, consisting of sample collection, sample transfer to the separation column, and chromatographic analysis.

Our new instrument combines several proven technologies. The impaction collection is a straightforward extension of our existing automated system for measuring particulate nitrate, wherein particles are preconditioned via humidification and then deposited on a metal surface by impaction (Stolzenburg and Hering 2000). Thermal desorption GC/MS has been used successfully for the analysis of time-integrated filter and impactor samples of atmospheric aerosols (Waterman et al., 2000, Neusüss et al., 2000, Falkovich and Rudich, 2001). The automation of the GC/MS is an extension of our well-established work for in-situ measurement of volatile organic compounds in the gas phase (Goldstein et al., 1995; Lamanna and Goldstein, 1999).

The analytical technique employed by TAG is very similar to published protocols for analysis of particulate filter samples. Compounds are separated chromatographically and then identified individually by comparing their mass spectrum fragmentation pattern to the published spectra on a NIST MS database. As such, our effort has the advantage of building on the existing source characterization data base for organic compounds. The major difference from filter-based work is that our instrument provides automated, in-situ analysis with high time resolution, and avoids known artifacts associated with filter collection.

Source Attribution through Factor Analysis. Two approaches have been used for source attribution of particulate matter. The first approach is based on chemical mass balance methods wherein the mix of elemental composition or chemical constituents found at the receptor site is compared to individual source profiles. Alternatively, if the ambient data set has sufficient time resolution and statistical power, source attribution may be accomplished through factor analysis. With factor analysis the variability over time in profiles measured at the receptor site can be described through the superposition of several independent “factors”. Each factor is associated with a characteristic ratio of compounds, much like a source signature (e.g. Lamanna and Goldstein, 1999). The independent factors are then associated with sources based on comparison with literature data on source profiles (Rogge et al., 1997a, 1997b, 1998; Schauer et al., 1999; Fine et al., 2001).

To date, the resolution of organic particulate matter has focused on the first approach. These efforts have utilized data sets derived from integrated filter samples collected over 24 hour intervals, and or composite samples collected over time periods of as much as one year. With the hourly data set provided by our new instrument, source attribution for organics can be done by the second approach, namely through factor analysis. For the first time, we will have a data set that provides the statistical power necessary to utilize factor analysis for identifying origins of particulate organic matter. No other technique has this capability.

Hourly time resolution is critical to these analyses. In an urban or suburban location such as Fresno, the various source types have different temporal patterns. Compounds associated with primary emissions will have a different diurnal cycle (e.g. mobile sources peaking in the morning and evening rush hour) than compounds whose production is secondary through gas to particle conversion (e.g. peaking in mid to late afternoon). Light duty vehicles and heavy diesel vehicles have different temporal traffic patterns. With our method we will be able to resolve these differences in temporal patterns.

Factor analysis will identify those sets of compounds that are associated with a single source, and will show the relative strength of that source. Available source profile data permits identification of the source types associated with these sets of co-varying compounds. Additionally, since we observe at high time resolution, we may be able to identify additional compounds whose variability matches the variability of known source profiles, and thus refine the profiles for the major source categories we observe, and to make observations regarding the relative stability of primary organic compounds in the atmosphere. In summary, the focus of our approach is to capture the time variability in the measured organic marker profiles that corresponds to the inherent time variability in source contributions. We will associate specific source types with these factors based on published source profiles.

3. Experimental Methods: The TAG System

The fundamental principal of TAG is collection of ambient PM_{2.5} aerosols onto an inert substrate by means of impaction, immediately followed by thermal desorption onto a GC column, with subsequent GC/MS-FID analysis. As illustrated in Figure 1, TAG system has two basic modes of operation. These are: (1) ambient sampling with concurrent GC/MS analysis, (illustrated in Figure 1a) and (2) thermal desorption and sample injection (illustrated in Figure 1b). The sample collection and concurrent GC/MS analysis takes approximately 50 minutes. The thermal desorption mode is operational only during the time required to desorb and inject the sample into the head of the GC/MS column. This step takes approximately 10 minutes, giving an overall cycle time of one hour.

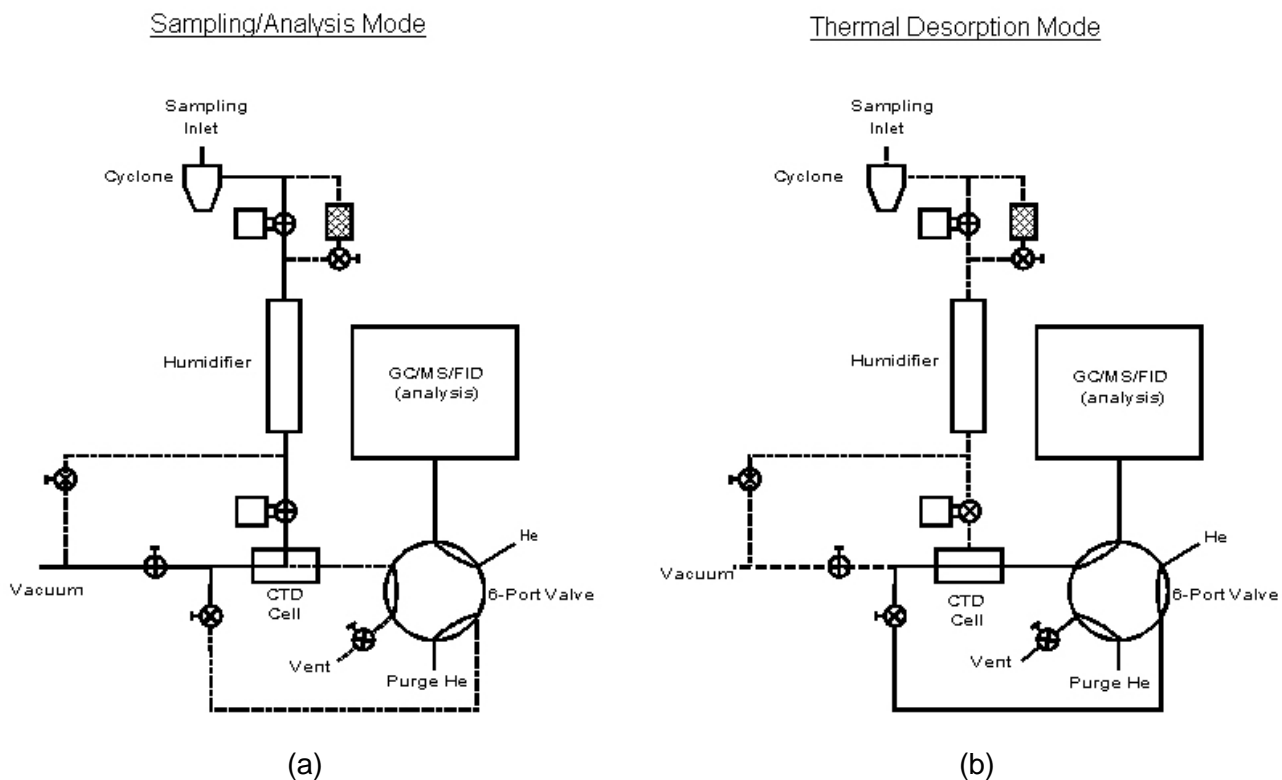


Figure 1. Schematic of the TAG system, showing flow configuration for two modes of operation: (a) concurrent sampling and analysis, and (b) thermal desorption. Most of the time the system is in the sampling/analysis mode. The thermal desorption mode is used for transfer of collected sample onto the analytical column.

Components of the TAG system shown in Figure 1 are: an inlet; a PM_{2.5} precut cyclone; a humidifier; an isolation ball valve; an integrated collection and thermal desorption (CTD) cell, the GC/MS-FID, and associated transport lines and valves. The cyclone provides a PM_{2.5} precut that excludes particles above 2.5 μm in aerodynamic diameter. Cyclones have the advantage that they do not require oil or grease to prevent particle bounce and re-entrainment, thus eliminating a potential source of contamination. The humidifier is used to increase the relative humidity of the sample air stream to a value of 65% or higher. This reduces the bounce of solid particles within the impaction region of the CTD by adding a thin coating of water to the sampled particles. The CTD cell collects the humidified particles by impaction, and then desorbs the collected sample through heating. The CTD has nine 0.34-mm diameter orifices and is fabricated from 316 stainless steel that is chemically passivated using an Inertium treatment (Advanced Material Components Express., St. College, PA). The CTD collector is mounted in an aluminum block with a cartridge heater that is controlled by a proportional integral differential (PID) controller. These are housed within an insulated box equipped with a fan that permits cooling of the cell at the end of the desorption step. A ball valve immediately above the CTD cell is open during sampling and closed during the thermal desorption step. The system has an upstream particle filter that may be switched in line automatically to provide routine measures of the background signal when no aerosol is sampled and to test

for potential gas phase artifacts. System automation is handled through switching of the various valves, and programmed temperature control.

For sample collection the CTD is cooled to a temperature of 30° C prior to switching the valves so ambient air sample flows through the cyclone, humidifier and CTD cell. For the measurement of dynamic blanks, defined as the signal for particle-free sampling, the upstream valves are switched to divert the sample flow through a filter, but is otherwise the same as for aerosol sampling. At the end of the approximately 30-min sample collection period, the sample flow is directed around the cell through bypass line. With the GC oven at 50°C, the CTD cell is purged with He gas, and the cell is slowly heated. Material that desorbs from the cell at low temperature, below approximately 80°C, is mostly water, and is vented. After the initial heating, the six-port valve is switched so that the He carrier gas is directed through the cell and into the GC/MS. Heating of the CTD continues to approximately 300° C to desorb the organic compounds in the collected sample. The transfer lines between the CTD and GC column and the 6-port valve are heated to 300°C. During desorption the head of the column is held at 50°C, and thus acts as a “trap”, refocusing the desorbed compounds onto the beginning of the column. At the end of desorption, the system returns to the sampling and analysis configuration, allowing the GC/MS analysis of the current sample, and the collection of the subsequent sample, to proceed.

The GC/MS-FID provides analysis of the sample using a DB-5MS column with a He carrier gas flow of 2 cm³/min and a 28.5-minute temperature ramp to 300°C, followed by a 6-min soak at 300°C, similar to the published analytical protocols for aerosol filter analyses. Compounds eluting from the column are split between the MS and FID detectors to provide simultaneous mass spectra for identification and flame ionization detection for quantification. The analysis proceeds during the collection of the subsequent sample, so that nearly uninterrupted measurement is possible. At the end of the analysis the GC oven temperature is cooled in preparation for the next sample. The collection and analysis steps are automated, yielding around the clock speciation with hourly time resolution.

4. Laboratory Evaluation

Specific aspects of the TAG system were evaluated in the laboratory. We examined (1) the particle collection efficiency within the CTD, (2) the system response to known standards (3) the efficiency of sample transfer to the chromatographic column via thermal desorption and (4) the system reproducibility for collocated sampling.

Particle Collection Efficiency: The particle size dependent collection efficiency of the CTD cell is shown in Figure 2. These data were obtained with two types of challenge aerosols: oleic acid, a nonhygroscopic oil and mixture of ammonium sulfate and oxalic aerosol, to form a hygroscopic aerosol. Results are shown for two configurations, both operating at a sample flow rate of 7 L/min. The CTD cell had 10, 0.28 mm diameter jets. It collected particles with diameters of 0.09 μm and larger with an efficiency of 50%, increasing to above 90% at 0.18 μm . For the hygroscopic test aerosol the collection efficiency is higher, with 50% efficiency at 0.06 μm , increasing to 90% at 0.11 μm . Higher collection efficiencies are found for the 9-jet CTD, which has a 50% efficiency collection of oleic acid particles at 0.07 μm , increasing to 90% at 0.12 μm .

Thermal Desorption Efficiency: The efficiency of thermal desorption and transfer from the CTD cell to the head of the chromatography column was evaluated using a standard solution comprised of a wide range of compounds including Dodecane, Hexadecane, Eicosane, Octacosane, Decanoic acid, Benzaldehyde, 4,4-Dimethoxybenzophenone, Acenaphthene, Chrysene, Levoglucosan, and Cholestane. Specifically, a comparison of the results obtained by introducing the standard with a microliter syringe through the GC injection port (traditional approach), to that obtained by thermal desorption of the same size standard aliquot from the CTD. For the CTD analysis, the standard aliquot was placed in a glass boat, the solvent was allowed to evaporate, and then the standard was thermally desorbed and transferred through the sampling valve directly onto the GC column. For these tests the GC/MS was configured to incorporate a flame ionization detector (FID) in parallel to the mass spectrometer detector (MSD). The FID has the advantage of offering a more linear response with respect to the mass of carbon, and of better stability over time. Multipoint calibration curves were generated for both the direct injection and thermal desorption modes.

Multipoint calibration curves for several representative compounds are shown in Figure 3. Chrysene is a polycyclic aromatic hydrocarbon formed through combustion. Cholestane is one of the hopanes that serves as a biomarker for petroleum. Levoglucosan is a product of the combustion of cellulose, and is a powerful tracer for wood combustion. Eicosane is one of the many alkanes found in ambient particles. The FID and the MSD responses for sample introduction via thermal desorption from the CTD were compared to those obtained by sample introduction via the injection port, as is standard practice for filter extracts. We obtained excellent linear responses ($R^2 > 0.95$) and near zero intercepts for both injection modes for almost all compounds in the standard mixture, as listed in Table 1.

Desorption and transfer efficiencies from the CTD relative to that for direct injection are displayed in the fourth column of Table 1. Results are calculated as the ratio of the CTD response to that of the direct injection for 10 ng of analyte, where individual response is calculated by the corresponding regression line from the multipoint calibration using data from the FID that is more stable over time than the MSD. The relative transfer efficiency among compounds is roughly indicated by the FID response per femtomole of carbon (fMC), as listed in the last two columns of Table 1. As is evident, the transfer efficiency from the CTD is equivalent to that for direct injection for most compounds, and even better for levoglucosan, octacosane and cholestane. Neither approach shows good efficiency for levoglucosan or decanoic acid. For these compounds, the FID signal relative to the number of carbon atoms is much lower than that for the alkanes, indicating incomplete transfer of these compounds through the analytical system, regardless of the introduction technique. These compounds are known to be very difficult to transfer through gas chromatography systems, so they are sometimes derivatized prior to analysis.

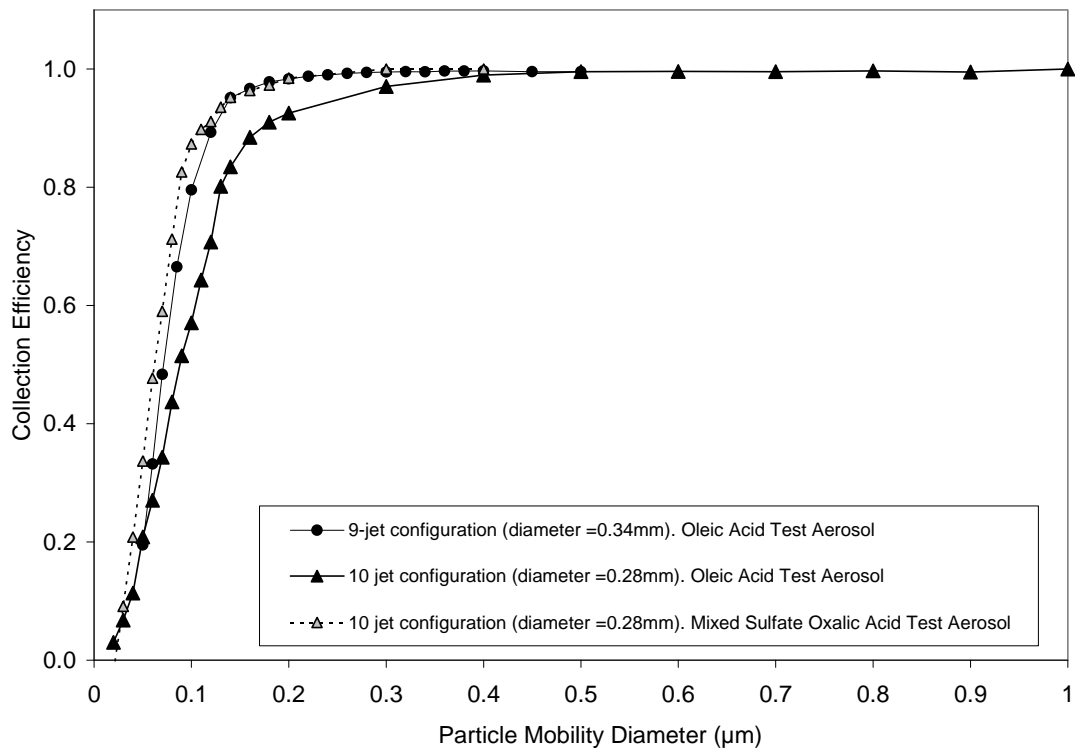


Figure 2. Particle-size dependent collection efficiency of the CTD cell for an organic aerosol, oleic acid, and for a hygroscopic aerosol comprised of a mixture of oxalic acid and ammonium sulfate. Results are shown for both a nine-jet and ten-jet configuration.

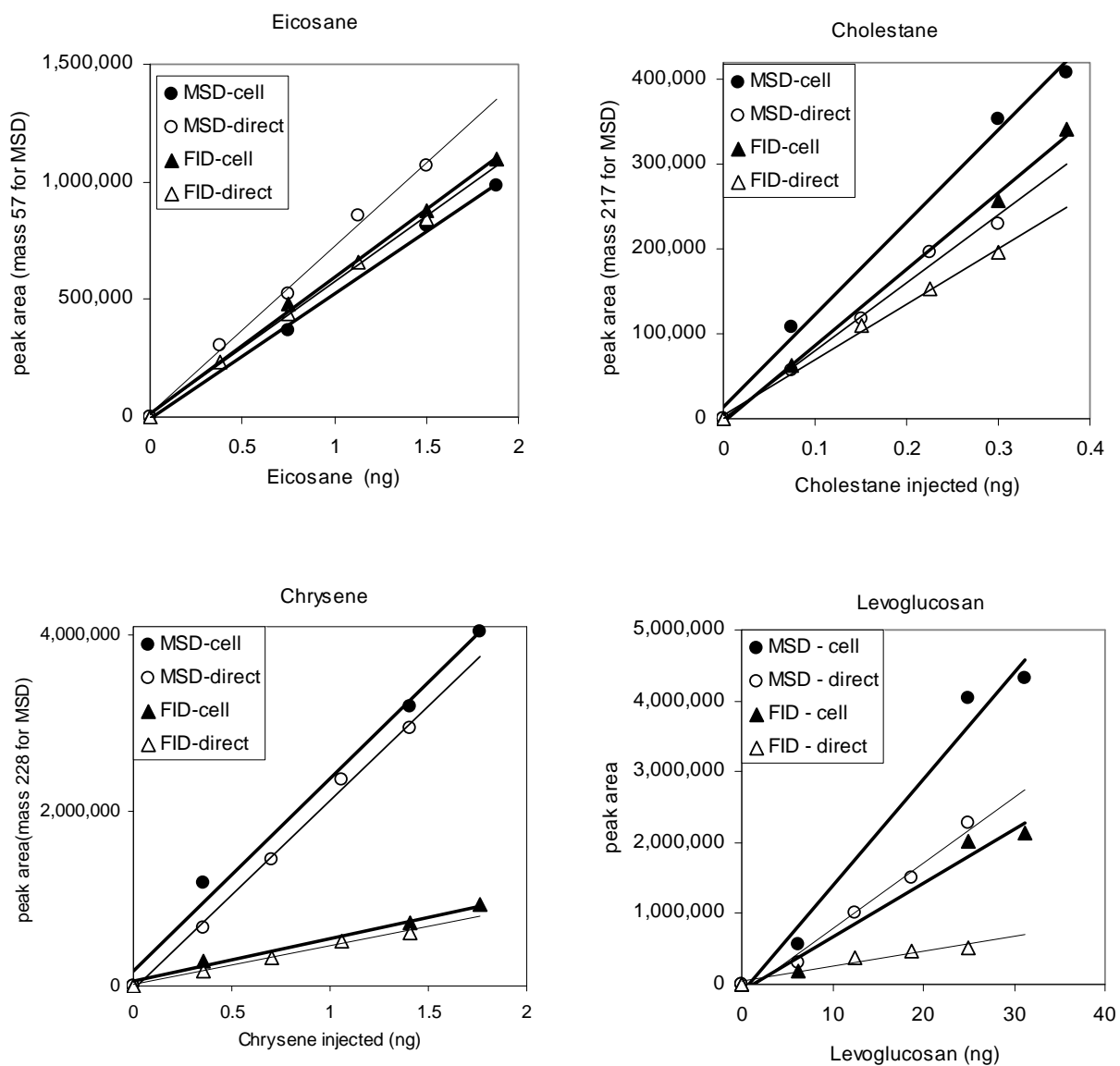


Figure 3. Calibration curves for the CTD cell for four representative marker compounds, eicosane, cholestane, chrysene and levoglucosan, with comparison to the FID response for direct injection.

Table 1. Thermal Desorption Response to Laboratory Standards

Compound	CTD - MSD Response			Efficiency (CTD/Direct)	Flame Ionization Detector	
	slope (10 ³ cts/ng)	intercept (10 ³ cts)	R ²		CTD (cts/fMC)	Direct (cts/fMC)
Acenaphthene	795	-146	0.976	1.00	6,071	6,120
Hexadecane	581	-51	0.995	1.26	8,416	6,667
Eicosane	812	10	0.999	1.19	9,376	7,909
Dimethoxybenzo- phenone	153	4	0.999	0.97	4,218	4,342
Chrysene	2,192	172	0.991	1.11	6,228	5,638
Octacosane	838	182	0.999	1.41	8,454	5,944
Cholestane	1,090	13	0.994	1.38	12,419	9,019
Levoglucosan	151	-128	0.981	2.59	2,057	577
Decanoic acid	83	32	0.816	0.53	2,045	3,691

Notes: Simultaneous analysis by MSD and FID.
 CTD refers to thermal desorption from CTD cell,
 DIRECT refers to sample introduction with syringe through the injection port.
 Efficiency calculated as relative CTD to DIRECT response at 10 ng as given by regression line.

Detection Limits: The response to Acenaphthene, Hexadecane, Eicosane, Octacosane, Cholestane, and Chrysene was evaluated at the 0.1 to 0.4 ng level. All yielded very clear signals, well above baseline. Corresponding ambient concentrations for 30-min sampling (one-hour cycle time) with the TAG are 0.4-2 ng/m³. Reported concentrations for Fresno and Bakersfield during the IMS95 experiment were 2 to 200 ng/m³, depending on day and compound (Schauer and Cass, 2000). Our laboratory data show very clear signals at levels well below expected concentrations for California's Central Valley.

Detection limits for TAG are estimated from the area of a chromatographic peak equal to 3 times the baseline noise level for our standard injections. This detection limit is 0.01 ng for hexadecane, and, with the exception of levoglucosan, is within a factor of 3 for other compounds measured. At 0.03ng the corresponding ambient concentration is 0.1 ng/m³, well below expected levels for California urban areas. Levoglucosan is not transferred efficiently through the system, as shown in Table 1, and its detection limit is correspondingly higher. However, concentrations of levoglucosan are quite high when wood burning occurs, and are clearly observed with this instrument, as shown in our Berkeley samples presented below.

Reproducibility for Ambient Sampling: Reproducibility for identifying and quantifying individual compounds in ambient aerosol samples was tested with ambient aerosol using off-line collection and subsequent analysis. This allowed collection of multiple samples in parallel for assessing measurement precision, and for assessing possible vapor adsorption artifacts. Collection was done on 4th street in Berkeley, California located in the vicinity of an interstate highway. After collection, samples were transported to the GC/MS and the glass collection boats were inserted into the CTD cell mounted on the GC/MS for thermal desorption and analysis. Figure 4 shows a scatter plot of peak areas for a selection of compounds measured between the first of these triplicate samples and the other two. A minor variability between the peak areas scales linearly indicating slight differences in sample size, but nearly identical relative responses. Standard deviations for measurements of individual compounds in the triplicate samples ranged from 0.04 to 0.33 for 11 selected representative compounds with a pooled std dev of 0.12, and reproducibility for the majority of these compounds was better than 10%.

To summarize these laboratory experiments, we find that the TAG provides

- efficient collection of particles in the size range above 0.1 μm
- efficient sample transfer via thermal desorption from the CTD to the GC column
- linear response to a suite of organic compounds with detection limits better than 0.1 ng/m³ for efficiently eluted compounds.

- precision of 10% or better for collocated samples

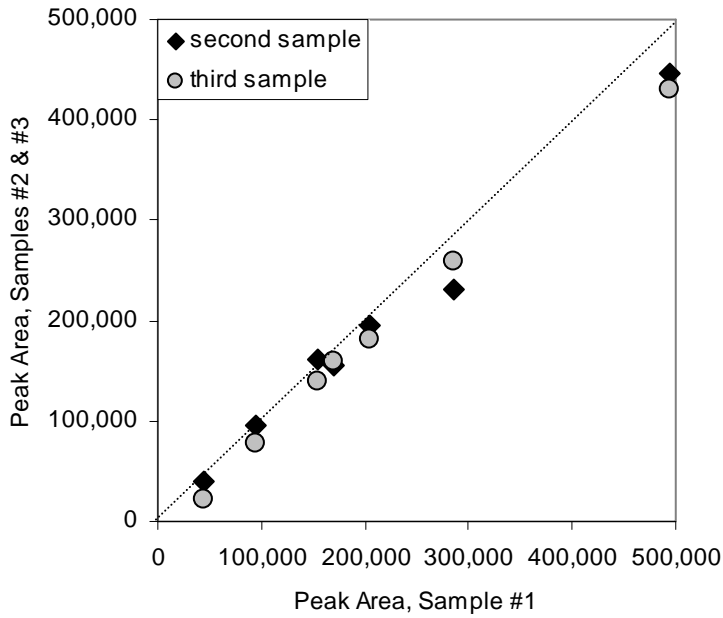


Figure 4. Comparison of peak areas for independent, collocated samples of ambient air in Berkeley California. Line shows 1:1 correspondence.

5. Atmospheric Aerosol Measurements in Berkeley, CA

In this section we demonstrate the utility of TAG for identifying specific organics in aerosols with approximately hourly time resolution. We further show that the data can be used for Factor Analysis and serve as a basis for source apportionment studies.

TAG was tested in the laboratory at UC Berkeley, an urban environment, by running continuous automated analyses of ambient air for approximately 1 full day on January 10-11, 2004. An example chromatogram from one of the air samples is shown in Figure 5. We have identified 74 of the major peaks using the NIST 1994 mass spectral database, many of which are labeled in Figure 5. Examples of the mass spectral matches for several compounds are shown in Figure 6.

Notable in the chromatogram is the presence of levoglucosan (31.4 min) which is strongly associated with wood burning. Several alkanic acids are seen, including tetradecanoic acid, hexadecanoic acid and octadecanoic acid. All of the alkanes from C₁₇ through C₃₅ are present. Also, note the presence of many polycyclic aromatic hydrocarbons, especially later in the chromatogram. These include anthracene, fluoranthene, benzo[e]pyrene, benzo[k]fluoranthene, benzo[ghi]perylene, and indeno[1,2,3-cd]pyrene.

Timelines of the relative concentrations of each of these identified compounds are given in Appendix A. The individual timelines show that abundance of the measured compounds varies significantly over the one-day measurement period, and that some groups of compounds have similar temporal variations. The concentrations of individual compounds vary by factors 2 to 11. The concentration timeline patterns vary among sets of compounds, as can be seen through inspection of the timelines. This variability results from a combination of different sources with different temporal attributes (e.g. woodsmoke, mobile sources, etc.) along with meteorological variability. The covariance of groups of measured compounds should provide information about composition associated with specific source categories, and we can separate marker compounds for specific sources using statistical approaches that analyze for co-variance such as Factor Analysis. This 1 day data set is too short to do a complete factor analysis of all 74 compounds measured, but we have done a preliminary analysis of the first 14 compounds.

Abundance

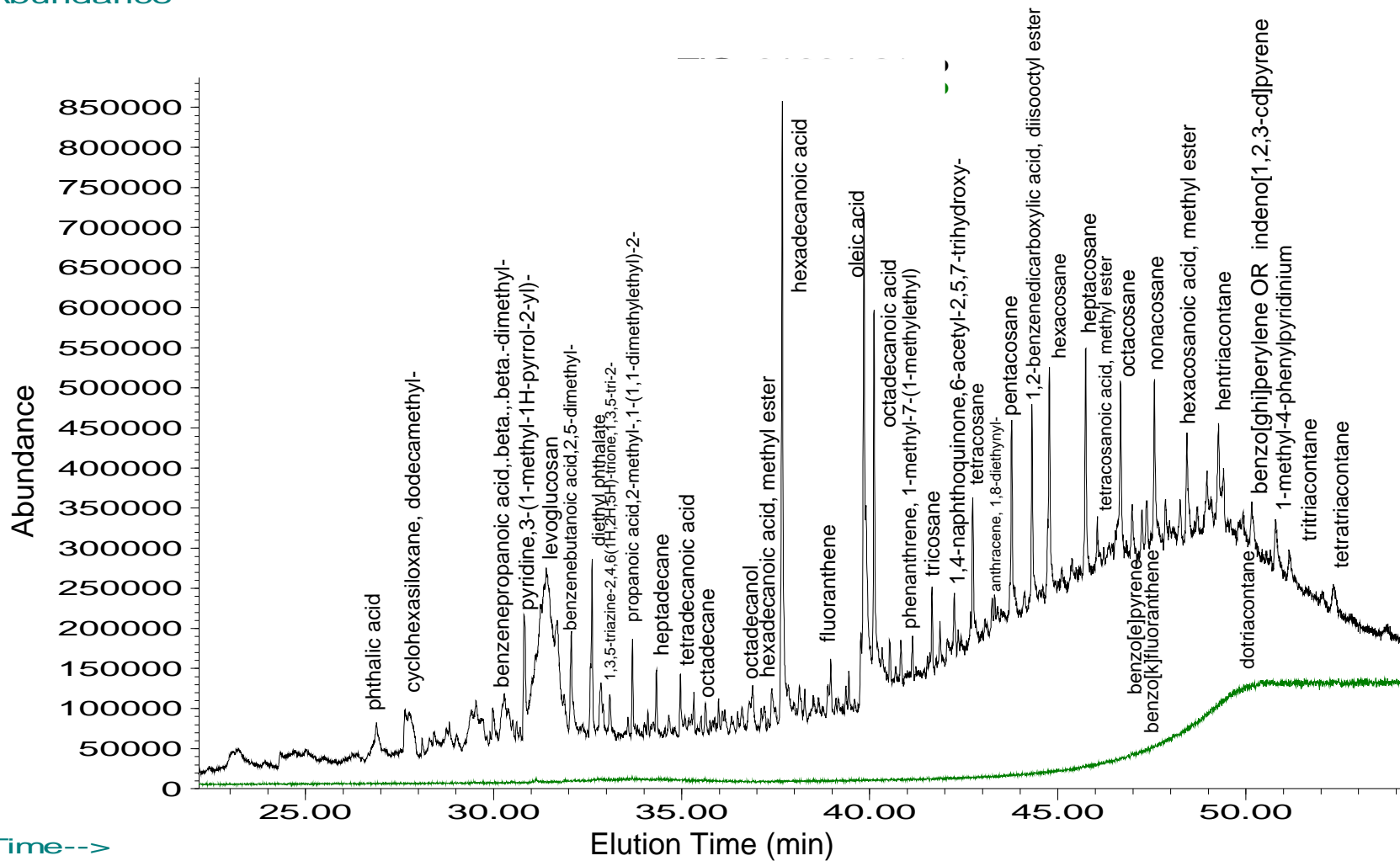


Figure 5. TAG Chromatogram from Berkeley California, with many of the identified peaks labeled. Lower green line shows signal from blank.

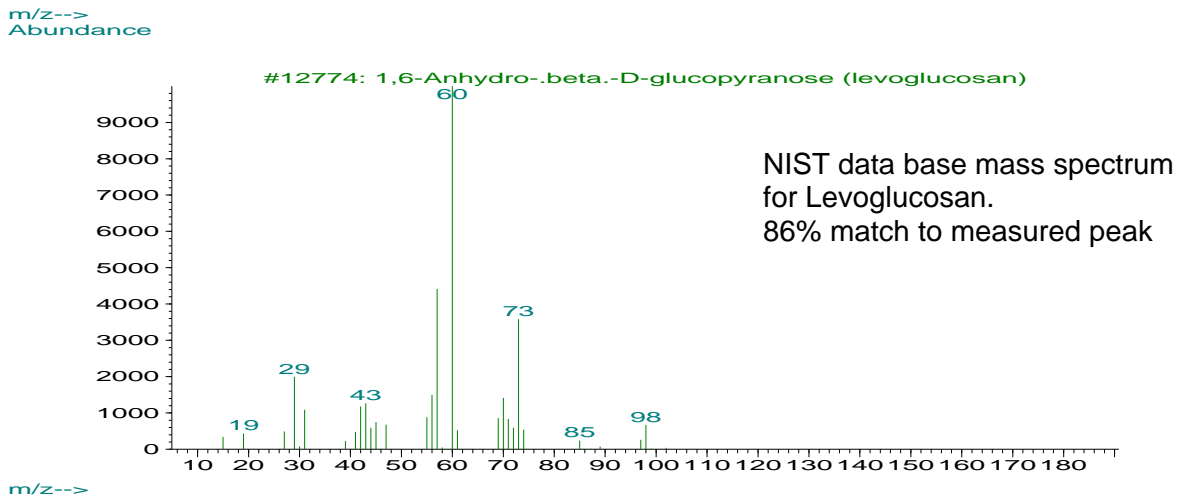
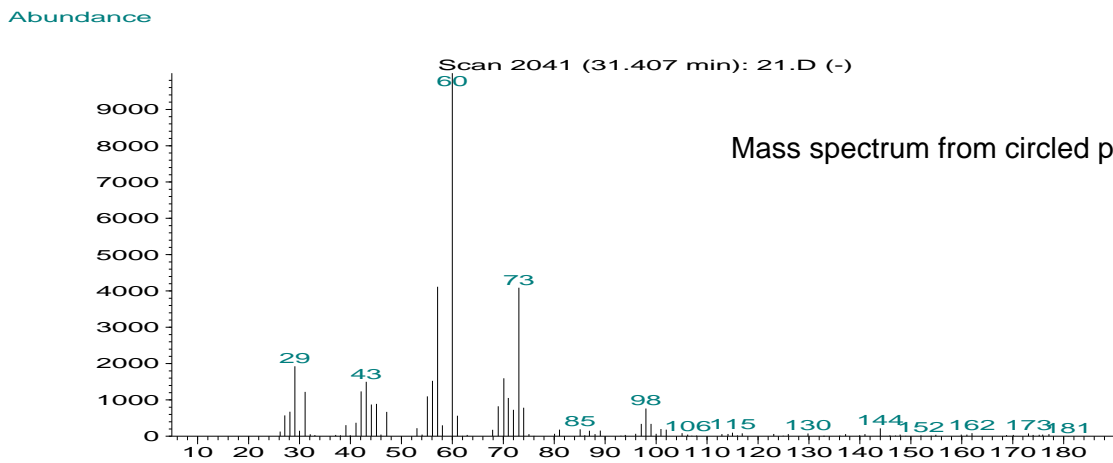
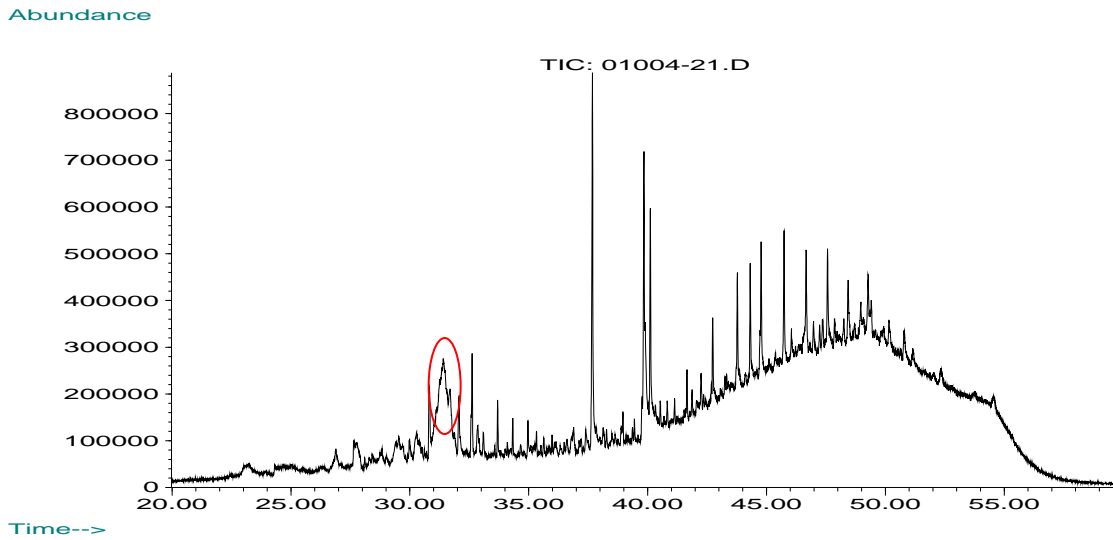


Figure 6a. Mass Spectral match for circled peak in chromatogram from ambient sample in Berkeley, CA.

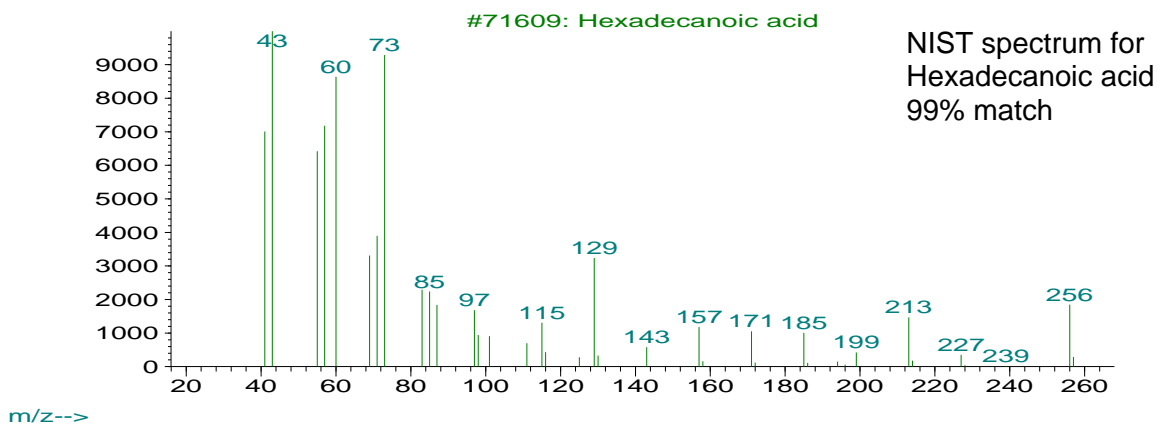
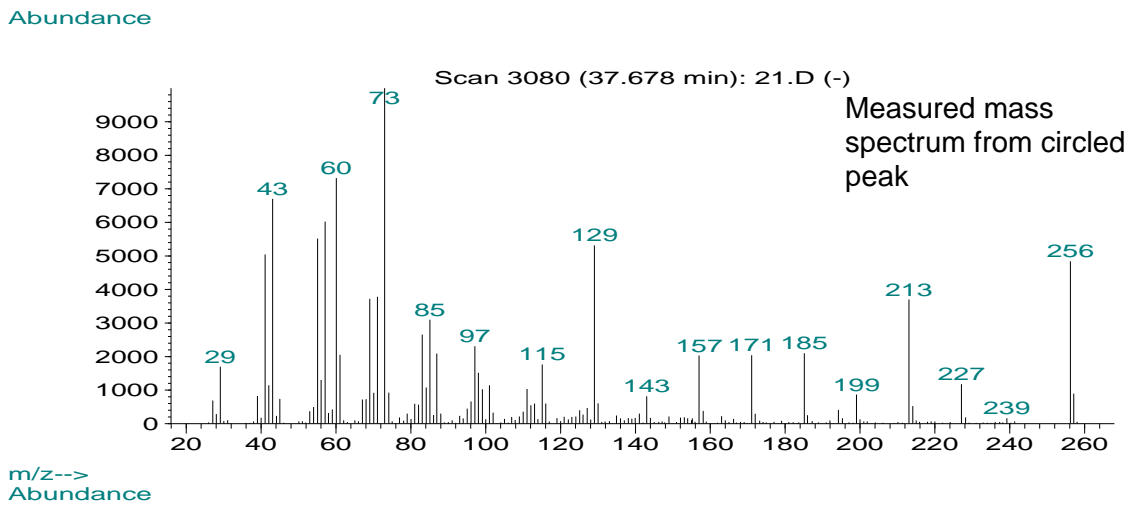
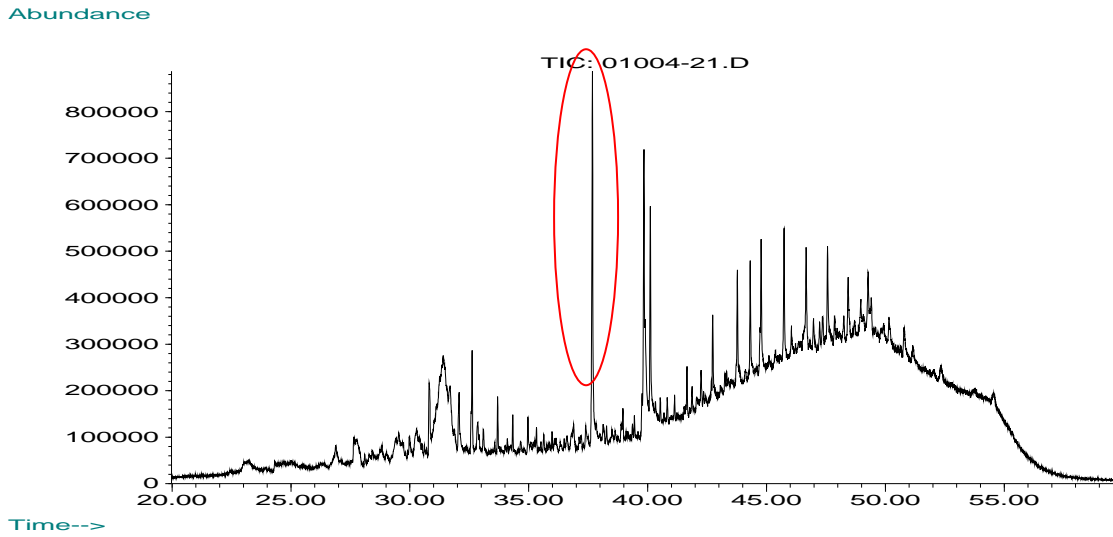


Figure 6b. Mass Spectral match for circled peak in chromatogram from ambient sample in Berkeley, CA.

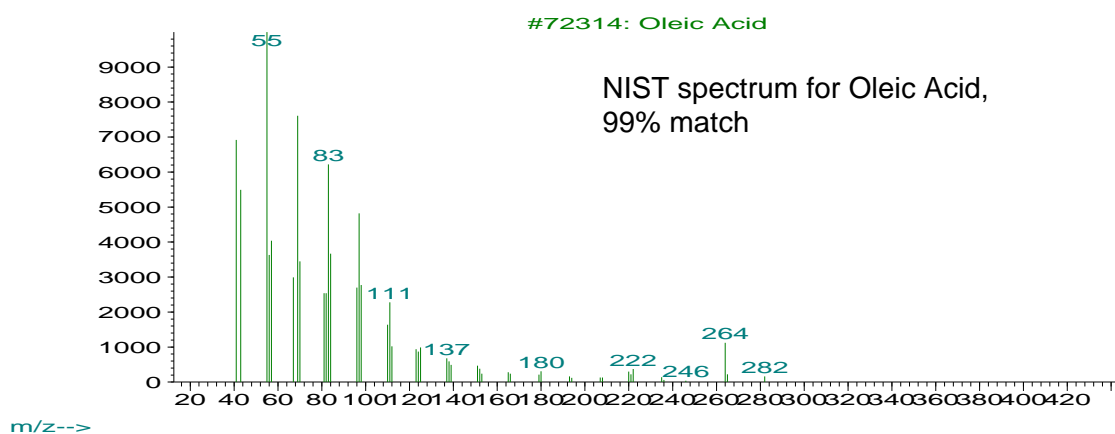
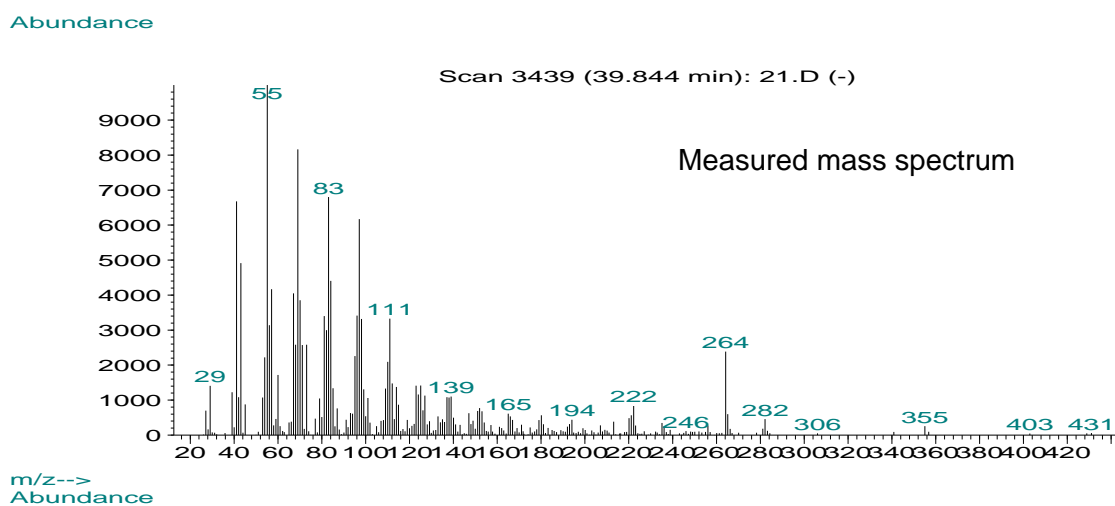
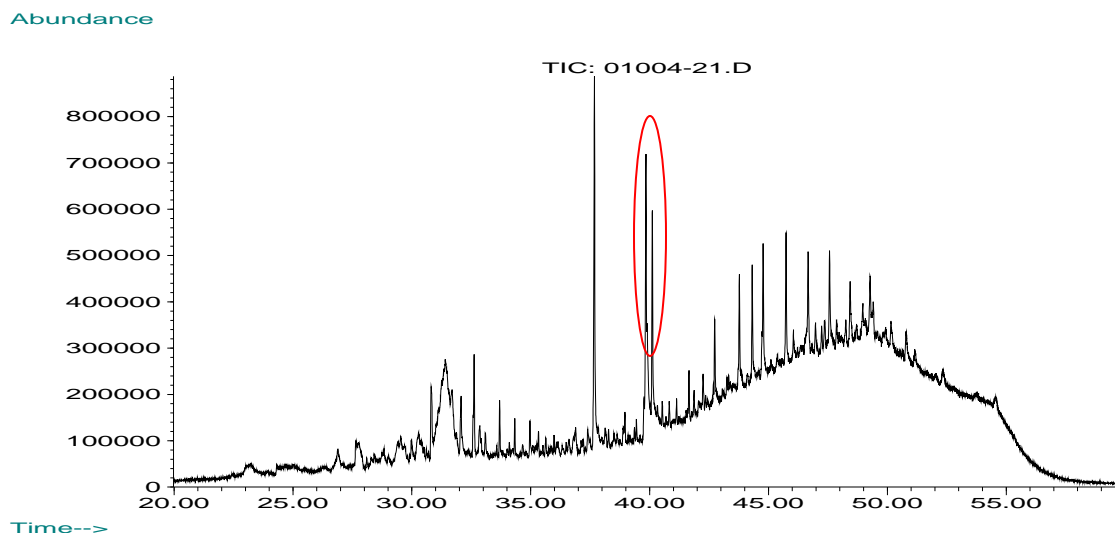
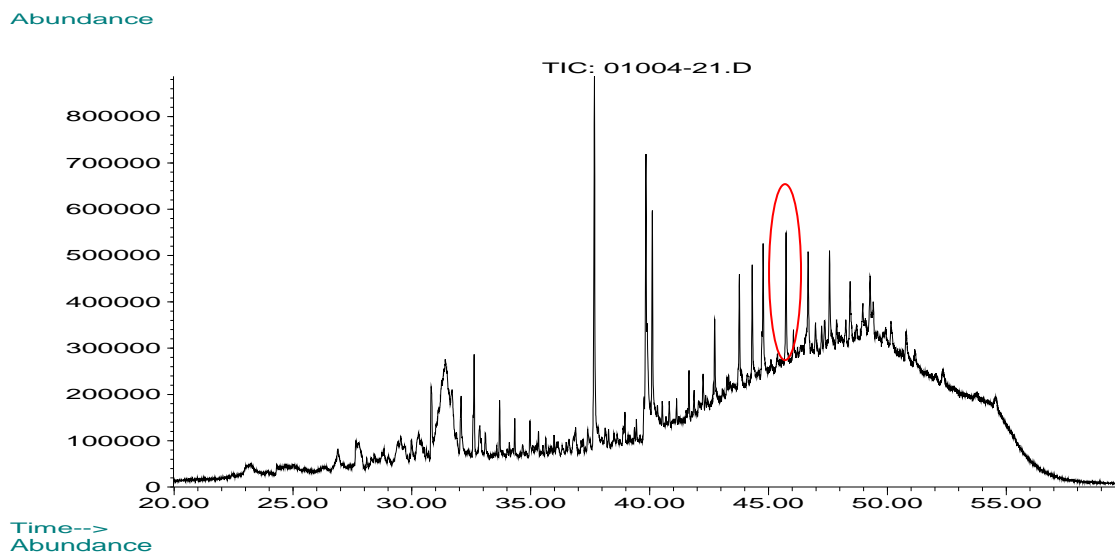
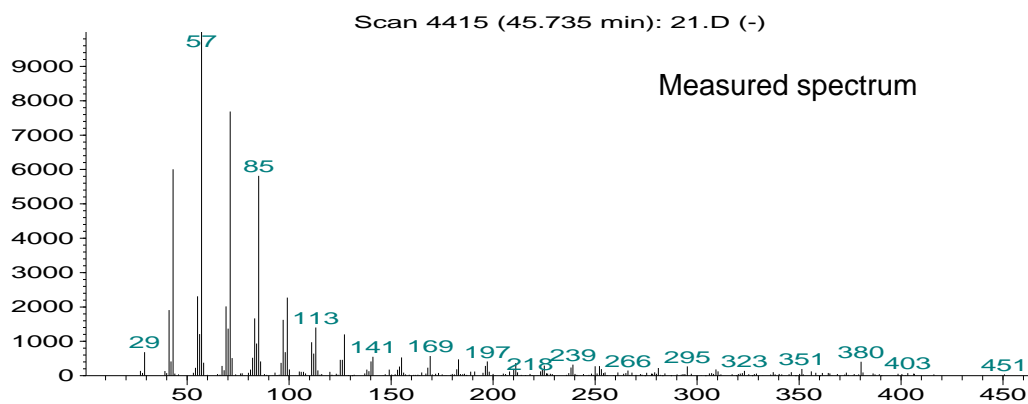


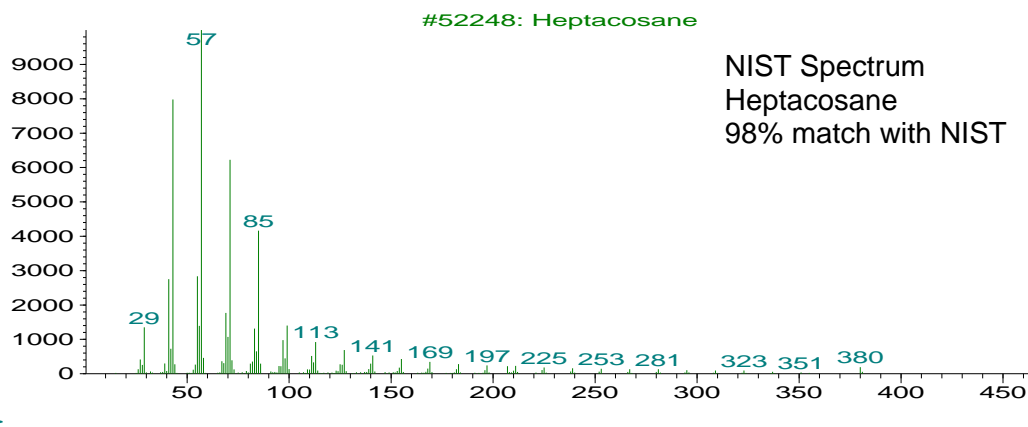
Figure 6c. Mass Spectral match for circled peak in chromatogram from ambient sample in Berkeley, CA.



Time-->
Abundance



m/z-->
Abundance



m/z-->

Figure 6d. Mass Spectral match for circled peak in chromatogram from ambient sample in Berkeley, CA.

Factor analysis results, shown in Table 2, are limited to 14 compounds because we only had 15 time measurement points in the data set. The dominant compound associated with Factor 1 is levoglucosan, a clear marker of wood burning (Simoneit et

al., 1999). The dominant compound associated with Factor 2 is propanoic acid,2-methyl-,1-(1,1-dimethylethyl)-2-methyl-1,3-propanediyl ester, Factor 3 is 1,3,5-triallylisocyanuric acid and the dominant compound associated with Factor 4 is heptadecane. The dominant compounds for Factors 2-4 do not offer enough information alone to determine a source type (i.e. heptadecane has several potential sources). These source types will become clearer as more compounds are added into the factor analysis, resulting in a characteristic set of marker compounds within each factor. We expect that with a longer data set this type of factor analysis will prove to be very effective at separating source categories as the basis for source apportionment studies, particularly when paired with the wide range of additional aerosol and gas phase observations that are planned for the Fresno field experiment.

We note that the 24 hour period analyzed above is representative of a time period where traditionally only 1 or perhaps 2 sequential filter analyses of organic aerosol composition would typically have been measured. Our TAG measurements clearly show that having hourly time resolution dramatically enhances the amount of information that can be learned about the sources contributing to organic aerosol loading in the atmosphere, compared to traditional 12 or 24 hour filter sampling.

Table 2. Factor Analysis Results for Air Sampled in Berkeley, California, January 10-11, 2004.

Compound	Loadings (Values < 0.3 omitted)			
	Factor 1	Factor 2	Factor 3	Factor 4
phthalic acid	0.74	0.55		
cyclohexasiloxane, dodecamethyl-	0.58		0.49	0.54
benzenepropanoic acid,.beta.,.beta.-dimethyl-	0.50	0.44	0.45	0.57
pyridine,3-(1-methyl-1H-pyrrol-2-yl)-	0.89		0.37	
levoglucosan	0.96			
benzenebutanoic acid,2,5-dimethyl-	0.81	0.46		
diethyl phthalate		0.99		
propanoic acid,2-methyl-,1-(1,1-dimethylethyl)-2-		1.00		
benzophenone		0.73		0.44
benzaldehyde,4-hydroxy-3,5-dimethoxy-	0.89			
1,3,5-triazine-2,4,6(1H,2H,5H)-trione,1,3,5-tri-2-		0.35	0.79	0.47
heptadecane				0.90
tetradecanal	0.38		0.84	
tetradecanoic acid	0.96			
Importance of factors				
Sum square loadings	5.47	3.47	2.22	2.07
Proportion of variation	0.39	0.25	0.16	0.15
Cumulative variation	0.39	0.64	0.80	0.94

Factor analysis was performed in SPLUS 6.1 (MathSoft, Inc.), using varimax rotation and maximum likelihood estimation. The model was limited to four factors because additional factors did not have significant sum square loadings, and did not explain a significant portion of the variation (less than 0.02). Proportion variation defines the fraction of data explained by each factor. Cumulative variation is the sum of the proportion variation, indicating that these four factors explain 94% of observations. Only the first 14 compounds of the data set were included in this analysis due to statistical limitations resulting from the short sample period which contained 15 sequential measurements at approximately 1 hour intervals. Factor analysis of all the measured compounds will be possible with longer datasets, such as those we will collect in Fresno.

6. Field Campaign in Nova Scotia

The first field deployment with the TAG system was conducted as part of the ICARTT 2004 campaign last summer. Measurements were made on the southwest coast of Nova Scotia (Chebogue Point) during July and August, 2004. The project objective was to observe pollutants as they were transported from the Northeastern US towards the North Atlantic Ocean. This field campaign included many research groups, with measurements of trace gases, meteorological parameters, and aerosol parameters. Collocated measurements included a full suite of gas phase volatile organic compounds (Goldstein group/UCB) as well as an Aerosol Mass Spectrometer (Doug Worsnop/Aerodyne).

TAG was operated over a 6-week period, with around-the-clock, hourly, in-situ measurements. In total, we measured 750 samples of atmospheric aerosols with hourly time resolution (750 chromatograms x 2 detectors = 1500 total chromatograms). This recently acquired data is the first obtained with the new TAG instrument outside our laboratory, and is the first data with hourly time resolution over an extended period of time. It is a rich data set, and our analyses are not complete. Nonetheless, we believe the results to date indicate that our instrument is field worthy, and the data are important to understanding the origins of organic aerosols.

Here we present our “first look” at the TAG data focusing on a continuous subset of the observations from July 26 – August 15 (~3 weeks). During this period, the system ran automatically, with automated filtered air and zero air blanks, however calibrations were done manually with directly applied standards. The automated filtered and zero air blanks were periodically interspersed between the ambient air samples to check for potential artifacts due to carryover between samples or due to gas phase artifacts. We are still working on the quantification of our measurements using the applied standards, on the specific identification of compounds not found in the NIST mass spectral database, and integration of the remaining chromatograms.

Comparison of Aerosol and Background Chromatograms:

Figure 7 compares a typical ambient air sample (black) to that obtained when sampling through a Teflon filter (green). The sample time for these chromatograms was 30 minutes, and the sample size was 0.25 m³. The Teflon-filter sample is a dynamic blank that provides a measure of any positive gas phase artifacts or contamination from the TAG system itself. As is apparent from Figure 7, the dynamic blank is low by comparison to the aerosol signal. The vast majority of the individual peaks in the aerosol sample, which comprise the resolved compounds, are not present in the filtered blank. These resolved compounds are the focus of the data analysis reported here. The Total Organic Aerosol is the sum of Resolved Compounds that we see in the black chromatogram as peaks, plus the Unresolved Compounds that we see as the difference between the black and green chromatograms, plus any Non-Eluting Compounds that do not make it through our measurement system. Additional information is contained in the Unresolved Compounds and this is being explored, but this report focuses exclusively on the information contained in the Resolved Compounds.

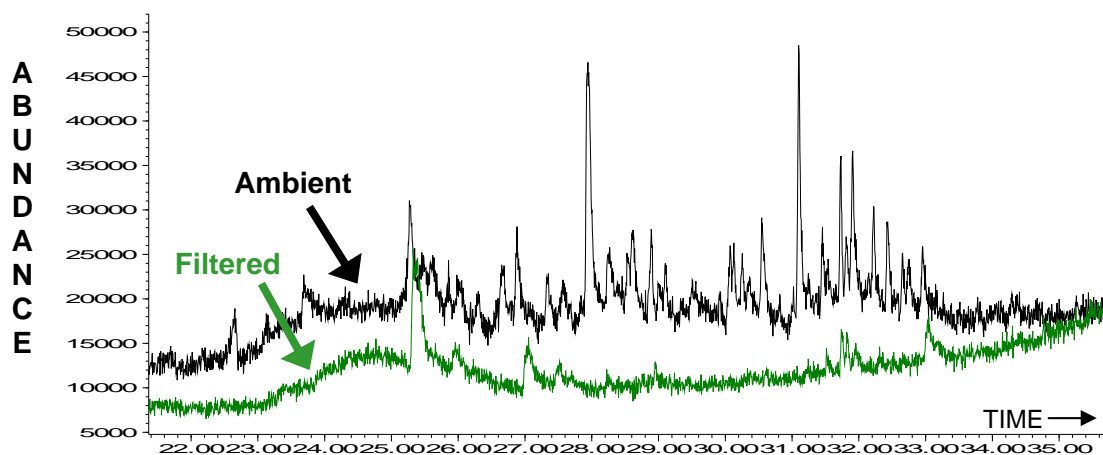


Figure 7. Chromatograms of mass spectrometer detector response (abundance) versus elution time from the gas chromatography column. This is a typical example of a sample (black) versus a filtered blank (green) for the portion of the chromatogram (22 to 35 minutes) where most speciated organics eluted from the chromatogram in Nova Scotia.

Compound Identification and Time Series

Unlike the measurements for Berkeley aerosols reported above, most of the resolved compounds from the Nova Scotia campaign are not in the NIST mass spectral data base. This is not surprising for a remote site where the concentration of primary compounds is low compared to the concentration of oxygenated, secondary material. Some of these unidentified compounds are also found in our Berkeley, CA samples, albeit at much lower relative concentrations.

Although we are not able to identify these compounds by name, we are able to track them throughout the study based on their retention time and mass spectral signal. The abundance of these compounds is evaluated from each chromatogram by integration of the baseline corrected signal strength for the characteristic mass/charge ratio over the characteristic retention time window. This is done for each of the individual ion chromatograms, to construct a time line of compound abundances. For our initial analysis we have integrated peaks for 28 of the most prominent of the individual compounds, creating a data matrix for analyzing timelines, comparing to other observations made at the site, and for performing factor analysis.

The timeline for four of the 28 individual compounds that we integrated for the three week period July 26-August 15, 2004 are shown in Figure 8. Also shown are the filtered blanks for these compounds. For each of the 28 compounds evaluated the blanks were low, indicating that there was no significant gas phase or other artifacts impacting our observations for these compounds. Note that the time variability of Compounds A and C are similar, as is that for Compounds B and D. The hourly time resolution of the data make it quite clear that the temporal patterns for these two pairs of compounds were very different, suggesting therefore that the sources of these organic compounds were also quite different.

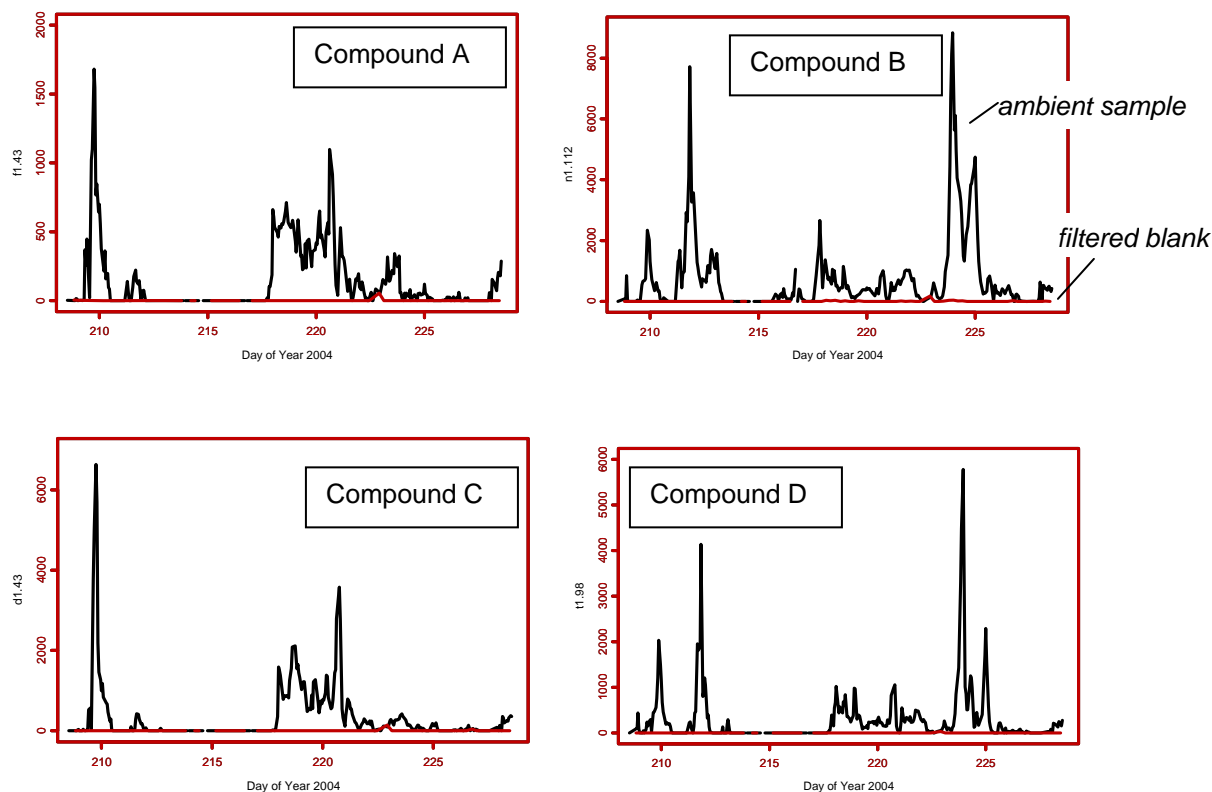


Figure 8. Timeline of concentration (July 26-August 15, 2004) for four compounds (A, B, C, D) measured by TAG and the FILTERED blank for these compounds (red) showing there were no significant gas phase artifacts present.

Comparison to Collocated Measurements

We have compared our TAG data to observations from an Aerosol Mass Spectrometer (AMS) (Data from Doug Worsnop and James Allan et al., Aerodyne Inc. and University of Manchester Institute of Science and Technology). The AMS provides a useful comparison point for several reasons. First, the AMS measures Total Organic Aerosol with high time resolution, but cannot differentiate the individual organics in the aerosols. Second, the AMS can measure many inorganic components in the aerosols such as total sulfate or total nitrate, thus allowing us to investigate whether specific organic compounds measured by TAG are associated with sulfate sources for example. An additional reason this comparison is useful for ARB is that our planned Phase II deployment in Fresno is being coordinated with planned measurements by Kim Prather's group whose single particle aerosol mass spectrometer can measure a similar range of aerosol components (e.g. total organics, sulfate, nitrate, etc.) as the Aerodyne AMS instrument.

In Figure 9, the time series for TAG compounds A and B are compared to the AMS signals for total organic and sulfate aerosols. This figure clearly shows that the total organic aerosol (green) is actually the sum of a variety of organic compounds that TAG is able to separate. At least two types of organic aerosol mixtures were measured at different times in Nova Scotia. The first aerosol event (Event Type 1) which occurred around August 6-7 contained organic compounds, but no

sulfate, and was associated with TAG compound A. The second aerosol event (Event Type 2), which occurred around August 11, contained both organics and sulfate and is associated with TAG compound B. Together the temporal patterns of TAG compounds A and B sum to a pattern resembling that of the Total Organic Aerosol measured by AMS.

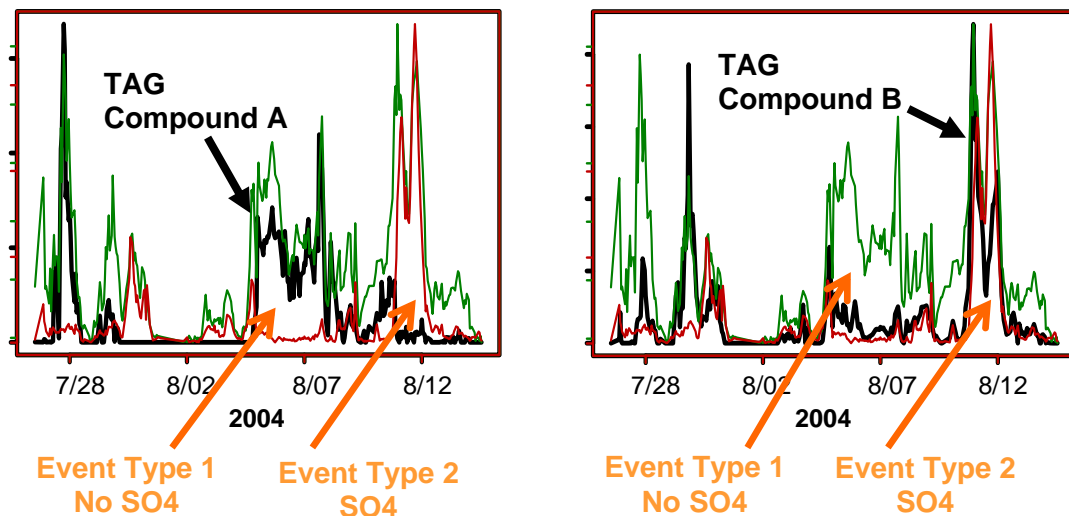


Figure 9. Timeline of aerosol concentrations (July 26-August 15, 2004, shown as Day of Year (DOY)) for TAG compounds A and B (black), and AMS measurements of Total Organics (green) and Sulfate (SO₄) (red). The vertical axis indicates concentration for the purpose of timeline comparisons, but is not calibrated for this preliminary analysis. The individual TAG compounds (black) are 2 or 3 orders of magnitude smaller than Total Organics (green) by mass.

Source Resolution

We have performed factor analysis using all the TAG preliminary data (28 resolved compounds using MS single ion peak area), combined with AMS (Total Organic Carbon, SO₄, NO₃, NH₄), elemental carbon (EC), and gas phase O₃, CO, and Radon data. The purpose of this analysis was to see how these 36 elements varied with each other to see if the factor analysis could elucidate some underlying processes or source types leading to the observed inter-variability of gases and aerosols.

Results of the Factor analysis show that the variability in the observed gases and aerosols could be dominantly explained by three Factors.

- Factor 1 contained the majority of TAG compounds (including Compounds A and C), AMS Total Organic Aerosol, and Radon, thus we will call it the “Organic Only Factor”. The high Radon values also tell us that this Organic Only Factor must be associated with significant continental influence because the only significant source of Radon is soil emissions.
- Factor 2 was associated with a few TAG compounds (including Compounds B and D), but was dominated by the AMS observations of Total Organic Carbon, SO₄, NO₃, and NH₄, by elemental carbon, and gas phase O₃ and CO. These constituents can be thought of as markers of oxidized urban plumes which lead to high O₃ concentrations in air a few days downwind of the continental United States.
- Factor 3 consisted of just 4 of the 28 TAG compounds and was not strongly associated with any of the other species used in the factor analysis. Examination of meteorological data indicates a local to regional source that provides an interesting but not dominant contribution to the Total Organic Aerosol at this site.

Time series of the strength of Factors 1 and 2 are shown in Figure 10. Comparison to Figure 3 above shows that “Event 1” is

associated with Factor 1, while “Event 2” is associated with Factor 2. For these two events we examined the 8-day back trajectory estimates of air arriving at Nova Scotia provided by NOAA. As shown in Figure 4, Event 1 (organic only) is associated with air descending from the North which had spent time recently over Eastern Canada. The airmass for the time period of Event 2 (organics plus sulfate) originated over the Eastern Seaboard of the United States. These back trajectories support our interpretation of the origins of Factor 1 as a continental air mass, and Factor 2 as an aged urban plume.

Given the slow deposition rates of sub-micron sized aerosols from the atmosphere, by the time air pollution events reach the coast of Nova Scotia from the United States they may have been aloft and undergoing photochemical transformations for at least several days. This has important consequences for the observations we report here that make them quite different from what we expect to observe in Fresno during Phase II of our ARB contract. First of all, what we observed in Nova Scotia as a Type 2 event was a plume that integrated over a wide variety of source types and was highly homogenized by the time we observed it. Therefore, making measurements days downwind of the sources we would not necessarily expect to discern differences in the temporal patterns from individual sources within the source region. The TAG observations in Nova Scotia consisted of highly oxidized aerosols that are quite different than the mostly primary aerosols we observed in Berkeley (shown in Section 5 above) and those we expect to observe in an urban area such as Fresno. In Fresno, we also expect that primary and secondary aerosols will have very different diurnal patterns, allowing us to further separate source contributions.

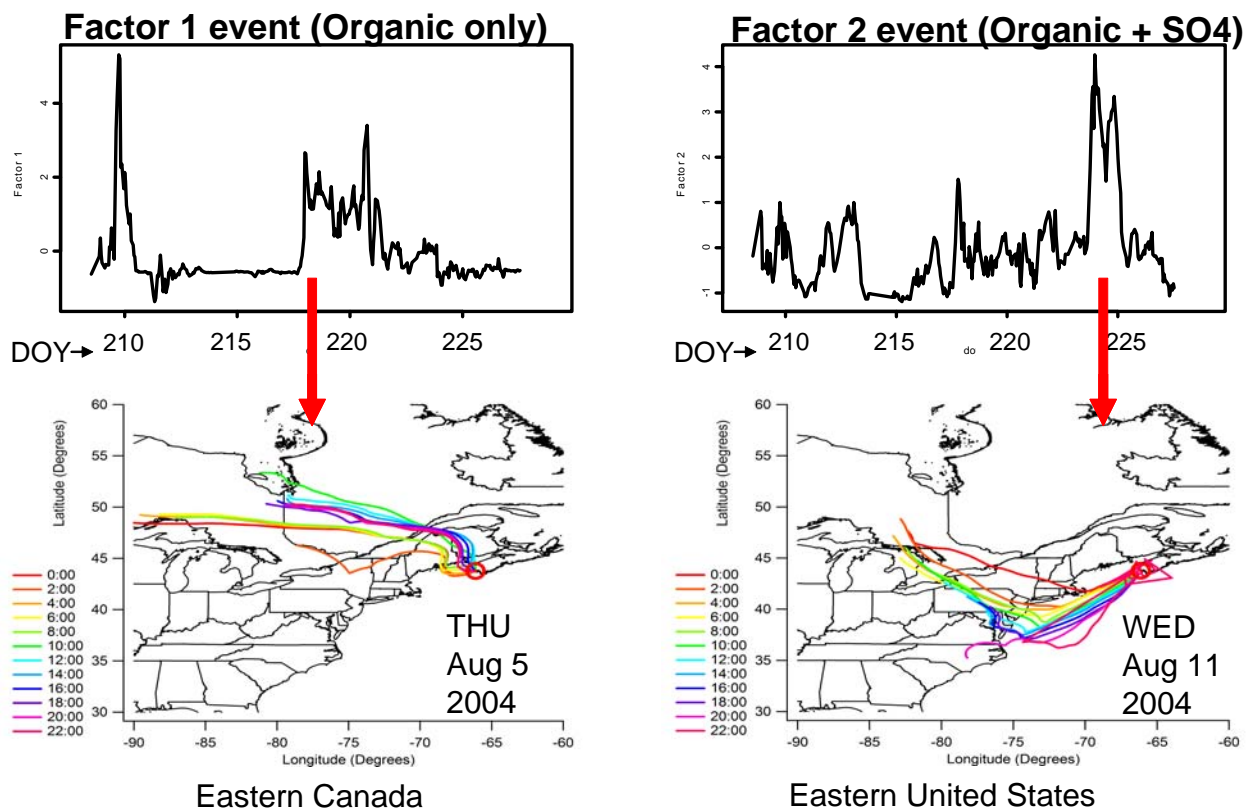


Figure 10. Timelines of Factors 1 and 2, and the calculated back trajectories from a period representing a Factor 1 event and a period representing a Factor 2 event, showing the different spatial origins of the chemically different organic aerosol events observed at Chebogue Point. (DOY means Day of Year, starting from January 1, 2004).

7. Gas Phase VOC Measurements

In order to aid in interpretation of aerosol observations it is extremely useful to measure a suite of trace gases whose source types and atmospheric lifetimes are better known than those of aerosols. The best suite of trace gases to observe when studying sources of organic aerosols is gas phase volatile organic compounds (VOCs). These VOCs are most useful because of their wide variety of lifetimes (minutes to months) functional types (alkanes, alkenes, alkynes, alcohols, aldehydes, aromatics, organic nitrates, etc) and sources (anthropogenic, biogenic, photochemical, combination). Some VOCs have sources dominated by tailpipe emissions (e.g. alkenes with 4 or 5 carbons), others are dominated by evaporative emissions (e.g. methylpentanes), and others are indicative of solvent use (e.g. toluene), liquid propane (e.g. propane), biomass burning (e.g. acetonitrile), secondary production in the atmosphere (e.g. acetaldehyde or organic nitrates), or biogenic sources (e.g. isoprene, methylbutenol, terpenes). We have built and deployed instrumentation for measuring a wide variety of gas phase VOCs (including all compounds listed above) with hourly time resolution and have showed that the data is extremely useful for identification of source types through factor analysis and correlation with tracers of known origin (e.g. Lamanna and Goldstein, 1999; Goldstein and Schade, 2000; Millet et al., 2004).

Subsequent to our initial contract, we have been asked by ARB staff (Nehzat Motallebi and Eileen McCauley) to submit a supplemental proposal along with the interim report to include time resolved gas-phase VOC measurements using a second automated in-situ GC/MS/FID instrument built in our laboratory. These gas phase measurements are to be done alongside the particle phase measurements during both summer and winter in order to provide supporting information for resolution of aerosol source types.

A schematic diagram of the gas phase VOC instrument is shown in Figure 11. To provide information on as wide a range of compounds as possible, two separate measurement channels are used, equipped with different preconditioning systems, preconcentration traps, chromatography columns, and detectors. Channel 1 was designed for preconcentration and separation of C₃-C₆ non-methane hydrocarbons, including alkanes, alkenes and alkynes, on an Rt-Alumina PLOT column with subsequent detection by FID. Channel 2 was designed for preconcentration and separation of oxygenated, aromatic, and halogenated VOCs, NMHCs larger than C₆, and some other VOCs such as acetonitrile and dimethylsulfide, on a DB-WAX column with subsequent detection by quadrupole MSD (HP 5971).

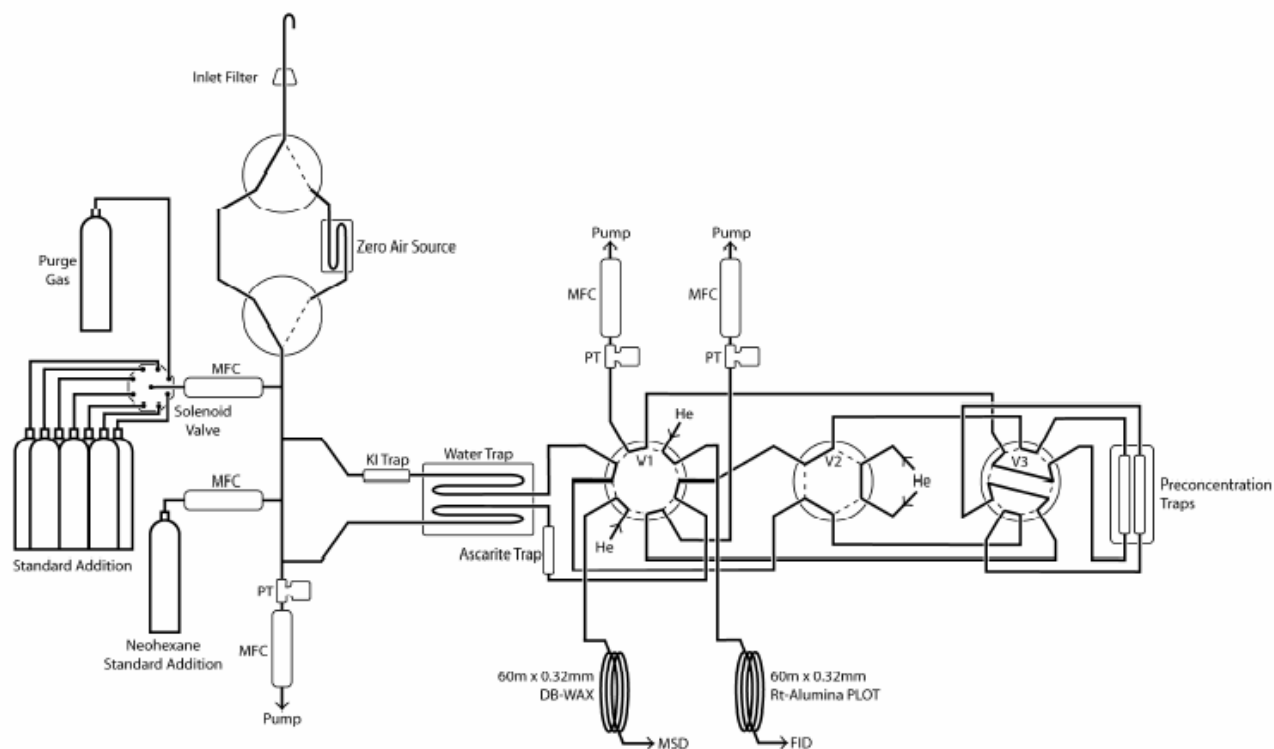


Figure 11. Schematic diagram of automated in-situ GC/MS/FID VOC instrument (Millet et al., 2004).

Ambient air samples are drawn at 4 sl/min through a 2 micron Teflon particulate filter and 1/4" OD Teflon tubing (FEP fluoropolymer, Chemflour) mounted outside the laboratory. Two 15 scc/min subsample flows are drawn from the main sample line, and through pretreatment traps for removal of ozone, water, and carbon dioxide. For 30 minutes out of every hour, the valve array (V1, V2, and V3; valves from Valco Instruments) are switched to sampling mode (Figure 11, as shown) and the subsamples flow through 0.03" ID fused silica-lined stainless steel tubing (Silcosteel, Restek Corp) to the sample preconcentration traps where the VOCs are trapped prior to analysis. When sample collection is complete, the preconcentration traps and downstream tubing are purged with a forward flow of UHP helium for 30 seconds to remove residual air. The valve array is then switched to inject mode, the preconcentration traps heated rapidly to 200 °C, and the trapped analytes desorbed into the helium carrier gas and transported to the GC for separation and quantification. As non-inert surfaces are known to cause artifacts and compound losses for unsaturated and oxygenated species, all surfaces contacted by the sampled airstream prior to the valve array were constructed of teflon (PFA or FEP). All subsequent tubing and fittings, except the internal surfaces of the Valco valves V1, V2, and V3, are Silcosteel. The valve array, including all silcosteel tubing, is housed in a temperature controlled box held at 50 °C to prevent compound losses through condensation and adsorption. All flows are controlled using Mass-Flo Controllers (MKS Instruments), and pressures are monitored at various points in the sampling apparatus using pressure transducers (Data Instruments). In order to reduce the dew point of the sampled airstream, both subsample flows pass through a loop of 1/8" OD teflon tubing cooled thermoelectrically to -25 °C. Following sample collection, the water trap is heated to 105 °C while being purged with a reverse flow of dry zero air to expel the condensed water prior to the next sampling interval. A trap for the removal of carbon dioxide and ozone (Ascarite II, Thomas Scientific) is placed downstream of the water trap in the Rt-Alumina/FID channel. An ozone trap (KI-impregnated glass wool) is placed upstream of the water trap in the other channel leading to the DB-WAX column and the MSD.

Sample preconcentration is achieved using a combination of thermoelectric cooling and adsorbent trapping. The preconcentration traps consist of three stages (glass beads/Carbopack B/Carboxen 1000 for the Rt-Alumina/FID channel, glass beads/Carbopack B/Carbosieves SIII for the DB-WAX/MSD channel; all adsorbents from Supelco), held in place by DMCS-treated glass wool (Alltech Associates) in a 9 cm long, 0.04" ID fused silica-lined stainless steel tube (Restek Corp). A nichrome wire heater is wrapped around the preconcentration traps, and the trap/heater assemblies are housed in a machined aluminum block that is thermoelectrically cooled to -15 °C. After sample collection and the helium purge, the preconcentration traps are isolated via V3 until the start of the next chromatographic run. The traps are small enough to permit rapid thermal desorption (-15 °C to 200 °C in 10 seconds) eliminating the need to cryofocus the samples before chromatographic analysis (following *Lamanna and Goldstein* [1999]). The samples are thus introduced to the individual GC columns, where the components are separated and then detected with the FID or MSD.

Chromatographic separation and detection of the analytes is achieved using an HP 5890 Series II GC. The temperature program for the GC oven is: 35 °C for 5 minutes, 3 °C/minute to 95 °C, 12.5 °C/minute to 195 °C, hold for 6 minutes. The oven temperature is then ramped down to 35 °C in preparation for the next run. The carrier gas flow into the MSD is controlled electronically and maintained constant at 1 mL/min. The FID channel carrier gas flow is controlled mechanically by setting the pressure at the column head such that the flow is 4.5 mL/min at an oven temperature of 35 °C. The carrier gas for both channels is UHP (99.999%) helium which is further purified of oxygen, moisture and hydrocarbons. Zero air for blank runs and calibration by standard addition is generated by flowing ambient air over a bed of platinum heated to 370 °C. This system passes ambient humidity, creating VOC free air in a matrix resembling real air as closely as possible. Zero air is analyzed daily to check for blank problems and contamination for all measured compounds.

Compounds measured on the FID channel are quantified by determining their weighted response relative to a reference compound (see *Goldstein et al.* [1995] and *Lamanna and Goldstein* [1999] for details). Neohexane (~5 ppm, certified NIST traceable $\pm 2\%$; Scott-Marrin Inc.) is employed as the internal standard for the FID channel, and is added by dynamic dilution to the sampling stream. Compound identification is achieved by matching retention times with those of known standards for each compound (Scott Specialty Gases, Inc.). The MSD is operated in single ion mode (SIM) for optimum sensitivity and selectivity of response. Ion-monitoring windows are timed to coincide with the elution of the compounds of interest. Calibration curves for all of the individual compounds are obtained by dynamic dilution of multi-component low-ppm level standards into zero air to mimic the range of ambient mixing ratios. A calibration or blank is performed approximately every 6th run.

The system is fully automated for unattended operation in the field. The valve array (V1, V2 and V3) and the preconcentration trap resistance heater circuit are controlled through the GC via auxiliary output circuitry. The PC controlling

the GC is also interfaced with a CR10X datalogger (Campbell Scientific Inc.), which is triggered at the outset of each analysis run. The inlet valve, the standard addition solenoid valve and the water trap cooling, heating and valve circuitry are switched at the appropriate times during the sampling cycle by a relay module (SDM-CD16AC, Campbell Scientific) controlled by the datalogger. Relevant engineering data (time, temperatures, flow rates, pressures, etc.) for each sampling interval are recorded by the CR10X datalogger with a AM416 multiplexer (Campbell Scientific Inc.), then uploaded to the PC and stored with the associated chromatographic data. Chromatogram integrations are done using HP Chemstation software. All subsequent data processing and QA/QC is performed using routines created in S-Plus (Insightful Corp.).

Measurements made using this gas phase VOC instrument have been published from a series of studies which occurred in 2001-2004 including field campaigns at Trinidad Head California during the spring NOAA ITCT 2002 campaign, the EPA/DOE Pittsburgh Air Quality Study in both summer and winter, and a summer campaign in Granite Bay California (Millet et al. 2004a, 2004b, 2004c). Table 3 provides a list of the compounds measured during the Trinidad Head campaign along with their detection limit, precision, accuracy, and the range of concentrations measured. Trinidad Head was a very clean coastal site, remote from urban pollution. In urban environments such as Pittsburgh and Granite Bay (and we expect Fresno), an even larger number of species could be identified and quantified.

This instrumentation was also deployed at Chebogue Point in summer 2004, thus we show below a small subset of these in-situ VOC measurements and discuss them in comparison to the TAG observations and Factors 1-3 described above. We also note that these data will be extremely useful for other investigators who plan to do ARB supported measurements at the same site in Fresno including Kim Prather's group (UC San Diego), Judy Chow's group (DRI), and Ron Cohen's group (UC Berkeley).

The three factors determined using the TAG data (section 6) were clearly associated with different wind flow patterns as observed at Chebogue Point (Figure 12). Factor 1 was associated mainly with moderate wind speeds coming from the north suggesting that they originated somewhere in Eastern Canada. Factor 2 was associated with air coming from the south at moderate wind speeds suggesting that it came from the Eastern United States. Factor 3 was associated with slower wind speeds and air that was coming from the land rather than off the ocean (Chebogue Point is located at the south-west tip of Nova Scotia).

Table 3. Precision, detection limit, accuracy and concentration quantiles for measured VOCs at Trinidad Head, California (Millet et al., 2004c).

	Precision (%) ^a	Detection Limit (ppt)	Accuracy (%) ^b	Concentration Quantiles (ppt)		
				0.25	0.50	0.75
1-butene	1.9	0.6	7.5	4.9	8.5	14.9
1-pentene	1.9	0.5	7.5	2.0	3.9	6.1
acetone	3.2	13	10	529.4	629.1	801.0
acetonitrile	10.5	5.8	13	30.8	36.3	42.4
benzene	1.9	4.5	10	41.0	55.1	79.0
butanal	6.2	4.6	10	15.2	18.5	23.3
butane	1.9	0.6	7.5	24.6	44.0	69.8
c-2-pentene	1.9	0.5	7.5	0.0	1.1	2.0
CFC-11	1.2	0.3	10	232.7	235.8	240.0
CFC-113	2.2	0.3	10	86.9	88.2	89.2
chloroform	2.0	0.5	10	8.3	9.1	10.2
DMS	7.3	1.3	10	23.6	50.6	80.8
ethanol	16.9	21	19	74.7	112.1	167.5
ethylbenzene	7.5	0.5	10	0.7	1.4	4.0
hexane	1.9	0.4	7.5	2.8	4.7	7.8
isopentane	1.9	0.5	7.5	10.0	19.0	40.9
isoprene	1.9	0.5	7.5	2.2	4.0	6.3
isopropanol	14.7	17	17	10.9	17.2	27.2
MACR	3.7	8.0	10	8.7	15.2	23.7
MBO	20.4	1.0	22	2.2	7.6	17.7
MEK	6.4	4.9	10	44.6	57.1	75.8
methanol	16.4	70	18	611.0	778.0	1021.1
methyl iodide	4.2	1.8	10	1.1	1.5	2.0
methylpentanes ^c	1.9	0.4	7.5	4.6	8.7	21.0
MTBE	1.2	0.4	10	1.3	2.1	5.5
MVK	8.0	4.0	10	3.1	5.8	9.4
m-xylene	7.5	0.5	10	0.8	2.4	7.3
o-xylene	7.5	0.5	10	0.5	1.4	3.9
pentane	1.9	0.5	7.5	6.9	12.9	20.9
C ₂ Cl ₄	8.0	0.3	10	4.4	4.8	5.4
propane	1.9	0.9	7.5	217.3	312.4	416.4
propene	1.9	0.8	7.5	12.8	22.4	43.3
propyne	1.9	0.8	7.5	0.5	2.1	3.6
p-xylene	7.5	0.5	10	0.6	1.5	4.0
t-2-butene	1.9	0.6	7.5	0.0	1.1	1.8
t-2-pentene	1.9	0.5	7.5	0.0	0.6	1.3
toluene	3.3	4.9	10	5.6	12.8	30.8

^a Precision is defined here as the relative standard deviation of the calibration fit residuals. ^b The measurement accuracy was estimated by propagating the uncertainties associated with the measurement precision, the calibration slope accuracy, mass flow measurements, and the accuracy of the calibration standards. ^c The sum of 2-methylpentane and 3-methylpentane, which coelute from the chromatography column.

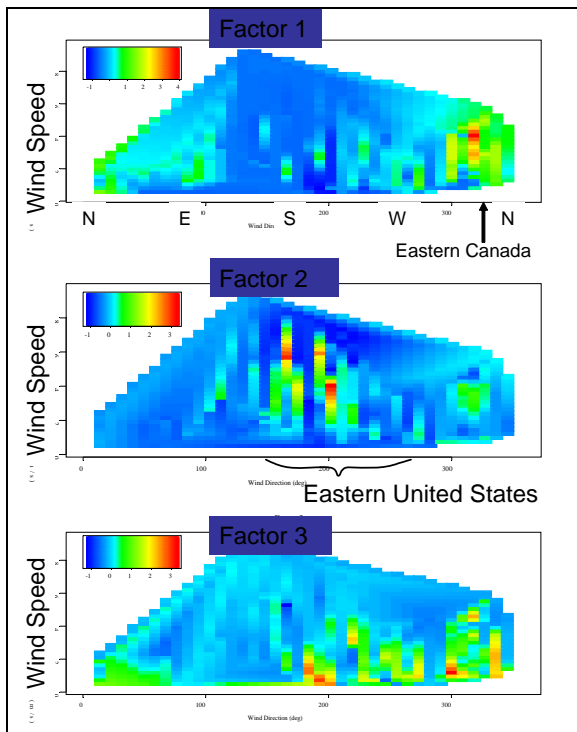


Figure 12. Factors 1, 2, and 3, plotted as an interpolated function of wind speed and direction.

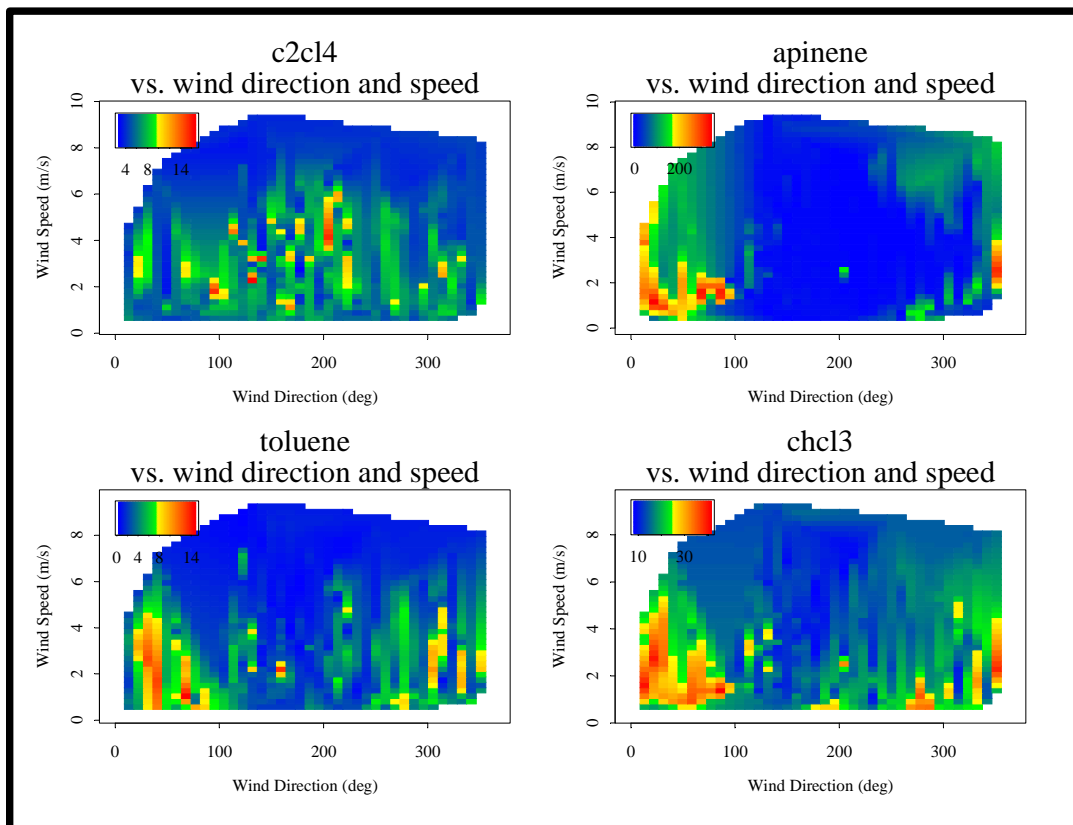


Figure 13. Ethylene chloride, alpha-pinene, toluene, and trichloromethane as a function of wind speed and direction, measured for at Chebogue Point Nova Scotia (~July 1 – August 19, 2004).

Observations of gas phase VOCs show relationships with wind speed and direction (Figure 13) that are quite similar to those discerned for Factors 1-3 from the TAG organic aerosol data. Ethylene chloride is a long lived anthropogenic pollutant that is clearly coming from the Eastern Seaboard of the United States (based on back trajectory analyses which are not shown), and its pattern with respect to back trajectories and local wind speed and direction is extremely similar to that of Factor 2, the organic aerosol plus sulfate events that we wrote were likely indicative of emissions from the Eastern United States. Thus, ethylene chloride provides a clear and unique marker of anthropogenic emissions that can be used to verify and aid in our interpretation of the TAG data. In addition, since ethylene chloride emission rates from the US are reasonably well known from sales data, and it is a long lived compound compared to the transport time from sources of a few days to a week, we could extrapolate an estimate of specific organic aerosol marker compounds using this combination of observations.

Toluene and trichloromethane patterns with respect to wind speed and direction, and also with respect to back trajectories, are similar to Factor 1 events (organic only aerosol). Therefore, these compounds are likely emitted along with the organic only aerosols from sources that are not associated with sulfur emissions from locations along the back trajectories from Eastern Canada. While we have not identified the major sources of these aerosols specifically yet, we have learned a significant amount from this preliminary analysis about the required source characteristics needed to explain its origin.

Finally, we see some correlation between the patterns for Factor 3 organic aerosol compounds and some of the more locally derived gas phase organic compounds including biogenics such as alpha-pinene. This analysis is very preliminary, and we are currently working hard to identify the four compounds in this Factor to determine whether they could indeed be of local origin from gas to particle conversion of biogenic VOCs.

The comparison of gas phase VOC observations with speciated organic aerosol observations (TAG) should be dramatically more straightforward in Fresno than it was for Nova Scotia for two main reasons. The first reason is that the organic aerosols will have a MUCH higher proportion that is primary compounds in Fresno which are easier to identify, up to 80% of total organic mass (Hildemann et al., 1991; Schauer et al., 1996). The second reason is that the diurnal patterns in Fresno will reveal a great deal about primary versus secondary compounds, tailpipe versus evaporative compounds, biomass burning versus mobile sources, and other source types that have significantly different temporal patterns and can be identified by the suite of proposed gas phase VOC observations.

8. Comparison between Berkeley, California and Nova Scotia

Through comparison of chromatograms collected in Nova Scotia with those collected in Berkeley California on the UC Berkeley campus, we have discerned some striking differences. The chromatograms from Berkeley contain a much higher fraction of compounds that are easily identified through the NIST mass spectral database as shown in section 5. These compounds are consistent with the suite of compounds reported in the literature from filter collection and solvent extraction analysis over the past 20 years. Many are primary compounds associated with sources. In contrast, the chromatograms from Nova Scotia include a wide variety of compounds that contain oxygen but are not readily identified from the NIST data base. We believe this difference is telling us that the Nova Scotia measurements are indicative of highly oxidized aerosols and that the transformation to oxidized form happens over the span of a few days travel time in the atmosphere. This difference also tells us that we should expect a much higher proportion of primary compounds in Fresno than in Nova Scotia, and that we should be able to identify a very large fraction of them using the NIST mass spectral database.

9. Conclusion

Our first look at TAG measurements from Berkeley California clearly shows that we can routinely identify more than 70 individual organic compounds in the chromatograms using the NIST mass spectral database in this type of urban

environment. We also show that even with this initial data set of 1 day hourly time resolution observations, we can use Factor Analysis to indicate at least four distinct diurnal patterns associated with different source types, one of which can already be conclusively identified as biomass burning.

Our campaign in Nova Scotia demonstrates that we have successfully operated TAG under field conditions for a 6-week period, yielding hourly-resolved data on the organic aerosol constituents. Significantly, our routine collection of dynamic blanks shows that the signal from TAG is uniquely associated with the aerosol, and is not a gas phase artifact. Our first look at hourly time resolution data from Chebogue Point Nova Scotia clearly shows that at least three source categories (Factors) can be identified for organic aerosol loading at this site. Comparison with the AMS data show that the three Factors together represent the total organic aerosol observations, and show that our time resolved data can be used to separate sources in a way that AMS Total Organic Aerosol measurements cannot. At Chebogue Point Nova Scotia we learned that the speciated organics in aerosols are highly oxidized during transport from the source region. The transport time from the sources is typically at least 2 days. Recent work by Molina et al (GRL, 2004) has shown that OH oxidation of primary organics in organic aerosols (e.g. long alkanes) occurs efficiently in the atmosphere resulting in organic aerosol lifetimes of order 6 days. Because of this phenomenon, our data from Chebogue Point are extremely valuable and interesting, but they differ significantly from what we observed in Berkeley and what we expect to observe in Fresno. At Chebogue Point we learned that the air mass history (or back trajectories) leading to the site determine the variety of organics in the aerosol, with major differences in observed compounds for pollution events coming from the Eastern Seaboard of the United States compared to those coming from Northern Canada or those coming South from nearby influence of the Maritime Provinces of Canada.

With the TAG data sets we have contracted to collect in Fresno in both summer and winter (4 weeks of hourly data in each season), we will be able to provide a strong source attribution analysis of the major contributors to the organics in PM 2.5. In Fresno we expect to observe a high fraction of identifiable primary compounds rather than secondary compounds in the organic aerosols, similar to what we observed in Berkeley. These primary compounds and their temporal variability at the diurnal scale should be useful for attribution of aerosol loading to specific regional source categories. In summer we expect a higher fraction of secondary oxidized compounds than in winter, but we still expect the organic aerosol to contain a large fraction of identifiable primary compounds in this region due to the proximity to sources. Because we have a much stronger understanding of gas phase VOC sources than of organic aerosol sources, hourly observations of gas phase VOC in Fresno alongside the particle phase observations will be invaluable for helping to discern source categories and relative source strengths for organic aerosols.

10. References

- Chow, J.C., Watson, J.G., Lowenthal, D. H., Solomon, P.A., Magliano, K.L., Ziman, S.D., Richards, L.W., 1993. PM10 and PM2.5 compositions in California's San Joaquin Valley. *Aerosol Science and Technology* 18: 105-128.
- Christoforou, C.S., Salmon, L.G., Hannigan, M.P., Solomon, P.A., Cass, G.R., 2000. Trends in fine particle concentration and chemical composition in southern California. *J. Air and Waste Management Assoc.* 50: 43-53;
- Falkovich A. H. and Rudich Y. (2001) Analysis of semivolatile organic compounds in atmospheric aerosols by direct sample introduction thermal desorption GC/MS, *Environ. Sci. Technol.* 35: 2326-2333.
- Fine, P. M., Cass G. R., Simoneit, B. R. T. (2001) Chemical characterization of fine particle emissions from fireplace combustion of woods grown in the northeastern United States, *Environ. Sci. Technol.* 35: 2665-2675.
- Forstner, H. J. L., Flagan, R. C., Seinfeld J. H. (1997), Molecular speciation of secondary organic aerosol from photooxidation of the higher alkenes: 1-octene and 1-decene, *Atmos. Environ.* 31: 1953-1964.
- Fine, P. M., Cass G. R., Simoneit, B. R. T. (2001) Chemical characterization of fine particle emissions from fireplace combustion of woods grown in the northeastern United States, *Environ. Sci. Technol.* 35: 2665-2675
- Fraser M. P., Kleeman, M. J., Schauer, J. J., Cass, G. R. (2000) Modeling the Atmospheric Concentrations of Individual Gas-Phase and Particle-Phase Organic Compounds, *Environ. Sci. Technol.*, 34: 1302-1312.
- Goldstein, A.H., and G.W. Schade. (2000) Quantifying biogenic and anthropogenic contributions to acetone mixing ratios in a rural environment, *Atmospheric Environment*, V 34, N 29-30, 4997-5006.
- Goldstein, A. H., Daube, B. C., Munger J. W., and Wofsy S. C. (1995) Automated in-situ monitoring of atmospheric nonmethane hydrocarbon concentrations and gradients, *J. Atmos. Chem.* 21: 43-59.
- Hildemann L.M., Markowski G.R. and Cass G.R. (1991) Chemical composition of emissions from urban sources of fine organic aerosol. *Envir. Sci. Technol.* 25, 744-759.
- Jayne, J. T., Leard D. C., Zhang X-F, Davidovits P., Smith K. A., Kolb, C. E., Worsnop D. R. (2000) Development of an aerosol mass spectrometer for size and composition analysis of submicron particles, *Aerosol Sci. Technol.* 33: 49-70.
- Kim, B.M., Teffera, S., Zeldin, M.D., 2000. Characterization of PM2.5 and PM10 in the South Coast air basin of southern

- California: Part 1n-- spatial variation. *J. Air and Waste Management Assoc.* 50: 2034-2044
- Lamanna, M. S. and Goldstein, A. H. (1999) In situ measurements of C_c-C₁₀ volatile organic compounds above a Sierra Nevada ponderosa pine plantation, *J. Geophysical Research* 104, D17: 21247-21262.
- Liu, D. Y., Prather, K. A., Hering, S. V. (2000) Variations in nitrate containing particles in Riverside California, *Aerosol Science and Technology*. 33:71-86.
- Millet, D.B., A.H. Goldstein, J.D. Allan, T.S. Bates, H. Boudries, K.N. Bower, H. Coe, Y. Ma, M. McKay, P.K. Quinn, A. Sullivan, R.J. Weber, and D.R. Worsnop. (2004) VOC measurements at Trinidad Head, CA during ITCT 2K2: Analysis of sources, atmospheric composition and aerosol residence times, *Journal of Geophysical Research*, Vol. 109, No. D23, D23S16, 10.1029/2003JD004026.
- Millet, Dylan B., Neil M. Donahue, Spyros N. Pandis, Andrea Polidori, Charles O. Stanier, Barbara J. Turpin, and Allen H. Goldstein, Atmospheric VOC measurements during the Pittsburgh Air Quality Study: Results, interpretation and quantification of primary and secondary contributions, *Journal of Geophysical Research*, PAQS special issue, in press, 2004a.
- Millet, D.B., and A.H. Goldstein, Evidence of continuing methylchloroform emissions from the United States, *Geophysical Research Letters*, 31, 17, L17101, 10.1029/2004GL020166, 2004b.
- Millet, D.B., A.H. Goldstein, J.D. Allan, T.S. Bates, H. Boudries, K.N. Bower, H. Coe, Y. Ma, M. McKay, P.K. Quinn, A. Sullivan, R.J. Weber, and D.R. Worsnop, VOC measurements at Trinidad Head, CA during ITCT 2K2: Analysis of sources, atmospheric composition and aerosol residence times, *Journal of Geophysical Research*, Vol. 109, No. D23, D23S16, 10.1029/2003JD004026, 2004c.
- Molina, M. J., A. V. Ivanov, S. Trakhtenberg, and L. T. Molina. (2004) Atmospheric evolution of organic aerosol, *Geophysical Research Letters*, VOL. 31, L22104, doi:10.1029/2004GL020910.
- NARSTO. (2003). Particulate Matter Sciences for Policy Makers, A NARSTO Assessment, Chapter 6.
- Neusüss, C., Pelzing, M., Plewka, A., and Herrmann, H. (2000), A new analytical approach for size-resolved speciation of organic compounds in atmospheric aerosol particles: Methods and first results, *J. Geophysical Research* 105, 4513-4527.
- Noble C. A. and Prather K. A. (1996) Real time measurement of correlated size and composition profiles of individual atmospheric aerosol particles, *Environ. Sci. Technol.* 30: 2667-2680.
- Nolte C. G., Schauer J. J., Cass, G. R., and Simoneit, B. R. T. (1999) Highly polar organic compounds present in meat smoke, *Environ. Sci. Technol.*, 33: 3313-3316.
- Rogge, W. F., Hildemann, L. M. Mazurek, M. A., Cass, G. R., and Simoneit, B. R. T. (1997a) Sources of fine organic aerosol. 7. hot asphalt roofing tar pot fumes, *Environ. Sci. Technol.*, 31:2726-2730.
- Rogge, W. F., Hildemann, L. M. Mazurek, M. A., Cass, G. R., and Simoneit, B. R. T. (1997b) Sources of fine organic aerosol. 8. boilers burning no. 2 distillate fuel oil, *Environ. Sci. Technol.*, 31:2731-2737.
- Rogge, W. F., Hildemann, L. M. Mazurek, M. A. and Cass, G. R. (1998) Sources of fine organic aerosol 9: pine oak and synthetic log combustion in residential fireplaces, *Environ Sci Technol.* 32: 13-22.
- Schauer J. J., Kleeman M. J., Cass G. R., and Simoneit B. R. T. (1999) Measurement of Emissions from Air Pollution Sources. 2. C₁ through C₃₀ Organic Compounds from Medium Duty Diesel Trucks, *Environ. Sci. Technol.*, 33: 1578-1587.
- Schauer J. J. and Cass G. R. (2000) Source apportionment of wintertime gas-phase and particle phase air pollutants using organic compounds as tracers, *Environ. Sci. Technol.* 34: 1821-1832.
- Schauer J.J., Rogge W.F., Hildemann L.M., Mazurek M.A., Cass G.R. and Simoneit B.R.T. (1996) Source apportionment of airborne particulate matter using organic compounds as tracers. *Atmos. Environ.* 30 (20) 3837-3855.
- Simoneit, B.R.T.; Schauer, J.J.; Nolte, C.G.; Oros, D.R.; Elias, V.O.; Fraser, M.P.; Rogge, W.F.; Cass, G.R. *Atmos. Environ.* 1999, 33, 173-182.
- Stolzenburg, M. R. and Hering, S. V. (2000) A new method for the automated measurement of atmospheric fine particle nitrate, *Environmental Science and Technology* 34: 907-914.
- Tobias H. J. and Ziemann P. J., (1999) Compound identification in organic aerosols using temperature programmed thermal desorption particle beam mass spectrometry, *Anal. Chem.* 71: 3428-3435.
- Tobias, H. J., Kooiman, P. M., Docherty K. S., Ziemann P. J. (2000) Real time chemical analysis of organic aerosols using a thermal desorption particle beam mass spectrometer, *Aerosol Sci. Technol.* 33: 170-190.
- Waterman, D., Horsfield, B., Leistner, F., Hall, K., and Smith, S. (2000) Quantification of Polycyclic Aromatic Hydrocarbons in the NIST Standard Reference Material (SRM1649A) Urban Dust Using Thermal Desorption GC/MS, *Analytical Chemistry*; 2000; 72(15); 3563-3567.
- Yue, Z. and Fraser, M.P. (2003a). Characterization of non-polar organic fine particulate matter in Houston, Texas. Submitted for publication;
- Yue, Z. and Fraser, M.P. (2003b). Polar organic compounds measured in Fince Particulate matter during TexAQs 2000. Submitted for publication).

